CRETACEOUS STRATIGRAPHY AND BASEMENT INFLUENCES, PEACE RIVER ARCH REGION, WESTERN CANADA SEDIMENTARY BASIN

A Thesis

Submitted to the Faculty of Graduate Studies and Research

in Partial Fulfillment of the Requirements

for

the Degree of

Doctor of Philosophy in Geology

by

DONGQING CHEN

University of Regina

Regina, Saskatchewan

December, 2000

ABSTRACT

Geophysical data, including data from well logs (GR, SP, resistivity, sonic), seismic reflection (PRAISE) and aeromagnetic anomaly (Alberta Basement Transects), together with data from the Geological Atlas and SAMS databases (GSC-Calgary), were used to investigate Phanerozoic formations in the Peace River Arch (PRA) region and their possible relationship to basement features. Detailed stratigraphic correlations in the Cretaceous section were made on the southeast flank of the PRA (23 cross sections, 719 wells, 73 surfaces). More than 100 isopach and structural maps were constructed for the defined Cretaceous stratigraphic intervals.

Many formation boundaries in the Cretaceous appear to be time transgressive surfaces. Three major stratal re-orientations occurred during Cretaceous time. Repeated, abrupt, ~90° angle changes in stratal orientation were influenced by PRA collapse and tectonic loading (convergence of plate boundaries and accretion of terranes) on the western margin.

Three different stacking processes of sediments (linear progradation of elongate zones, differential subsidence and aggradation) occurred in the Cretaceous, and appear to have been controlled by changes in the regional stress field during Cretaceous time. Linear shifting of elongate zones is interpreted to have occurred when lateral compression was strong; differential subsidence of blocks is believed to have occurred when lateral compression was weak; and aggradation developed probably when lateral compression was moderate.

Long acting basement faults are developed in the PRA region. These faults either trend NW-SE parallel to the short axis of the PRA or the Rocky Mountain deformation front,

or NE-SW (NEE-SWW), parallel to the long axis of the PRA. Throughout Phanerozoic time, these faults are interpreted to have played important roles in relieving intra-plate stresses, shaping subsidence processes, and affecting local sediment accumulations. Reverse motion on faults has been observed in the Arch region.

Five stages of development are recognized during PRA evolution. (1) The Arch remained high from Cambrian to Early Devonian time, and this was related to a much broader regional uplift. (2) The Arch was subsiding from Middle Devonian to Permian time. Subsidence rate was accelerated from the Middle to Late Devonian, reached its peak in Wabamun time, and decreased from the Carboniferous to Permian. (3) The long subsidence history of the PRA was interrupted by Mesozoic convergence events on the western margin. Depositional processes in the Arch region were dominated by convergence events from Jurassic to Early Cretaceous Aptian time. (4) Collapse of the PRA occurred during Early Cretaceous Albian time when the effect from early convergence events waned. (5) Subsequent convergence events dominated the PRA region after the Albian and initiated Arch uplift in late Turonian time (Cardium), and the final uplift began in the latest Cretaceous.

ACKNOWLEDGMENTS

Foremost I like to thank Dr. Katherine Bergman, the University of Regina, for the research opportunity and supervision of this thesis. I am grateful for financial support from that University through their Graduate Study Scholarships, and from Dr. Bergman through her NSERC Lithoprobe Supporting Geoscience Grant and NSERC Research Grant during 1995-1998.

I owe a great deal of gratitude to the Geological Survey of Canada - Calgary, especially to Dr. Grant Mossop for access to the database of the Geological Atlas of the Western Canada Sedimentary Basin and comments; to Dr. Gerry Ross for access to the Lithoprobe seismic data and discussion; to Jim Dietrich and Tom Brent for access to the Lithoprobe seismic data, help with the seismic software, and discussions; to Dr. Barry Richards for the data on Carboniferous faults; to Bruce Palmer (now Rakhit Petroleum Consulting Ltd.) for facilities access and coordination; to Ken Nairn †, David Rose, Graham Lai, Ping Tzeng and Parry Houvardes for computer support; to Philip Lawrence for help with the seismic workstation; to Mike Staniland (now Petro-Canada), Bill McDougall, Peter Neelands, Paul Wozniak, Doug Lemay, Bryan Ortman, Steve Orzech, Elizabeth Macey and Glen Edwards for help with the mapping software and hardware; to Dr. Jan Jansonius for helpful literature advice; to John McIsaac, Edward Hau and Joanne McCloskey for help with the search of publications; and many others at the Geologic Survey of Canada-Calgary.

I appreciate the advice from Dr. Kathryn Bethune, the University of Regina, on the mechanisms of igneous intrusion and comments on the thesis. I thank also the Chair of the Geology Department of that University, Dr. Donald Kent, and other committee members, Dr.

Roger Walker, Dr. Ken Ashton and Dr. Stephen Bend, as well as the external examiner, Dr. David Eaton, the University of Western Ontario, for their advice, comments and discussions.

I also like to acknowledge the discussions with my former colleagues Dr. Hongliu Zeng, the University of Texas, and Dr. Zuoheng Chen, the Geological Survey of Canada - Calgary.

TABLE OF CONTENTS

LIST OF FIGURES

CHAPTER 1: THESIS OBJECTIVES AND METHODOLOGY

1-1. Introduction

The study area for this thesis is located in the Peace River Arch (PRA, Fig. 1-1) region, Western Canada Sedimentary Basin (WCSB), within the quadrilateral bounded longitudinally by the border of Alberta – British Columbia and the Fifth Meridian and latitudinally by Townships 56 and 92 (Fig. 1-2). Geographically, the study area occupies the southeast part of the Northwest Plain and extends into the Northeast Plain and Central Plain of Alberta.

The PRA, one of the most prominent and long-acting basement features in the WCSB, is about 140 km wide, trends in an east-northeast direction, and extends about 400 km cratonward from the Cordillera (Cant, 1988). Figure 1-1 (modified from Keith, 1990) shows the outline of the Arch in Middle Devonian time. In fact, both appearance and extent of the PRA vary through time (refer to Fig. 5-2).

Granitic Precambrian rocks in the PRA were uplifted about 1,000 m above regional basement elevation and are unconformably overlain by Paleozoic formations (Cant, 1988). After initial uplift, the PRA evolved in a passive continental margin setting during Paleozoic time (Stewart, 1972; Speed, 1994; Kent, 1994). The depositional succession from the Paleozoic to the Jurassic is dominated by carbonate rocks in the Arch region (Fig. 1-3). During Mesozoic time, the process of foreland basin development was superimposed on the evolution of the Arch. The foreland basin depositional succession from the Mid-Jurassic to the Paleocene is dominated by clastic rocks in the Arch region (Speed, 1994; Mossop and Shetsen, 1994). Both arch evolution and foreland basin development have profound influences on the

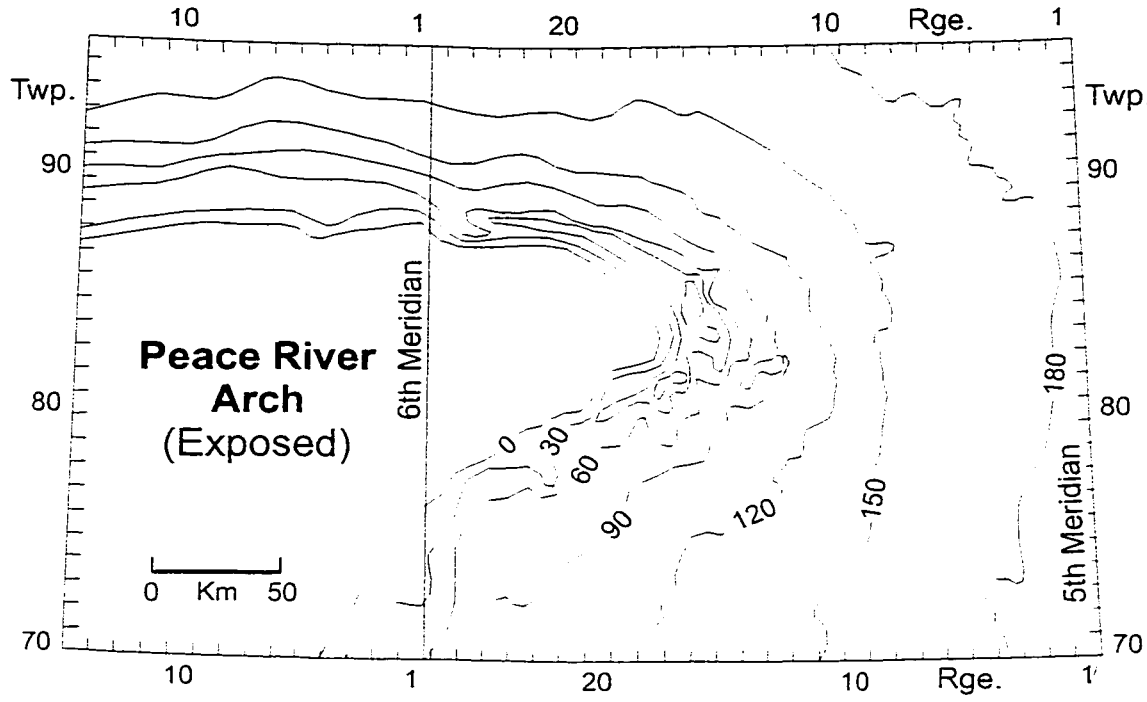

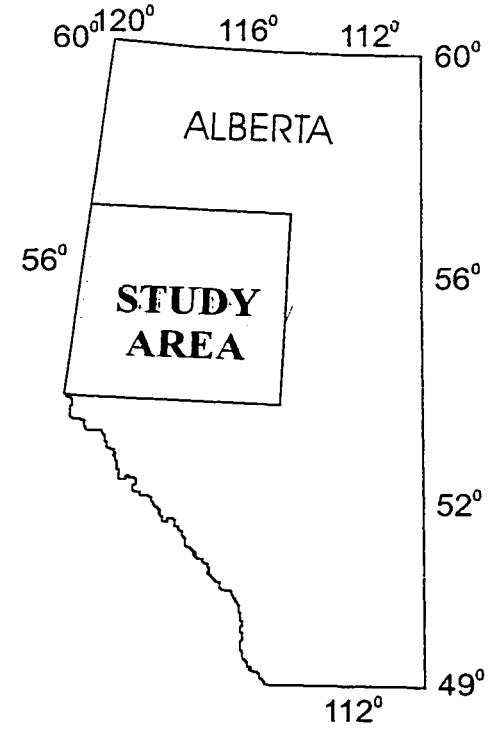

Figure 1-1. Peace River Arch in the Devonian Beaverhill Lake Group, modified from Keith (1990), showing details of the northern part of the study area. The appearance and extent of the Peace River Arch vary through time.

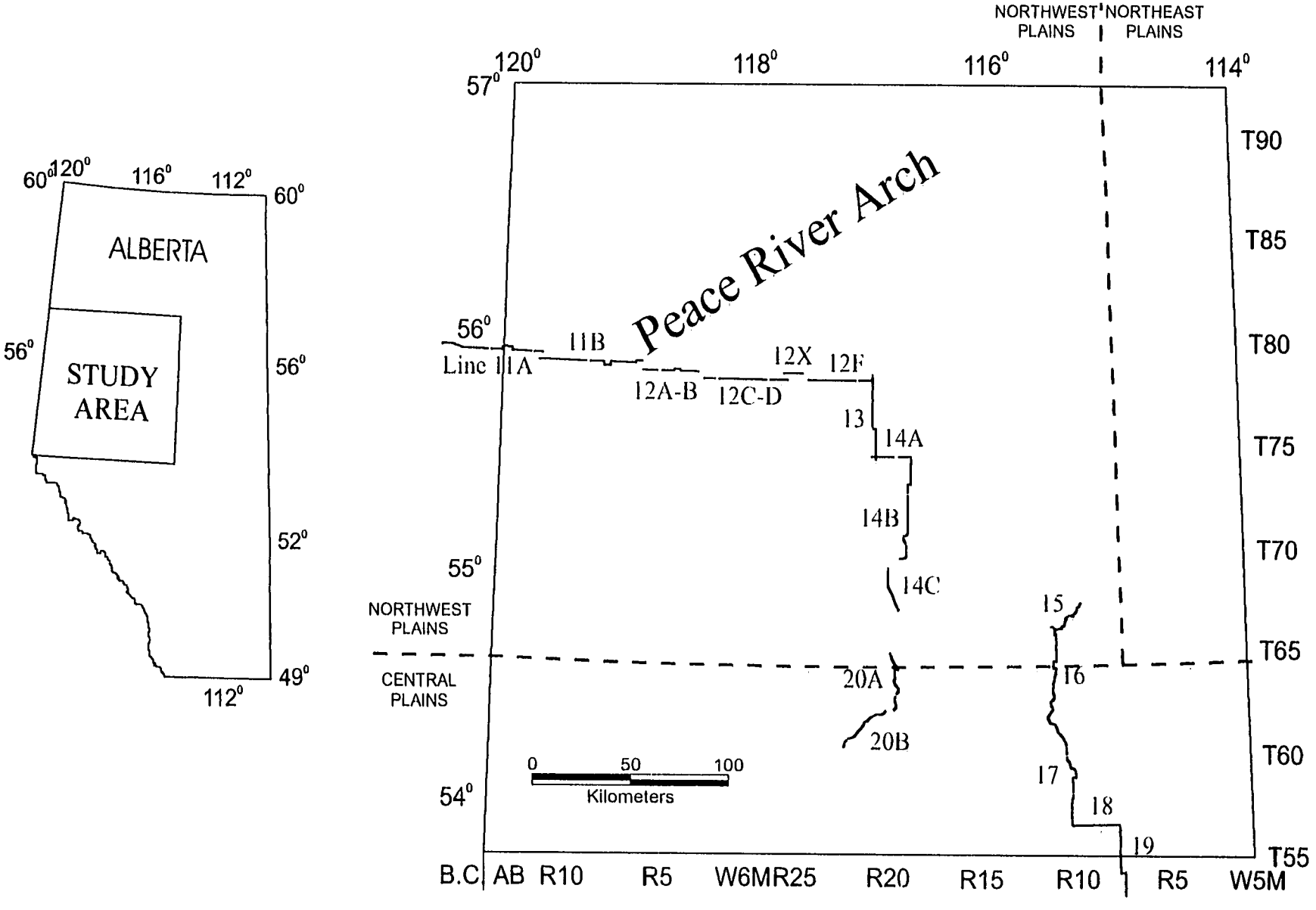

Figure 1-2. Study area, plain boundaries, and seismic survey lines. Dashed line, boundary of Alberta plains (Energy Resources Conservation Board of Alberta, 1992). Solid line, seismic line (Peace River Arch Industry Seismic Experiment of Lithoprobe, 1994).

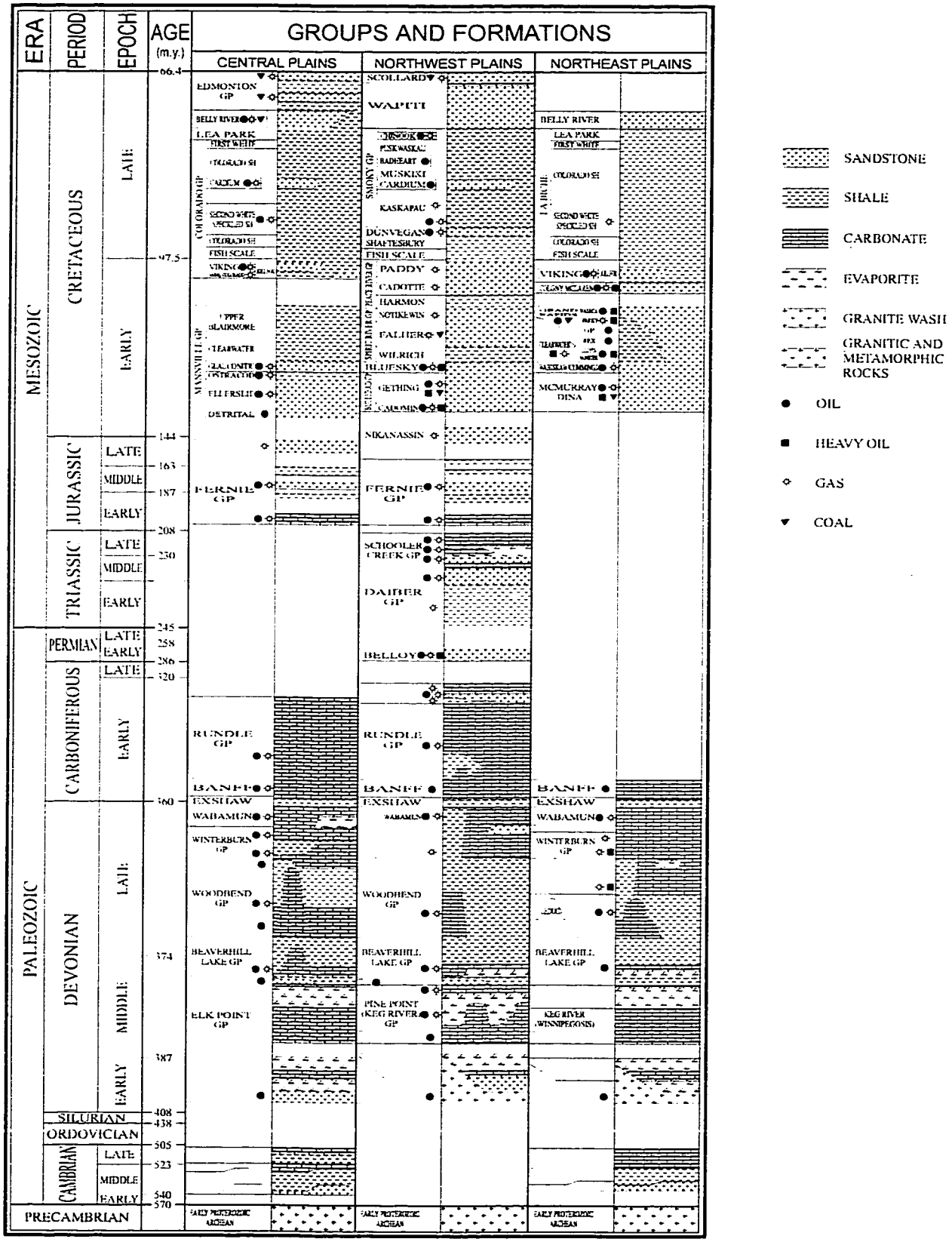

Figure 1-3. Stratigraphic table modified from AGAT Laboratories (1987) and the Energy Resources Conservation Board of Alberta (1992), showing formation variation and nomenclature comparison in the study area.

composition and distribution of reservoir rocks in the region (refer to Figs. 2-3, 2-5, 2-6; Leckie, 1984; Dix, 1990; Hart and Plint, 1993).

Since Imperial Spirit River No. 1 was drilled in 1949 (deMille, 1958), abundant oil and gas reserves have been found in the PRA region and have made the region one of the richest hydrocarbon provinces in the WCSB. Hydrocarbons are accumulated in various reservoirs throughout the Phanerozoic (Fig. 1-3). According to the SAMS database of the Geological Survey of Canada (Calgary), more than thirty-three thousand wells have been drilled in the study area. Many large oil and gas fields have been found and a huge amount of commercial hydrocarbon has been produced from the Arch region.

Figure 1-4 focuses on the Elmworth area in the south of the PRA, which is known as the largest gas accumulation in Canada. The Elmworth area contains 17 tcf of proved plus probable gas and 1 billion barrels of natural gas liquids (Marsters, 1984). The Elmworth field has 250 recognized pools of commercially recoverable gas in 23 distinct stratigraphic zones (Marsters, 1984). In fact, the entire rock section is saturated with gas.

Uplift and subsidence of the Arch and its profound control on regional sedimentation during Phanerozoic time have attracted academic research for many decades. One targeted research conference on the PRA was held in Calgary, Alberta, on December 10, 1957 (Scott, 1958). Two specific volumes: (1) Symposium on the Peace River Arch (Journal of the Alberta Society of Petroleum Geologists, V. 6, No. 3) and (2) Geology of the Peace River Arch (Bulletin of Canadian Petroleum Geology, Special Volume 38A) were published in 1958 and 1990, respectively.

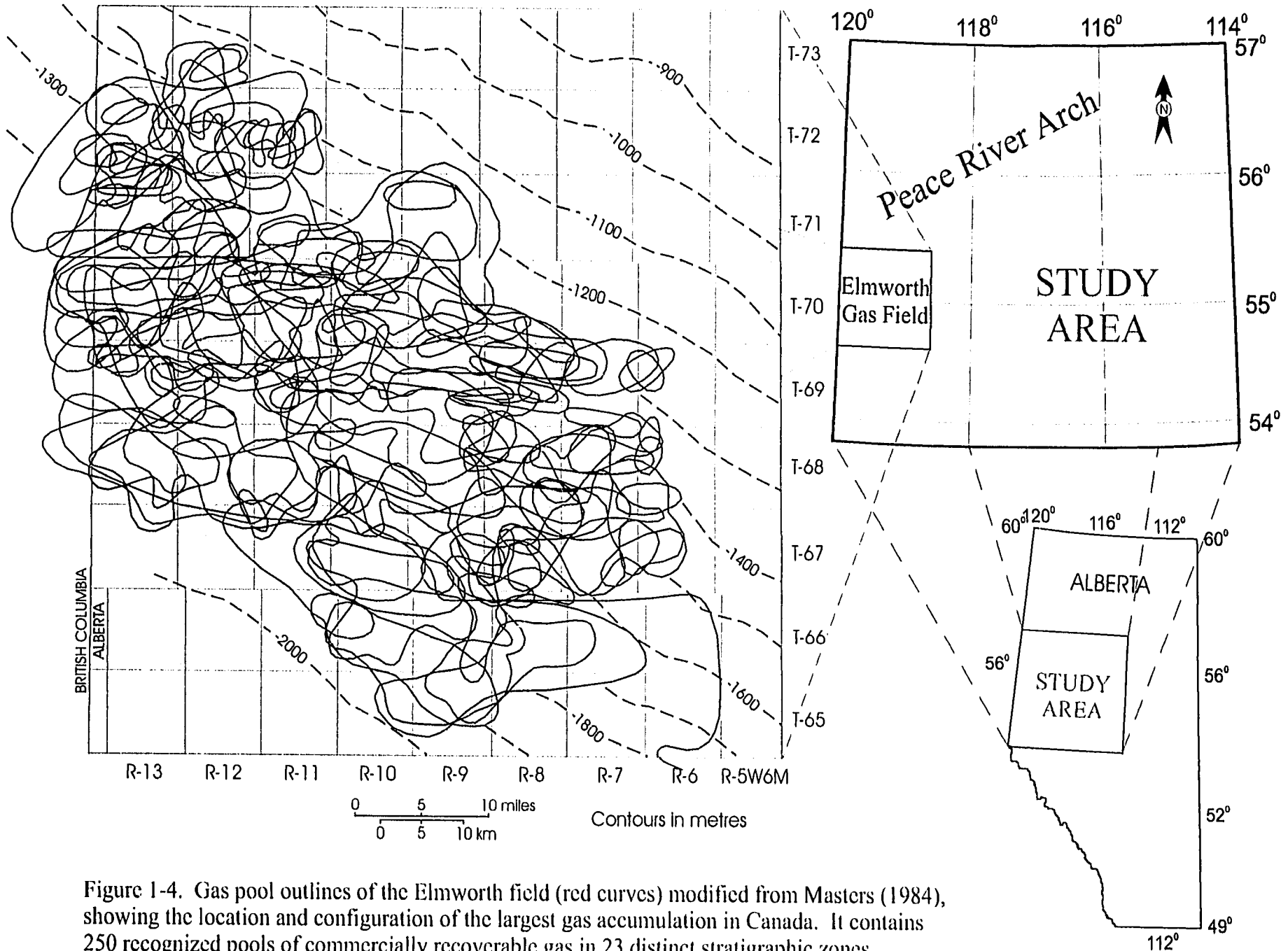

Figure 1-4. Gas pool outlines of the Elmworth field (red curves) modified from Masters (1984), showing the location and configuration of the largest gas accumulation in Canada. It contains 250 recognized pools of commercially recoverable gas in 23 distinct stratigraphic zones.

Since the initial 1957 conference, many mechanisms have been suggested for the origin of Arch uplift and subsidence (e.g. thermal extension and decay, Cant, 1988; failed continental margin rifting, O'Connell *et al.*, 1990; flexural-isostatic adjustment, Ross, 1990; Beaumont *et al.*, 1993). A correlation between foreland basin clastic wedges and the events of terrane accretion on the western boundary has been made by Cant and Stockmal (1989). Effect of basement reactivation on Cretaceous formations in the Arch area have been speculated by Smith *et al.* (1984), Hart and Plint (1990), Donaldson *et al.* (1998). Influences of sea level fluctuations in the Cretaceous Interior Seaway have been discussed by Bergman and Walker (1987), Pattison and Walker (1992), Posamentier *et al.* (1992), and Leckie and Reinson (1993).

In the past decade, more data were collected, including 1) database (Agis Associates Ltd., 1994) for the Geological Atlas of the WCSB (Mossop and Shetsen, 1994) and 2) Peace River Arch Industry Seismic Experiment (PRAISE) seismic profiles acquired by Canadian Lithoprobe across and adjacent to the PRA in northwestern Alberta and northeastern British Columbia in 1994 (Fig. 1-2). The digital database of the Geological Atlas contains abundant structural and stratigraphic data for the Phanerozoic in the WCSB and enables an integrated study of the stratigraphic development and modification in the PRA region. The obtained PRAISE regional seismic survey combines resolution of reservoir-scale and crustal-scale tectonic elements (Eaton *et al.*, 1997) and allows an investigation of both deep crust and shallow sedimentation.

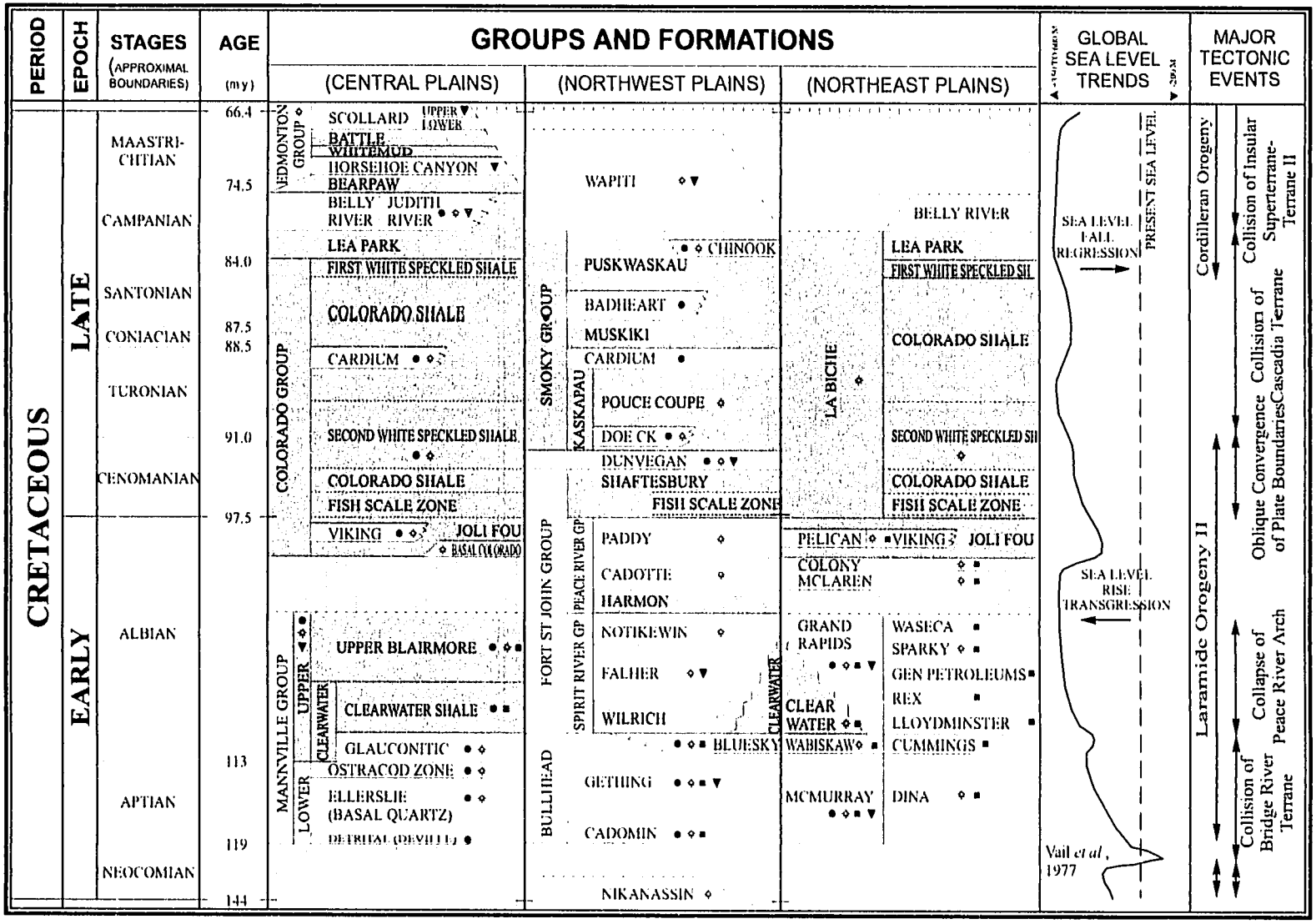

Figure 1-5. Stratigraphic table for the study area, modified from AGAT Laboratories (1987) and the Energy Resources Conservation Board of Alberta (1992), showing Cretaceous formations, nomenclature comparison, global sea level trends, and major tectonic events.

The nomenclature of the stratigraphic system varies between the plains of Alberta. A comparison of the nomenclature for the three plains is shown in Figure 1-5. The stratigraphic table in Figure 1-5 was modified from the Energy Resources Conservation Board of Alberta (ERCBA, 1992) and provides general information of formations' age, lithology and hydrocarbon occurrence for the Phanerozoic in the study area.

The ERCBA well log database provides the data source for the construction of formation distribution in the Alberta Basin. However, detailed correlation of the Cretaceous successions for the PRA region is not available from the database. Inconsistencies in formation identifications (picks), stratigraphic nomenclature, and definitions, as well as data entry errors, exist in the database (Cant, 1988). To minimise the effects of these errors, Cant (1988) used large stratigraphic intervals to examine the regional structure and development of the PRA during the Cretaceous. The Geological Atlas database (Agis Associates Ltd., 1994) is a reliable data source for Phanerozoic studies in the WCSB. However, detailed subdivisions of the Cretaceous in the Arch region are not available from the database.

Since the PRAISE seismic data were acquired in 1994, crustal reflection sheets and several tops in the Phanerozoic section in the PRA region have been interpreted (Ross and Eaton, 1996, 1997; Eaton *et al.*, 1997, 1999). However, detailed seismic calibration and interpretation for most of the Cretaceous formations in the Arch region have not been published. Debates (Ross, Eaton, Brent, Dietrich, personal communications, 1999, 2000) arose from seismic interpretations, including discussions surrounding location, orientation and timing of basement faults and crustal reflection sheets (Ross and Eaton, 1996, 1997; Eaton *et al.*, 1997, 1999; Hope *et al.*, 1999).

1-2. Thesis Objectives

This thesis has two objectives: (1) to document continuous and detailed changes in Cretaceous stratigraphy and depositional process and identify anomalies in Cretaceous formations on the southeast flank of the PRA, and (2) to examine basement features in an attempt to isolate possible influences from basement. Geophysical data including well log, seismic and aeromagnetic anomalies were employed in the study and various computer programs were used to assist with stratigraphic correlation, data processing, and isopach and structural mapping. Seven objectives were identified.

(1) To provide a detailed correlation of the successions from the base of the Cretaceous to the Upper Cretaceous Belly River/Lea Park transitional zone (Fig. 1-5) on the southeast flank of the PRA.

(2) To record stratigraphic anomalies, stratal changes, and stacking processes of the Cretaceous formations in the study area.

(3) To analyze the causes for shoreline re-orientation between the Lower Cretaceous Spirit River Group and the Upper Cretaceous Cardium Formation.

(4) To examine the factor(s) controlling the maximum southward transgression in the Spirit River Group (Cant, 1984; Leckie, 1986) and shoreline trends in the Cardium Formation (Plint and Hart, 1990).

(5) To identify areas of possible basement-sediment interaction.

(6) To time Arch uplift and subsidence and to examine possible relationships between

formation changes and Arch activity, basement fault reactivation, and tectonic events on the western continental margin.

(7) To examine factors that may have controlled arch uplift and subsidence, and formation development in the PRA region.

1-3. Thesis Methodology

This study uses a top down approach to examine potential sediment-basement interaction. Detailed stratigraphic correlations in the Cretaceous section were constructed. An area (Fig. 1-6) about 47,000 km^2 was selected within the rectangle bounded by the fifth and sixth meridians and Townships 56 and 74. The pilot area was selected on the southeast flank of the PRA because less of the Cretaceous section has been eroded.

Cretaceous lithology and well log signatures vary greatly in the PRA region. To minimize correlation mistakes, a three-dimensional correlation grid (Fig. 1-6) was constructed, consisting of six E-W cross sections, five N-S linking sections, and twelve additional infill cross sections, comprising 719 wells and covering every township in the pilot area. Seventy-three surfaces (Fig. 1-7) in the Cretaceous were identified and entered into an Excel spreadsheet database. Isopach and structural maps were constructed using Surfer and ArcView for each of the defined stratigraphic intervals.

The Geological Atlas database (Agis Associates Ltd., 1994) was used for constructing the formation maps from the Jurassic to the Cambrian. These maps were compared with each other and with Cretaceous maps to identify possible areas of basement influence. Important

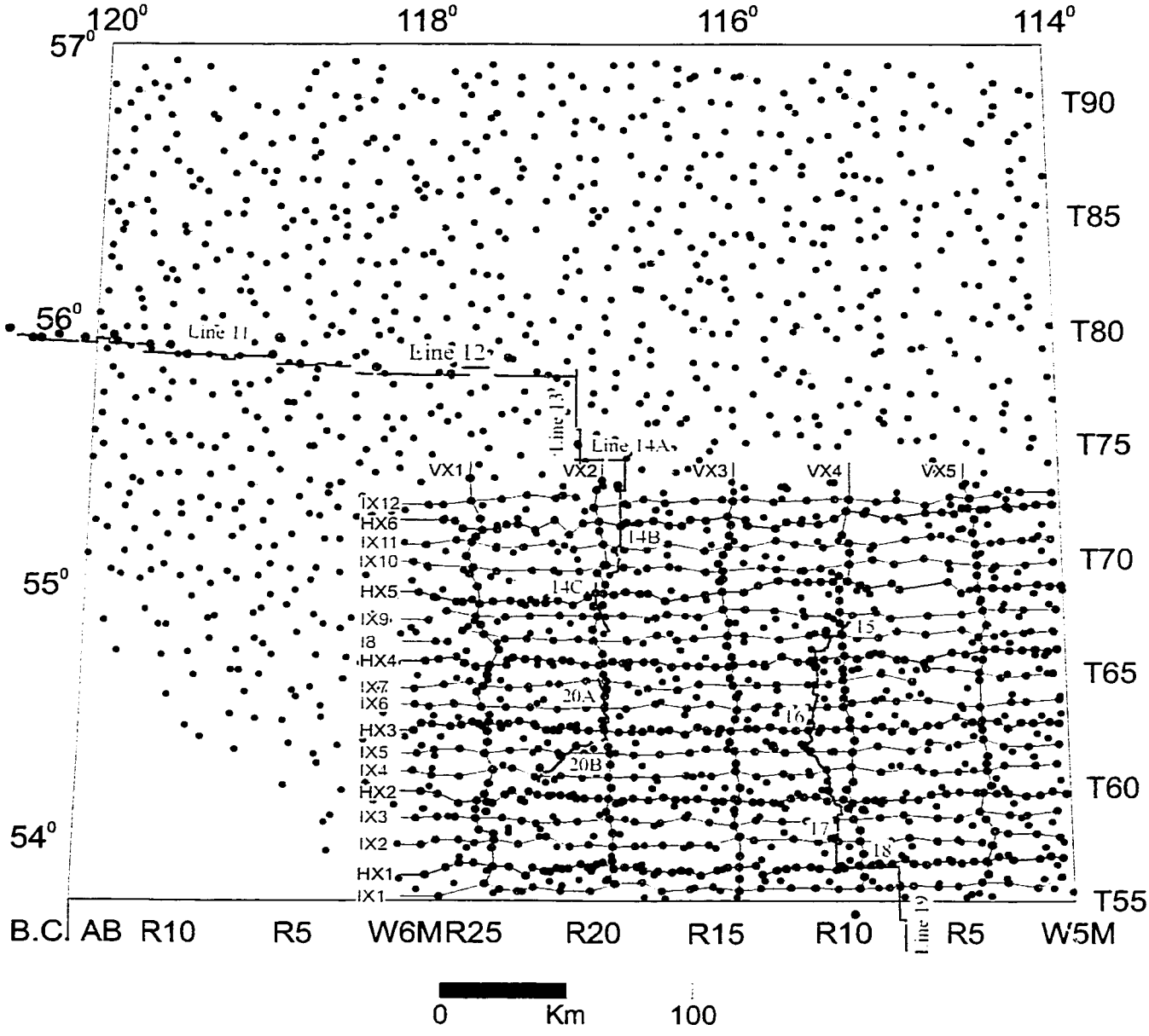

Original correlation grid of well log cross sections.
Infill well log cross section.
Seismic line with locations of synthetic seismograms.
Control point from the database for the Geological Atlas of the Western Canada Sedimentary Basin (Mossop and Shetsen, 1994).

Figure 1-6. Geophysical data and correlation grid employed in the study.

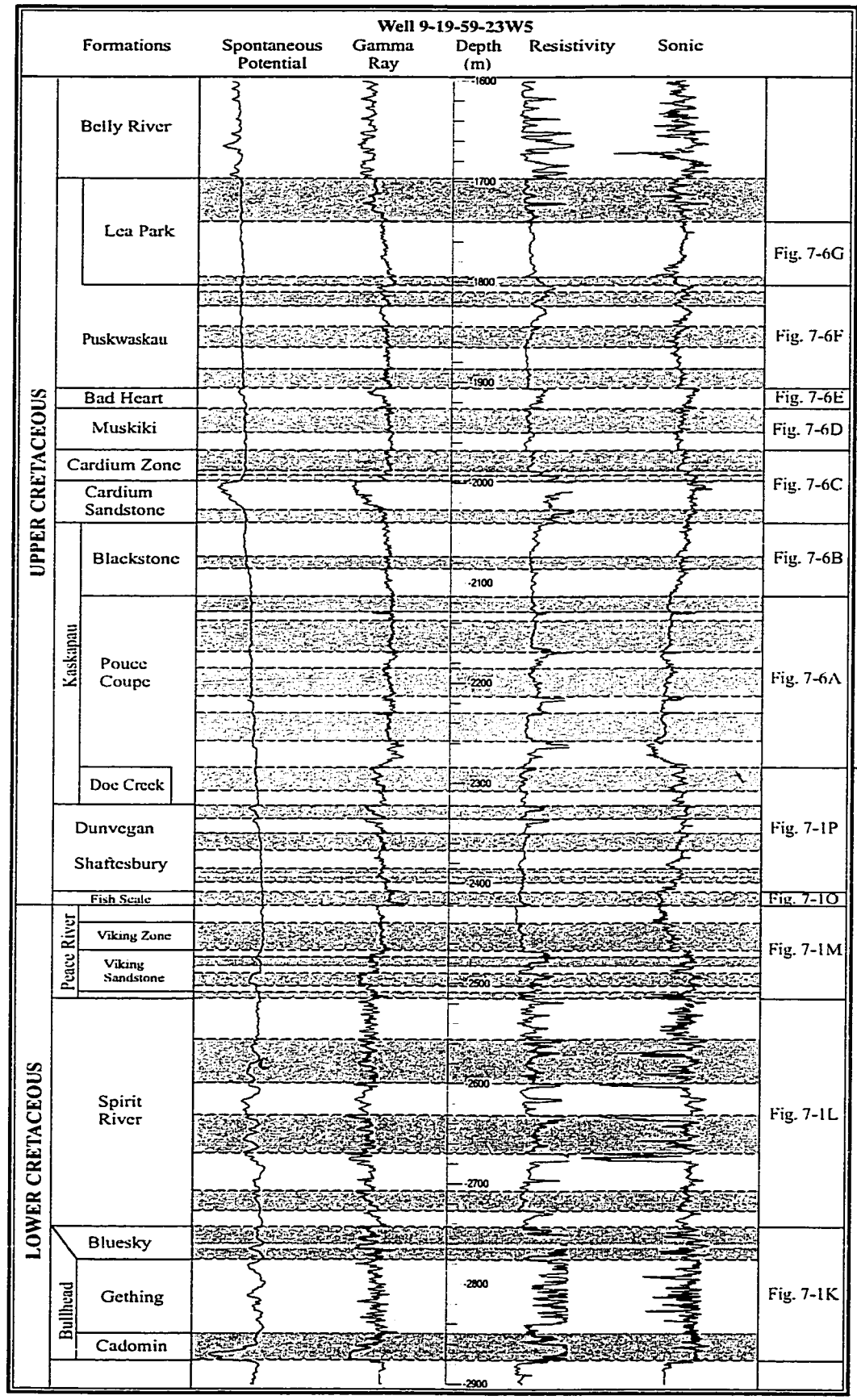

Figure 1-7. Type log showing correlated intervals in the Cretaceous. Some layers pinched out and are not shown in this well.

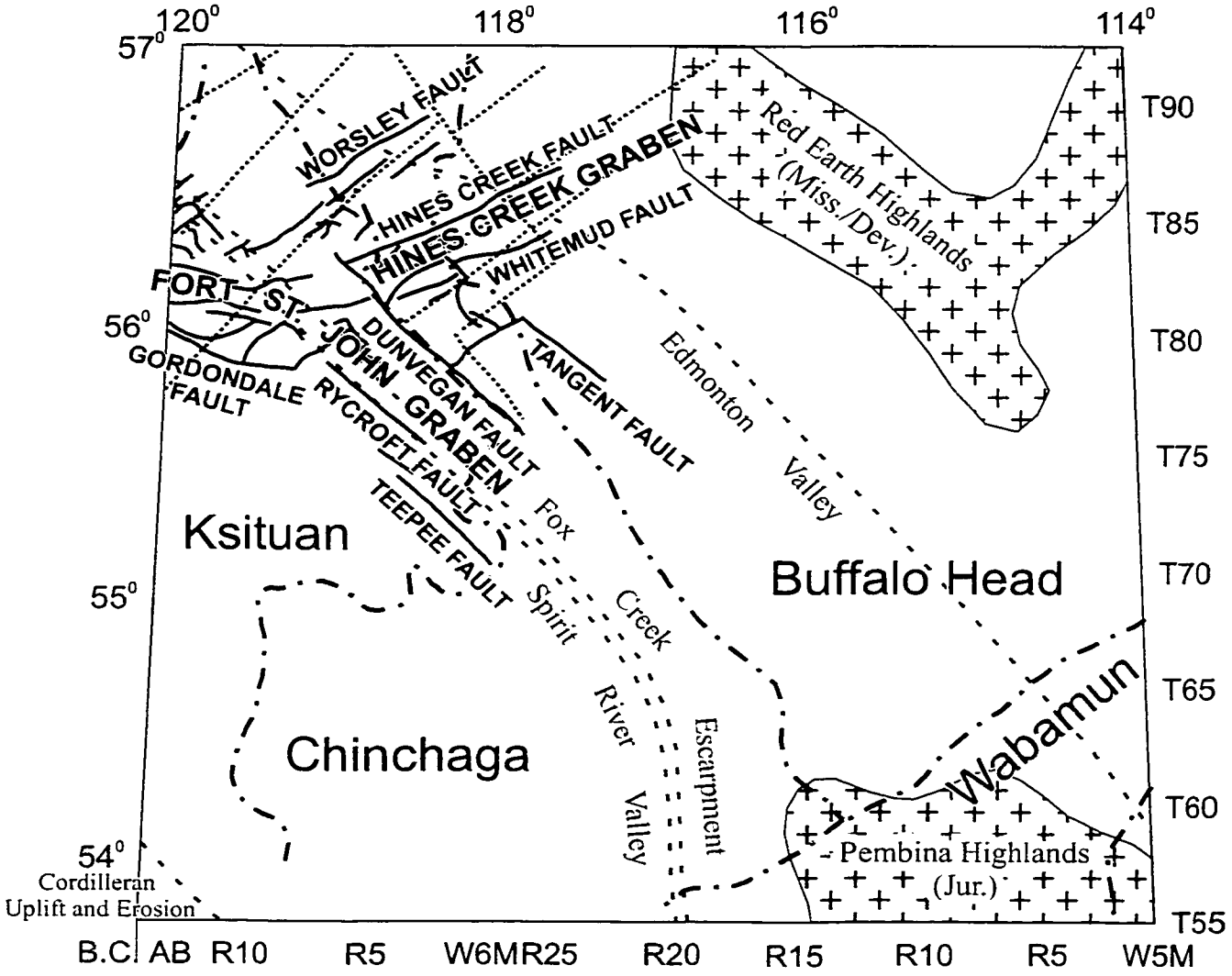

Precambrian domain boundary (Ross, 1990).
Inferred Precambrian fault/shear zone (Burwash *et al.*, 1994).
Carboniferous extensional fault (Richards *et al.*, 1994).
Other geological structures are from Leckie and Smith (1992).

Figure 1-8. Basement architecture and major structural components in the study area.

geological elements in the study area (Fig. 1-8), such as Precambrian domain boundaries (Ross *et al.*, 1989), inferred Precambrian fault/shear zones (Burwash *et al.*, 1994), Carboniferous extensional faults (Richards *et al.*, 1994), and other geological components (Leckie and Smith, 1992) were digitized, converted and overlain on the isopach maps with the help of MicroStation, WinDig, Fgraph, and ArcInfo.

As an important step in the research, the well log analysis was supplemented with seismic and aeromagnetic data to investigate both sedimentary and crustal features. Although seismic reflection methods are extensively used in this region by the oil and gas industry, published sections are rare. This study used PRAISE seismic data and interpreted lines 11 to 14 and 20, 15 to 19 (Fig. 1-6). Observed seismic data from the ten lines were calibrated with synthetic seismograms generated with velocities from sonic logs using GMAplus (Fig. 1-9). The calibrated seismic data were interpreted using GeoQuest IESX, Graphic Workshop, and CorelDRAW.

Aeromagnetic data were also used in this study. Computer programs ArcView, ArcInfo and Surfer were used in data conversion and display. The Transects' seismic and aeromagnetic data were supplemented to (1) identify basement faults, (2) delineate lateral extent of unconformities, (3) define sequence configurations, (4) search for terminal reflectors of tracts, (5) constrain time of displacements, (6) explore characteristics of crustal sheets, and (7) investigate interactions between Phanerozoic formations and crustal fabrics.

Possible influences on deposition were analyzed and include not only tectonic factors but also the effects of eustatic change. For example, the onlap seismic reflectors at the bottom of the Middle Cambrian and toplap/truncation reflectors at top of the Upper Cambrian (Fig. 1-

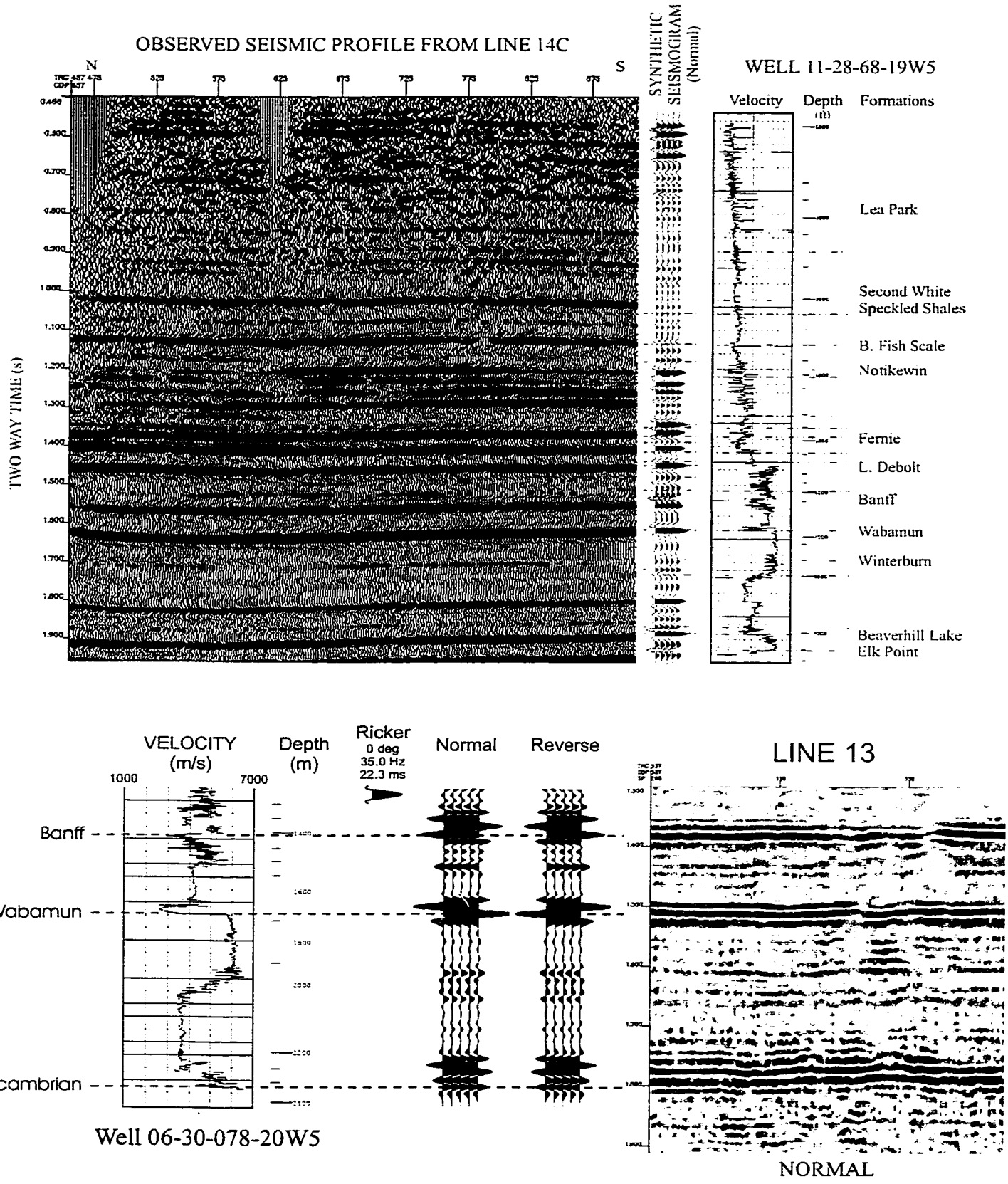

Figure 1-9. Calibration of observed seismic data with syntheticseismograms generated from velocity data of sonic logs. Wavelet, Ricker (0 deg, 35 Hz, 22.3 ms). Line location, refer to Fig. 1-2.

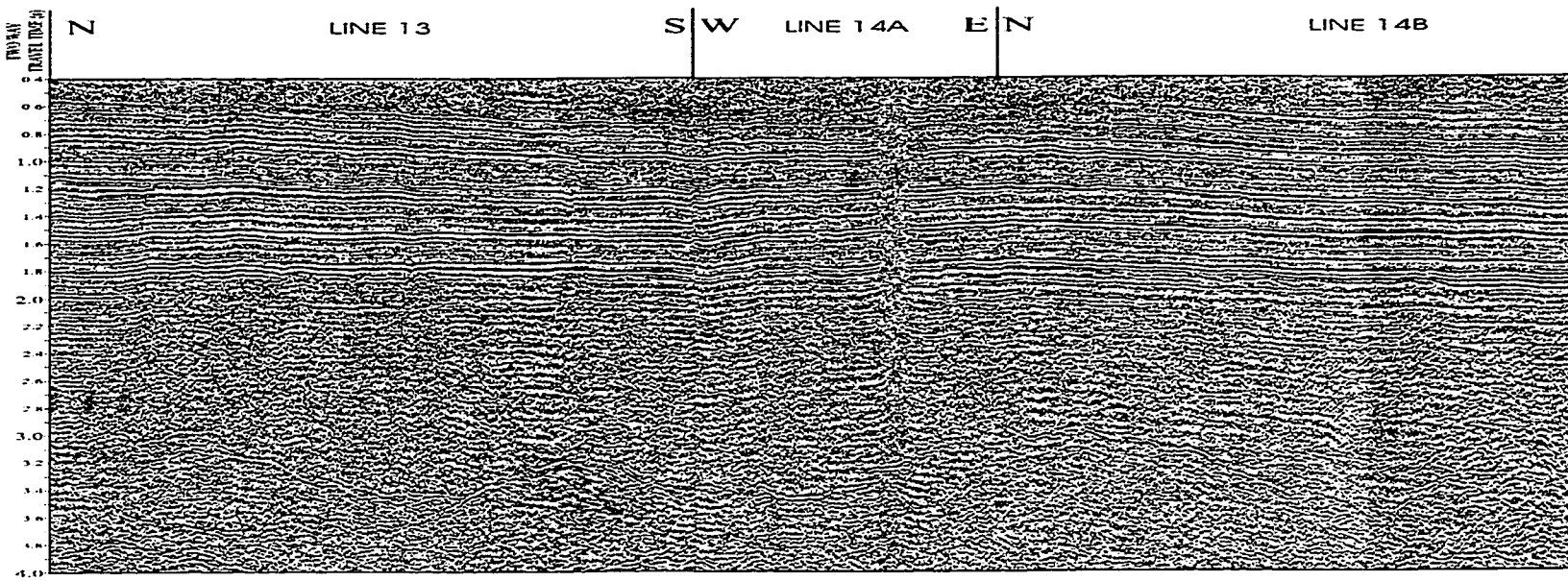

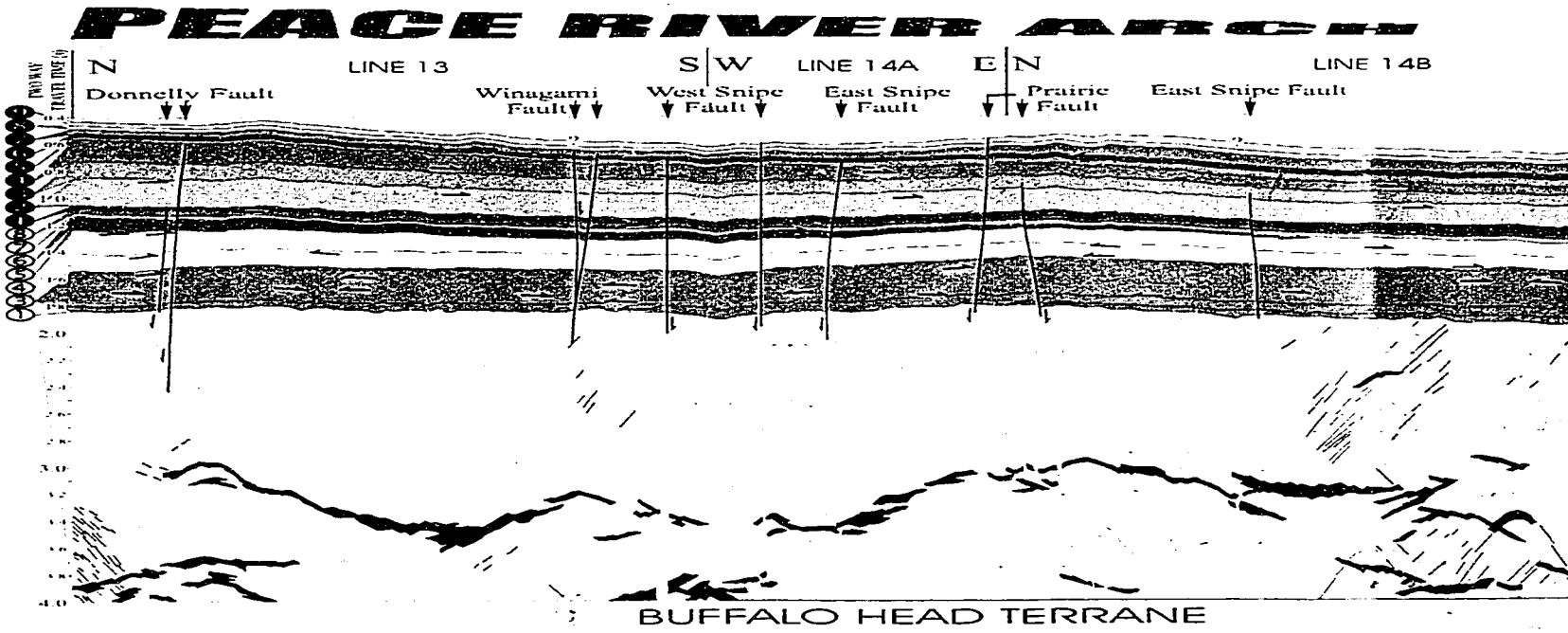

① Precambrian
② Cambrian
③ Devonian
④ Mississippian
⑤ U. Debolt, Mississippian
⑥ Permian
⑦ Triassic
⑧ Jurassic
⑨ Inferred Tertiary
❶ Lower Mannville Group
❷ Upper Mannville Group
❸ Peace River Group
❹ Shaftesbury and Dunvegan formations
❺ Middle Second White Speckled Shale
❻ Upper Second White Speckled Shale
❼ Black Stone and Cardium formations
❽ Bad Heart and upmost Colorado
❾ Lea Park Formation
❿ Belly
⓫ Inferre
Ⓐ Top of
Ⓑ Top of
Ⓒ Top of
Ⓓ Top of

Figure 1-10. Composite migrated seismic sections (vertical exag
of the Peace River Arch. Upper, un-interpreted section; lower, i

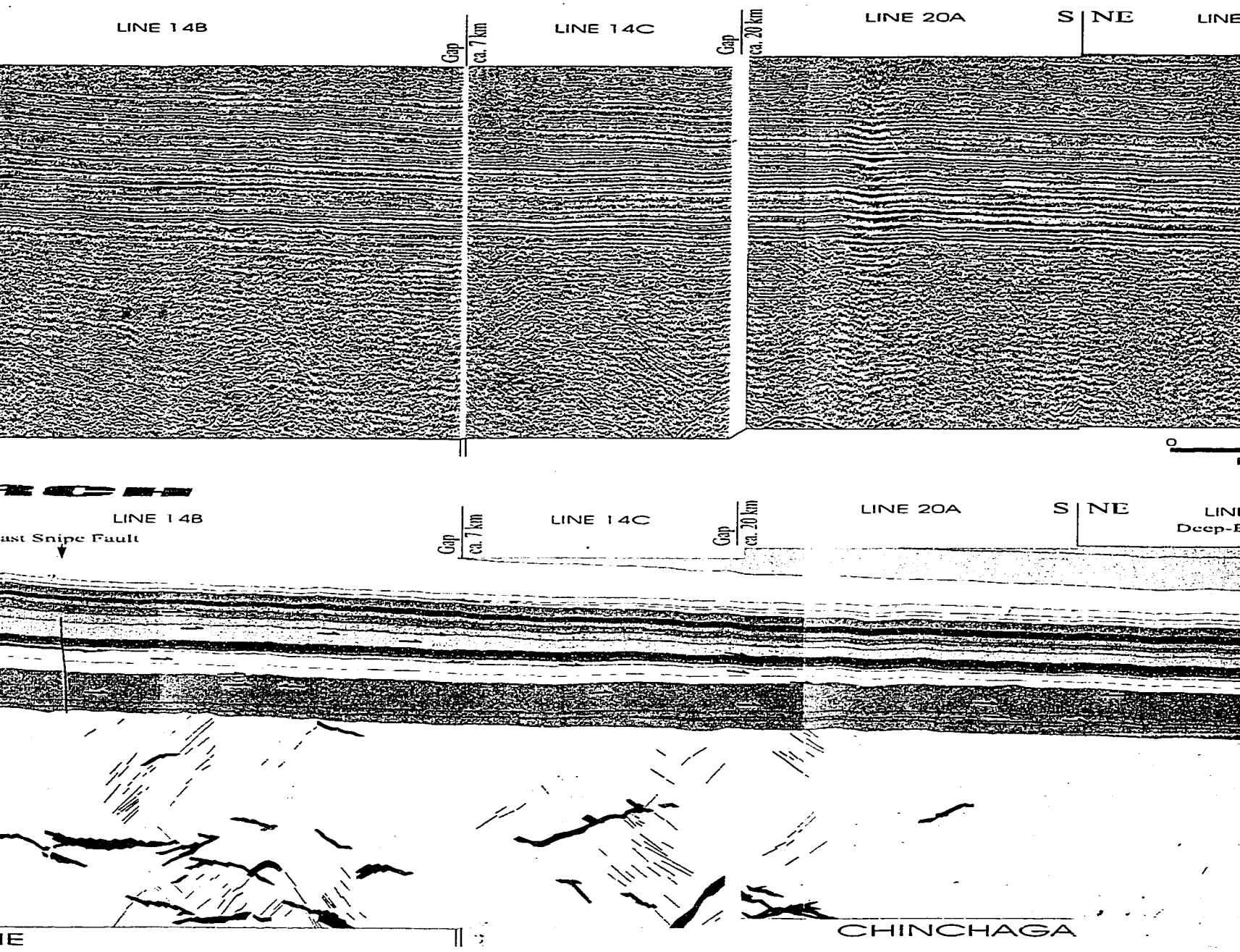

nvegan formations
ite Speckled Shale
c Speckled Shale
rdium formations
ost Colorado

Belly River Group
Inferred Edmonton Group
Top of Middle Cambrian
Top of Upper Cambrian
Top of Beaver Hill Lake Group
Top of Wabamun Group

Top of Banff Formation
Cretaceous bottom
Base of Fish Scale
2nd White Speckled Shale marker
Top of Cardium Formation
Top of Bad Heart Formation

Inferred Cretaceous top
Onlap/downlap of reflecti
Toplap/truncation of reflec
Fault with main direction
Crustal reflection sequenc
Strain in crustal rocks

seismic sections (vertical exaggeration, 2 times), showing structures of the south flank
n-interpreted section; lower, interpreted section. Line location, refer to Fig. 1-2.

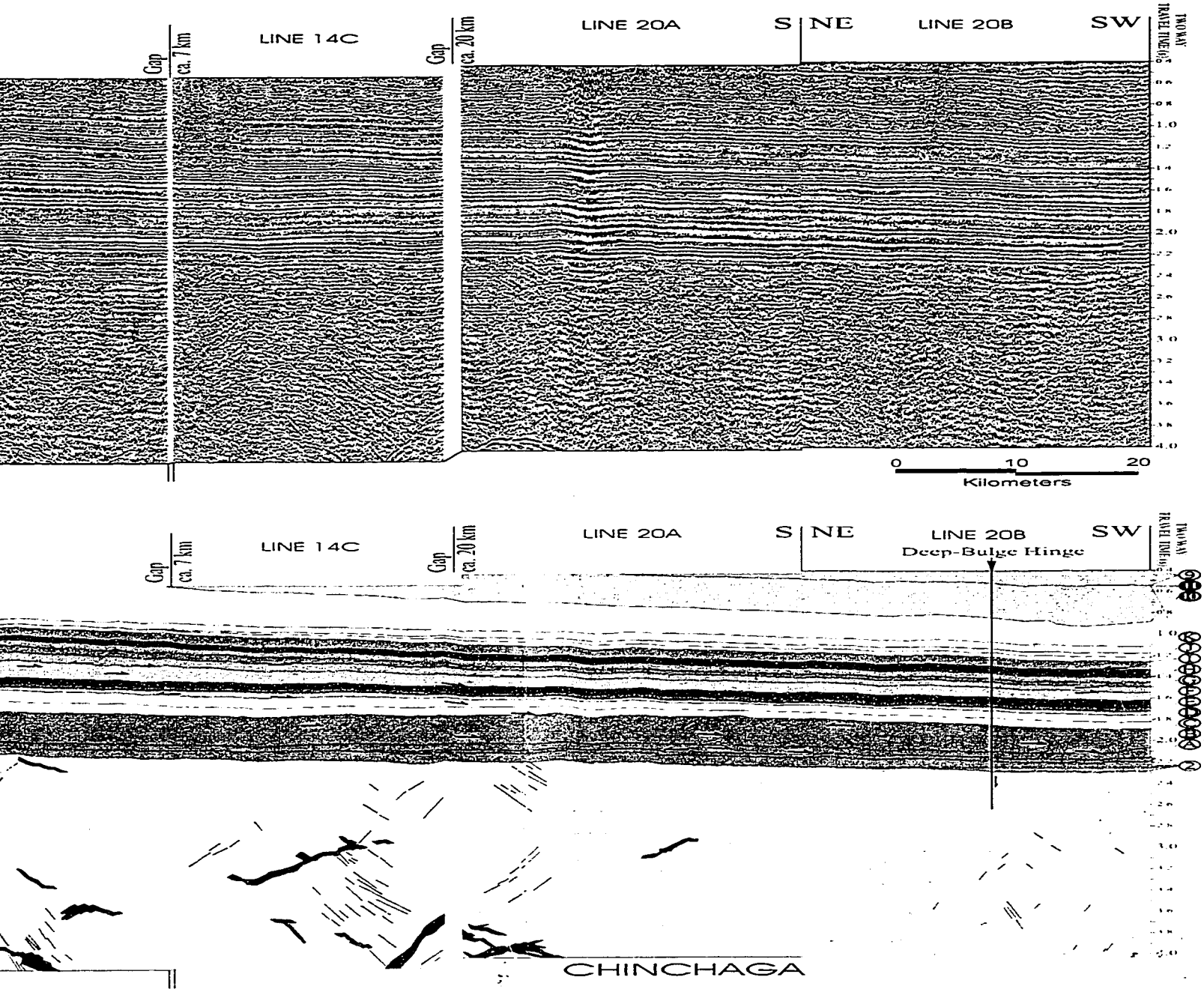

River Group
ed Edmonton Group
f Middle Cambrian
f Upper Cambrian
f Beaver Hill Lake Group
f Wabamun Group

Top of Banff Formation
Cretaceous bottom
Base of Fish Scale
2nd White Speckled Shale marker
Top of Cardium Formation
Top of Bad Heart Formation

Inferred Cretaceous top
Onlap/downlap of reflection
Toplap/truncation of reflection
Fault with main direction of dislocation
Crustal reflection sequence
Strain in crustal rocks

ggeration, 2 times), showing structures of the south flank
interpreted section. Line location, refer to Fig. 1-2.

10) on the southeast flank of the PRA do not necessarily mean the Arch subsided in Middle Cambrian time and rose again in Late Cambrian time. Regional tectonics, basement configuration and global sea level change suggest that the transgression of the Middle Cambrian toward the PRA may have been related to the rapid rise of global sea level during Middle Cambrian time. The regression/truncation of the Upper Cambrian may have been caused by broad regional uplift and erosion during Early Paleozoic time.

1-4. Thesis Layout

The thesis is composed of six chapters. As a preludial chapter, Chapter 1 introduces thesis objectives, methodology, and layout in four sections. Chapter 2 focuses on the regional geology of the PRA area and discusses basement architecture, regional tectonic development, the PRA, faulting systems, and links between western continental margin tectonism and foreland basin development. Chapter 3 reviews previous studies and existing problems, including the timing and origin of PRA uplift and subsidence as well as control mechanisms on Cretaceous stratal re-orientations. Based on detailed stratigraphic correlation and mapping, Chapter 4 illustrates the Cretaceous formations, including the diachronism of many traditional boundaries, major stratal re-orientations, and stacking processes of sediments. The chapter also discusses possible control mechanisms on the stratigraphic variations. Supported by the Geological Atlas

database (Agis Associates Ltd., 1994) and Lithoprobe PRAISE seismic survey, Chapter 5 threads seismic, isopach, and eustatic information and describes the PRA evolution by illustrating key features through many cross sections, isopach and structural maps. As an

epilogue. Chapter 6 summarizes key points from the study, briefly discusses the significance of this stratigraphic and structural study to petroleum exploration, discusses Cretaceous reservoirs in the study area, and suggests fields for future work.

CHAPTER 2: REGIONAL GEOLOGY

2-1. Basement Architecture and Regional Tectonic Development

Sm-Nd isotopic data support the interpretation almost all of the WCSB is underlain by sialic crust that was differentiated from the mantle during the Archean, with linear belts to which a significant juvenile Proterozoic component has been added (Burwash *et al.*, 1994). The crystalline basement in the study area is composed primarily of four Early Proterozoic domains: Buffalo Head, Chinchaga, Wabamun, and Ksituan (Fig. 1-8). These domains were identified on the basis of aeromagnetic and gravity anomaly data, and U-Pb zircon and monazite geochronology (Ross *et al.*, 1989). The Buffalo Head and Wabamun were identified as accreted terranes (2.4-2.0 Ga); the Chinchaga as a magnetic low (2.4-2.0 Ga); and the Ksituan as a magmatic arc (2.0-1.8 Ga, Hoffman, 1989; Ross *et al.*, 1989; Burwash *et al.*, 1994). The assemblage of these domains is by collision and accretion onto the western margin of the Canadian Shield in 2.0- 1.9 Ga (Ross, 1990).

Extending cratonward from the Canadian Cordillera (Fig. 2-1), the PRA initiated in the western margin of North America. Since North America was separated from Rodinia by multi-phase rifting in the Late Precambrian (about 0.7 Ga), passive margin sedimentation occurred on all edges of Laurentia (Stewart, 1972; Speed, 1994; Kent, 1994). Divergent boundaries drifted away and a passive margin developed in the west over various periods into the Paleozoic. In the Canadian portion, the passive margin from the end-Proterozoic breakup of Rodinia existed until Jurassic time and carbonate rocks are dominant in the section from the Paleozoic to the Jurassic. Since Jurassic time, collisional events transformed the western

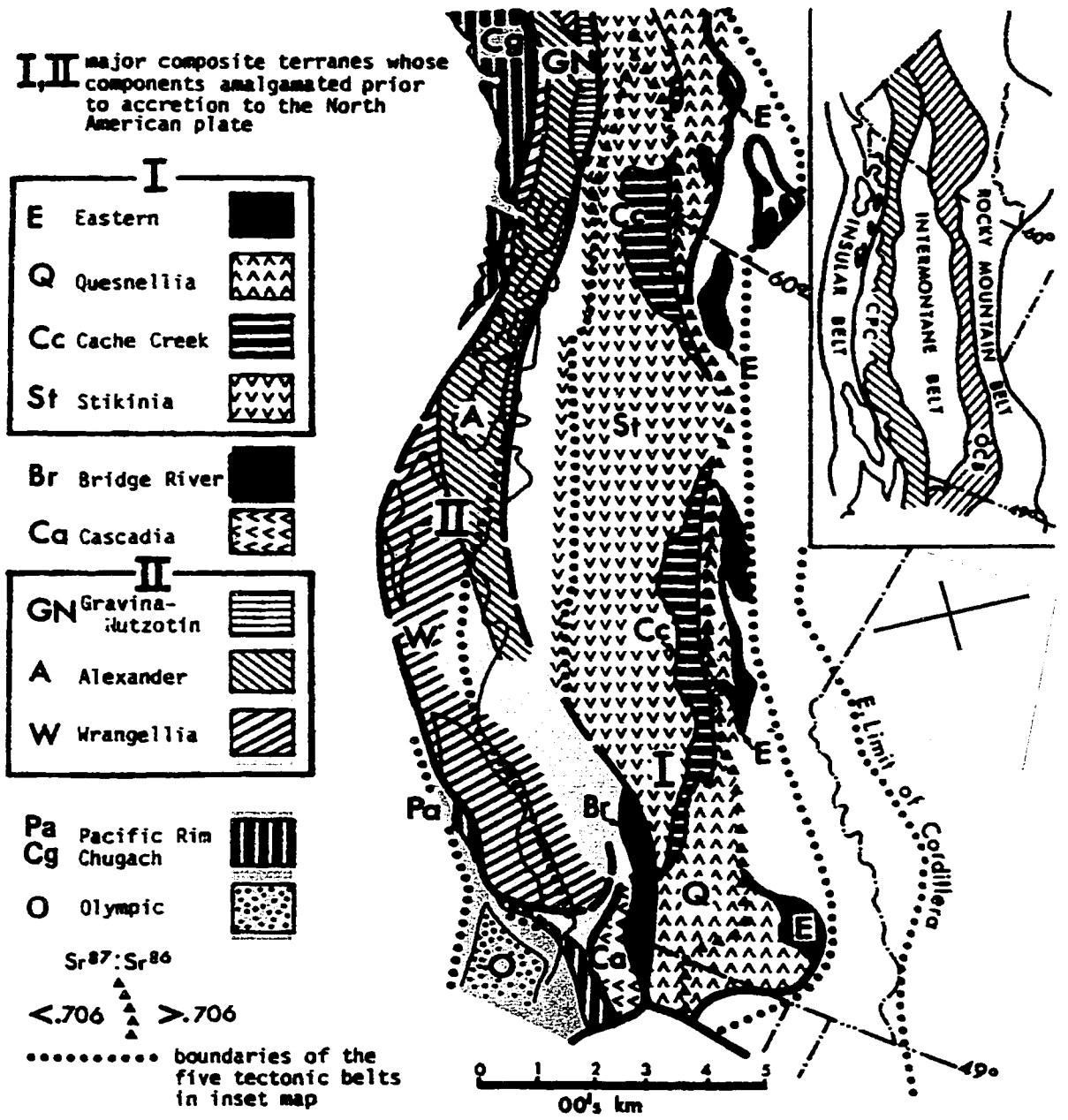

Figure 2-1. Physiographic belts in Canadian Cordillera, modified from Monger *et al.* (1982). Green box, study area of the thesis. Red cross, location of the Peace River Arch.

continental margin into an active margin and clastic rocks are dominant in the foreland basin section from the mid-Jurassic to the Paleocene in the WCSB (Speed, 1994; Mossop and Shetsen, 1994).

Beginning in the mid-Jurassic, the western margin of North America was subjected to at least two major episodes of compressional tectonism, as a result of collision with large oceanic terranes. As a consequence of these collisions, sedimentary rocks that were deposited outboard of the ancient margin were compressed and displaced eastward over the continental margin. In the southwest of the PRA region, platformal rocks were thrusted and folded to form a portion of the Canadian Rocky Mountains and the Rocky Mountain Foothills. Emplacement of the imbricate thrust slices, progressively from west to east, produced thickening of the crust and downwarp of the foreland, forming an eastward-migrating foredeep that trapped clastic detritus shed from the developing mountains (Mossop and Shetsen, 1994).

The foreland basin is divided into five zones (Kauffman and Caldwell, 1993). They are, from west to east, western foredeep, forebulge, west-median trough, east median hinge, and eastern platform. These zones rose or subsided differentially in response to deformational events in the Cordillera.

The study area occupies the three western zones (Fig. 2-2). According to Kauffman and Caldwell (1993), the western foredeep, a narrow zone bordering the tectonic front, had the highest subsidence and sedimentation rates and received coarse-grained, synorogenic, terrigenous clastic sediments as coastal-plain to shallow-water marine facies. The forebulge, separating the foredeep from the broad eastern parts of the basin, was a discontinuous set of

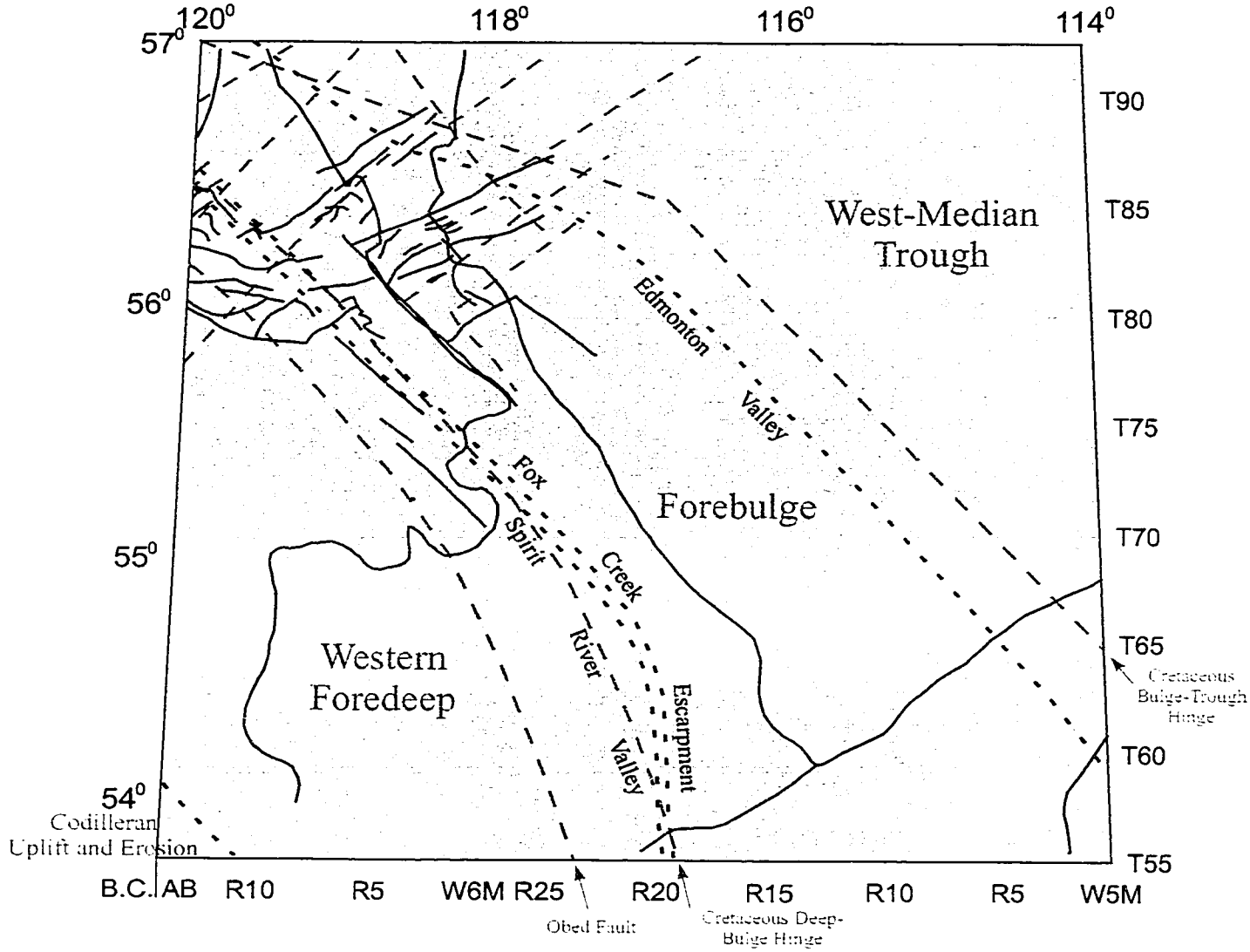

Precambrian domain boundary (Ross, 1990).
Inferred Precambrian fault/shear zone (Burwash *et al.*, 1994).
Carboniferous extensional fault (Richards *et al.*, 1994).
Discontinuity in the foreland basin (Leckie and Smith, 1992).

Figure 2-2. Tectonic belts of foreland basin within the study area.

arches parallel to the loading axis 50-200 km east of the foredeep. Importantly, the forebulge overlies reactivated Precambrian basement blocks and Lower Paleozoic supra-crustal rocks (Kauffman and Caldwell, 1993). The broad west-median trough, incorporating the axis of the foreland basin, was characterized by moderate levels of fine-grained sedimentation and episodic, strong, rapid subsidence (Kauffman and Caldwell, 1993).

In the study area, the three western zones were divided by the Deep-Bulge and the Bulge-Trough hinges in the Earliest Cretaceous (Fig. 2-3). These hinges are long-acting basement faults (refer to Figs. 2-7, 2-8). In the Peace River Arch region, reverse movement on basement faults is prevalent (refer to Fig 2-8; unpublished data of this thesis; Staniland, personal communication, 1998). These hinges are interchangeable with basement faults. Motion on basement faults over long periods of time and abrupt stratal changes have been observed in this study. Although the migration of the forebulge and other elongate foreland zones has been discussed by some flexural models (Quinlan and Beaumont, 1984; Beaumont *et al.*, 1993; Catuneanu *et al.*, 1997), no long-acting basement faults and abrupt stratal changes have been defined/considered in existing flexural models.

Figure 2-2 shows major faults and boundaries defined by previous studies and this thesis. Several NW-SE trending faults have played important roles in the development of the foreland zones. They are, from west to east, the Obed Fault, Deep-Bulge Hinge, Chinchaga-Buffalo Head Boundary, and Bulge-Trough Hinge. The Obed Fault is new to this study and the name is taken from the town close to the fault. The Obed Fault in part overlaps Fault 1 of Donaldson *et al.* (1998, Fig. 2-4). The earliest Cretaceous Deep-Bulge Hinge in part overlaps the Fox Creek Escarpment (Leckie and Smith, 1992) and Fault 2 of Donaldson *et al.* (1998).

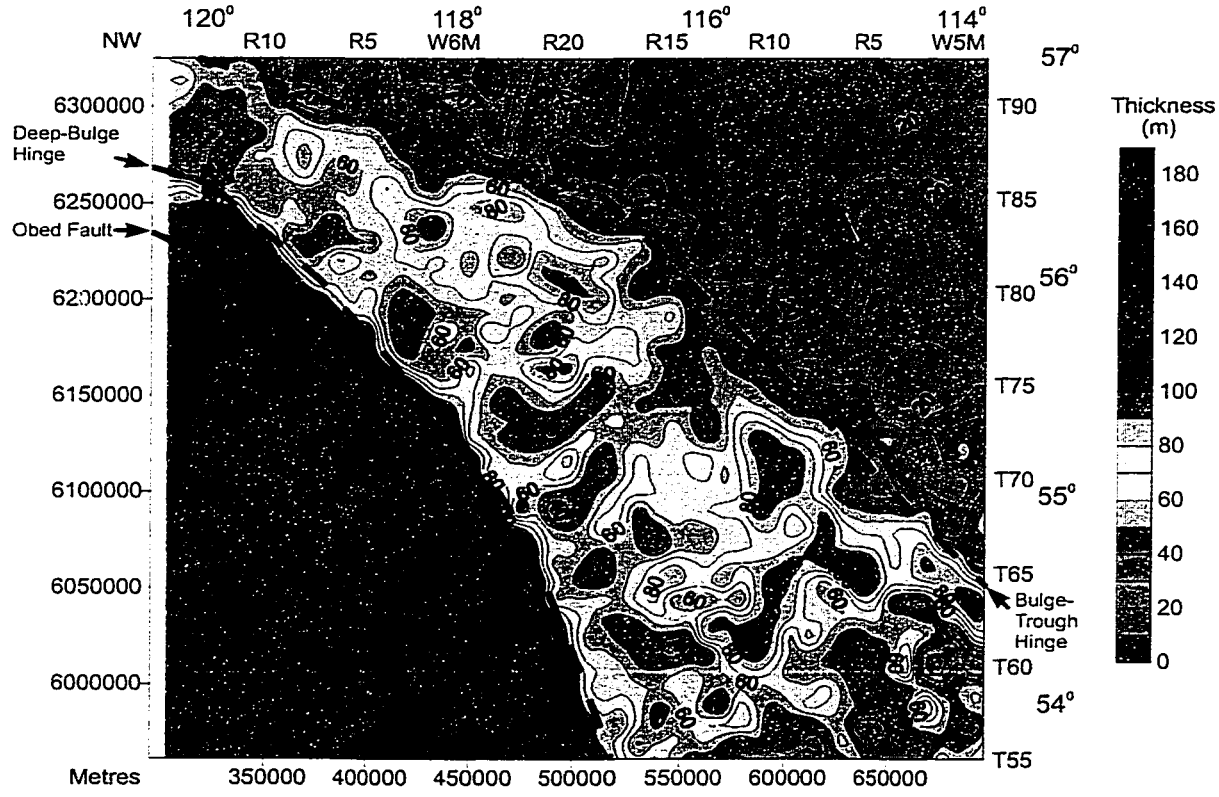

Figure 2-3. Isopach map of Cretaceous Lower Mannville, showing stratal trend and isopach pattern influenced by basement and boundary tectonics.

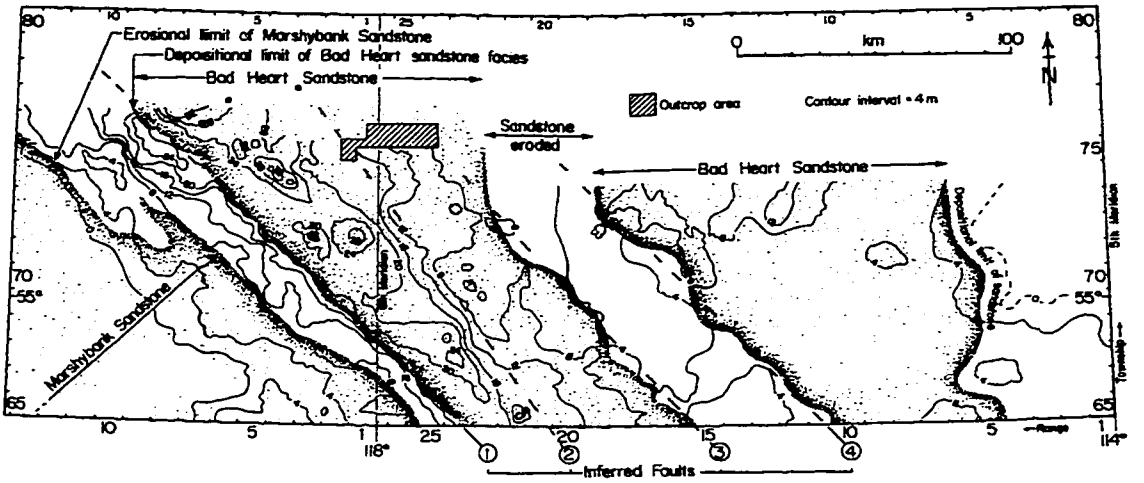

(A)

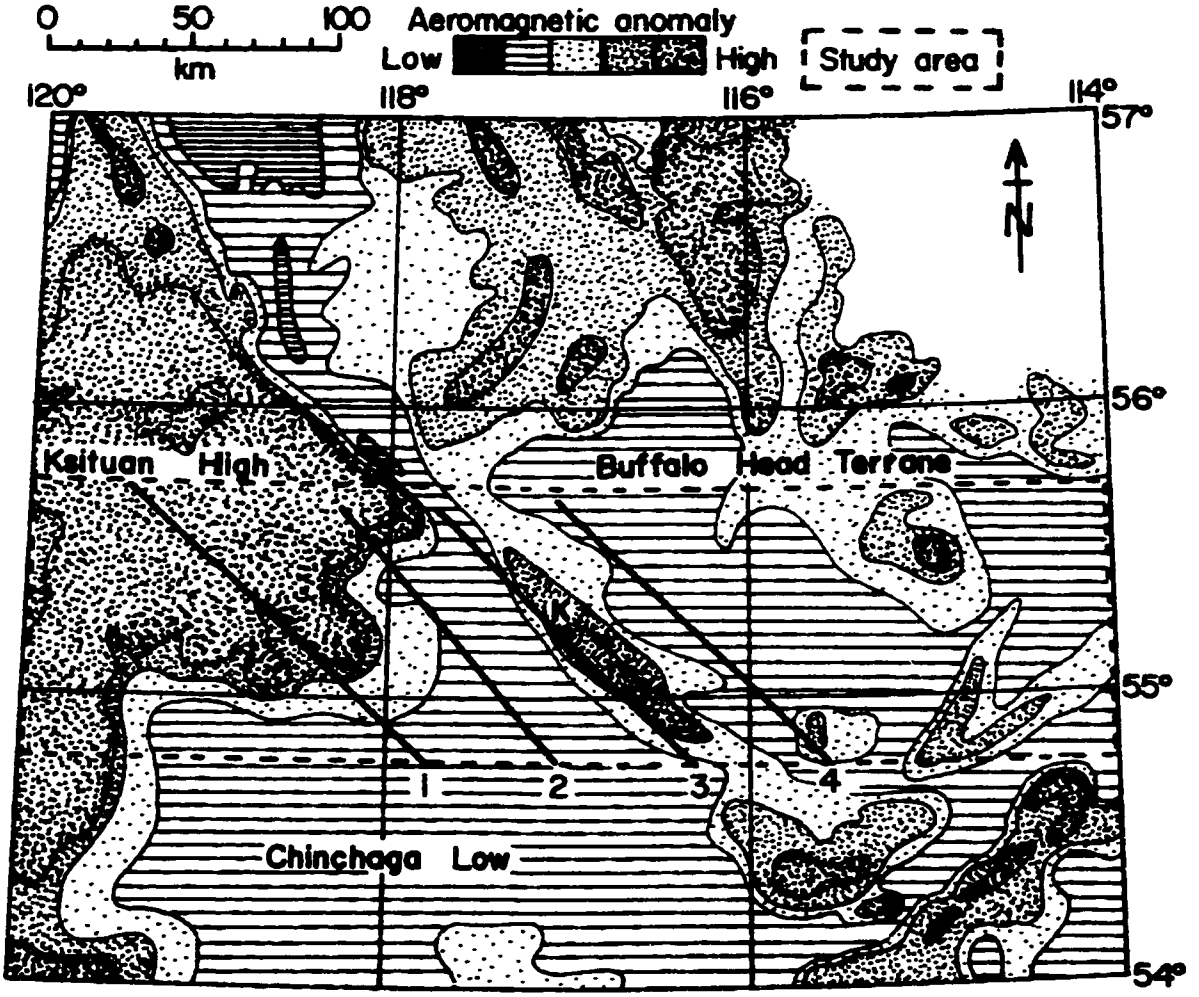

(B)

Figure 2-4. Diagrams from Donaldson *et al.* (1998). (A) Marshybank and Bad Heart sandstone distribution. (B) Correspondence between Upper Cretaceous faults and acromagnetic anomaly.

The Chinchaga-Buffalo Head Domain Boundary (Ross, 1990) in part overlaps Fault 3 of Donaldson *et al.* (1998). The earliest Cretaceous Bulge-Trough Hinge is parallel to the Edmonton Valley (Leckie and Smith, 1992). The deviation of the Edmonton Valley outline from the Bulge-Trough Hinge may have resulted from the mapping scale used by Leckie and Smith (1992).

2-2. Peace River Arch and Basement Faults

The PRA is a long-acting basement element in the WCSB (Fig. 1-1). During its history, the Arch has existed in three different forms: a Late Proterozoic to early Paleozoic Arch, a late Paleozoic to earliest Mesozoic Embayment, and as a deep basin component of a Mesozoic foreland basin (O'Connell, *et al.*, 1990). During times of collapse, the PRA was under a regional extensional regime with graben systems oriented parallel and normal to the arch axis (refer to Fig. 4-8; Cant, 1988; Richards *et al.*, 1994).

The Arch has had a significant influence on Phanerozoic sedimentation controlling the basement floor and overlying water body. For example, the collapse of the Arch during Early Cretaceous Albian time appears to have influenced the distribution of Upper Mannville Group sediments. The isopach pattern of the Upper Mannville Group (Fig. 2-5) is dish-shaped around top of the Arch. The formation strike is changeable but parallel to the trends of Arch axes (Cant, 1988; Chen and Bergman, 1997). The Upper Mannville Group is composed of several transgressive – regressive successions that thicken toward the Arch axis (Williams, 1958). The Falher Member is nonmarine south of Township 68 and marine over the Arch north of Township 75. Between Townships 68 and 75, a zone of transgression and regression

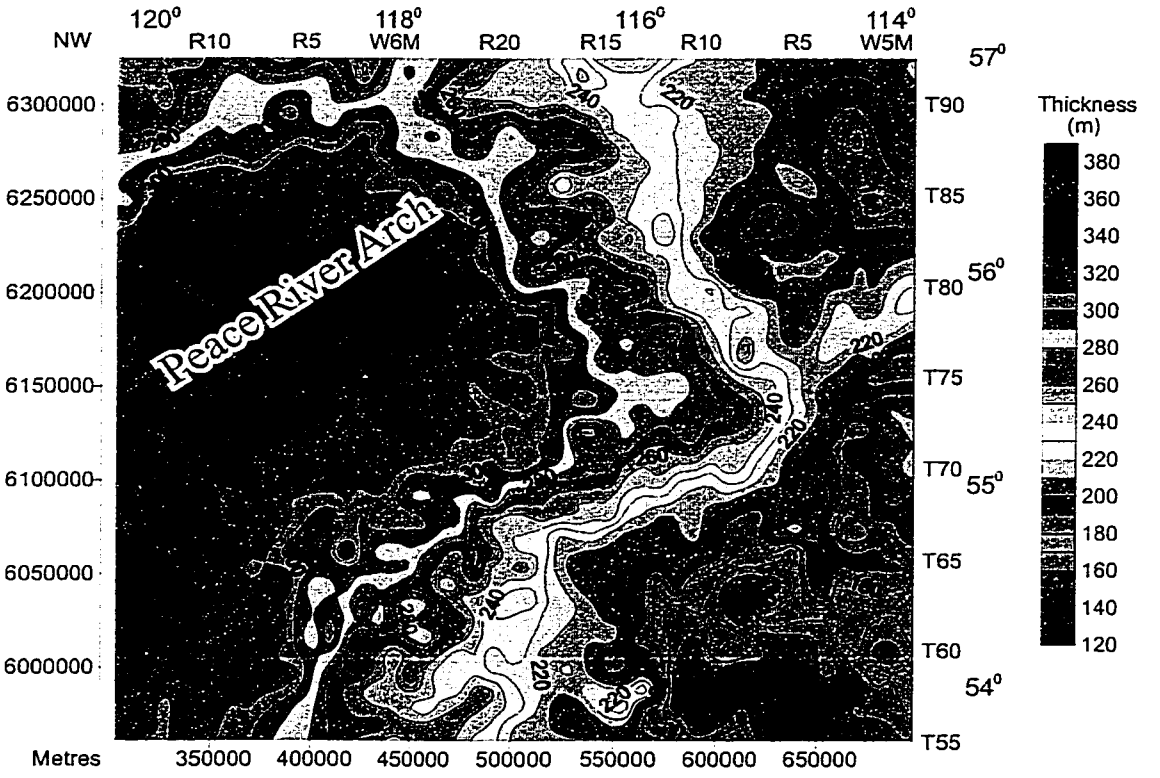

Figure 2-5. Isopach of Upper Mannville Group, Lower Cretaceous, showing the dish-shaped isopach pattern controlled by the collapse of the Peace River Arch.

occurs at the southern edge of the Arch (Cant, 1988). In the Moosebar and Gates formations, northeastern British Columbia, several of the Falher transgressive and regressive limits fall within a 30 to 40 km E-W trending zone that parallels the location and trend of the PRA (Leckie, 1984; Smith *et al.*, 1984).

Faults on the exposed shield in Saskatchewan and under the thin cover of eastern Alberta trend NEE-SWW (Garland and Bower, 1959), and are parallel to those of the Arch. The Arch structure overprinted the preexisting Precambrian basement structure, and several Archean to Early Proterozoic fault zones may have been reactivated throughout the Phanerozoic. Many of the faults associated with Arch block faulting can be traced into the overlying Devonian, Mississippian, and Pennsylvanian sediments (O'Connell *et al.*, 1990). Horsts and grabens orientate parallel to the arch axes by Mid-Devonian time. Large fault blocks in the Mid-Devonian faulting system moved downward at varying rates (Cant, 1988). A graben system also developed during the Carboniferous and normal faulting during this period involved rejuvenation of old basement blocks (Lavoie, 1958; Richards *et al.*, 1994).

On the southeast flank of the PRA, basement faults can be grouped into two sets of faults intersecting each other at high angles. One set trends largely NW-SE parallel to the Rocky Mountain deformation front. The other set trends largely NE-SW (NEE-SWW) parallel to the long axis of the PRA. Throughout Phanerozoic time, these faults played important roles in relieving intra-plate stresses, shaping structural styles, and affecting local accumulations of sediments. Among NE-SW (or NEE-SWW) trending faults, the Carboniferous Hines Creek Graben appears to affect the Lower Cretaceous Viking Formation (Fig. 2-6). On the isopach map of the Viking Formation, the NEE-SWW bend of the dense contours corresponds closely

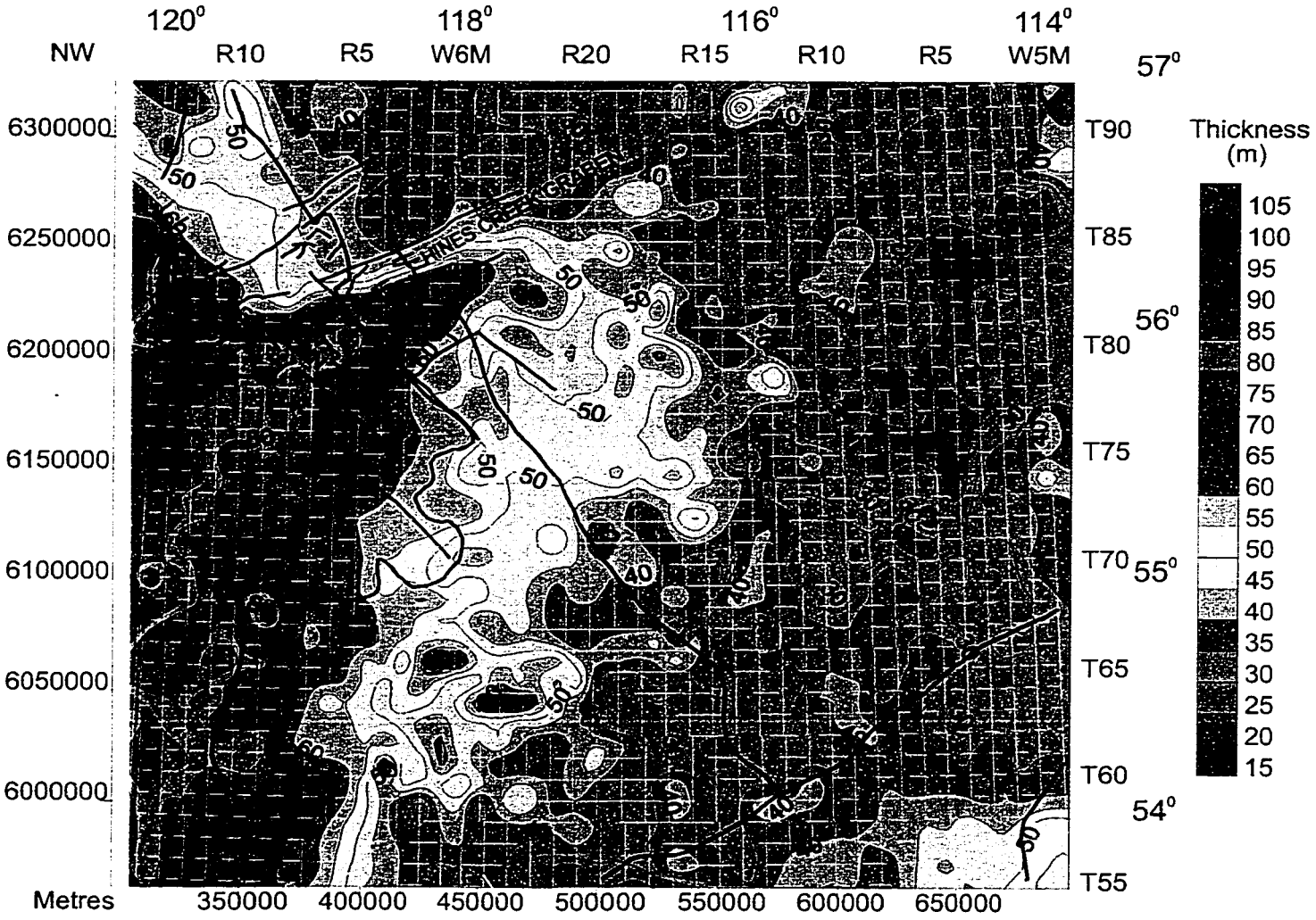

Figure 2-6. Isopach map of Lower Cretaceous Viking Formation, showing influence of the Peace River Arch and reactivation of the Carboniferous fault system (Richards *et al.*, 1994) in late Albian time.

to the trend of the Hines Creek Graben reflecting the influence by PRA collapse during Albian time.

In the study area, most basement faults are structural hinges because reverse displacement along fault planes occurred in response to changes in regional stress fields. Among the basementfaults on the southeast flank of the PRA, the Deep-Bulge Hinge, Obed Fault, Bulge-Trough Hinge, Donnelly Fault, and Chinchaga-Buffalo Head Boundary appear to be more active and have played important roles.

The Deep-Bulge Hinge (Fig. 2-2) was originally observed on the isopach of the Lower Cretaceous Lower Mannville Group (80-120 m contours in Fig. 2-3). The Deep-Bulge Hinge deflects along the Fox Creek Escarpment (Leckie and Smith, 1992; Fig. 2-2) and coincides with the location of the Fort St. John Graben (Fig. 1-8) that was defined in the Carboniferous. The Deep-Bulge hinge cuts the proximal edge of the earliest Cretaceous forebulge and has persistently influenced Cretaceous formations (Figs. 2-7, 2-8). In the Upper Cretaceous Cardium Formation (refer to Figs. 4-9, 4-10), the Deep-Bulge Hinge coincides with the location where Succession 1 terminated (refer to Fig. 4-10A) and Succession 4 started (refer to Fig. 4-10D). In the Upper Cretaceous Bad Heart Formation (refer to Fig. 3-5), the dense contours (10-15 m) in the northwest of the mapping area follow the Deep-Bulge Hinge and form a step in the formation.

The Deep-Bulge Hinge separated the forebulge from the western foredeep. Differences between the foredeep and the forebulge are observable on seismic reflection data (Fig. 2-9). Line 20B in Figure 2-9 is about normal to the strike of the Deep-Bulge Hinge. In the cross section of Line 20B, reflection characteristics between 0.5-1.0 second vary across the

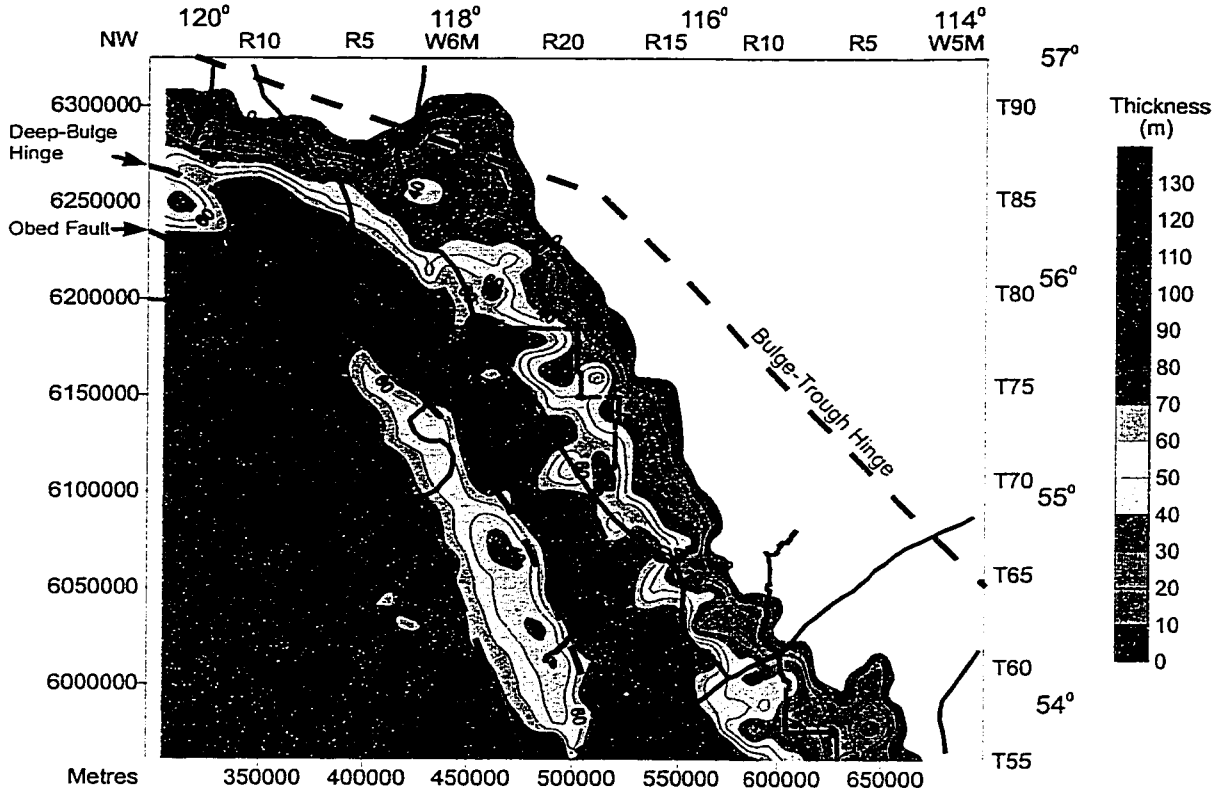

(A) Jurassic Fernie Group

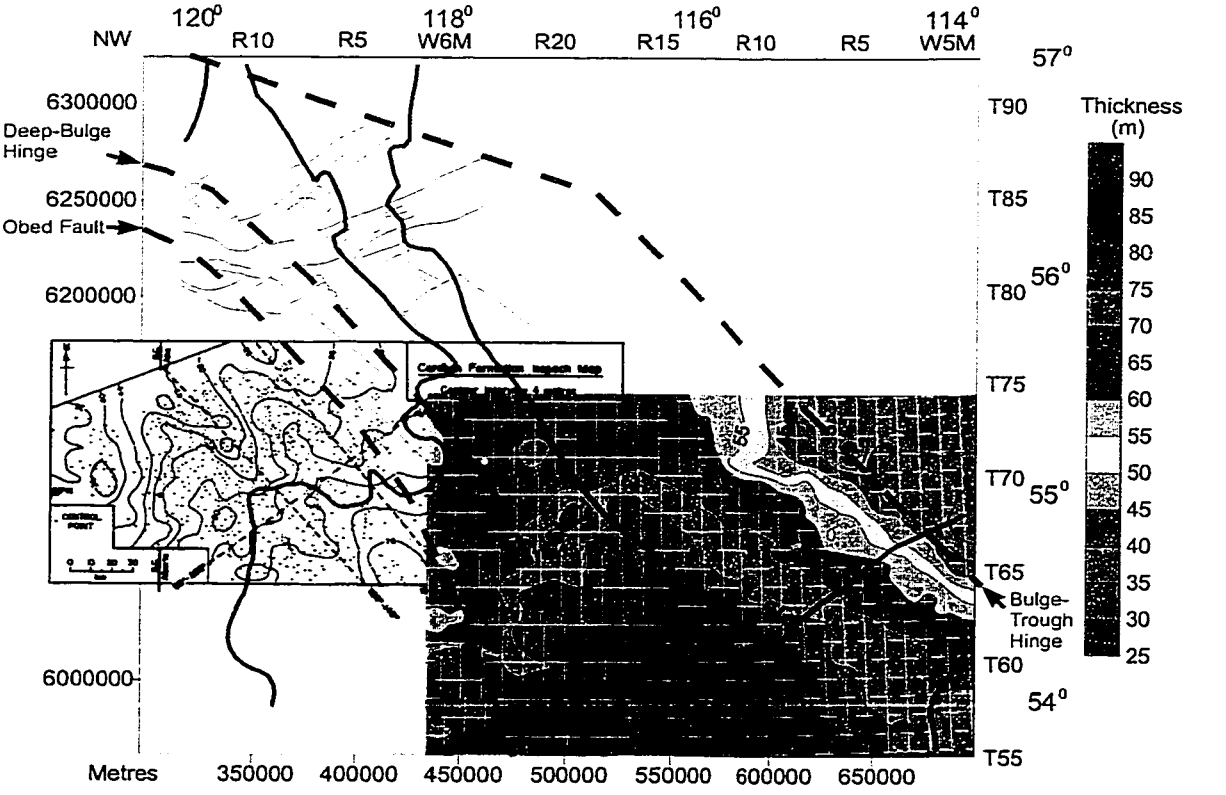

(B) Cardium Formation of Upper Cretaceous

Figure 2-7. Isopach maps, showing influence of basement discontinuities on the formations. Black and white isopach of the Cardium Formation, from Hart and Plint (1990). Blue line, Proterozoic domain boundary (refer to Fig. 1-8). Red line, Carboniferous fault (refer to Fig. 1-8). Pink line, seismic line; line number, refer to Fig. 1-2.

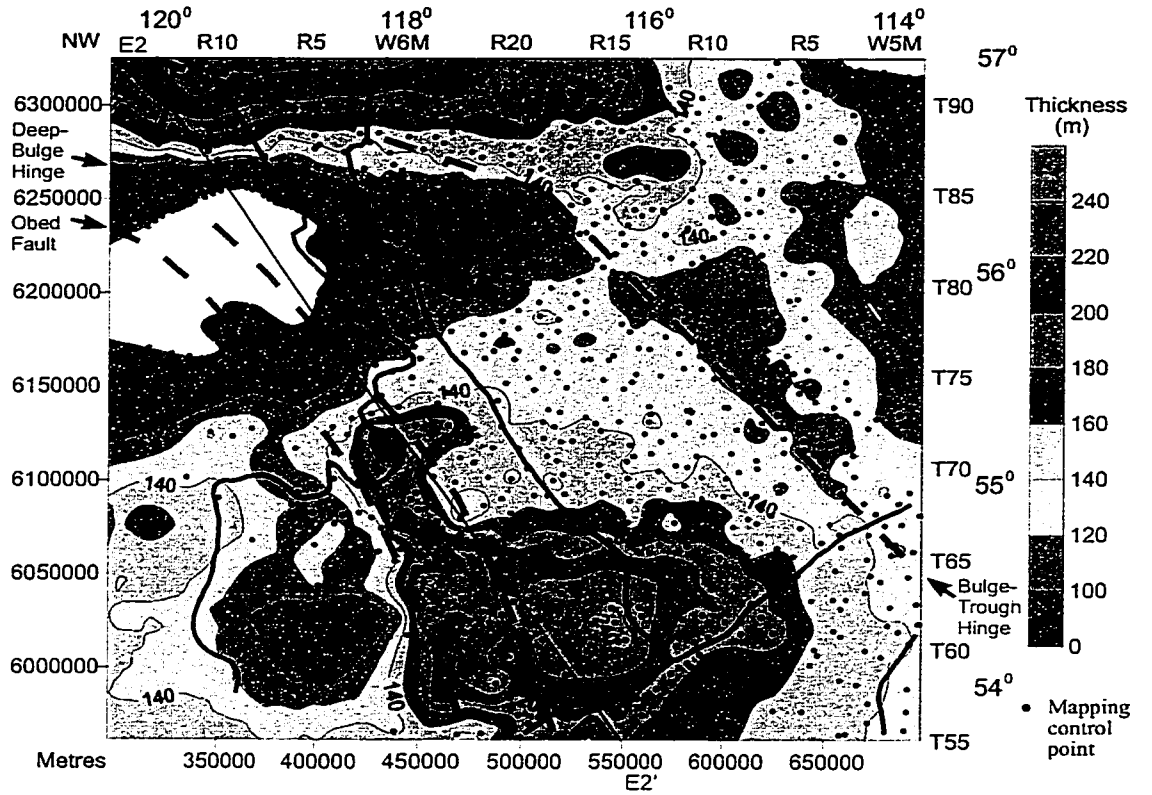

(A) Devonian Winterburn Group

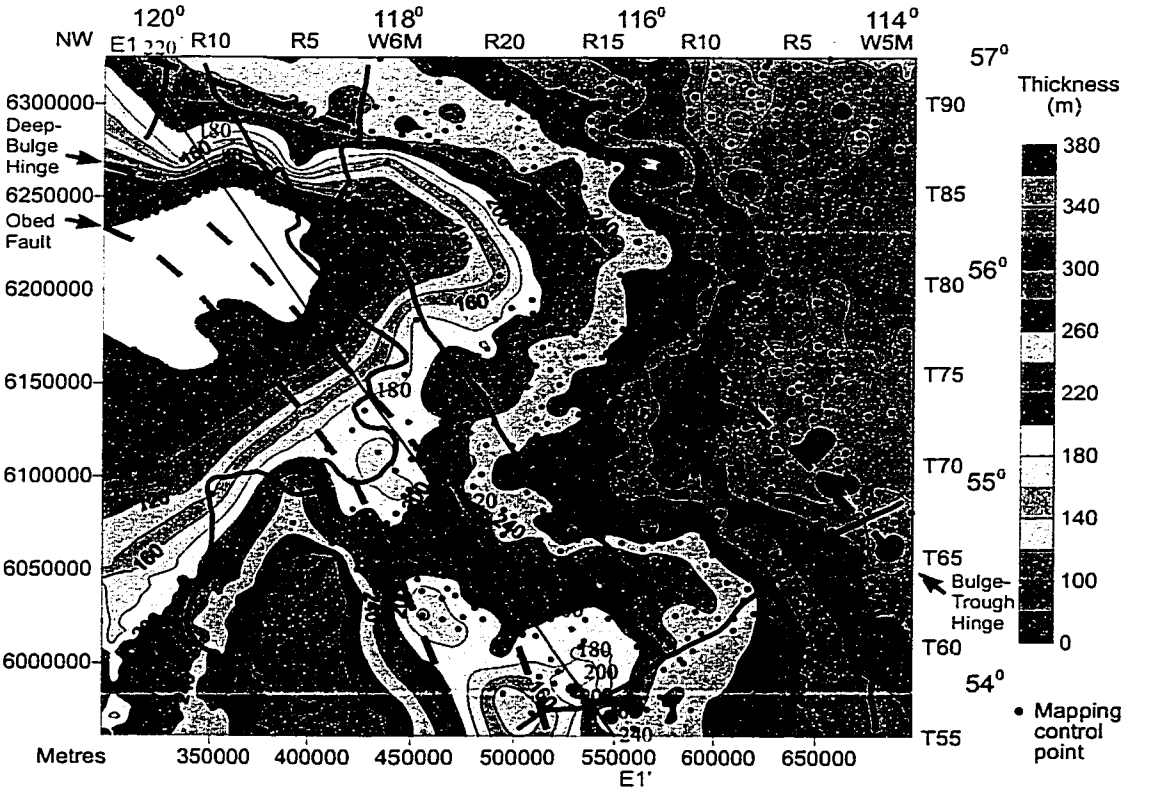

(B) Devonian Woodbend Group

Figure 2-8. Isopach maps showing basement impact. Blue line, Proterozoic domain boundary (refer to Fig. 1-8). E1-E1' and E2-E2', refer to Fig. 5-2.

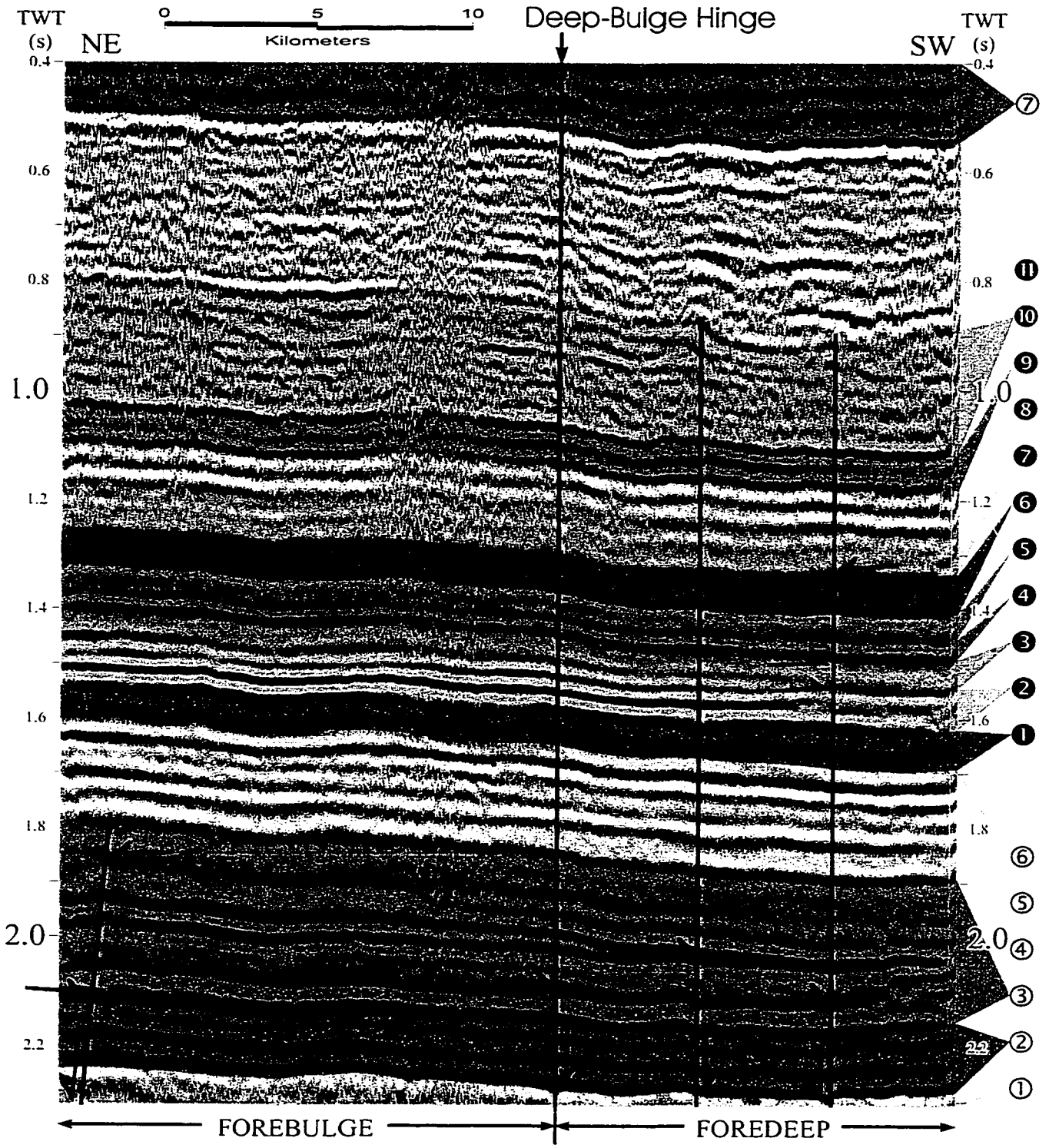

① Precambrian
② Cambrian
③ Devonian
④ Mississippian
⑤ Triassic
⑥ Jurassic
⑦ Inferred Tertiary

❶ Lower Mannville Group
❷ Upper Mannville Group
❸ Peace River Group
❹ Shaftesbury and Dunvegan formations
❺ Middle Second White Speckled Shales
❻ Upper Second White Speckled Shales
❼ Black Stone and Cardium formations

❽ Bad Heart and upmost Colorado
❾ Lea Park Formation
❿ Belly River Group
⓫ Edmonton Group
Fault
Onlap/downlap
Toplap/truncation

Figure 2-9. Migrated seismic section of Line 20B (vertical exaggeration, 4 times), showing reflection characteristics across the Deep-Bulge Hinge. Line location, refer to Figs. 1-2.

hinge. Formations on the forebulge northeast of the hinge appear relatively flat and have less disturbed phase lineups; while formations in the foredeep southwest of the hinge show deformation/disturbance of phase lineups. Terminal reflections (onlap, downlap, and toplap/truncation) are common against the hinge or other basement faults in the foredeep. The Deep-Bugle Hinge intersects some strong reflections (Fig. 2-10) in the upper crust of the Winagami Reflection Sequence (WRS, Ross and Eaton, 1996, 1997). The sub-horizontal reflection sheets in the WRS are well developed on the forebulge but die out in the foredeep (Fig. 2-10).

About 40 km west of the Deep-Bulge Hinge, the Obed Fault was firstly identified on the isopach map of the Jurassic Fernie Group (Fig. 2-7A). The fault is also a long acting fault and can be detected in many formations (Figs. 2-7B, 2-8). The Obed Fault appears to have functioned like a hinge. For example, the fault was east-wall-up and west-wall-down in the Woodbend Group (Fig. 2-8B) and west-wall-up and east-wall-down in the Winterburn Group (Fig. 2-8A). The Obed Fault and the Deep-Bulge Hinge cut the basement into an elongate zone between them. Appearing as a narrow neck in the Woodbend and Winterburn groups (Fig. 2-8), the elongate zone emerged as a scar in the Jurassic Fernie Group (Fig. 2-7A) and appears to affect the same place in the Cardium Formation (Fig. 2-7B).

Sub-parallel to the Canadian Cordilleran deformation front, the Bulge-Trough Hinge was developed on the remote, gentle side of the forebulge (Fig. 2-2). This hinge is associated with linear structures/discontinuities not only in compressional (Figs. 2-3, 2-7) but also extensional (Figs. 2-5, 2-8A) regimes. The Bulge-Trough Hinge is coincident with a linear structure on the aeromagnetic anomaly map (Fig. 2-11).

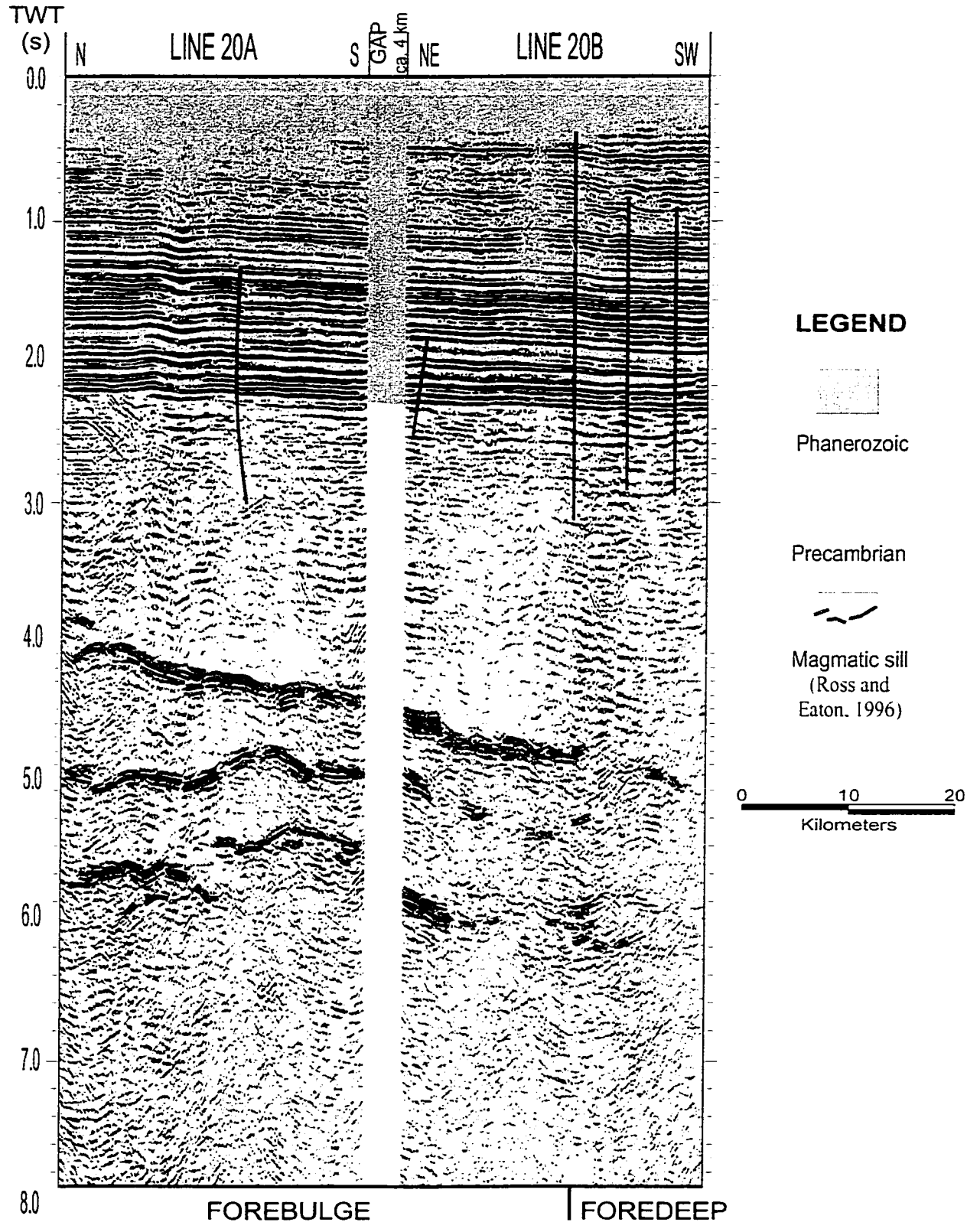

Figure 2-10. Migrated seismic section (vertical exaggeration, 2 times), showing location of the Deep-Bulge Hinge. Line and Hinge locations, refer to Figs. 1-2, 5-6A.

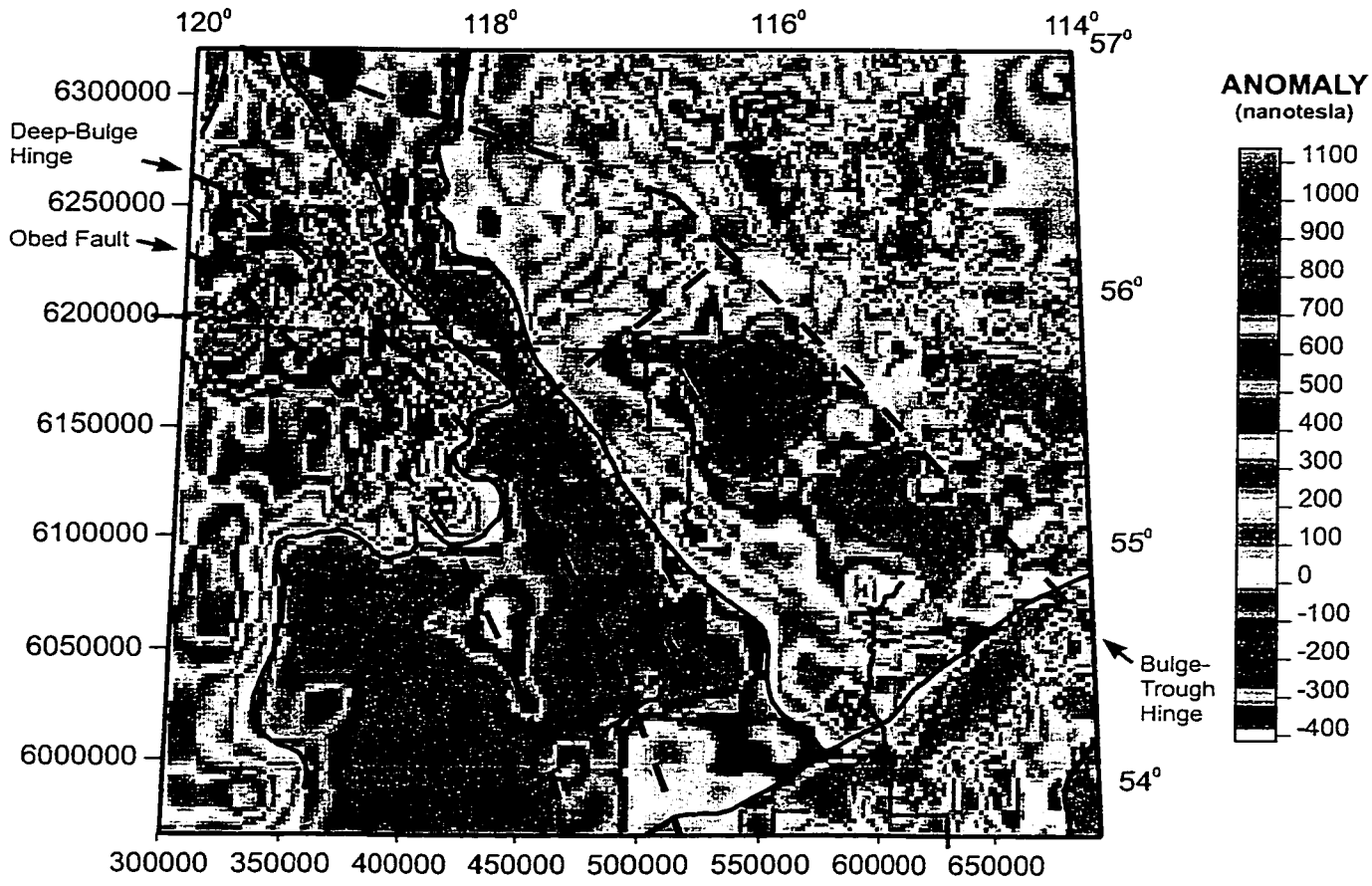

Figure 2-11. Aeromagnetic anomaly map for the Peace River Arch region, showing relations between magnetic anomalies and basement faults (red dashed line) and Proterozoic domain boundary (blue line, refer to Fig. 1-8). Pink line, seismic line; line number, refer to Fig. 1-2.

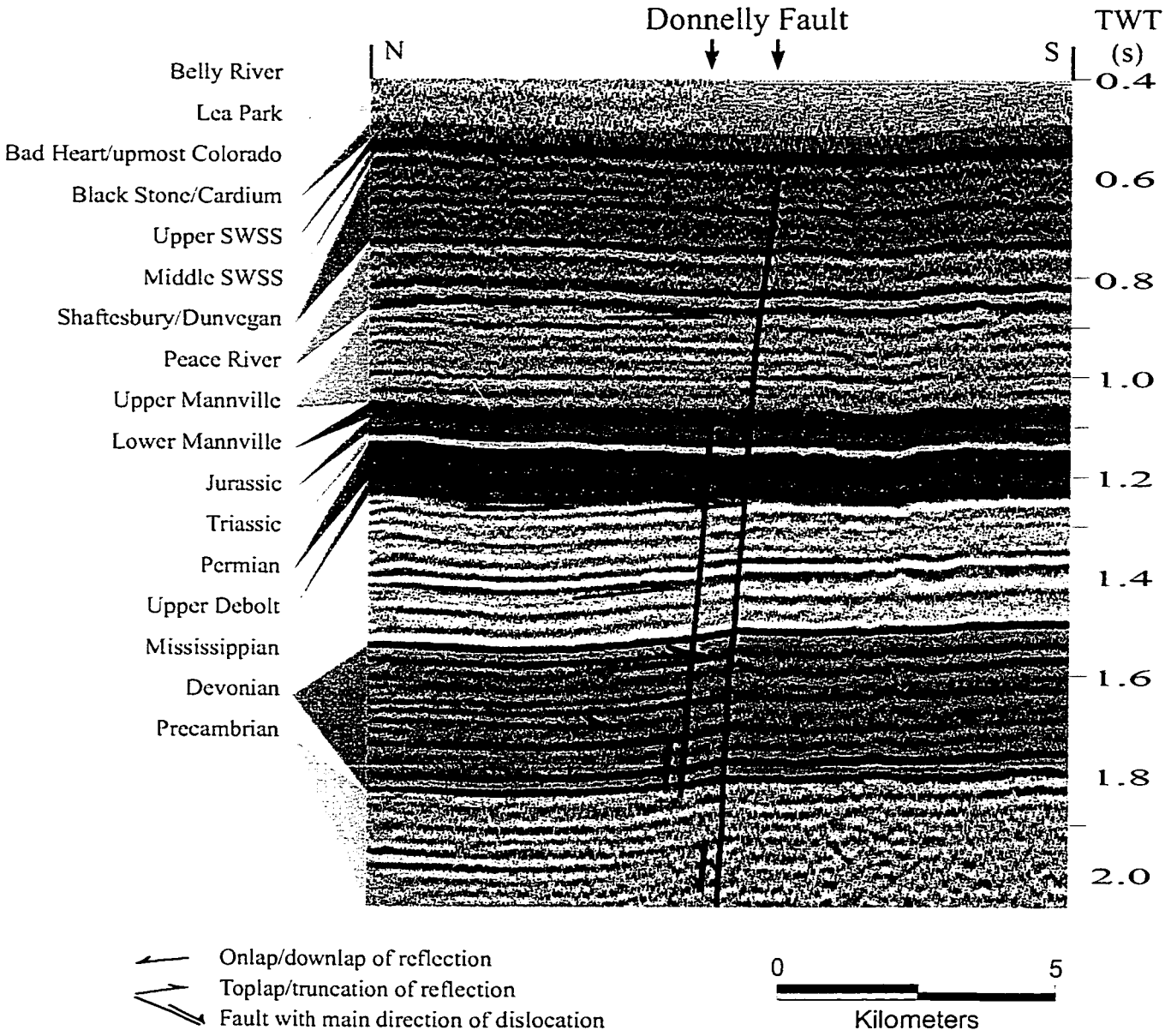

Figure 2-12. Migrated seismic section (vertical exaggeration, 2 times), north of Line 13, showing reactivations of the Donnelly Fault. Line location, refer to Fig. 2-1.

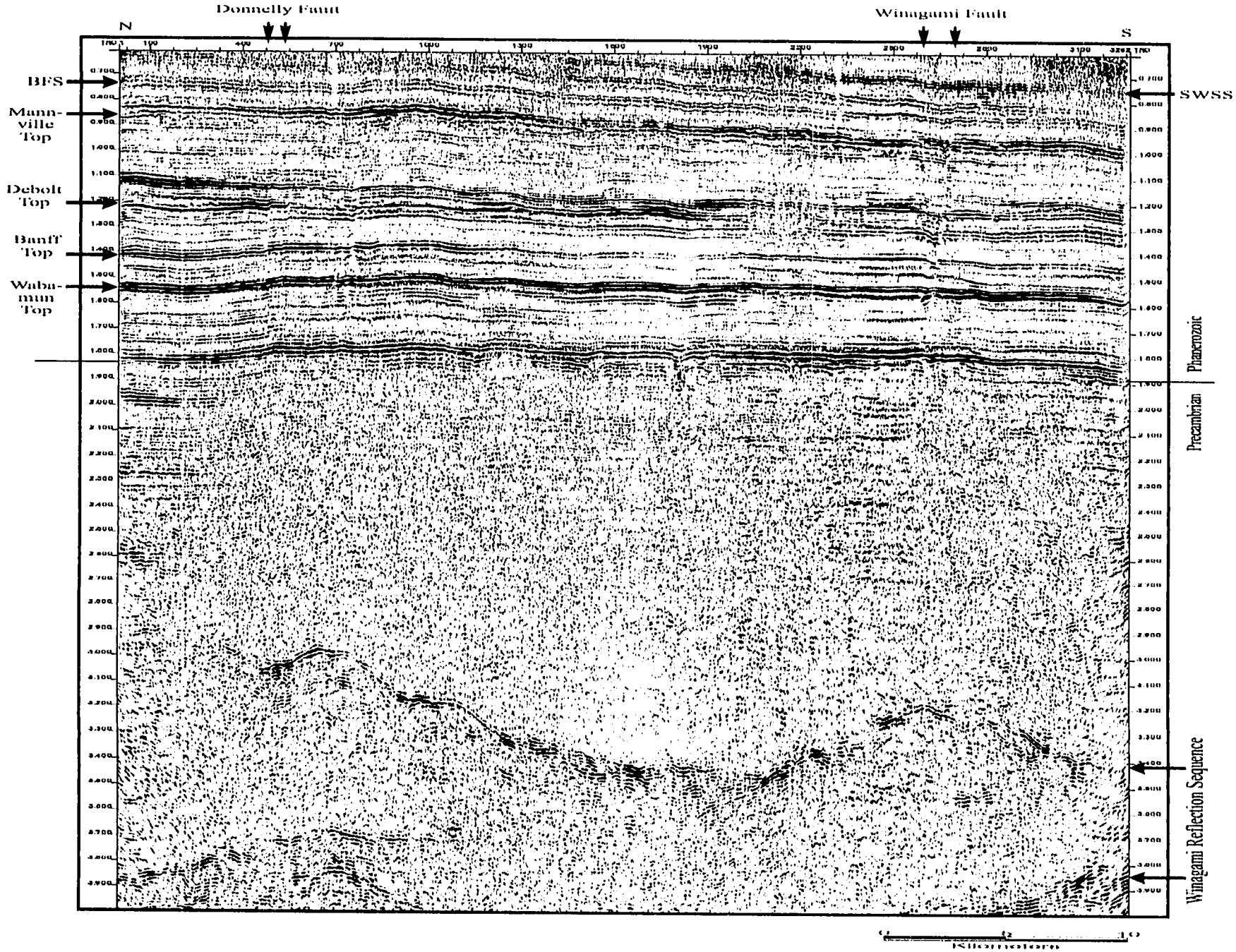

Figure 2-13. Un-interpreted seismic reflections of Line 13 (migrated, vertical exaggeration 2 times), showing faults and related crustal features. Normal polarity display: red, peak; blue, trough. Line location, refer to Fig. 2-1.

The Donnelly Fault (Tangent Fault, Eaton *et al.*, 1999; Hope *et al.*, 1999) consists of a faulting zone with two planes about 1 km apart, forming steps in the Carboniferous, especially at the Debolt top where vertical offset is about 50 m (Figs. 2-12, 2-13). Permian thickness changes across the Donnelly Fault and the fault also appear to influence the Devonian, Mississippian, and Cretaceous Upper Mannville Group. Onlap and toplap/truncation terminal reflections againstthe fault are observable in formations of the down-thrown wall, indicating intermittent movement of the fault.

The Proterozoic domains assembled in Paleoproterozoic time appear to have been well welded and functioned as a uniform crustal block during most of the Phanerozoic Era. The boundaries of the domains appear to have had a minor impact on sedimentation. The boundaries may have been weak planes in the crust and could be mobilized under certain conditions. For example, in the Cardium Formation, the axis of the elongate depositional centre (Fig. 2-7B) seems to follow the Chinchaga-Buffalo Head Boundary. Thickest accumulation of Cardium deposits was received along the down-warped boundary. In the Dunvegan and Doe Creek formations, differential subsidence of blocks occurred (Fig. 4-12). The quadrilateral subsidence appears to be in a clockwise shifting pattern, firstly confined in the Chinchaga domain (Fig. 4-12A), and subsequently distributed on the Buffalo Head-Wabamun Boundary (Fig. 4-12B), and finally developed on the Wabamun domain (Fig. 4-12C).

2-3. Links between Western Continental Margin Tectonism and Foreland Basin Deposition

It is generally agreed that western Canada has been under the influence of a convergent tectonic regime since mid-Jurassic time and the stages of Cordilleran development have dominated depositional processes in the foreland basin. The Canadian segment of the Cordillera is divided into five physiographically distinct belts (Fig. 2-1). These are westerly Rocky Mountain Belt, Omineca Crystalline Belt, Intermontane Belt, Coast Plutonic Complex, and Insular Belt (Monger *et al.*, 1982).

Monger *et al.* (1982) suggested that small terranes mainly in the Intermontane Belt but extending into the Omineca Crystalline Belt and the Coast Plutonic Complex formed the large composite terrane (Terrane I) that was accreted to the ancient margin of North America in Jurassic time. Terranes mainly in the Insular Belt but extending into the Coast Plutonic Complex were amalgamated and formed the composite terrane (Terrane II) that collided with and accreted to western North America about middle Cretaceous time.

In contrast, van der Heyden (1992) suggested that the western Canadian Cordillera is a single composite superterrane accreted to ancestral North America in Middle Jurassic time based on (1) widely scattered Middle to Late Jurassic plutons and (2) lack of vestiges of a major Late Jurassic to Early Cretaceous ocean between the superterranes I and II. Instead of using terrane collisions, van der Heyden (1992) attributes regional compression for the western Canadian Cordillera during the Cretaceous to external adjustments in plate motions. Oblique subduction of plates was responsible for the change of regional stress fields and structures.

Based on estimated pressures of more than 7 kb during prograde metamorphism in high-grade meta-sedimentary rocks in both the coast Plutonic Complex and the southern Omineca Crystalline Belt, burial depths were inferred to be greater than 25 km. It is speculated that one terrane may have overridden or compressed the other during the collision between Terranes I and II (Monger *et al.*, 1982). As foreign terranes impinged on the craton, they exerted a downward force causing a crustal flexure. Sediments were eroded from the new relief in the orogen and shed eastward, filling the down-flexed area (Mossop and Shetsen, 1994).

CHAPTER 3: PREVIOUS STUDIES AND EXISTING PROBLEMS

The tectonic and sedimentary history of the PRA was first discussed in the 1957 Symposium on the Peace River Arch (Scott, 1958). Since then, understanding of the complexities of the Arch has been aided by significant increases in geological and geophysical data. A comprehensive study of the PRA was undertaken by O'Connell *et al.* (1990). Several authors contributed to the Peace River Arch special publication in 1990. In addition to that volume, several studies, Leckie (1984), Bergman and Walker (1987), Cant (1988), Rouble and Walker 1994, Kent (1994), Richards *et al.* (1994), Eaton *et al.* (1997, 1999), Donaldson *et al.* (1998), Chen and Bergman (1999) have discussed a variety of aspects in the PRA region. A second special publication (1999), based on studies in the PRA area supported by Lithoprobe, has been published.

The Cretaceous history of the Arch region has been qualitatively and quantitatively approached. Williams (1958), Burk (1962), Hart and Plint (1990), and Underschultz and Erdmer (1991) quantitatively measured sediments in the foreland basin using well logs and isopach maps. Cant and Stockmal (1989) matched six clastic wedges in the foreland basin to the six tectonic episodes in the Canadian Cordillera. Bergman and Walker (1987) calibrated stratigraphic changes to global eustatic sea-level fluctuations. Jones (1980) and Donaldson *et al.* (1998) related sedimentary patterns to the reactivation of basement faults.

3-1. Timing of Peace River Arch Uplift and Subsidence

3-1-1. Initial Uplift of Peace River Arch

The initial uplift of the PRA was dated at post-Cambrian time by deMille (1958), at Early Cambrian time by Cant (1988), and at latest Proterozoic time by McMechan (1990). Based on correlations, deMille (1958) suggested that the Precambrian basement underlying the Peace River area was up-warped in post-Cambrian time. This timing is coincidental with the period of broad regional uplift in the WCSB during Ordovician and Silurian time. Three decades later, with increased data control, Cant (1988) demonstrated that the initial Arch uplift was in Early Cambrian time. Pre-Middle Cambrian uplift is supported on the seismic profile (Fig. 1-10). At the Middle Cambrian bottom, seismic reflectors onlap the PRA. Consequently, McMechan (1990) investigated the outcrops around the Precambrian top unconformity in the Canadian Cordillera west of the PRA region and proposed that the Arch may have been uplifted during latest Proterozoic time. This appears to be a generally accepted time for initial uplift of the Arch.

3-1-2. Major Subsidence of Peace River Arch

Though deMille (1958) presumed that the basement of the PRA remained high during much of the Paleozoic Era, most recent studies suggest that the Arch remained high from Cambrian to Devonian time and then collapsed, becoming an embayment during most of Carboniferous and Permian time (O'Connell *et al.*, 1990). The long subsidence of the PRA was interrupted by Mesozoic collisional events along the western margin (Figs. 2-1, 2-3). Collapse of the PRA was resumed during Early Cretaceous Albian time (Fig. 2-5). The Albian

collapse of the Arch has been identified because of its influence on sedimentation in the Upper Mannville Group (Cant, 1984; Leckie, 1984, 1986; Leckie *et al.*, 1990; Rouble and Walker, 1994). However, the origin of the Albian collapse of the Arch and its relationship to the mechanism causing the Arch collapse during Paleozoic time have not been examined.

3-1-3. Final Uplift of Peace River Arch

Williams (1958) suggested that the Peace River area was stable during the Late Cretaceous, stating that "marine shale beds thicken uniformly and gradually to the west and north, as if the Arch had never been there." The Arch became a positive feature toward the end of Upper Cretaceous time (Williams, 1958). Instead of "toward the end" of Upper Cretaceous time (Williams, 1958), Burk (1962) suggested that the final uplift of the Arch was "during" Late Cretaceous time based on isopach data from the Upper Cretaceous. The present southern flank of the PRA shows a history of continued subsidence throughout most of the Cretaceous and began to redevelop as an arch during the Late Cretaceous and evolved to its present form (Burk, 1962). Chen and Bergman (1999) mapped out detailed intervals for the Cretaceous on the southeast flank of the PRA and illustrated that the PRA region was uplifted during late Turonian (Cardium Formation) and early Campanian (Lea Park Formation) time but subsided again in middle Campanian (Belly River Formation) time. The final uplift of the Arch was apparently later than middle Campanian time (Fig. 3-1).

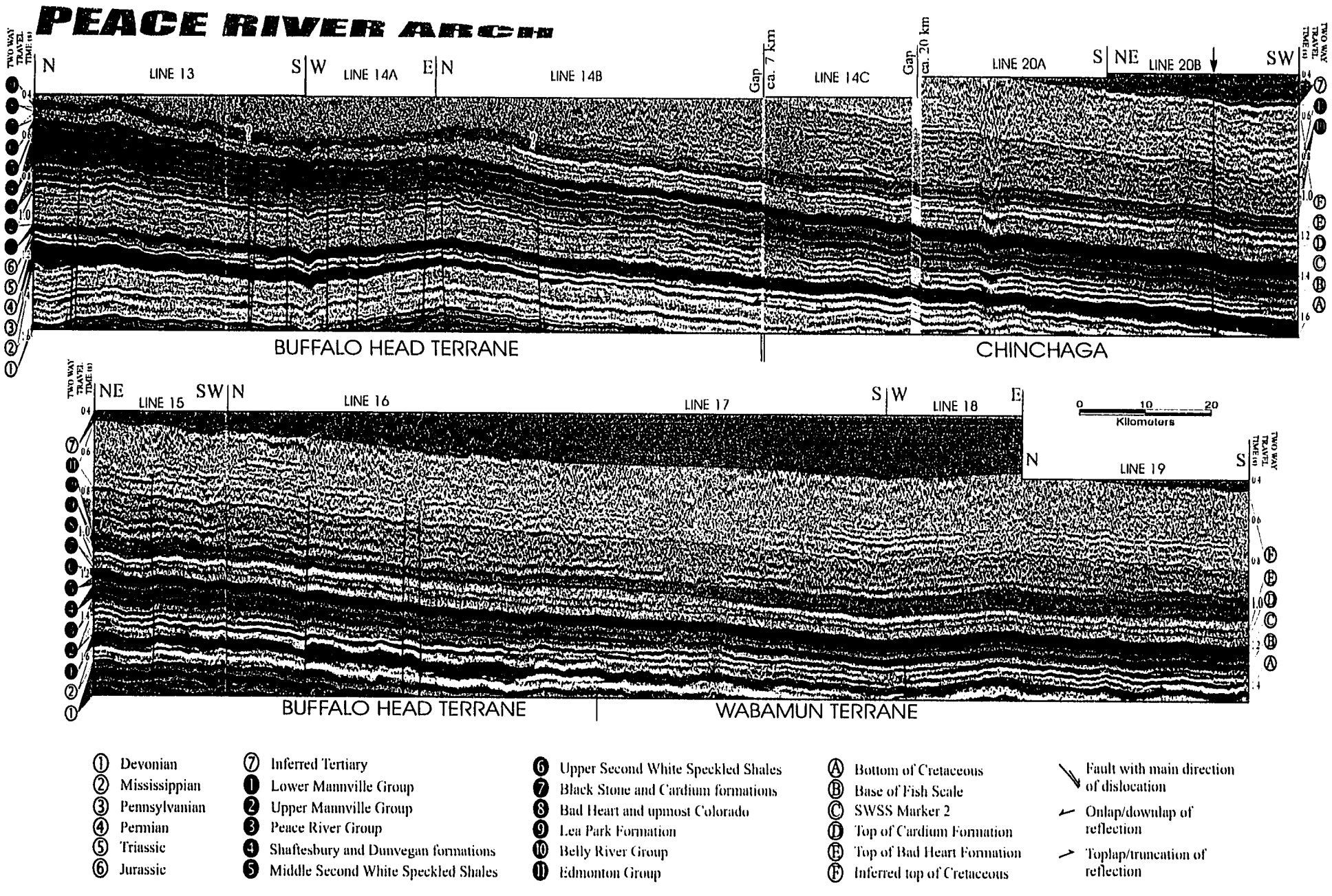

Figure 3-1. Migrated seismic sections (vertical exaggeration, 8 times), showing the Cretaceous in the southeast flank of the Peace River Arch. Line location, refer to Figure 1-2.

3-2. Origin of Peace River Arch Uplift and Subsidence

There have been considerable debates concerning the origin and mechanisms responsible for uplift and subsidence of the PRA. Many suggestions, such as thermal extension, rifting, isostatic adjustment, and phase change, have been proposed. Each of these hypotheses explains some aspects of the Arch movement but each has weaknesses/difficulties explaining all evidence/phenomena contained in the Arch region.

3-2-1. Thermal Extension and Rifting

The mechanism of thermal extension suggests that uplift of domes/arches could occur in areas of underlying mantle hotspots (Morgan, 1983; Crough, 1983). When lithospheric plates move over hotspots, fracturing of the crust may occur along planes of crustal weakness and lead to rifting with regional uplift. The Lithosphere could be thinned and rifted by thermal extension or stretching. The rate of lithospheric thinning and the width of a rift zone depend on the convection velocities in the underlying asthenosphere and on the viscosity – depth gradient near the lithosphere-asthenosphere boundary (Keen, 1985).

Cant (1988) speculated that thermal decay in the late Paleozoic may have caused the collapse of the PRA. Continued subsidence in the Mesozoic may have been caused by accretion of allochthonous terranes that loaded the lithosphere at the western end of the Arch (Cant, 1988). The suggestion of thermal decay has not substantially measured and calculated the amount of Arch region subsidence that is possibly driven by the mechanism of thermal decay.

O'Connell *et al.* (1990) suggested that the PRA was formed by uplift associated with the cratonward extension of an oceanic fracture zone in a failed rift setting and may have developed along lines of weakness in the pre-existing Precambrian crust. Richards *et al.* (1994) defined the major normal faults in the Carboniferous of the PRA and suggested the Peace River Embayment subsidence was fault-controlled in an extensive field on the western cratonic platform. Eaton *et al.* (1997, 1999) did not find seismic evidence of antecedent basement discontinuities that are responsible for the formation of Carboniferous faults and suggest these faults may have derived from the Devonian Granite Wash lithozone.

3-2-2. Isostatic Adjustment

As an alternative to thermal-extension and rifting, isostatic adjustment was proposed. According to the definition, there are three different mechanisms of isostatic adjustment, basement-prism-floating (e.g. Walcott, 1970; Jones, 1980), intact-basement-flexure (e.g. Quinlan and Beaumont, 1984; Beaumont *et al.*, 1993), and glacial rebound (e.g. Pirazzoli *et al.*, 1993; Wu, 1998).

3-2-2-1. Basement Prism Floating

Early studies (Goodman, 1951; Lavoie, 1958) supposed that basement in the Peace River area underwent periods of uplift and subsidence because of differential rising and sinking of basement blocks, not because of flexure of a completely intact basement surface. The hypothesis of basement-prism-floating isostatic adjustment (Walcott, 1970; Jones, 1980) suggests that the lithosphere could be considered as a collection of vertical prisms floating

independently under its own load when compressive force is absent. During times of horizontal compression the prisms are temporarily clamped together by friction to form a comparatively solid sheet effectively preventing independent vertical movement of the individual blocks. Isostatic adjustment faults are responsible for maintaining or restoring the isostatic equilibrium of the lithosphere during one or more geologic time periods.

The mechanism of basement-prism-floating isostatic adjustment could well explain many structural phenomena in the Cretaceous, such as the linear progradation of elongate zones in the Cardium and lower Shaftesbury/Dunvegan formations (refer to Figs. 4-9, 4-10, 4-16), differential subsidence of blocks in the upper Shaftesbury/Dunvegan and Doe Creek formations (refer to Figs. 4-11, 4-12), and aggradation in the Pouce Coupe Formation (refer to Figs. 4-13, 4-14). However, basement-prism-floating isostatic adjustment could not accommodate a collapse of the Peace River Embayment in an extensional stress field such as occurred during Carboniferous, Permian, and Early Cretaceous Albian time.

3-2-2-2. Intact Basement Flexure

The hypothesis of intact-basement-flexural isostatic adjustment (Beaumont *et al.*, 1993) suggests that the lithosphere under the WCSB was a flexural plate driven by loading in the Williston Basin and the rifted continental margin to the west. Relating subsidence in the foreland basin to loading on the western continental margin explains the macroscopic phenomena in the foreland basin during the Mesozoic. However, loading in the Williston Basin is not likely to affect uplift in the PRA during Mesozoic time (Beaumont, personal communication, 2000).

(A) Seismic Reflection of Lines 11 and 1

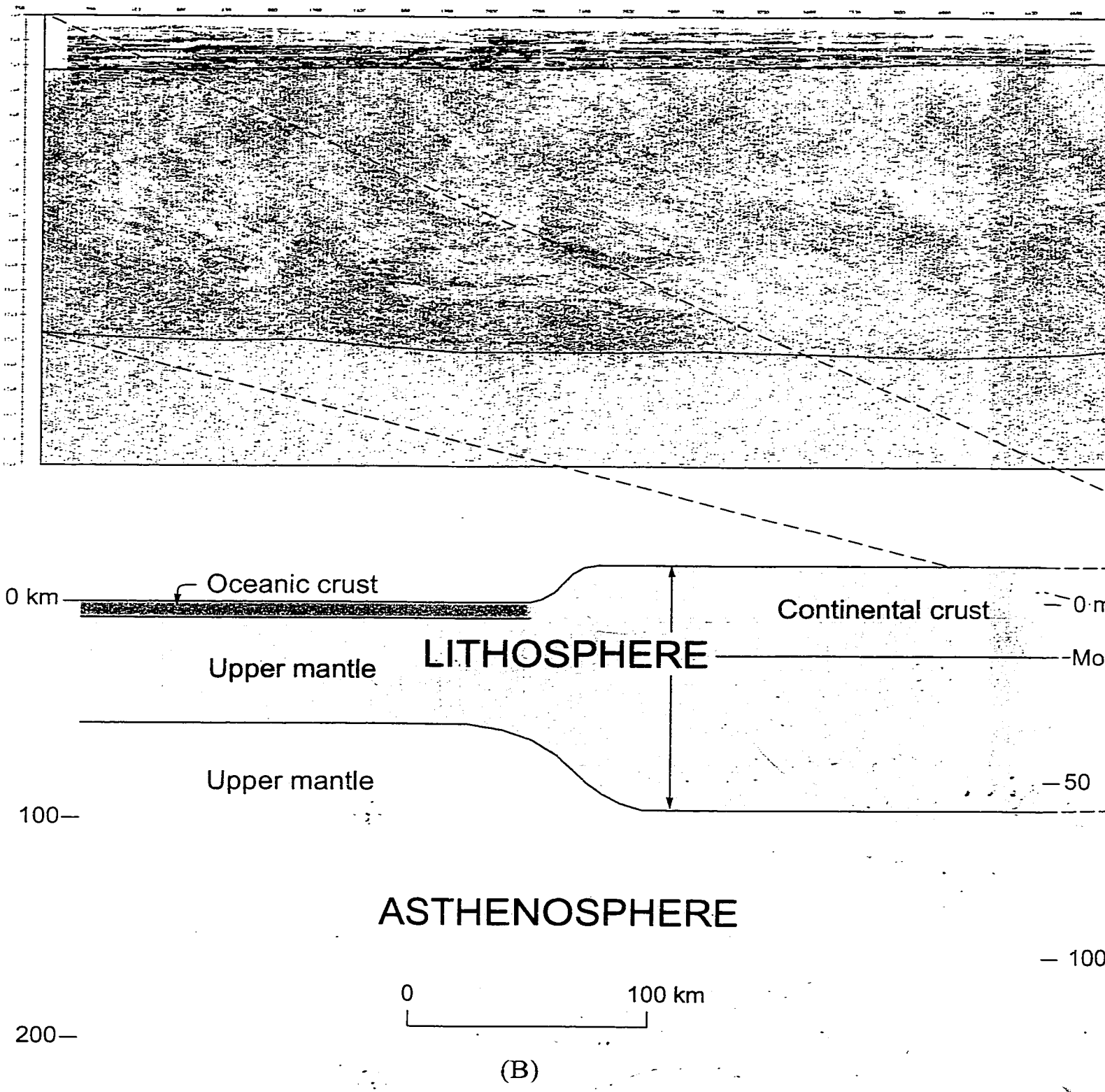

(B)

of Lines 11 and 12 across Peace River Arch Region

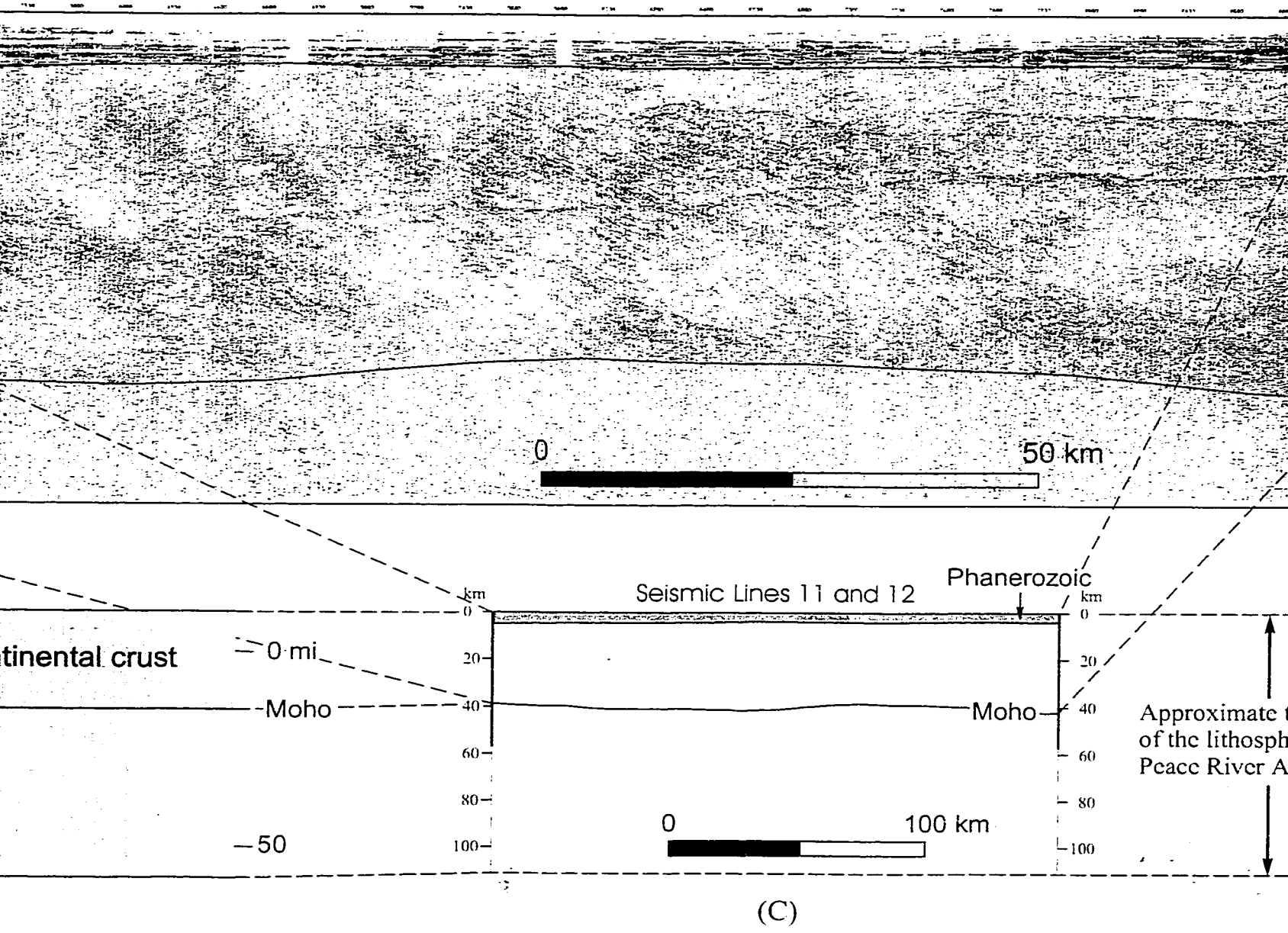

(C)

Figure 3-2. Phanerozoic of the Peace River Arch region plotted proportional t
outermost shell of the Earth. (A) Composite migrated seismic section showing
upper 8 seconds of data plotted with no vertical exaggeration (approximately).
Location of seismic lines, refer to Fig. 1-2. (B) Outermost shell of the Earth
modified from Press and Siever (1982). (C) Peace River Arch region plotted a
1:1 lateral to vertical scale. Average velocities are used to the time-depth
conversion: 4500 and 6500 m/s for Phanerozoic and crust, respectively.

d 12 across Peace River Arch Region

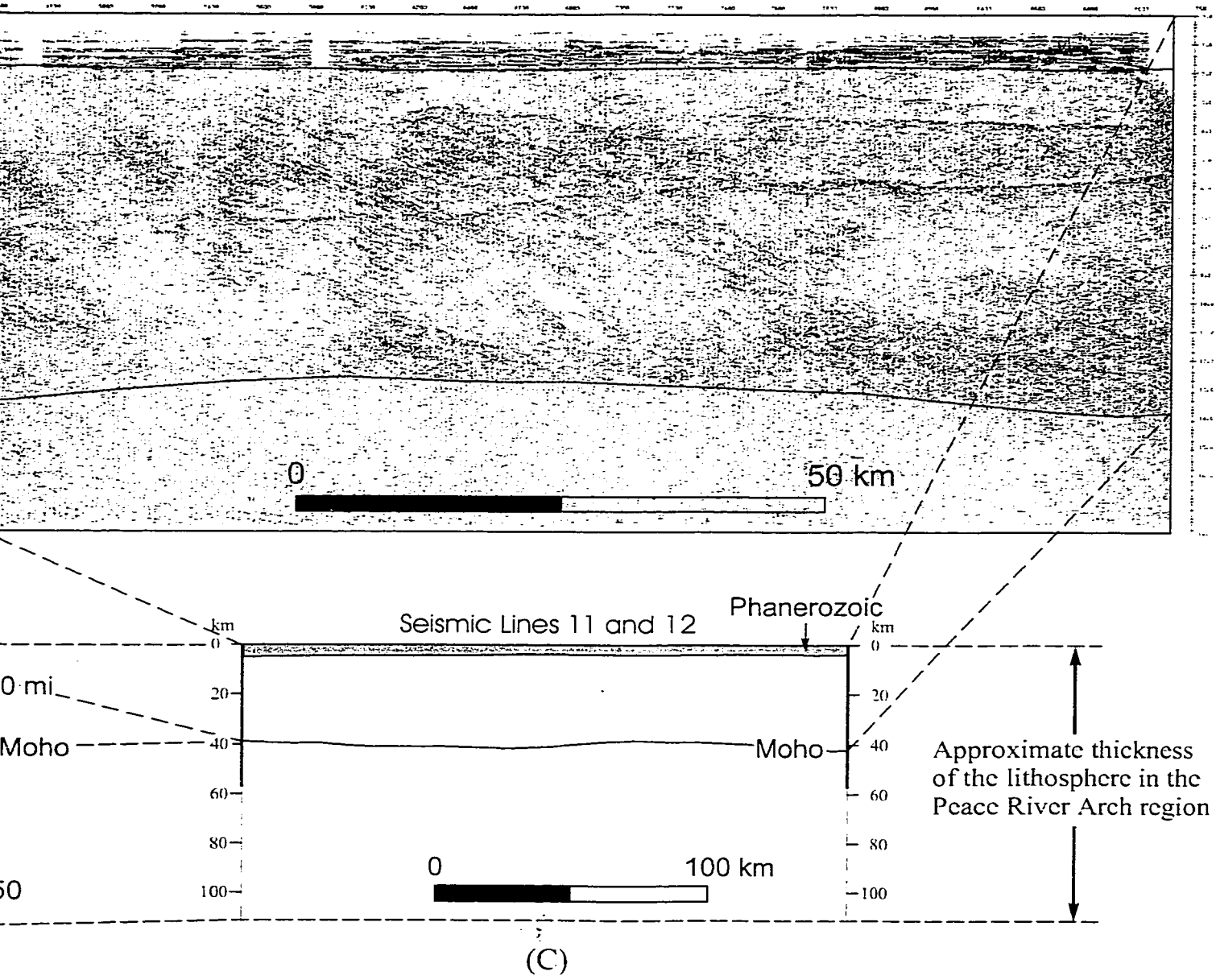

Figure 3-2. Phanerozoic of the Peace River Arch region plotted proportional to the outermost shell of the Earth. (A) Composite migrated seismic section showing the upper 8 seconds of data plotted with no vertical exaggeration (approximately). Location of seismic lines, refer to Fig. 1-2. (B) Outermost shell of the Earth modified from Press and Siever (1982). (C) Peace River Arch region plotted at 1:1 lateral to vertical scale. Average velocities are used to the time-depth conversion: 4500 and 6500 m/s for Phanerozoic and crust, respectively.

100

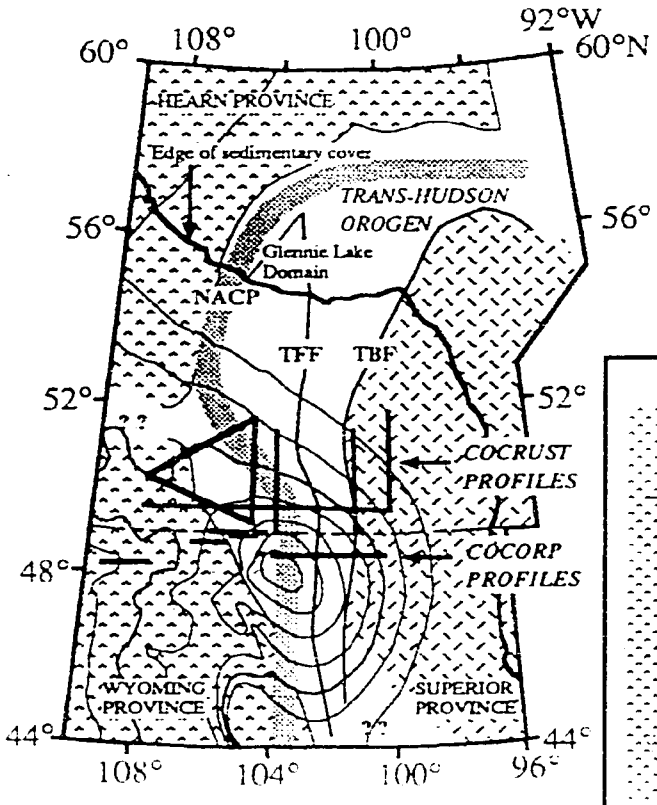
60°
108°
100°
92°W
60°N
HEARN PROVINCE
Edge of sedimentary cover
TRANS-HUDSON
OROGEN
56°
Glennie Lake
Domain
NACP
TFF
TBF
52°
COCRUST
PROFILES
COCORP
PROFILES
48°
WYOMING
PROVINCE
SUPERIOR
PROVINCE
44°
108°
104°
100°
96°

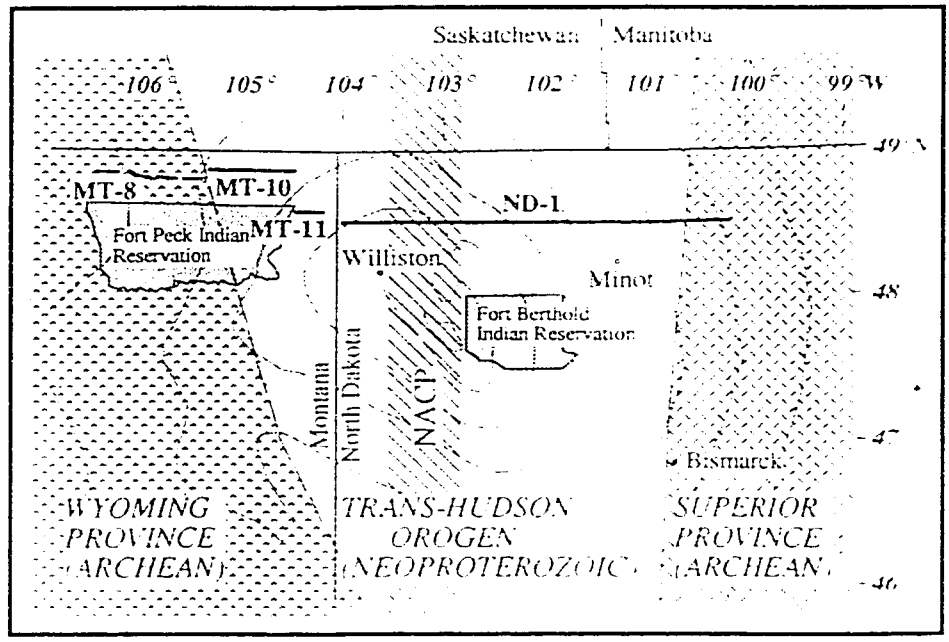
Saskatchewan
Manitoba
106°
105°
104°
103°
102°
101°
100°
99°W
49°
MT-8
MT-10
ND-1
Fort Peck Indian
Reservation
MT-11
Williston
Minot
48°
Fort Berthold
Indian Reservation
Montana
North Dakota
NACP
Bismarck
47°
WYOMING
PROVINCE
(ARCHEAN)
TRANS-HUDSON
OROGEN
(NEOPROTEROZOIC)
SUPERIOR
PROVINCE
(ARCHEAN)
46°

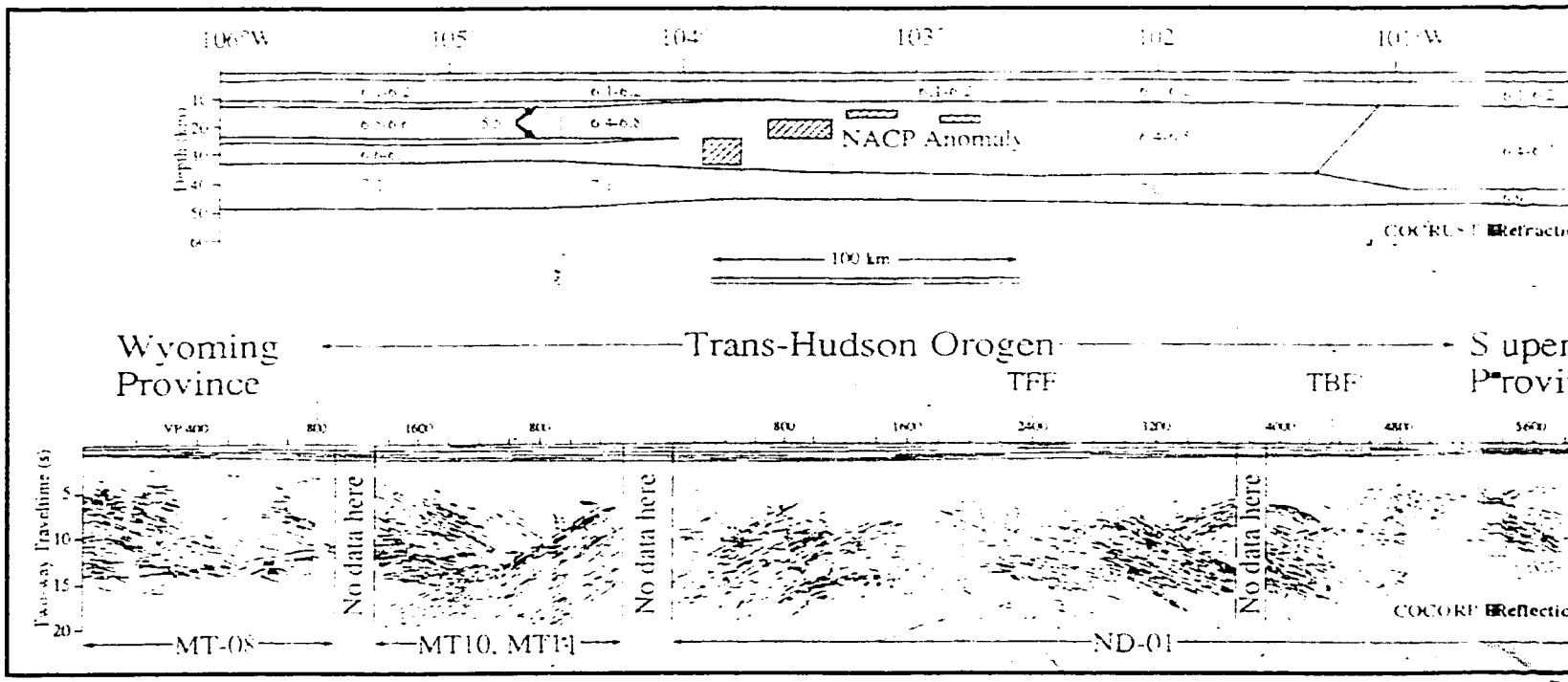
106°W
105°
104°
103°
102°
101°W
NACP Anomaly
100 km
Wyoming
Province
Trans-Hudson Orogen
TFF
TBF
Provi
No data here
No data here
No data here
MT-08
MT10, MT11
ND-01

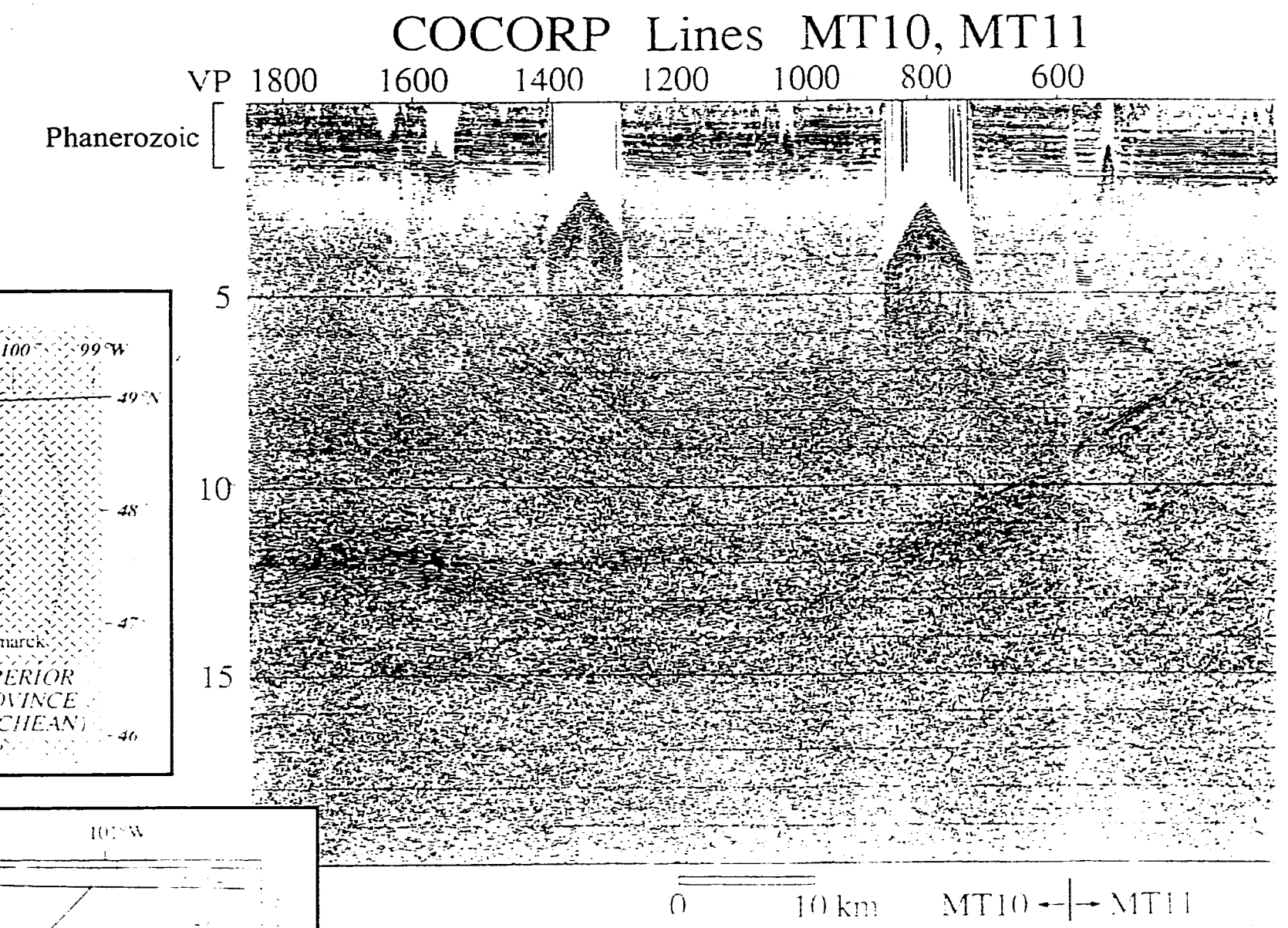

Figure 3-3. Maps from Nelson *et al.* (1993). Top-left and top-middle maps locations of COCORP seismic reflection profiles crossing the Williston Bas Top-right map, seismic reflections of lines MT10 and MT11. Bottom maps, average layer velocities (km/s) and line drawing (unmigrated) of the seismic reflections of lines MT08, MT10, MT11, and ND01.

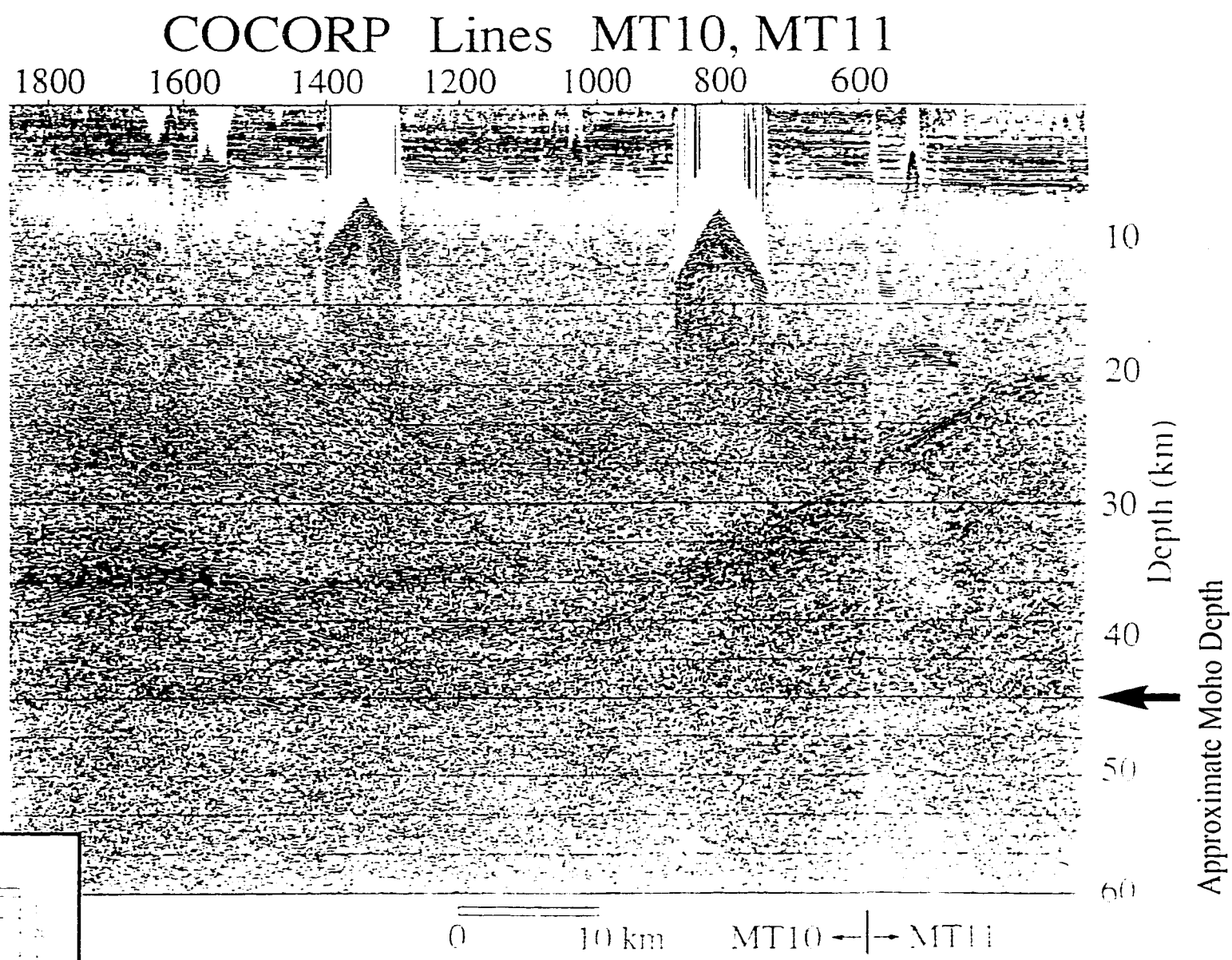

Figure 3-3. Maps from Nelson *et al.* (1993). Top-left and top-middle maps, locations of COCORP seismic reflection profiles crossing the Williston Basin. Top-right map, seismic reflections of lines MT10 and MT11. Bottom maps, average layer velocities (km/s) and line drawing (unmigrated) of the seismic reflections of lines MT08, MT10, MT11, and ND01.

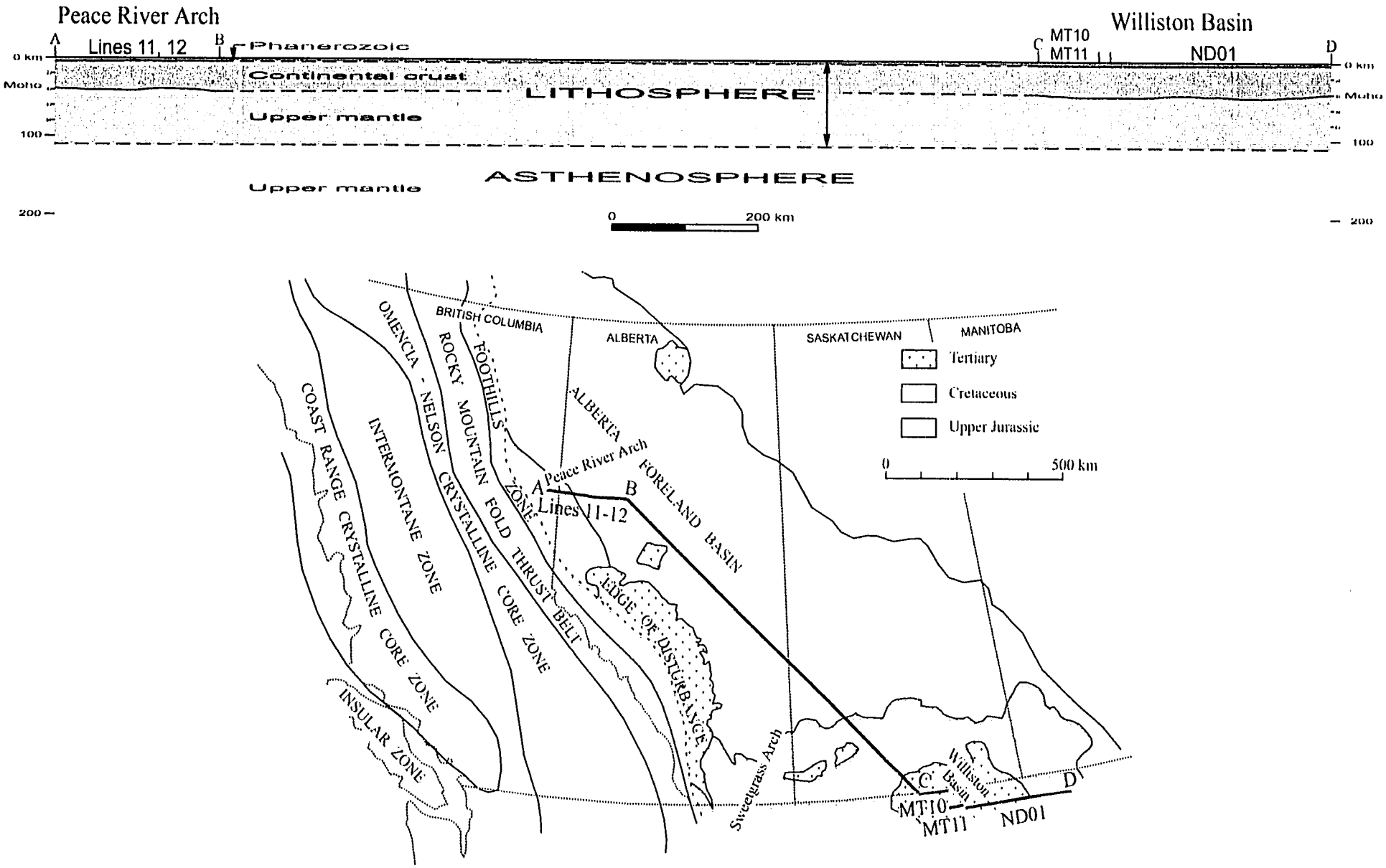

Figure 3-4. Outermost shell of the Earth from the Peace River Arch region to Williston Basin plotted at 1:1 lateral to vertical scale. Geometries for the Peace River Arch region and Williston Basin are scaled from Figs. 3-2 and 3-3. Bottom base map is modified from Beaumont *et al.* (1993).

Figures 3-2 to 3-4 illustrate several seismic profiles and derived depth cross sections, showing a correlation between the PRA region and the Williston Basin. Figure 3-2 shows the seismic profile across the PRA and a depth cross section converted from the seismic data. The cross section was plotted at 1:1 lateral to vertical scale and proportional to the outermost shell of the Earth (modified from Press and Siever, 1982). The thickness of the lithosphere in the PRA region various from about 100-120 km. The maximum thickness of the entire Phanerozoic record in this region is only about 5 km. The maps (Figs 3-3) were selected from Nelson *et al.* (1993), showing seismic reflections of the Phanerozoic and crust in the Williston Basin. In Figure 3-4, the non-dimensionally-exaggerated (1:1, vertical to lateral scales) geometries of the PRA region (Fig. 3-2) and the Williston Basin (Fig. 3-3) are linked to the base map modified from Beaumont *et al.* (1993). The data suggest that the entire Phanerozoic is a thin part of the lithosphere (Fig. 3-4). Any topographic relief or thickness change in the Phanerozoic is negligible on the scale of the entire lithosphere. The distance between the PRA and the centre of the Williston Basin is about 1,500 km. If the lithosphere reacts predictably, an uplift in the peripheral ring of the Williston Basin requires a load in the basin, probably ten times larger than the uplift (Beaumont, personal communication, 2000). Apparently, a few hundred metres of sediment load/unload in the Williston Basin could not generate an uplift/subsidence of the lithosphere in the PRA.

In addition to the geometry, the mechanical and thermal behavior of the lithosphere would be changed by its heterogeneous composition and faulty network. Microscopic and macroscopic geological and geophysical observations suggest that ductile faulting in the middle to lower crust and upper mantle may greatly influence the distribution and magnitude of differential stresses and the style of deformation in the overlying upper continental

lithosphere (Kirby, 1985).

A slight thinning of the crust occurs close to the axis of the Arch (from about 44 to 38 km), with a gently outward-dipping lower crustal structure and several kilometres of intermediate velocity lower crust beneath the Arch (Ross, 1990). Ross (1990) suggests that the intermediate velocity lower crust may not have been related to the thermal driving force; instead, it may have been related to a passive, flexural-isostatic origin of the PRA.

3-2-2-3. Glacial Isostatic Adjustment and Time Scale for Post-Glacial Rebound

The dynamics of the ice age Earth and post-glacial rebound have captured a growing interest and have been specifically discussed in a few publications (e.g. Pirazzoli *et al.*, 1993; Wu, 1998). "The post-glacial uplifts observed in North America, Fennoscandia, Scotland and elsewhere can be explained as retarded adjustment of the earth's interior to the removal of the Pleistocene ice-sheets in these regions" (Wolf, 1993). Glacial isostatic adjustment occurs because glaciers cause not only the warping and tilting of land around the ice sheets, but also the redistribution of the mass above and below the crust and the readjustment of the Earth to this redistribution (Wu, 1998). The time scale of glacial isostatic adjustment processes is suggested to be 0.001-0.1 m.y., which is much shorter than the long time scales of mantle convection and other tectonic processes (1-100 m.y., Peltier, 1998; Wu, 1998).

In the Cretaceous PRA region, four major abrupt 90^0 changes in strata have been documented in this thesis (refer to §4-2). These changes occurred between (1) the Lower and Upper Mannville groups, (2) the Peace River Group and Shaftesbury Formation, (3) the Dunvegan and Pouce Coupe formations, and (4) the Puskwaskau and Belly River formations.

The SW dipping (rooted in the Rocky Mountains) NW-SE striking (parallel to the Rocky Mountains) Lower Mannville Group continued for about 6 m.y. The Arch-centered Upper Mannville deposition continued for approximate 15.5 m.y. The NW dipping and NE-SW striking (perpendicular to the Rocky Mountains) of the Shaftesbury and Dunvegan formations lasted for roughly 6.5 m.y. The SW dipping (rooted in the Rocky Mountains) NW-SE striking (parallel to the Rocky Mountains) Smoky Group continued for nearly 11 m.y. The NW dipping Belly River Formation lasted for about 5 m.y.

The time scale for each of these processes is on the order of 5-15 million years and is consistent with the time scale of tectonic processes (1-100 m.y.), not glacial isostatic adjustment processes (0.001-0.1 m.y.). No documented glaciations in the Cretaceous could be correlated with the abrupt stratal changes. Furthermore, glacial isostatic adjustment or post-glacial rebound could not account for the repeated 90^0 changes in strata. Post-glacial rebound is not considered a modern analog that illustrates the time scale for basement tilting in the Cretaceous of the PRA region.

3-2-3. Phase Change

Based on deep-reflection profiles across the northern Williston Basin, Baird *et al.* (1995) suggested an origin of litho-phase change for the subsidence of the Williston Basin. In the region now underlain by the Williston Basin, a crustal root was generated during the Hudsonian collision and then incompletely eliminated by normal post-orogenic extension. "This remnant crustal keel much later underwent eclogite-facies metamorphism, which overprinted a new non-reflective Moho across the root and induced the subsidence of the Williston Basin" (Baird *et al.*, 1995).

Considering the unlikelihood of (1) PRA collapse by basement prisms floating in an extensional field (§3-2-2-1), (2) uplift of the PRA by loading in the Williston Basin (§3-2-2-2), and (3) Cretaceous basement tilting by post-glacial rebound (§3-2-2-3), litho-phase change as suggested for subsidence of the Williston Basin may have been the driving force for the anomalous behavior of the PRA in accordance with the structural anomaly in the Arch crust.

3-3. Influences on Foreland Basin Depositional Processes

In the PRA region, the orientation of sandbodies encased in marine mudstone has changed during Cretaceous time. An approximate 90^{0} change in shoreline trends took place between the Lower Cretaceous Spirit River Group (Cant, 1984; Leckie, 1984; Smith *et al.*, 1984; Rouble and Walker, 1994) and the Upper Cretaceous Cardium Formation (Wadsworth, 1989; Hart and Plint, 1990; Chen and Bergman, 1997). The origin of Cretaceous sandbodies and factors that influence foreland basin depositional processes have been the topics of many discussions. Sedimentologic interpretations (*e.g.*, offshore bars, Tillman and Martinsen, 1984) and eustatic fluctuations (*e.g.*, incised shorefaces; Bergman and Walker, 1987; Pattison and Walker, 1992; Posamentier *et al.*, 1992) have been proposed for the origin of linear sandbodies in the WCSB. Based on sandbodies stacking in particular locations, underlying tectonics were suggested by Smith *et al.* (1984), Hart and Plint (1993), Plint *et al.* (1993), and Donaldson *et al.* (1998). Subsidence and sedimentation in the foreland basin have been related to collisional events on the western continental margin (Tankard, 1986; Cant and Stockmal, 1989; Underschultz, 1991). The crustal subhorizontal reflection sequence in the PRA region has been discussed by Ross and Eaton (1996, 1997). The crustal sequence appears to have some

relation to foreland basin components.

3-3-1. Sedimentologic and Eustatic Interpretations

The sedimentologic interpretation implies that sand was transported many tens of kilometres across the shelf and deposited in the basin. There is no discussion about the effects of tectonics and/or eustatic sea level fluctuations. The sedimentologic interpretation can neither predict where sands would accumulate nor explain the frequent right angle stratal re-orientations in the PRA region during the Cretaceous. Fluctuations of relative sea level cause changes in shoreline position and accommodation space and have been suggested as a mechanism for the accumulation of sandbodies encased in marine mudstone. During transgression, shoreface position is shifted landward and accommodation space is increased. Conversely, during regression, the shoreline is shifted basinward and accommodation space is reduced. Relative sea level change accounts for the basin position of the sandbodies but does not explain the right-angle re-orientations observed in regional Cretaceous strata.

3-3-2. Underlying Tectonic Suggestions

There was periodic movement of basement structural elements in eastern Colorado during the Cretaceous that influenced Cretaceous strata (Weimer, 1978, 1980). In the Canadian portion of the WCSB, basement influence on deposition in the PRA has also been suggested (Smith *et al.*, 1984; Hart and Plint, 1993; Plint *et al.*, 1993). Hart and Plint (1993) observed stacking in particular locations of Cardium incised shoreface sandbodies. Stacking in one location would not be expected if the shoreface locations are simply related to

transgressions and regressions. Hart and Plint (1993) proposed an underlying tectonic control perhaps involving movements of Precambrian basement or reactivation of Paleozoic reef trends.

Based on observations in individual formations, several faults cut the Cretaceous Cardium and overlying Marshybank and Bad Heart formations in the PRA area (Hart and Plint, 1993; Plint *et al.*, 1993). Continuous processes of stratal change affected by basement have not been documented. Without evidence from underlying systems and basement, it is not clear if these faults affected the overlying sedimentary cover and if they are related to basement discontinuities.

Donaldson *et al.* (1998) compared the isopach pattern in the Bad Heart sandstone (Fig. 2-4A) to the aeromagnetic anomaly map (Fig. 2-4B) for the area. However, in Figure 2-4B, with the exception of Fault 3 along the southwest edge of the Kimiwan anomaly, there is no linear anomaly associated with Faults 1, 2, and 4 of Donaldson *et al.* (1998). Faults 1 and 2 cut into the Ksituan High. Foreland structures may or may not be indicated by aeromagnetic anomalies. The aeromagnetic survey records all magnetic anomalies on the Earth, including assembled basement domains, intrusive magmatic rocks, and shallow deposits of magnetite. Faults and tensile strains both horizontal and vertical could not be recorded as aeromagnetic anomalies if they do not cause sufficient magnetic differences between displacements.

The isopach of the Bad Heart Formation (Donaldson *et al.*, 1998; Fig. 2-4A) was overlain on the isopach of the same formation generated by this thesis (Fig. 3-5). The contour values and isopach patterns on both maps are consistent. Fault 2 (Donaldson *et al.*, 1998) is largely along the 10-m contour line (Fig. 3-5). The area to the northeast of the 10-m contour is

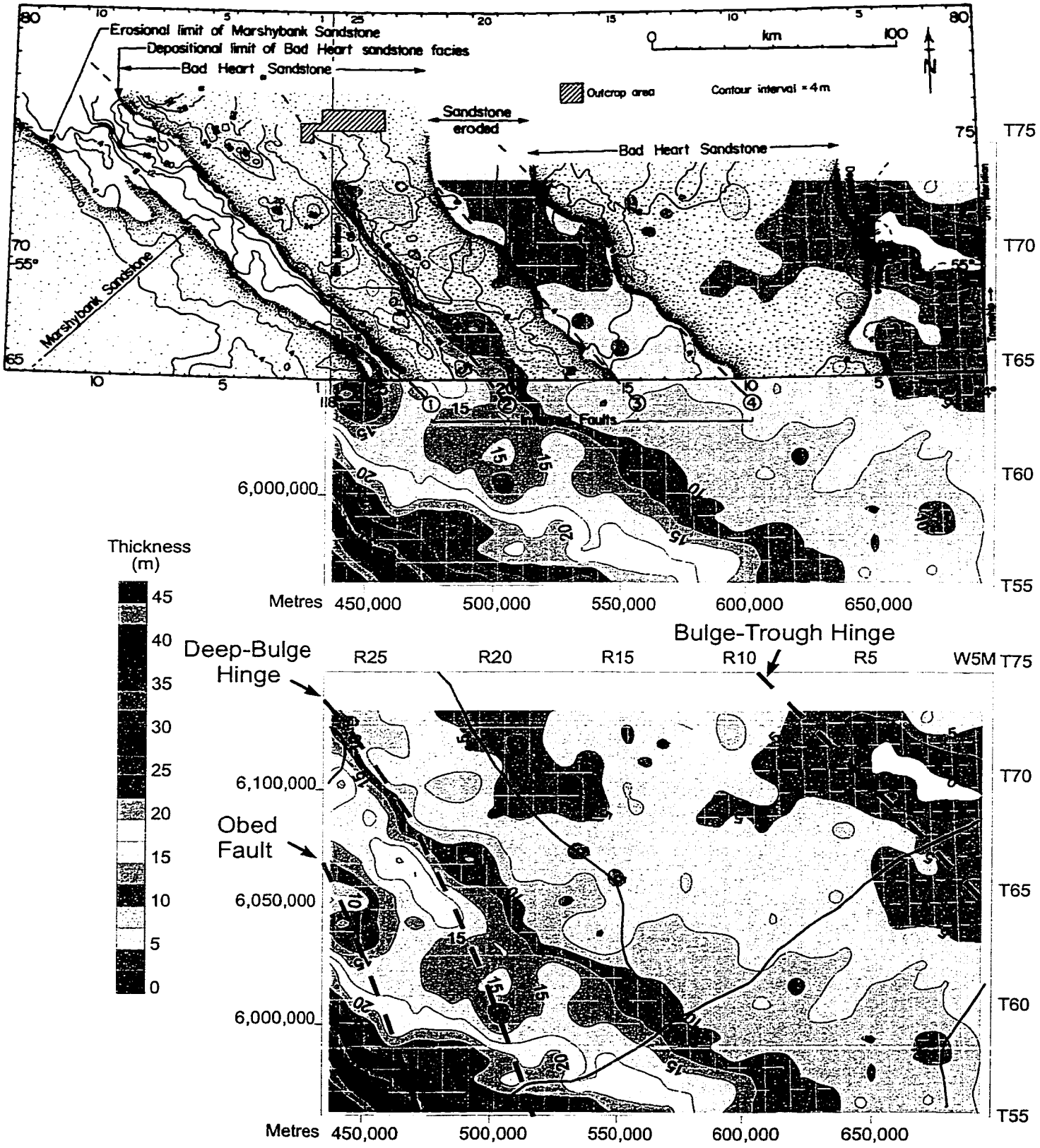

Figure 3-5. Comparison of isopach maps of the Bad Heart Formation. The black-white map derives from Donaldson *et al.* (1998) and the color map is created by this thesis. Blue line, domain boundary (refer to Fig. 1-8).

a broad shallow area with local highs delineated by 5-m contours.

This thesis documents continuous formation changes in the Cretaceous and analyzed possible influences from basement and boundary tectonic events. It is suggested that subsidence of the Bad Heart Formation was dominated by the compressional event on the western margin and that some basement faults were involved in deposition during this time.

3-3-3. Mechanism of Boundary Collisional Events

Much of the North American Cordillera is a collage of suspect terranes that seem to have collided and accreted to the North American cratonic margin mostly during Mesozoic and early Cenozoic time (Coney *et al.*, 1980). Monger *et al.* (1982) suggest that Terrane I was accreted to the cratonic margin of North America in Jurassic time and that Terrane II was accreted to the cratonic margin in middle Cretaceous time. Subsequent thrusting and northward translation on intra-plate strike-slip faults occurred primarily during Late Cretaceous to Early Tertiary time (Coney *et al.*, 1980). van der Heyden (1992) has subsequently suggested that the western Canadian Cordillera is a single composite superterrane that accreted to ancestral North America in Middle Jurassic time. In this interpretation (van der Heyden, 1992), the external adjustment in plate motion would cause regional compression along the western Canadian Cordillera during the Cretaceous. The debate surrounding whether one or two collisions have occurred on the western margin is beyond the scope of this study. For the purpose of analyzing basin floor tilting, timing of a compressional event is more important than the event itself. In terms of compression, it does not make a difference whether the compression came from terrane collisions or external adjustments in plate motion. The basin

floor was tilted, flexed, and subsided by a compressional force exerted on its boundaries. The observed formation changes record the tectonic influences and therefore could serve as a possible tool to constrain the timing of tectonic events.

Several studies (Tankard, 1986; Cant and Stockmal, 1989; Underschultz, 1991) have tried to relate sedimentation in the WCSB to stages of terrane collisions to western North America. Tankard (1986) suggested that the pulse of sediment in the Late Jurassic and Early Cretaceous was related to the accretion of terranes; thick marine shales of the mid-Cretaceous accompanied a period of tectonic quiescence; and sandstone and coal of the Upper Cretaceous were deposited in response to Laramide thrusting loading. Cant and Stockmal (1989) established a time correlation between the deposition of six clastic wedges in the Alberta foreland basin and the accretion of six terranes in the Canadian Cordillera:

(1) the Jurassic Fernie and Kootenay groups to the collision of Terrane I,

(2) the Cretaceous Mannville Group to the accretion of the Bridge River Terrane,

(3) the Dunvegan Formation to the docking of the Cascadia Terrane,

(4) the Belly River Formation to the collision of Terrane II,

(5) the Edmonton Group to the accretion of the Pacific Rim - Chugach Terrane, and

(6) the Tertiary Paskapoo Formation to the docking of the Olympic Terrane.

The collision-clastic wedge model (Cant and Stockmal, 1989) is oversimplified. There are three main problems with the model. (1) The Upper Cretaceous Cardium clastic wedge is missing. (2) There was a distinct regional stress change between the Early Cretaceous Aptian and Albian time. The model combines the Lower Mannville Group (dominated by the collisional event) with the Upper Mannville Group (dominated by PRA collapse as

documented in this study). (3) The clastic wedge of the Dunvegan Formation does not match the effect from the Cascadia Terrane accretion as shown in this thesis.

The Bridge River Terrane is a relatively small terrane that accreted to the continental margin from the southwest of the region (Fig. 2-1). The loading by the Bridge River Terrane could not be responsible for generating the accommodation space required in both Aptian (Fig. 2-3) and Albian (Fig. 2-5) time. Although both the Lower and Upper Mannville groups had abundant clastic supplies, the Lower Mannville was associated with a Rocky Mountain rooted subsidence in the southwest (Fig. 2-3); whereas, the Upper Mannville was associated with a collapse of the PRA in the northwest (Fig. 2-5), indicating a dramatic change in the regional stress field.

It is also unlikely that tectonic loading by the Cascadia Terrane, a relatively small terrane accreted in the southwest (Fig. 2-1), could cause the large scale subsidence in the northwest, coupled with the abundant clastic supply from the northwest during middle and late Cenomanian time. The large clastic wedge of the Dunvegan Formation was related to significant subsidence in the northwest (refer to Fig. 4-5A). Persistent subsidence in the southwest took place during Turonian, Coniacian, and Santonian time (refer to Figs. 4-16, 5-2R) and may have been related to the Cascadia Terrane docking in the southwest (Fig. 2-1).

3-3-4. Crustal Subhorizontal Reflection Sequence and Its Relation to Foreland Components

In the PRA region, a prominent set of subhorizontal reflections occurs between 3.5 and 18.5 km depth in the middle and upper crust, covers an area of at least 120,000 km^2, and has

been named as the Winagami Reflection Sequence (WRS, Ross and Eaton, 1996, 1997). The reflection sequence was interpreted as discordant intrusive igneous sheets (mafic suite) emplaced by a regional magmatic event during a period of brittle indentation of the western Canadian shield by the Slave province in the Late Proterozoic (1890-1760 Ma, Ross and Eaton, 1996, 1997). Seismic modeling suggests that the thickness of an igneous sheet is 70±10 m (Ross and Eaton, 1996, 1997). Figure 3-6 shows part of the WRS in Line 13 and it consists of about five subhorizontal strong reflection sheets.

Problems exist with the interpretation of the WRS as igneous intrusive sheets. On aeromagnetic maps "no lineaments likely to be associated with dikes are visible, we conclude that vertical mafic dikes are not present in the Winagami region" (Ross and Eaton, 1997). The ratio of thickness to length for a sheet in the WRS is about 1: 5,000. It is unlikely that a layer of magma with a thickness of 70 ± 10 m could intrude 120,000 km^2 in the middle and upper crust without dike/conduit during a brittle indentation.

To emplace the same volume of magma as in the WRS on an eruption basis with a very high volumetric flow rate – 500 m^3/s (Kinoshita *et al.*, 1969; Swanson, 1972; Swanson *et al.*, 1975) would take 2,664 years. The fact that mafic feeder dikes do not subcrop at the top of basement indicates that the real flow rate was much lower than the high eruption rate. So, the intrusion should have taken place over a very long time.

Magma flows by developing fractures and elastic dilations in country rocks and losing heat from itself (Kang, 1981; Delaney, 1980; Bruce and Huppert, 1990). It is the difference in temperature between melt-producing reactions that enables magma to migrate pervasively up through the orogenic crust without congealing (Brown and Solar, 1999). Mantle-derived

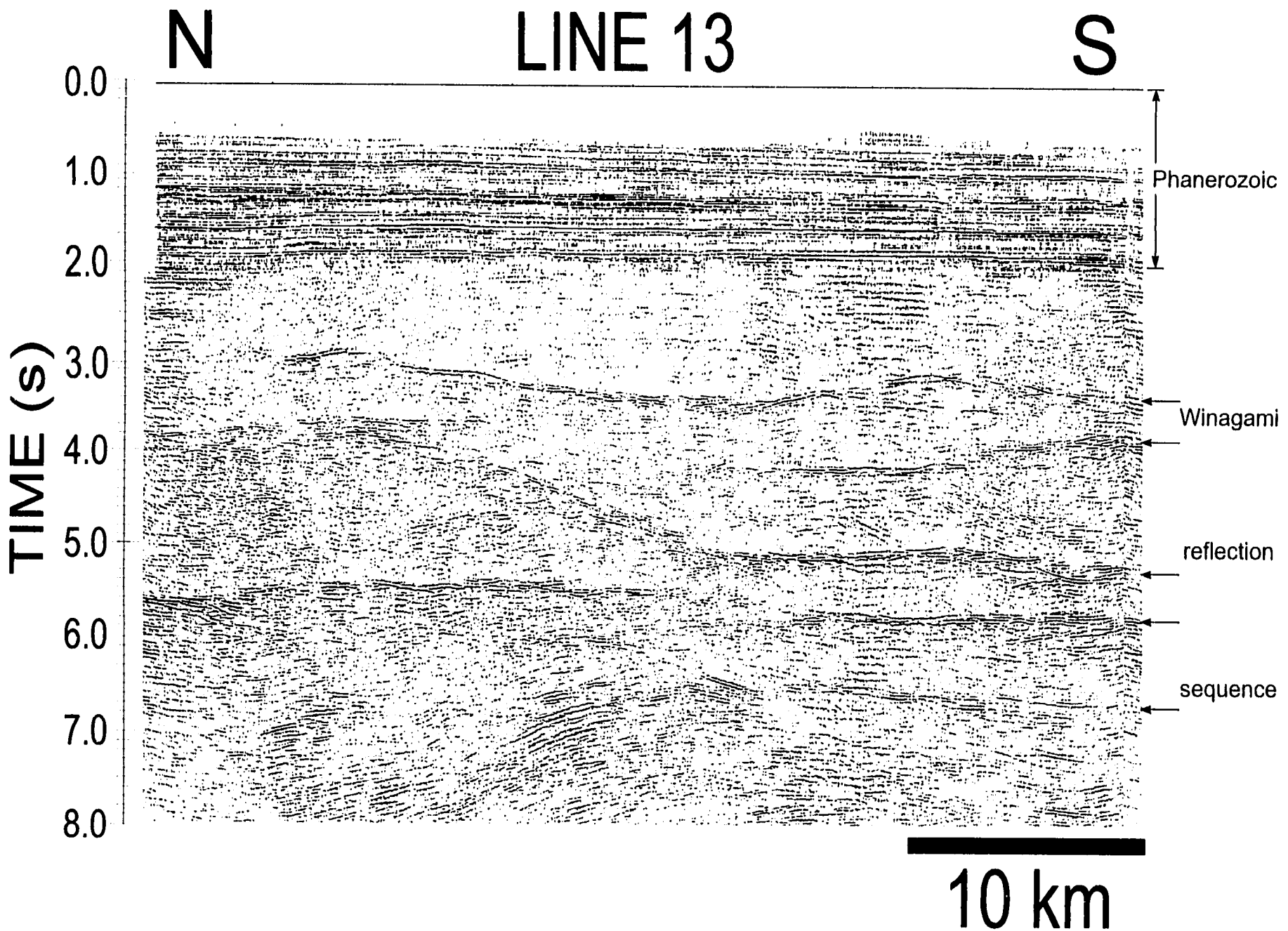

Figure 3-6. Migrated seismic section plotted almost without vertical exaggeration (refer to Ross and Eaton 1996, 1997), showing the Winagami Reflection Sequence in the south flank of the Peace River Arch. Line location, refer to Fig. 1-2.

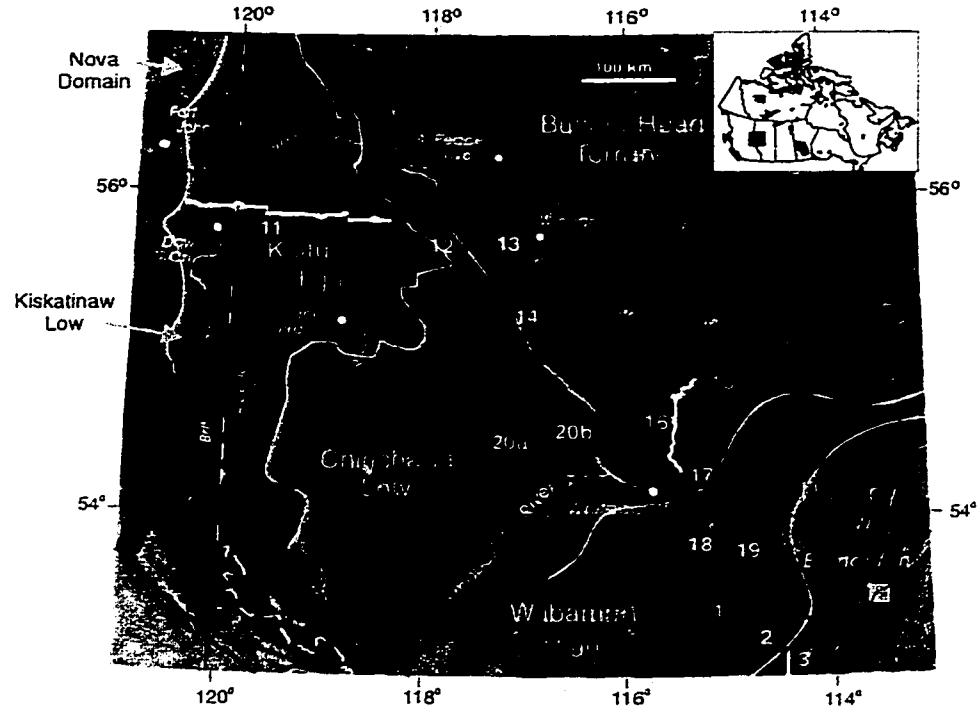

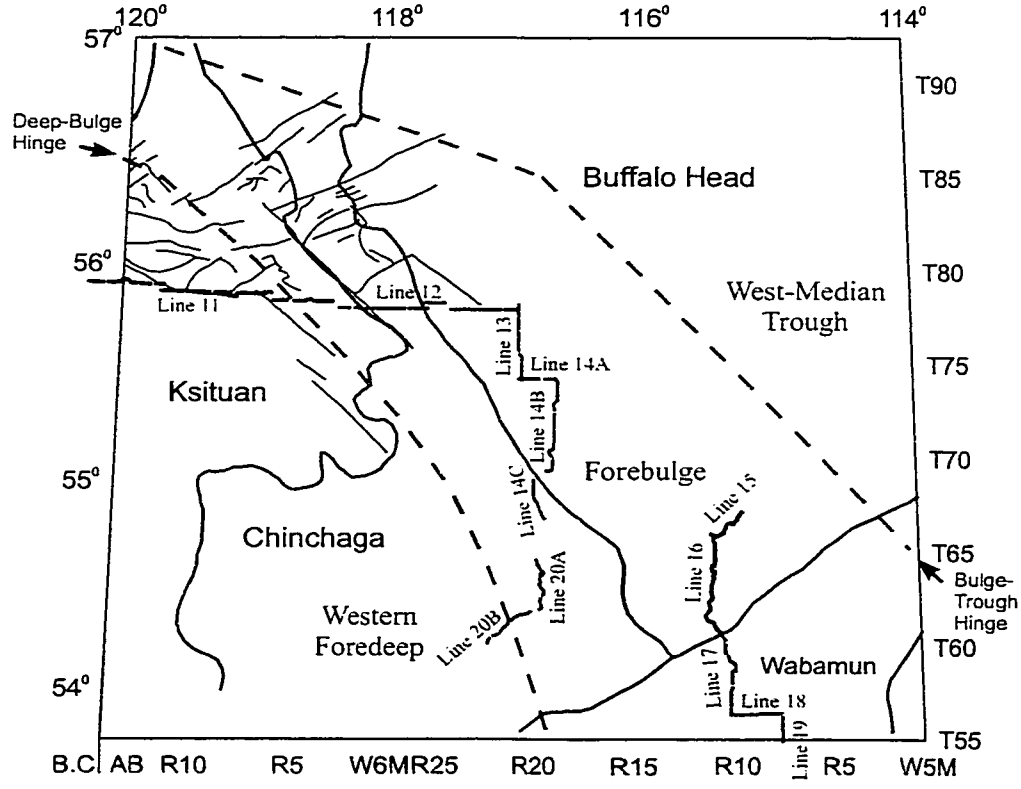

Figure 3-7. (A) Aeromagnetic anomaly data for Peace River Arch region from Ross and Eaton (1997). (B) Comparison of inferred extent of Winagami Reflection Sequence (light yellow shade) with tectonic features. Light blue line, location of Winagami Reflection Sequence. Dark blue line, Proterozoic domain boundary (Ross, 1990). Red line, Carboniferous extensional fault (Richards *et al.*, 1994). Foreland zone, refer to Fig. 2-1.

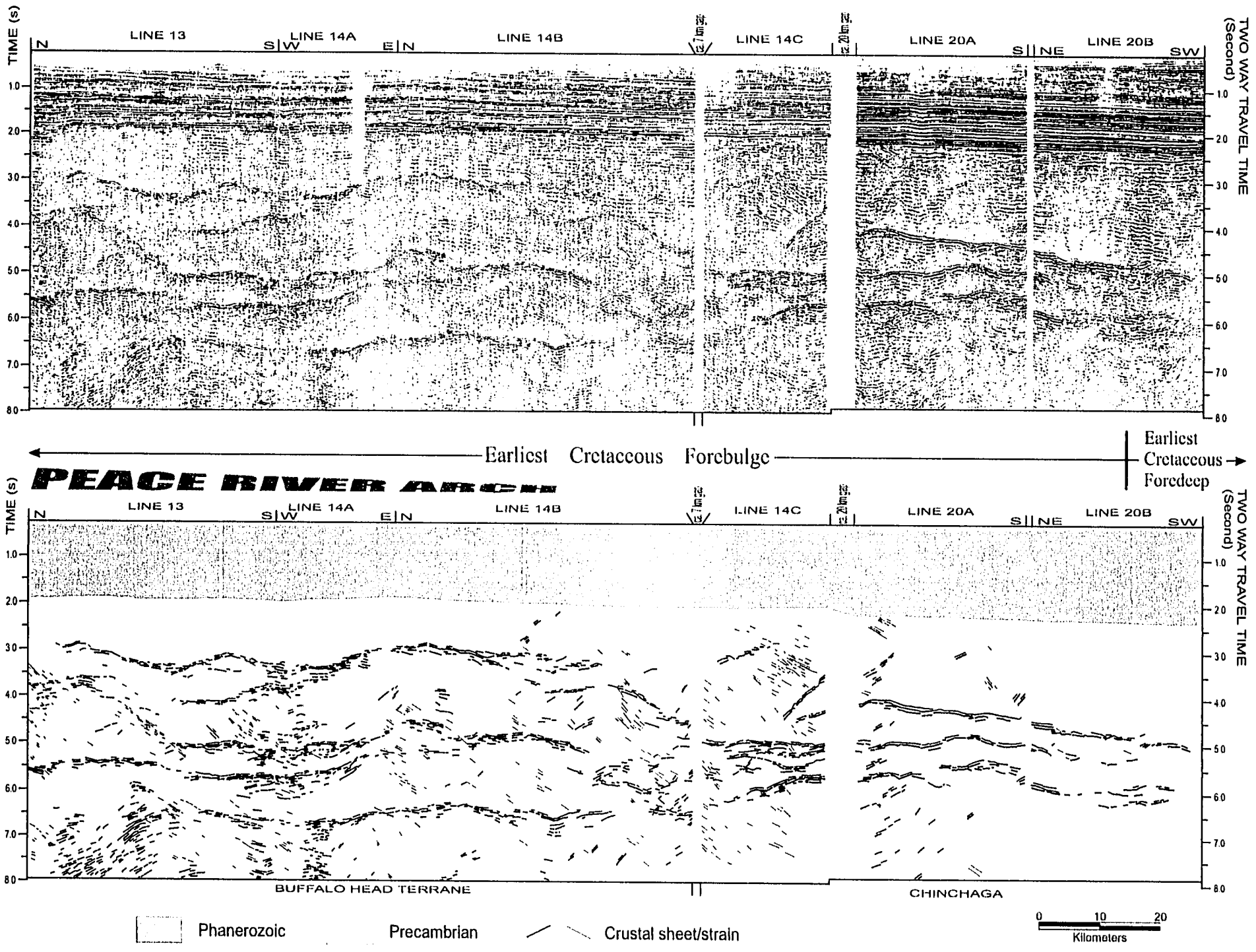

Figure 3-8. Seismic sections almost without vertical exaggeration, showing distribution of crustal reflection sheets and their relations with the Phanerozoic sedimentary cover and tectonic zones in the foreland basin. Line location, refer to Fig. 1-2.

magmas emplaced in the upper crust (depth < 10 km) are in thermal dis-equilibrium with the surrounding country rock. As a consequence of the large temperature contrasts not only will the magma cool quite rapidly, but the surrounding country rock will be heated and affected by large thermal stresses (Furling and Myers, 1985). A convective upwelling is unlikely in the upper crust because of cold temperatures and the possible presence of ground water (Ahern, 1980). In the situation of the WRS, heat convection between the magma source and the distant intrusive front is unlikely.

Temperature of magma invading the upper crust is influenced by cool host rocks over their path from source region to eventual destination. A large viscosity change corresponds to a small temperature change. For example, if the liquidus temperature of 1,200°C drops 55°C to the temperature of 1,145°C, this results in a five-fold increase in apparent viscosity (Delaney, 1980). Where the surroundings are at temperatures well below that corresponding to such an increase in viscosity, magmas flowing in dikes become stagnant due to relatively modest losses of heat. In these instances, magma can only flow very short distances, maybe on the order of only several kilometers (Delaney, 1980). Furthermore, the tabular form of the crustal sheets in the WRS maximizes heat loss and viscous drag.

The WRS is elongate and parallel to the Rocky Mountain deformation front (Fig. 3-7A). Noticeably, the WRS crosscuts Precambrian domain boundaries but coincidentally is distributed along the steeper (landward) side of the asymmetrical forebulge in the foreland basin (Fig. 3-7B). The number and volume of crustal sheets decrease toward the foredeep (SW of Line 20B) and are almost non-existent in the foredeep (Fig. 3-8), suggesting there could be an inherent relation between the WRS and the forebulge. This would require a

younger age for the WRS. The age limit of the WRS is poorly constrained (Ross and Eaton, 1996, 1997; Eaton, email, 2000), and it is possible that the age could be younger.

Figure 1-10 shows the seismic cross section crossing the south flank of the PRA. The Phanerozoic cover is elevated toward the Arch with its top eroded on the Arch. Along the seismic cross section, overall relief of the Precambrian topography is about 1,500 m. Although the thickness of formations on the PRA change as the Arch is uplifted and subsides, the polarity of the present Phanerozoic topography coincidentally corresponds to the polarity of the WRS top. There is a positive correlation between the topography of the present Phanerozoic cover and the topography of the crustal sheet top. The topographic relation between the present Phanerozoic and the crustal sheet indicates that the final uplift of the PRA and the latest modification of the WRS may have resulted from the same mechanism.

The reverse polarity in the WRS has been observed in this study (Fig. 2-13; unpublished data; Ross, Eaton, Brent, Dietrich, personal communications, 1999, 2000). It is noticeable that (1) the strong reflections of the reverse polarity are constant over a large area and insensitive to depth (frequency) changes, and (2) the high continuation of strong amplitude is developed in the reflections with reverse polarity and is not developed in the reflections with normal polarity. The origin of the reverse polarity is important to understanding the Arch origin and evolution history. Existing seismic modeling tests (Ross and Eaton, 1996, 1997) do not show a reverse polarity.

CHAPTER 4: VARIATION IN CRETACEOUS SEDIMENT

Cretaceous formations vary throughout the PRA region in terms of lithology, depositional process and orientation. For example, lithology varies not only vertically but also laterally. Siliciclastic sediments eroded from source areas are subject to reworking during transport to depositional sites. Sandbodies are incised into earlier deposits, grade basinward, and pass laterally into mudstone. Changes of regional stress fields cause the basin floor to behave in different ways, resulting in different depositional processes, progradation, aggradation, and differential subsidence. Abrupt 90^{0} reorientations of strata have been observed and may have resulted from changes in plate motion, and the direction and position from where a compressional/extensional force is exerted. More than one hundred Cretaceous isopach and structural maps were constructed during this study. The abundant stratigraphic data suggest a diverse Cretaceous depositional history in the Arch region.

4-1. Transgressive Formation Boundaries

In the Cretaceous, many traditional formation boundaries recognized by lithology are found to be time-transgressive surfaces. The characteristics of several correlation markers are modified across the basin. These markers include the sharp boundaries between the Belly River sandstone and the Lea Park shale (Fig. 4-1), the Bad Heart sandstone and the Puskwaskau shale (Fig. 4-2), and the Viking sandstone and the Joli Fou mudstone (Fig. 4-3).

The coarse clastic deposits of the Belly River Formation (Fig. 4-1) appear to interfinger with the fine clastic deposits of the Lea Park Formation. The "typical" correlation marker at

CROSS SECTION OF LOWER BELLY RIVER SANDBODIES

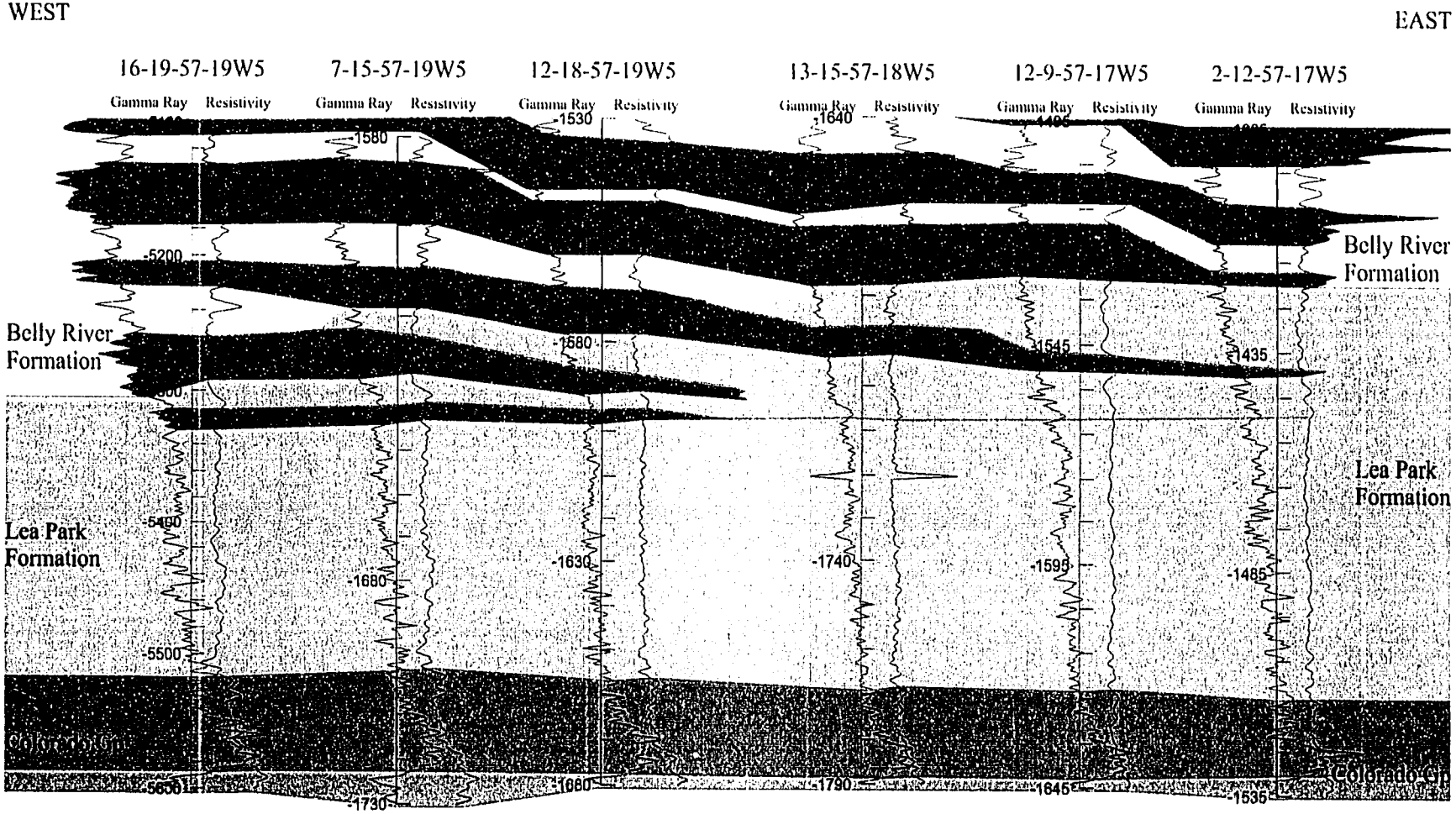

Figure 4-1. Well logs showing the diachroneity of the Belly River bottom sandbodies. The "typical" Belly River bottom marker appears to be time-transgressive.

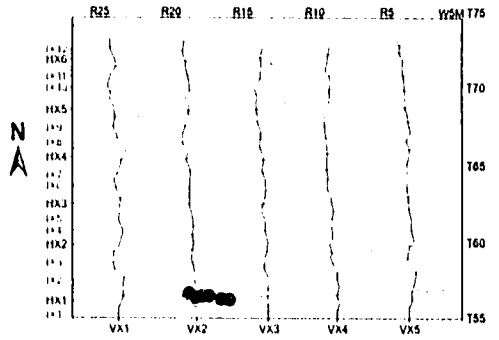

CROSS SECTION OF BAD HEART FORMATION

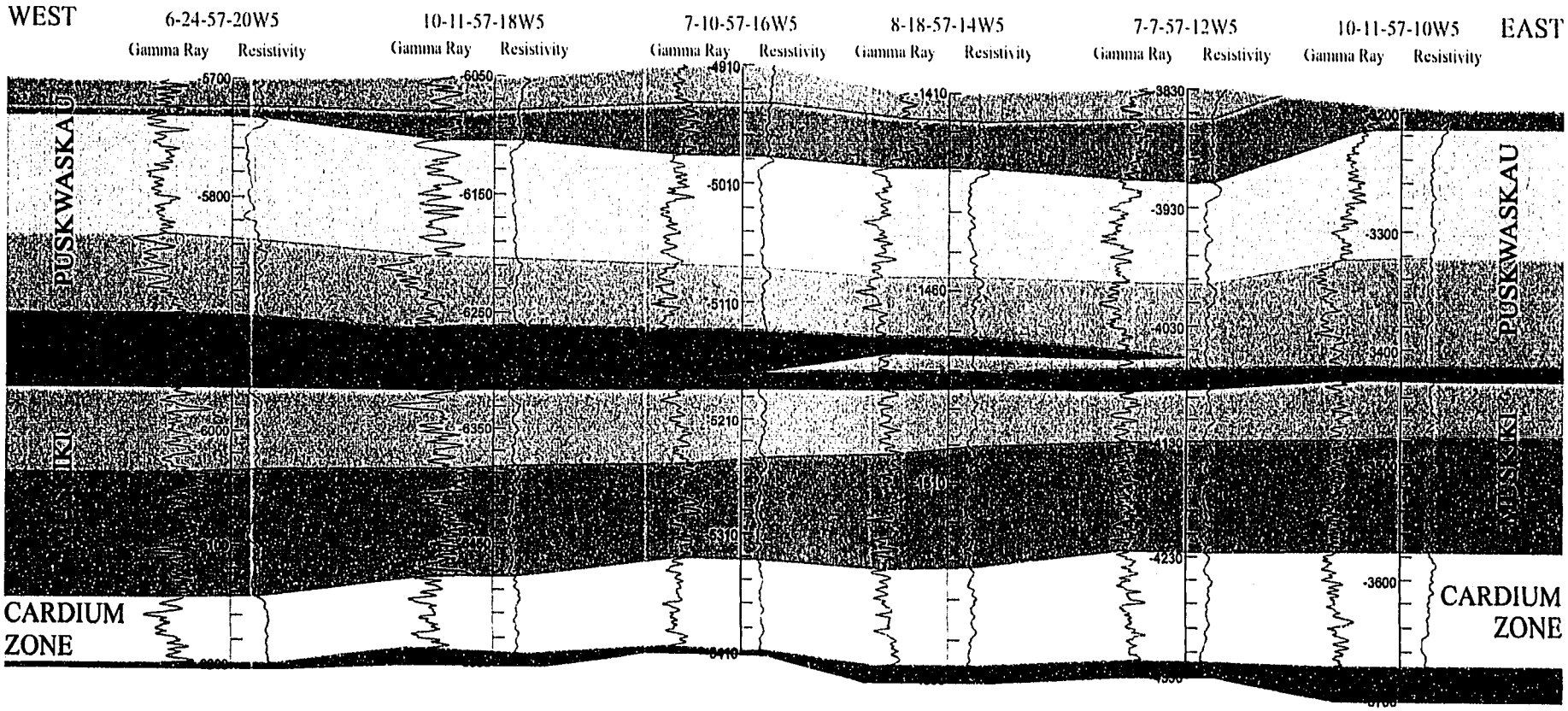

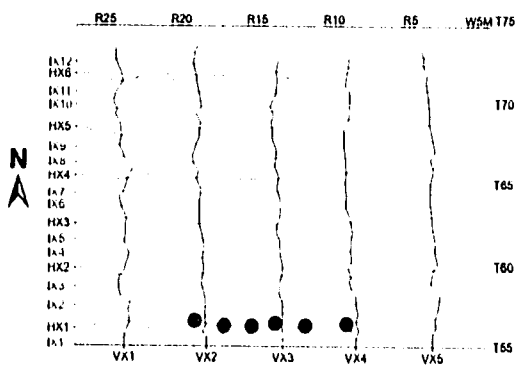

Figure 4-2. Well logs showing the diachroneity of the top of the Bad Heart Formation. The "typical" correlation marker that represents the top of the Bad Heart sandbodies at Well 6-24-57-20W5 changes character toward the east and disappears in the lower part of the Puskwaskau finer deposits at Well 10-11-57-10W5.

CROSS SECTION OF VIKING SANDSTONE AND JOLI FOU MUDSTONE

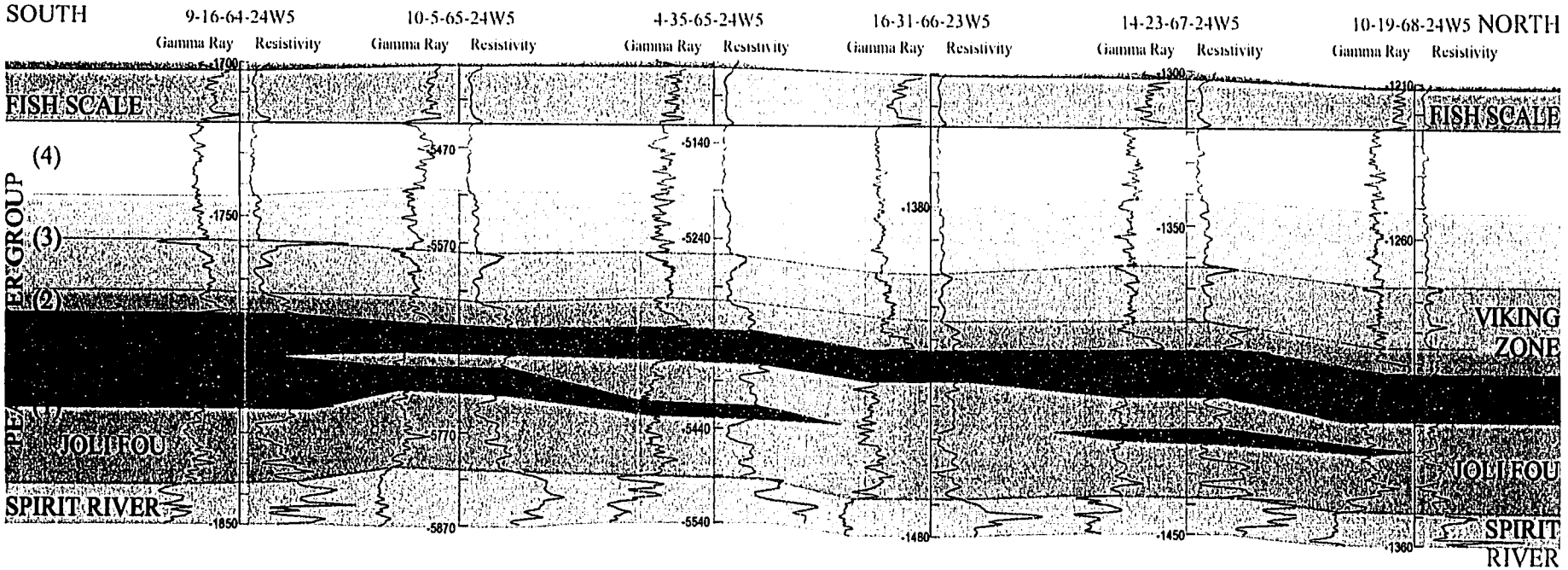

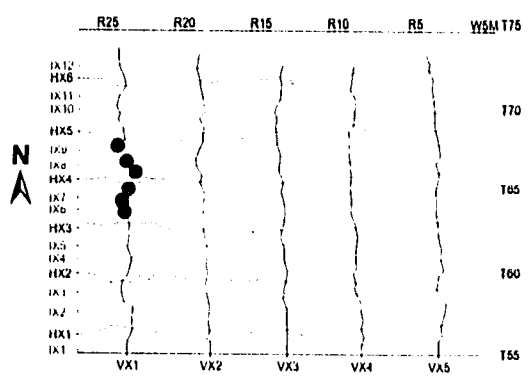

Figure 4-3. Well logs showing the correlation between the Viking and Joli Fou formations. Viking sandbodies are time-transgressive deposits. The lower Viking sandstone to the south (Well 9-16-64-24W5) gradually grades into the Joli Fou mudstone to the north (Well 6-16-68-24W5).

the base of the Belly River Formation disappears eastward in the Lea Park Formation, resulting in a diachronous boundary between the two formations. The Bad Heart sandstone (Fig. 4-2) fines toward the east and the "typical" correlation marker representing the top of the Bad Heart sandbodies at Well 6-24-57-20W5 disappears in the lower part of the Puskwaskau fine deposits at Well 10-11-57-10W5. The sandstone in the lower Viking Formation is synchronous with the Joli Fou mudstone. Figure 4-3 shows that the sandstone in the Viking Formation at Well 9-16-64-24W5 grades laterally into the Joli Fou mudstone at Well 6-16-68-24W5 toward the north.

4-2. Stratal Reorientation and Possible Controls

In the PRA region, a high angle change in shoreline trends occurs between the Lower Cretaceous Spirit River Group (NE-SW) and the Upper Cretaceous Cardium Formation (NW-SE). The time span is about 15 million years between the two formations. Much shorter time lengths for stratal reorientation have been identified in the study area. For example, the change in shoreline trends between the Dunvegan (NE-SW) and Cardium (NW-SE) formations could be as short as 2 million years.

There were three major stratal re-orientations in the Cretaceous: (1) from NW-SE in the Lower Mannville Group (Fig. 2-3) to NE-SW in the Upper Mannville (Spirit River) Group (Fig. 2-5), (2) from NE-SW in the Dunvegan Formation (Fig. 4-4A) to NW-SE in the Pouce Coupe Formation (Fig. 4-4B), and (3) from NW-SE in the lower Puskwaskau Formation (Fig. 4-5A) to NE-SW in the Lea Park (Figs. 4-5B, 3-1) Formation.

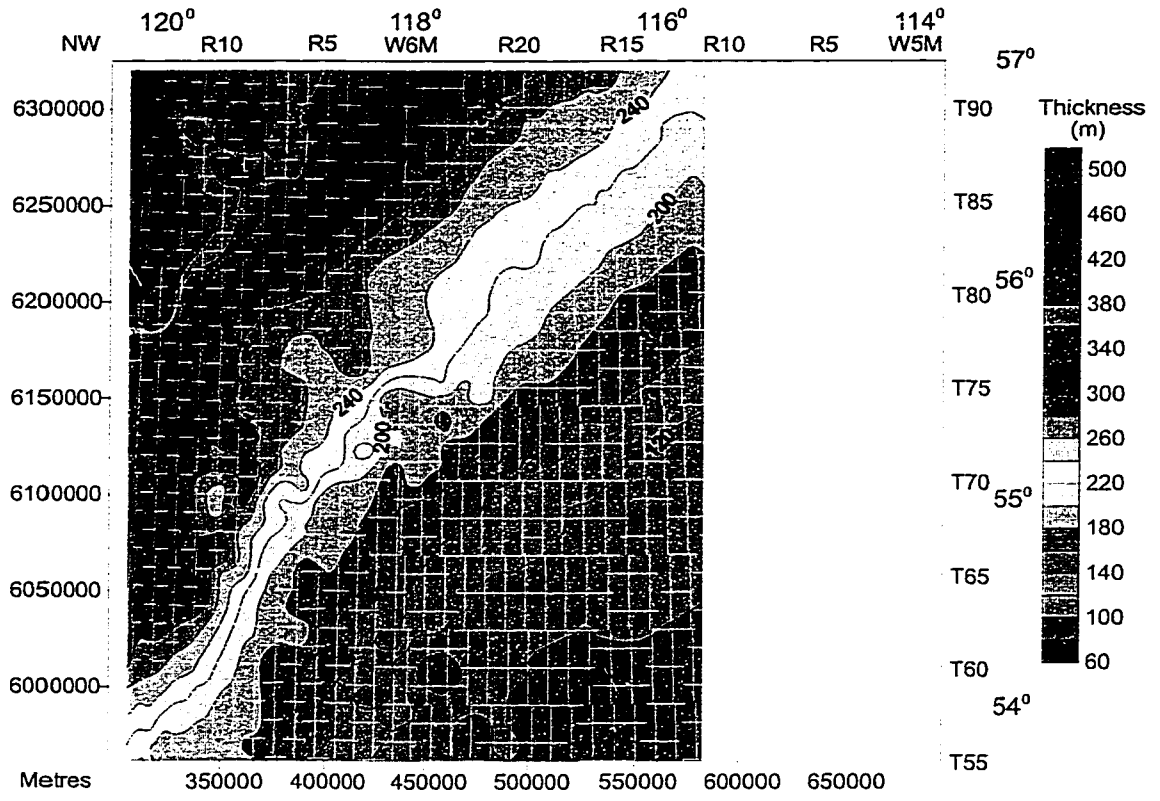

(A) Upper Cretaceous Dunvegan Formation

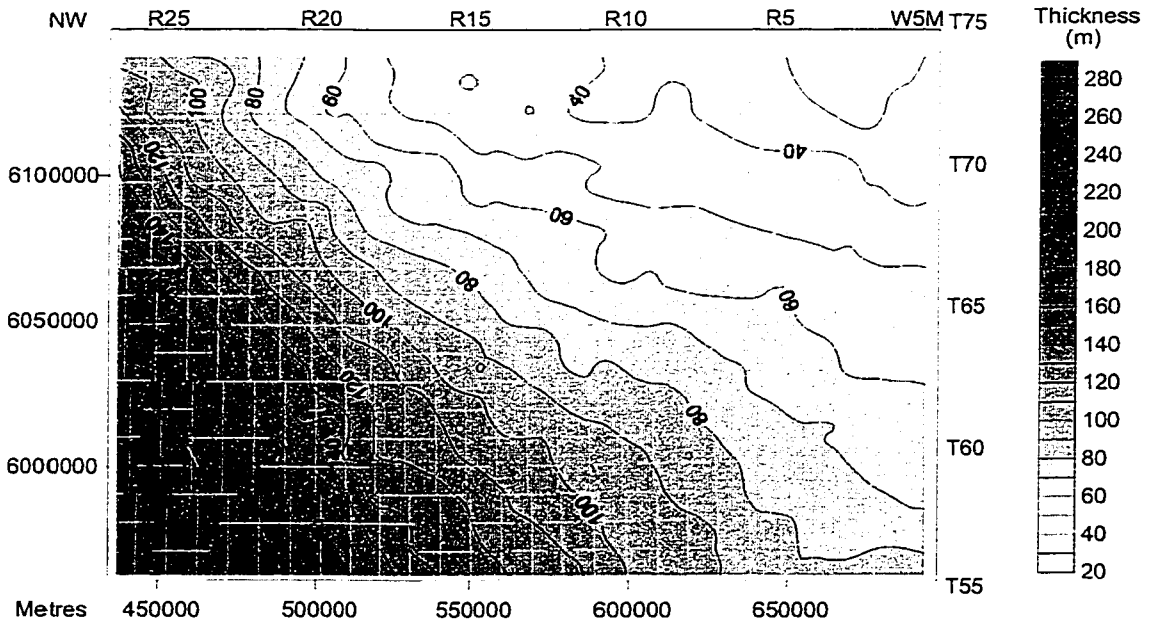

(B) Upper Cretaceous Pouce Coupe Formation

Figure 4-4. Isopach maps, showing an abrupt change of stratal orientation between the Dunvegan Formation and overlying the Pouce Coupe Formation.

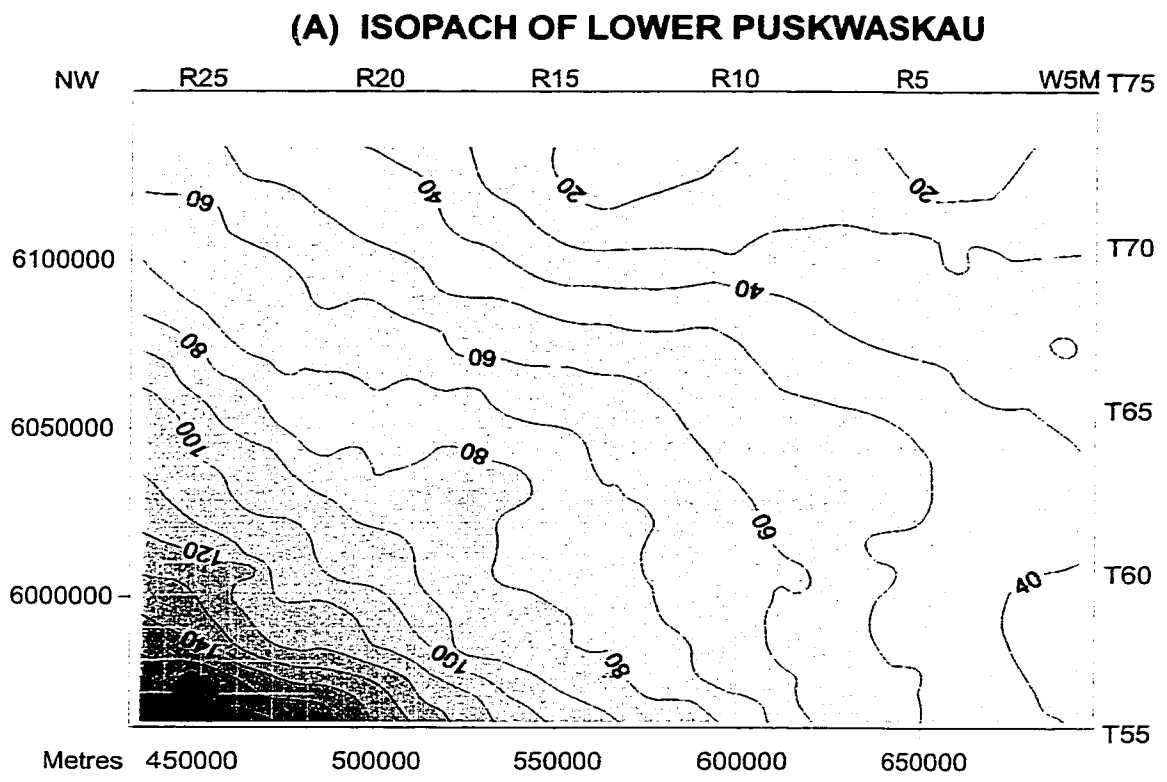

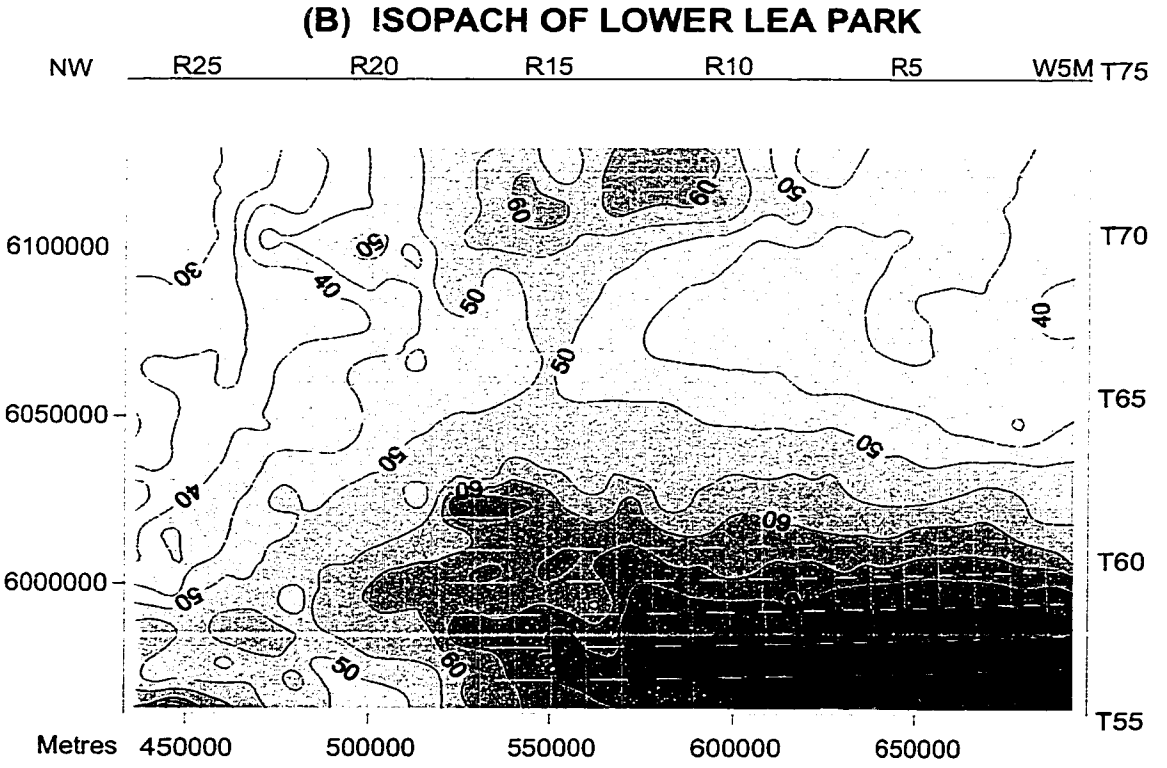

Figure 4-5. Isopachs of lower Puskwaskau and lower Lea Park formations, showing the stratal change between the formations.

4-2-1. Influence Level of Sea-Level Fluctuation, Tectonic Loading, and Sediment Supply on Deposition

Many factors, such as eustatic sea-level fluctuation, tectonic loading, and sediment supply, could affect depositional processes in the foreland basin. Eustatic sea level fluctuation could control the lithology and distribution of sediments in the basin by fluctuating shoreline position, water depth, and accommodation space. The effect of eustatic sea-level fluctuation is considerable on the margins of the basin. The following table shows mass accumulation rates for the sediments in the Alberta foreland basin (Underschultz, 1991).

Tectonic Loading	Eustatic Sea-Level	Sediment Accumulation	Sediment Distribution
Insignificant	Low	Slow	Coarse-grains cross basin
Significant	Low	Rapid	Coarse-grains cross basin
Significant	High	Rapid	Coarse-grains trapped on edges of basin, finer-grains fill in basin
Insignificant	High	Slow	Fine-grained sediments

It is suggested that tectonic loading controls the amount of sediment accumulated in the basin. Tectonic loading can control sediment supply and distribution by creating source areas in the orogen and accommodation space in the basin. A high angle stratal reorientation requires a change in the geometry of the basin floor, which is more likely caused by tectonic events. The effect of a terrane collision may provide the necessary tectonic event. For example, during the collision between Terranes I and II, one terrane may have overridden or compressed the other down to a depth of greater than 25 km (Monger *et al.*, 1982).

The amount of clastic supply from the west varies greatly with the lithology and erosion rate in the source areas. A lag effect between source areas and sediments accumulated in the basin has been suggested. "Even though Terrane I docked initially in the Jurassic, a

significant sedimentary response in the foreland basin in the study area is not seen until late Albian" (Underschultz and Erdmer, 1991). "Heating and uplift must precede thrusting and foredeep development, so a sediment source is activated before the sediment trap is effective" (Armstrong and Ward, 1993).

However, the calculation of modern orogeny erosion (Schumm, 1982) is quite different. The denudation rate is an exponential function of drainage-basin slope. The rate is about 3 feet (0.91 m) per 1,000 years in the early stage of the erosion cycle and about 25 feet (7.62 m) per 1,000 years in the modern orogeny. The largest daily load of sediments transported by the Colorado River is 15.8 x 10^6 tons (Wolman and Miller, 1982). It is about 6 x 10^6 m^3/d according to the Soil Mechanics Laboratory, University of Maine (i.e., most soils have a specific gravity of about 2.60-2.80 g/cm^3, http://umeciv.maine.edu). An average sedimentation rate is 6.3 m/ka from the Mackenzie River during the last 11 ka according to preliminary estimates based on pollen data (Duk-Rodkin and Hughes, 1994). In each process, the producing rate of erosion, transportation and deposition could be very high. An orogeny could be responsible for contemporaneous accumulation the same time of siliciclastic sediments trapped in the basin.

For example, in the study area, the maximum thickness of the Cardium Formation is about 90 m (Fig. 2-7) and was deposited during 0.5 m.y. The accumulation rate is about 0.18 m/ka and is much slower than the denudation rate of the modern orogeny (7.62 m/ka, Schumm, 1982). There could be no time delay for sediments to be denuded in the orogen and then trapped in the basin during the Cardium.

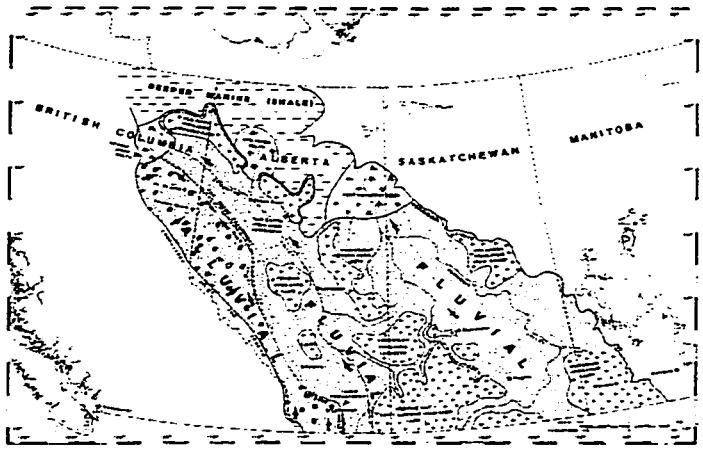

(A) Cadomin, Ellerslie, Gething, and Dina formations

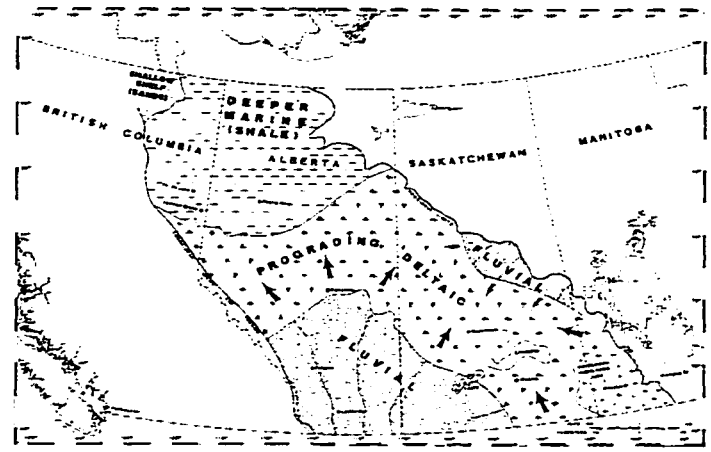

(B) Upper Mannville, Rex, General Petroleum, Waseca, and Clearwater formations and Falher Member of the Spirit River Formation

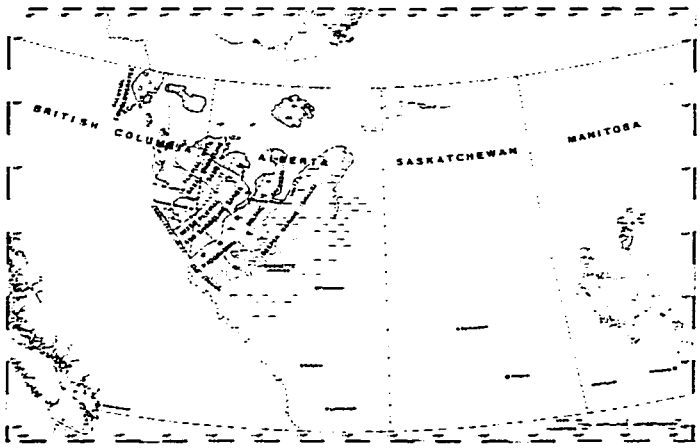

(C) Dunvegan Formation

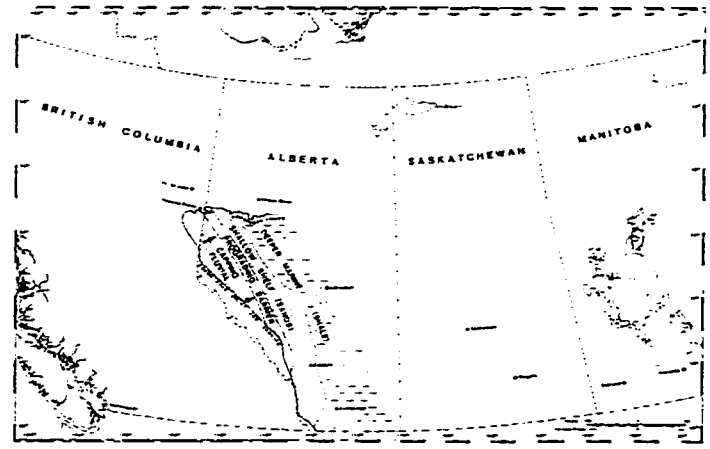

(D) Cardium Formation

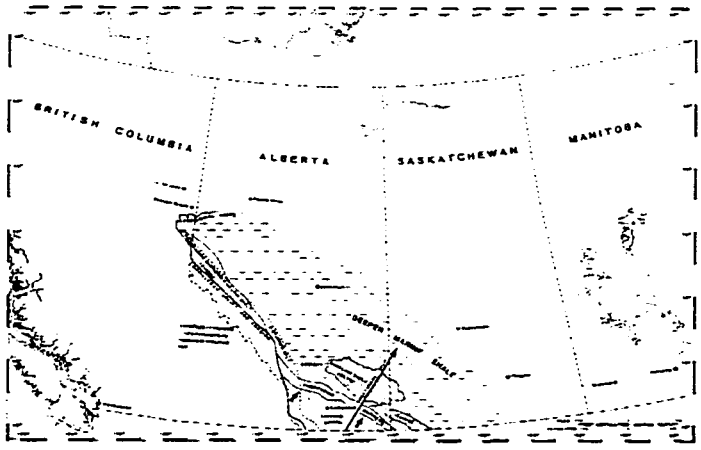

(E) Milk River Formation and Chungo and Chinook members

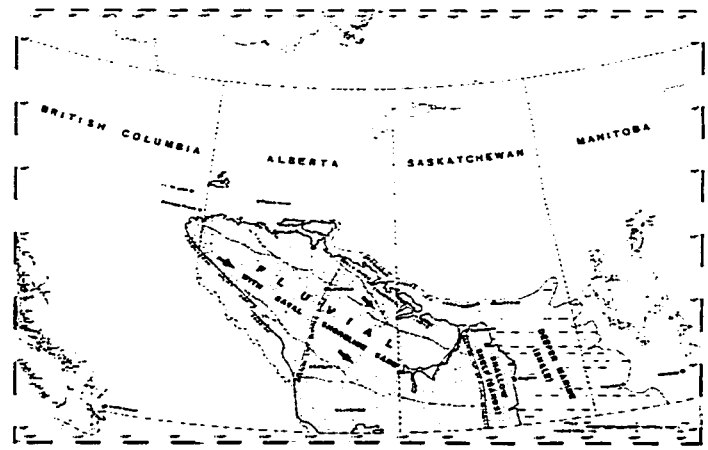

(F) Belly River Formation and equivalent units

Figure 4-6. Cretaceous paleogeographic reconstructions (modified from Leckie and Smith, 1992).

4-2-2. Stratal Change between Lower and Upper Mannville Groups

On the southeast flank of the PRA, there is a sharp change in stratal trend between the overlying Lower Mannville Group (NW-SE, Fig. 2-3) and Upper Mannville Group (NE-SE, Fig. 2-5). Paleogeographic reconstructions (Leckie and Smith, 1992) are shown in Figure 4-6 to compare the observed stratal changes with the depositional environments. In Lower and Upper Mannville groups, both isopach patterns and paleogeographic environments are distinct. The Lower Mannville Group (Fig. 2-3) shows evidence for a Mountain-rooted subsidence in the southwest and the Upper Mannville Group (Fig. 2-5) appears to be controlled by the PRA collapse. During Aptian time (Lower Mannville), facies prograded northeastward from alluvial to fluvial facies, striking NW-SE, parallel to the basin margin (Fig. 4-6A). The maximum thickness of the group was contained in coarse alluvial deposits in the foredeep along the Rocky Mountain deformation front. In contrast, during early Albian time (Upper Mannville), facies prograded northwestward from fluvial, prograding deltaic, to deeper marine (shale) facies, striking E-W, parallel to the PRA long axis (Fig. 4-6B). The maximum thickness of the group was contained in fine marine shale in the Peace River Embayment.

The stratal trend and isopach pattern of the Lower Mannville Group (Fig. 2-3) is comparable to those of the Jurassic Fernie Group (Fig. 4-7). Both groups are interpreted to have been strongly influenced by boundary tectonics and basement structures. The subsidence in the southwest was dominated by collisional events in the Canadian Cordillera (Terrane I and the Bridge River Terrane, Monger *et al.*, 1982). The Deep-Bulge Hinge affected deposition in both the Cretaceous Lower Mannville Group and the Jurassic Fernie Group. On the contrary, the stratal trend and isopach pattern of the Upper Mannville Group (Fig. 2-5) is comparable to

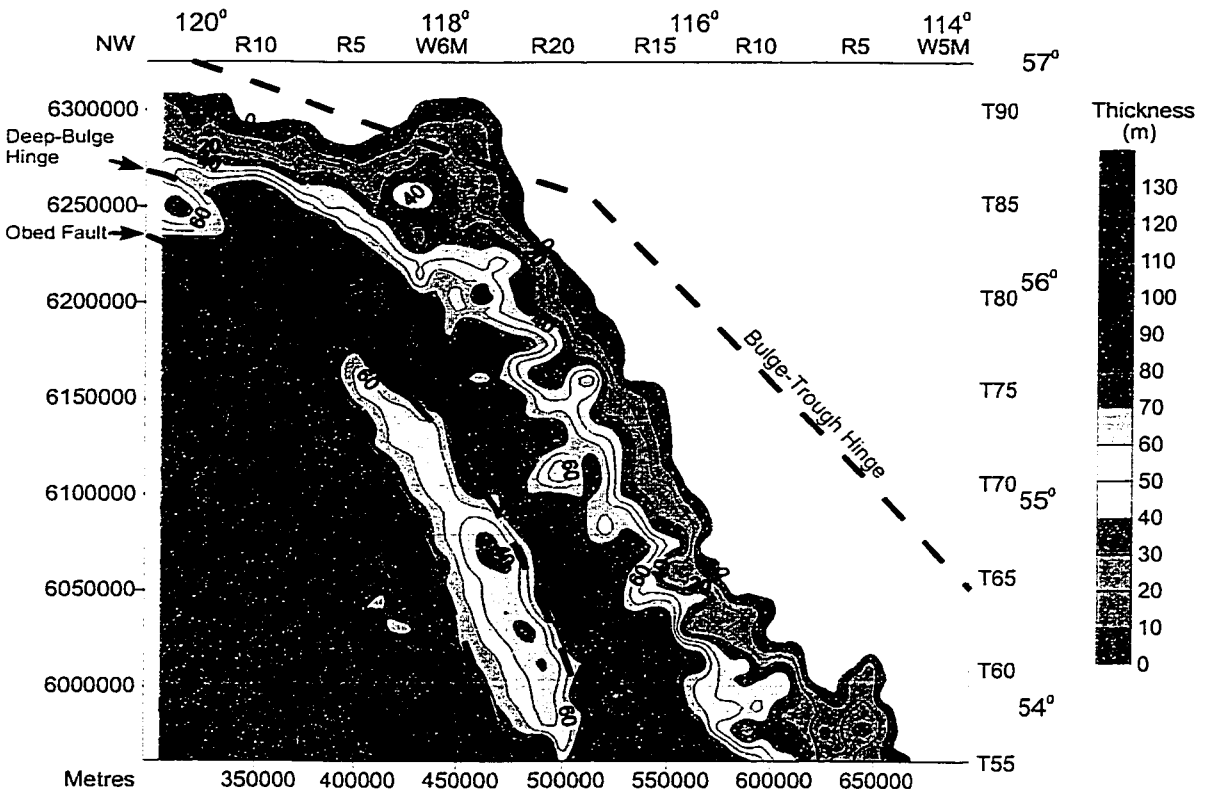

(B) Jurassic Fernie Group

Figure 4-7. Isopach map of Jurassic Fernie Group, showing stratal trends and isopach patterns influenced by basement and boundary tectonics.

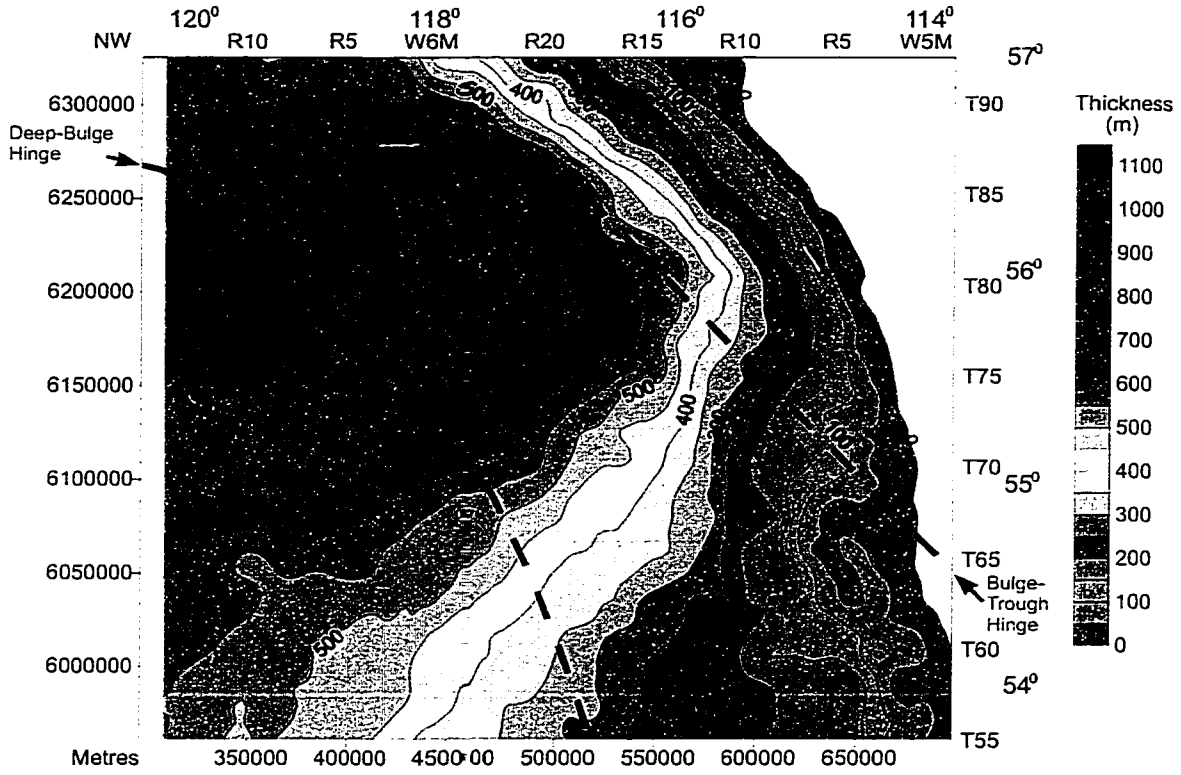

Figure 4-8. Isopach of Carboniferous, showing isopach pattern and change of stratal trends controlled by collapse of the Peace River Arch. Red line, Carboniferous extensional faults (Richards *et al.*, 1994).

those of the Carboniferous (Fig. 4-8) which was associated with regional extension. Both isopach maps show a dish-shaped pattern caused by collapse of the PRA. The stratigraphic trends are parallel to the long and short axes of the Arch.

The stratal change between Aptian and Albian time is interpreted to mark a shift in the regional stress field from compressional to extensional regime. The compressional effect from the collisions of Terrane I and the Bridge River Terrane waned and the mechanics causing the PRA collapse during the Paleozoic appear to have become dominant.

4-2-3. Stratal Change between Dunvegan and Pouce Coupe Formations

Following the Upper Mannville (>400 m, Fig. 2-5) and the Peace River (>200 m) groups that stacked in the same depo-centre in the Peace River Embayment/Inlet (refer to Fig. 5-3), the Shaftesbury/Dunvegan formations were deposited and continuously thicken toward the NW with stratal strike NE-SW (Fig. 4-4A). There is no apparent collapse of the PRA recorded on the Dunvegan isopach map, indicating that the northwest thickening was free from Arch related tectonism. The stratal trend shifted at a right angle to NW-SE in the overlying Pouce Coupe Formation (Fig. 4-4B). The NW-SE trend is present for most of the Smoky Group (Fig. 1-5) with the exception of the Cardium Formation on and around the Arch crest (Fig. 2-7B).

During Cenomanian time (Shaftesbury, Dunvegan, and part of the Doe Creek), facies prograded southeastward from fluvial, shoreline, prograding deltaic, to deeper marine (shale) facies and strike NE-SW (Fig. 4-6C). The maximum thickness of the formation was contained in coarse fluvial deposits in the northwest (>500 m). In contrast, during Turonian time

(Cardium), facies prograded northeastward from capping fluvial, prograding barrier, shallow shelf (sandstone), to deeper marine (shale) striking NW-SE, parallel to the basin margin (Fig. 4-6D). The maximum thickness of the formation was contained in coarse capping fluvial deposits along the Rocky Mountain deformation front in the southwest. Subsidence was in the southwest during Turonian, Coniacian, and Santonian time (>1,000 m).

Global sea level was rising from the Cenomanian to Turonian stage and fell in late Turonian (Fig. 1-5). The transition point of global sea level from rise to fall (in uppermost Pouce Coupe) does not match the stratal re-orientation time (between Dunvegan and Pouce Coupe). The abrupt regional changes in (1) stratal orientation, (2) location of major subsidence, (3) siliciclastic supply areas, and (4) out building direction of sedimentary facies are unlikely related to purely sedimentologic and/or eustatic processes during Cenomanian and Turonian time. The observed changes require tilting of the basin floor and shifting of the source area driven by a tectonic event.

Available tectonic events during Middle Cretaceous time include: (1) Cordilleran magmatic episode (greatest extent of magmatism in Canada at about 95-90 Ma in middle Cenomanian – earliest Turonian time), intense crustal shortening, and culmination of seaway expansion in the Western Interior Basin (Armstrong and Ward, 1993), (2) oblique convergence of plate boundaries (Coney et al., 1980; van der Heyden, 1992; Monger, 1983), (3) drifting of the Canada Basin continental margin that began by the end of Albian time (Dixon, 1993), and (4) docking of the Cascadia Terrane on the continental margin (Monger *et al.*, 1982). An oblique convergence of plate boundaries and drifting of the Canada Basin continental margin may have been responsible for the regional northwest tilting of the seafloor during

Cenomanian time. The oblique convergence of plate boundaries and docking of the Cascadia Terrane on the continental margin may have been responsible for the regional southwest tilting of the seafloor during Turonian time.

4-2-4. Stratal Change between Puskwaskau and Lea Park Formations

There was a change in stratal orientation between the Puskwaskau (Fig. 4-5A) and overlying Lea Park (Fig. 4-5B) formations on the southeast flank of the PRA. The lower Puskwaskau Formation trends NW-SE and subsidence remained in the southwest. The overlying Lea Park Formation trends roughly E-W with the depo-centre in the southeast. The paleogeographic reconstruction of the lower Puskwaskau Formation (Fig. 4-6E) shows facies lithologies that are finer but the facies distribution is similar to that of the Cardium Formation. Overlying the Lea Park Formation with a diachronous basal boundary (Fig. 4-1), the Belly River Formation was deposited as a large clastic wedge thickening northwestward (Fig. 3-1) while the Lea Park Formation was thinning toward the northwest. The siliciclastic sediments in the Lea Park and Belly River formations were shed eastward into the basin (Fig. 4-6F).

Global sea level was constantly high during Campanian time (Fig. 1-5) though stratal trend change are recorded between the lower Puskwaskau Formation and overlying Lea Park Formation and the lithologic change between the Lea Park Formation and overlying Belly River Formation. The changes in stratal orientation and lithology require basin floor tilting and source area alteration, which were very likely related to a tectonic event. Available tectonic events include (1) a minor culmination of magmatism in Canada at about 75 Ma to 80 Ma (middle to late Campanian, Armstrong and Ward, 1993), (2) northward translation along

the continental margin on dextral strike-slip faults in Campanian time (Monger, 1993), (3) accretion of the Insular Superterrane (Terrane II, Monger *et al.*, 1982; Cant and Stockmal, 1989) to western North America. The continental margin translation and Terrane II docking may have been responsible for the basin floor tilting and source area alteration during Campanian time.

4-3. Stacking Processes of Sediments

On the southeast flank of the PRA, three different stacking processes of sediments were recognized on the isopach maps, (1) linear progradation of elongate zones, (2) differential subsidence of blocks, and (3) aggradation (Figs. 4-9 to 4-16). During linear progradation, elongate depositional zones migrated back and forth in the direction perpendicular to the tectonic front. During differential subsidence, quadrilateral blocks subsided differentially across basement faults. During aggradation, the whole basement floor functioned as a uniform sheet and subsided.

4-3-1. Linear Progradation of Elongate Zones

The Cardium Formation can be described as a clastic wedge that was deposited along the western margin of the WCSB, and a stack of several allomembers defined by widespread erosion surfaces with undulatory topography of long, linear, erosive lows parallel to the basin strike (NW-SE) and asymmetrical steps that are consistently steeper on the landward (SW) side. The basin floor was uplifted in the southwest and then gradually subsided again; the

CROSS SECTION OF UPPER CRETACEOUS CARDIUM FORMATION

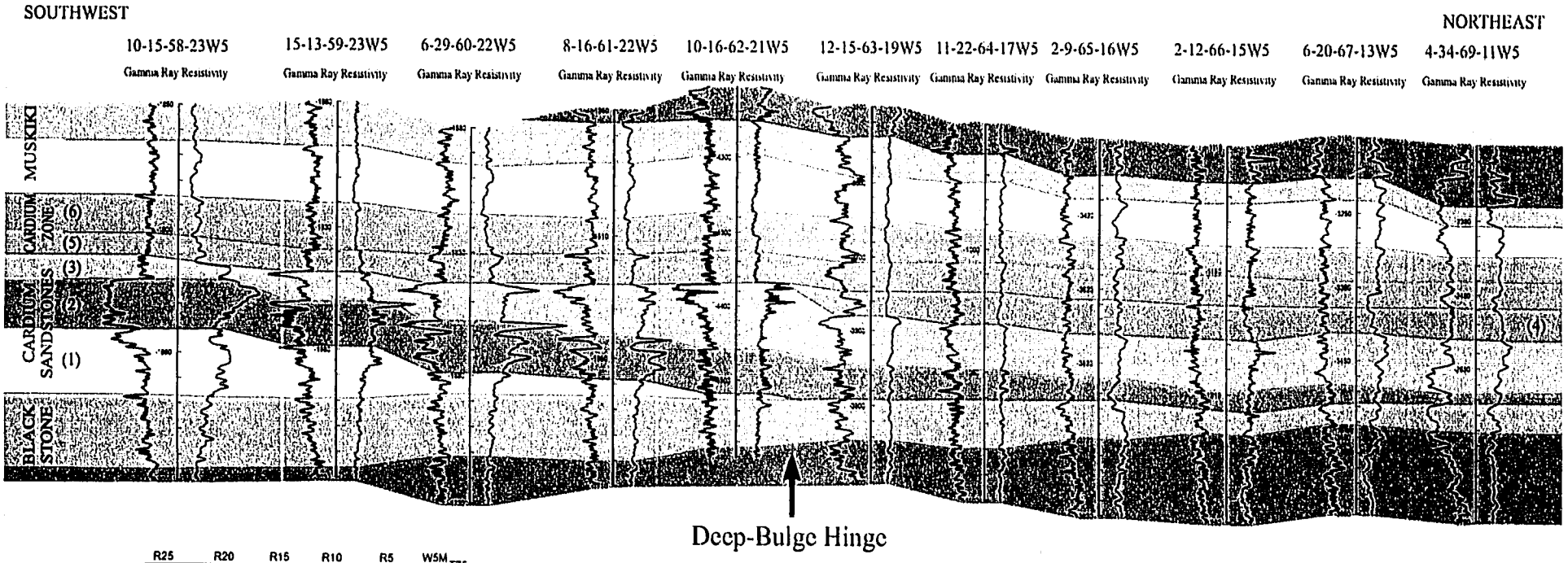

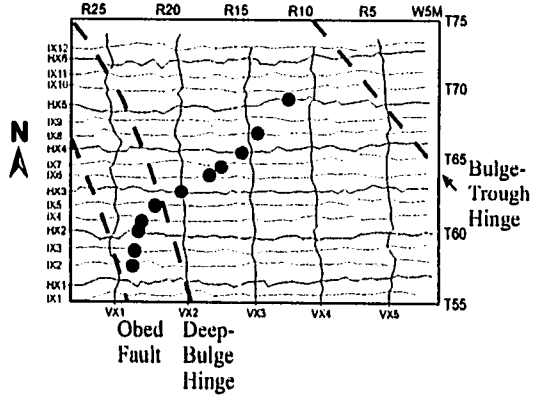

Figure 4-9. Well log cross section of the Upper Cretaceous Cardium F ormation, showing stratigraphic changes across the Deep-Bulge Hinge (Fox Creek Escarpment, Leckie and Smith, 1992; Fault 2, Donaldson *et al.*, 1998). Black dot, well location. Number, mapping unit in Figure 4-10.

LINEAR PROGRADATION OF ELONGATE DEPOSITIONAL ZONES

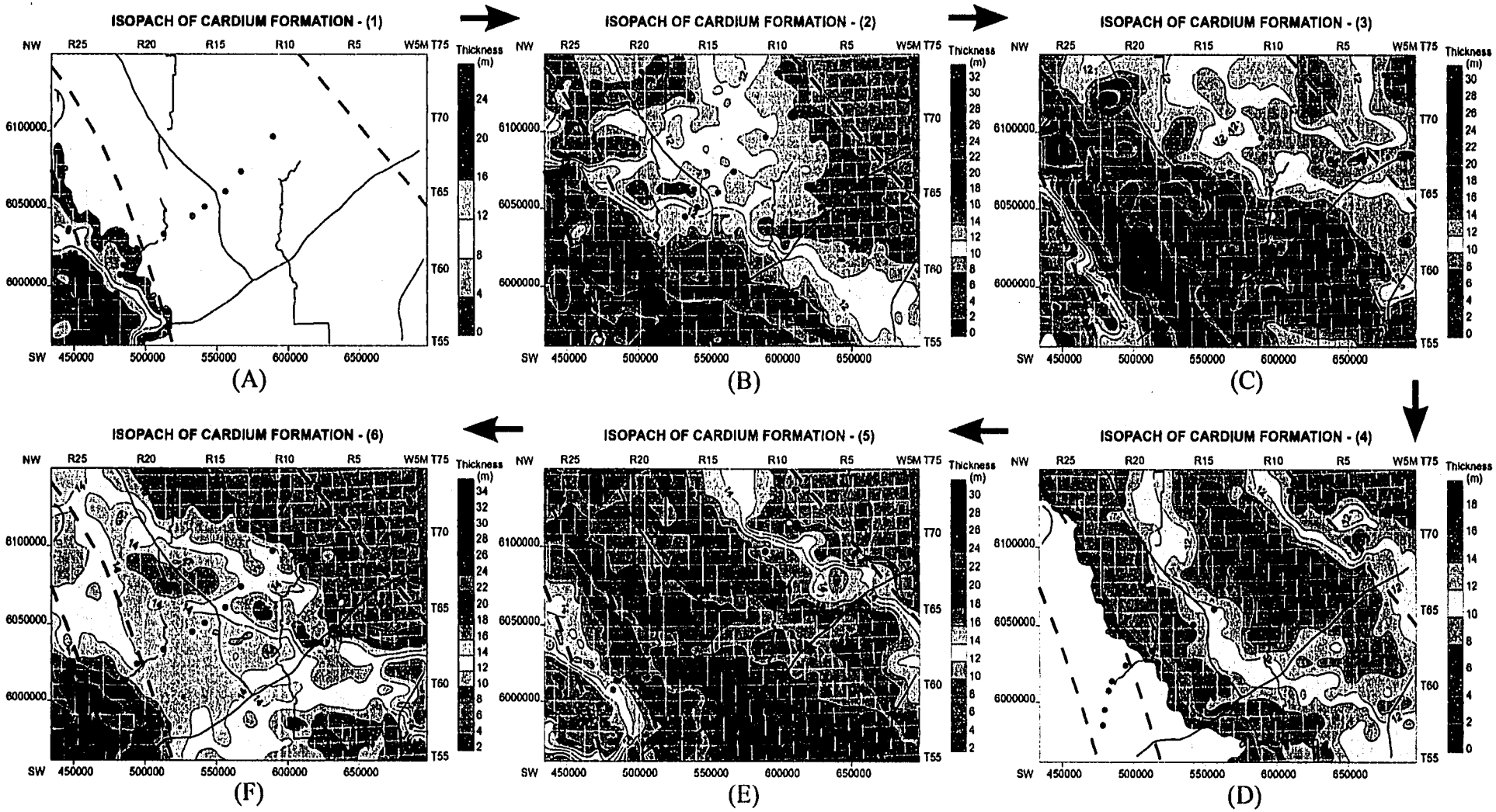

Figure 4-10. Isopach maps of the Upper Cretaceous Cardium Formation, showing linear progradation of elongate depositional zones. Red dot, location of well in Figure 4-9. Dashed red line, fault (refer to Fig. 2-1). Purple line, seismic line (refer to Fig. 1-2). Blue line, Proterozoic domain boundary (refer to Fig. 1-8). Number with formation name, refer to Figure 4-9. Red arrow toward an overlying succession.

shoreface was "moved" out into the basin and a series of stepped shorefaces were carved into the tilted sediments (Wadsworth, 1989). Observations of the Cardium Formation in this thesis (Figs. 4-9, 4-10) are consistent with Wadsworth's (1989) descriptions. The Cardium Formation on the southeast flank of the PRA shows elongate zones of linearly prograding sandbodies from the Cordilleran deformation front to the basin and then retreating back to the margin.

The shoreface translation back and forth could be explained by the process of regression and transgression during a cycle of sea level fall and rise. However, Cardium incised shoreface sandbodies are commonly stacked in particular locations (Hart and Plint, 1993) and their spatial extent and shifting show a relation to the foreland basin zones divided by basement discontinuities (i.e., Obed Fault, Deep-Bulge Hinge, Chinchaga-Buffalo Head Boundary, and Bulge-Trough Hinge).

The cross section in Figure 4-9 illustrates six correlated Cardium successions. The trend of the cross section is normal to the strike of the formation and the Deep-Bulge Hinge. The intersection of the Hinge and the cross section is between Wells 10-16-62-21W5 and 12-15-63-19W5. Thickness and log signatures of the successions vary gradually along the cross section but change abruptly across the Deep-Bulge Hinge. The Hinge coincides with the thinning of Succession 1 to zero (Fig. 4-10A) and the beginning of Succession 4 (Fig. 4-10D). Driven by tectonic loading and unloading, the elongate zones slivered by basement discontinuities were uplifted and subsided sequentially, resulting in migration of the forebulge basinward and subsequently landward.

CROSS SECTION OF LOWER UPPER CRETACEOUS

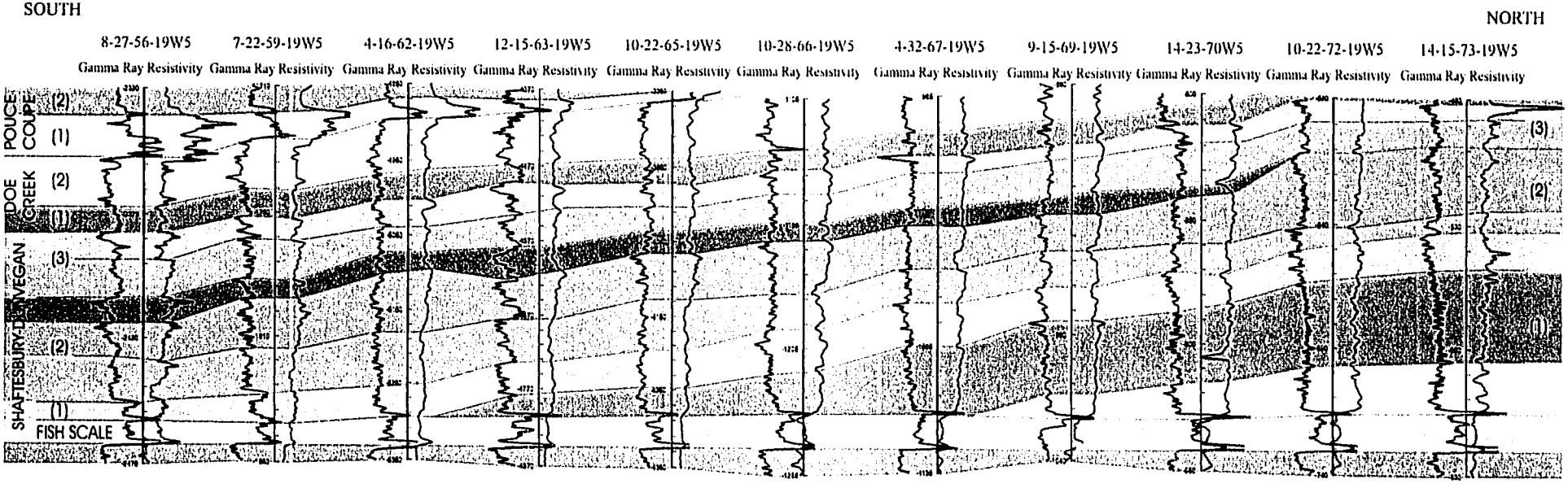

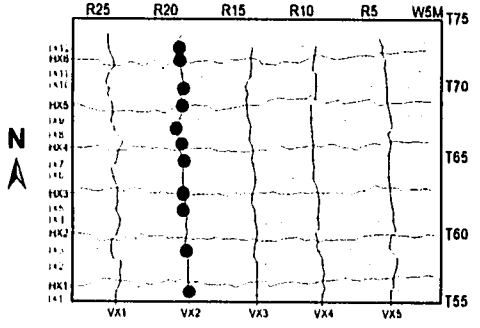

Figure 4-11. Cross section of lower Upper Cretaceous formations, showing changes of log signatures and thicknesses toward the Peace River Arch in northwest. Number, mapping unit in Figure 4-12. Black dot, location of well in the cross section.

DIFFERENTIAL SUBSIDENCE OF BLOCKS

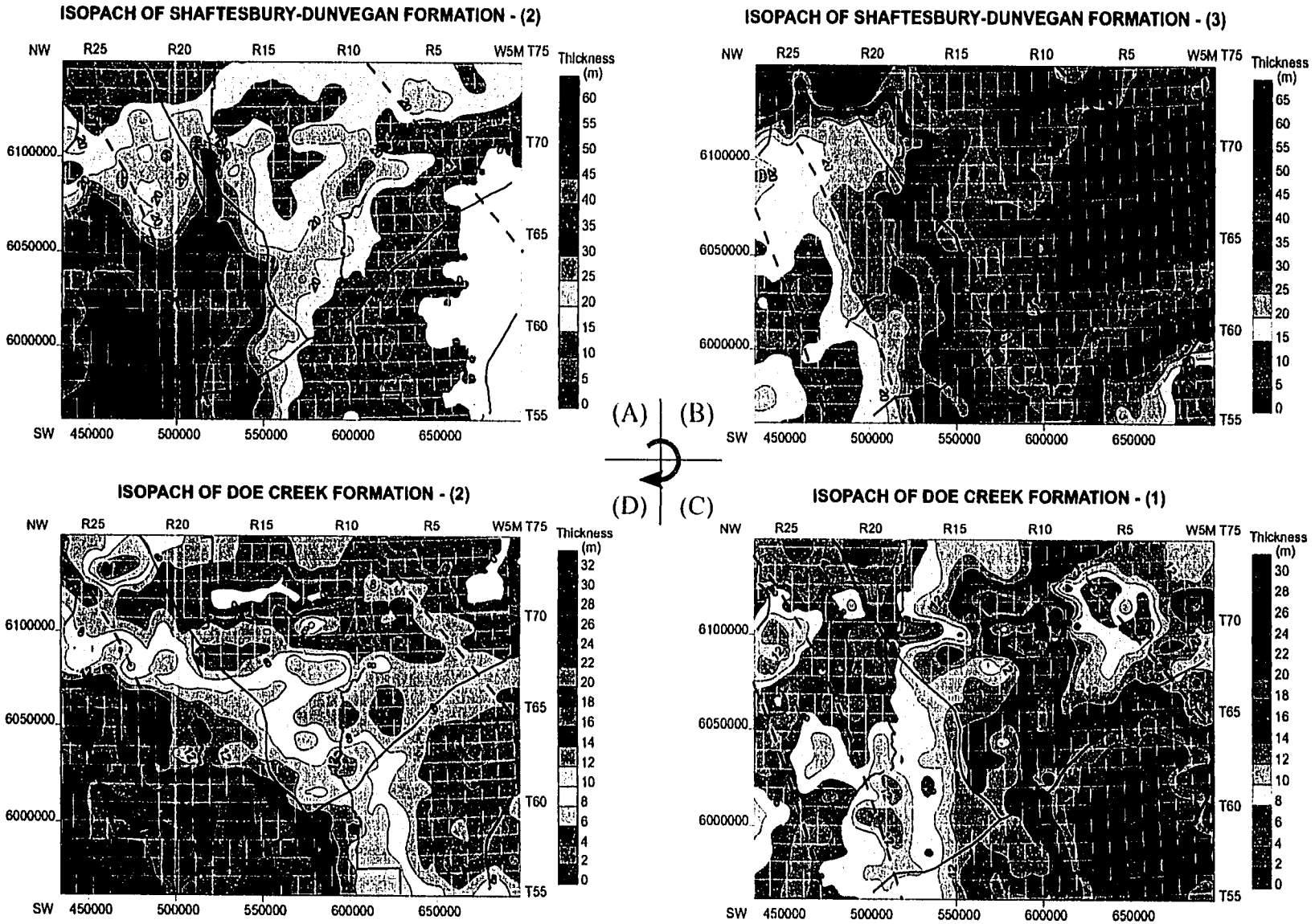

Figure 4-12. Isopach maps of the lower Upper Cretaceous showing differential subsidence of blocks and depositional centre shifting. Dashed red line, fault (refer to Fig. 2-1). Purple line, seismic line (refer to Fig. 1-2). Blue line, Proterozoic domain boundary (refer to Fig. 1-8). Number with formation name, refer to Figure 4-11. Red arrow toward an overlying secession.

4-3-2. Differential Subsidence of Blocks

On the southeast flank of the PRA, appearance of Cretaceous formations changes dramatically through time. Differential subsidence of blocks was observed on the isopach maps of the upper Shaftesbury/Dunvegan and Doe Creek formations. Sub-quadrate thickening of depositional loci shifted across Proterozoic domain boundaries (Fig. 4-12). A sub-quadrate thickening occurred in the Chinchaga domain when Succession 2 of the Shaftesbury/Dunvegan was accumulated (Fig. 4-12A). Subsequently, the thickening shifted to the east in the Buffalo Head and Wabamun domains when Succession 3 of the Shaftesbury/Dunvegan was accumulated (Fig. 4-12B). Thickening shifted to the Wabamun domain during Succession 1 of the Doe Creek deposits (Fig. 4-12C). Finally, the thickening appeared in the southwest when Succession 2 of the Doe Creek formed (Fig. 4-13D). A boundary condition is indicated by the clockwise shifting of the locus of deposition rather than shifting randomly. Differential subsidence of sub-quadrate blocks and shifting of depositional loci are interpreted to be related to changes in the regional stress field.

4-3-3. Aggradation

Aggradation of deposits was observed in the Pouce Coupe Formation on the southeast flank of the PRA. The Pouce Coupe Formation overlies the Dunvegan Formation and inter-fingers with the Doe Creek Formation (Figs. 1-5, 4-13). The appearance of the Pouce Coupe Formation on cross-sections is unique. The well log signatures indicate that the Pouce Coupe Formation may consist of fractured or poorly cemented shale interbedded with siltstone. Excluding the Doe Creek Formation, isopachs of the lower Pouce Coupe succession show an

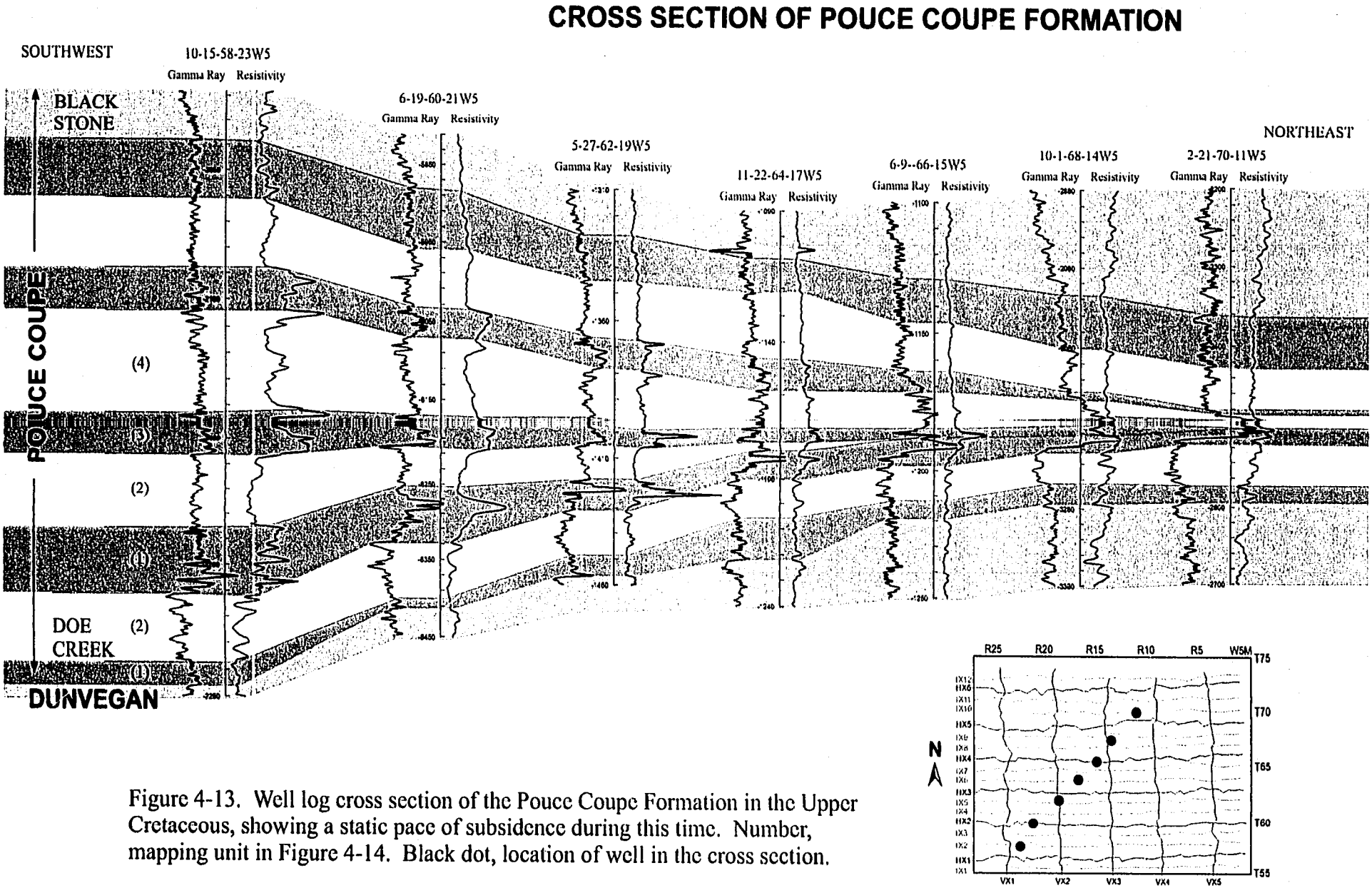

Figure 4-13. Well log cross section of the Pouce Coupe Formation in the Upper Cretaceous, showing a static pace of subsidence during this time. Number, mapping unit in Figure 4-14. Black dot, location of well in the cross section.

NON-SHIFTING AGGRADATION

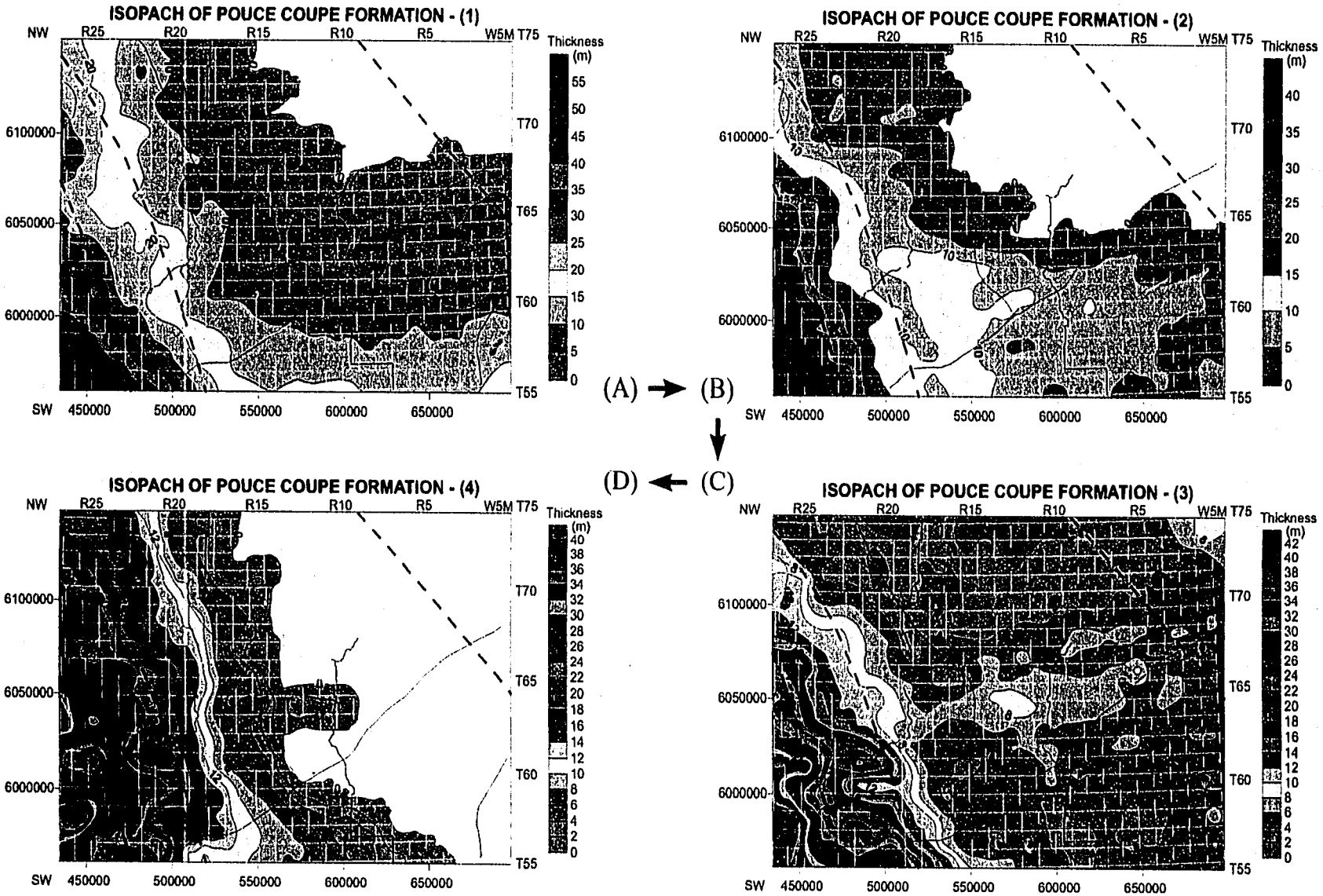

Figure 4-14. Isopach maps of the Pouce Coupe Formation, showing the non-shifting aggradation. Dashed red line, fault (refer to Fig. 2-1). Purple line, seismic line (refer to Fig. 1-2). Blue line, Proterozoic domain boundary (refer to Fig. 1-8). Number with formation name, refer to Fig. 4-13. Red arrow toward an overlying secession.

identical depositional pattern. Sediments derived from the west were trapped in the foredeep. The stratal strike remained NW-SE with subsidence in the southwest (Fig. 4-14), indicating a constant basin floor tilting. The basin floor is interpreted to have functioned as a uniform plate without differentiation of crustal blocks or migration of linear zones as if there was a persistent loading in the southwest and a pivot in the northeast of the plate. Every point in the section maintained subsidence at a constant rate.

4-4. Mechanism of Basin Floor Subsidence

According to the above description, the basin floor in the PRA region sank sometimes as discrete blocks and at other times as a broad sheet during the Cretaceous. The lithosphere in the Arch region appears to have behaved as a collection of vertical prisms or a stack of floating piles as defined by Walcott (1970) and Jones (1980). The three stacking processes observed in the Cretaceous sedimentary record can not be explained by sea level fluctuation and changes in sediment supply rates alone. Each of the stacking processes observed (linear propagation, differential subsidence, and aggradation) as well as the change from one process to the other require a basin floor adjustment that could be driven only by tectonic events. Although the Cardium Formation coincides with the 90 m.y. lowstand (Fig. 1-5), Cardium incised shoreface sandbodies stack in particular locations (Hart and Plint, 1993) and steps of Cardium shorefaces coincide with the foreland zones divided by basement discontinuities (Figs. 4-9, 4-10).

Three tectonic driving forces possibly existed in the PRA region during Cretaceous time: (1) compressional forces from plate convergence along the western continental margin,

(2) subsidence force from (a) thermal decay (Cant, 1988) or (b) mantle convection (Beaumont *et al.*, 1993; Currie, 1997) or (c) phase change (Baird *et al.*, 1995), and (3) buoyant force (uplift) from the replacement of heavier crust by lighter crust (Jones, 1980). Each of the forces is obliquely exerted on the plate and can be divided into lateral and vertical components. Two resultant forces – horizontal and vertical forces – are combined from lateral and vertical components of the forces. The resultant horizontal and vertical forces varied through time and dominated uplift and subsidence processes in the PRA region during the Mesozoic.

4-4-1. Strong Horizontal Compression: Linear Progradation of Elongate Zones and Uplift of the Peace River Arch

Elongate zones in the Cardium Formation were defined by basement faults parallel to the Rocky Mountain deformation front, and were migrating back and forth (Figs. 4-9, 4-10) under the regional compressional regime during late Turonian time. The shifting back and forth of the elongate zones could be driven by tectonic loading and unloading coupled with a drop of eustatic sea level.

In the PRA region, a cycle of tectonic loading and unloading occurred in Turonian-Santonian time and culminated in late Turonian time. Figure 4-15 shows six isopach maps from the Pouce Coupe to the First White Speckled Shale formations varying from Turonian to Santonian age. Strikes of the six formations were largely NW-SE. Elongate zones of subsidence migrated basinward in the first half cycle from the Pouce Coupe through Blackstone to Cardium. The elongate zones moved landward in the last half cycle from the Cardium through Muskiki and Bad Heart to lower Puskwaskau. The contour lines in the end

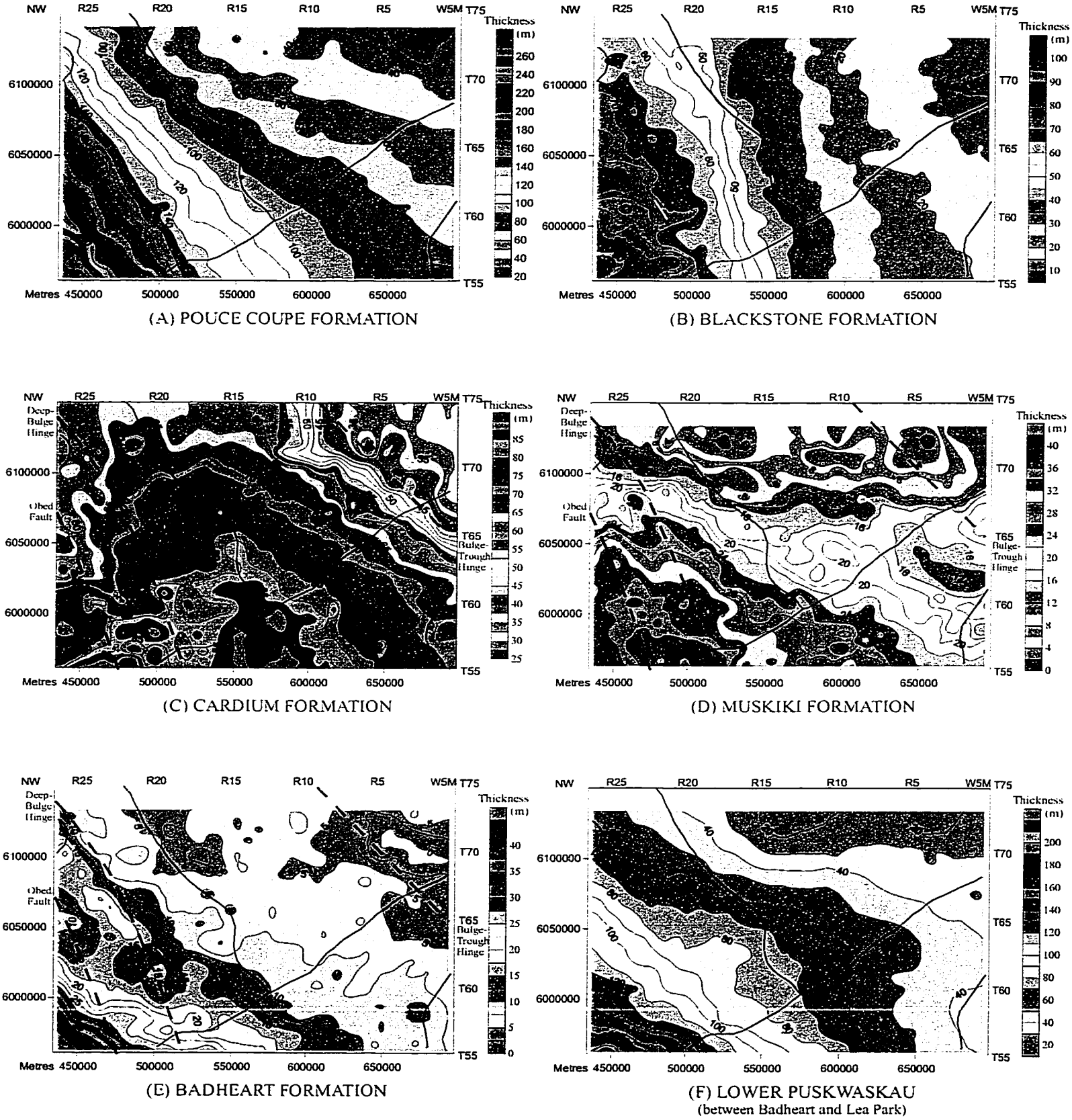

(A) POUCE COUPE FORMATION

(B) BLACKSTONE FORMATION

(C) CARDIUM FORMATION

(D) MUSKIKI FORMATION

(E) BADHEART FORMATION

(F) LOWER PUSKWASKAU
(between Badheart and Lea Park)

Figure 4-15. Isopach maps of Cretaceous Pouce Coupe to First White Speckled Shale formations. Contour interval in metres. Blue line, Proterozoic domain boundary (refer to Fig. 1-8).

formations (Pouce Coupe, Blackstone, and lower Puskwaskau) are consistent. However, in the middle formations (Cardium, Muskiki, and Bad Heart), the contour lines vary. Basement discontinuities are more readily observed in the middle formations. An uplift of the PRA occurred during deposition of the middle formations (Cardium and Muskiki). From the Pouce Coupe to lower Puskwaskau, the effect of basement appears to be stronger and then fades, suggesting that the regional compression on sedimentation varied from becoming stronger and then weaker.

Basinward progradation of depo-centres was also observed in the lower Shaftesbury/Dunvegan Formation (Fig. 4-16). This is not consistent with the global sea level rise recorded for this time (Fig. 1-5). Basal deposits of the Shaftesbury/Dunvegan Formation prograded on top of the Fish Scale Zone from northwest to southeast (Figs. 4-11, 4-16). Although progradation is similar in the developing processes in the basal layers of the Shaftesbury/Dunvegan and Cardium successions, two major differences exist in (1) the fluctuation of sea level (fall in Cardium, rise in Shaftesbury/Dunvegan) and (2) progradational direction (Cardium in NE, Shaftesbury/Dunvegan in SE).

Progradation in the Cardium and the lower Shaftesbury/Dunvegan appear to be driven by strong regional compression although global sea level fluctuations may have overprinted the tectonic effect on sandbody migration. Active elongate zones of the basin floor cut by basement faults shift progressively, perpendicular to the contemporaneous compressional force. As the squeezing force from tectonic loading increases, the elongate blocks are progressively activated and the forebulge migrates along the compressional force.

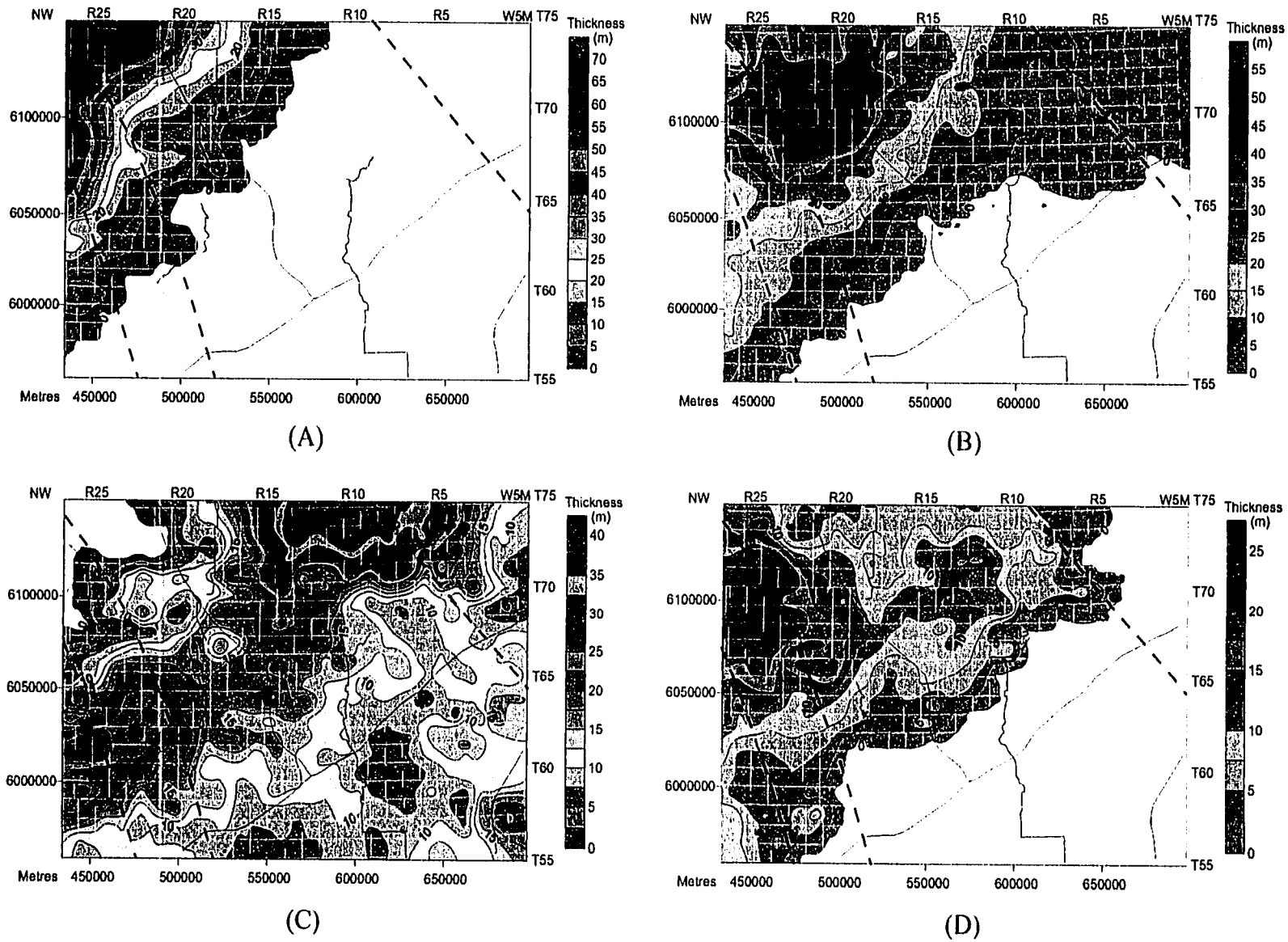

Figure 4-16. Isopach maps of lower portion of Shaftesbury-Dunvegan formations, showing depo-centre shifting. Blue line, Proterozoic domain boundary (refer to Fig. 1-8). Purple line, seismic line (refer to Fig. 1-2).

4-4-2. Weak Horizontal Compression: Differential Subsidence of Blocks

Differential subsidence of blocks crossing basement discontinuities was observed in the upper Shaftesbury/Dunvegan and Doe Creek formations on the southeast flank of the PRA (Fig. 4-12). Global sea level was constant/slightly rising during latest Cenomanian and earliest Turonian time (Fig. 1-5). Sea level fluctuations alone could not have created the sub-quadrate shifting depocentre. Differential subsidence coincides with the regional change (from NW to SW) of the basin floor orientation during latest Cenomanian and earliest Turonian time. During the change, the stress field was probably less compressive.

When the vertical force was greater than the frictional force caused by compression, individual blocks of the basement were moving vertically independently (refer to Walcott, 1970; Jones, 1980). This motion may have been responsible for the apparent differential subsidence and nonlinear shifting of basement blocks in the upper Shaftesbury/Dunvegan and Doe Creek formations.

4-4-3. Medium Horizontal Compression: Aggradation

Aggradation was observed on maps of the Pouce Coupe Formation on the southeast flank of the PRA (Figs. 4-13, 4-14). The formation maps show continuous building up of identical sediment wedges. Vertically, the Pouce Coupe Formation is between the underlying upper Dunvegan and Doe Creek formations (differential subsidence, less compression) and the overlying Cardium Formation (progradation, strong compression). From the Pouce Coupe to Cardium formations, regional compression on sedimentation became stronger (refer to §4-4-1). In early middle Turonian time, accretion of the Cascadia Terrane on the western margin of

North America was initiated but the regional compression had not reached peak level until the late Turonian (Cardium Formation).

Aggradation could occur when the lateral component of compressional force clamped basement prisms together to effectively prevent individual blocks from independent vertical movement (refer to Walcott, 1970; Jones, 1980) but was not sufficiently strong to cause folding and rolling of the crust. While the lateral component of the compressional force was holding basement prisms together, the vertical component of the compressional force was pushing down the clamped block sheet.

It may be concluded that aggradation could be a middle state between weak and strong compression: (1) linear shifting of elongate zones occurs when the lateral compression is strong; (2) differential subsidence of blocks takes place when the lateral compression was weak; and (3) aggradation appears during times when lateral compression was moderate.

CHAPTER 5: EVOLUTION OF PEACE RIVER ARCH

Proterozoic basement of the PRA consists of granodiorites, schists and gneisses, with minor amounts of quartzite and marble (Burwash, 1957). Granitic Precambrian rocks in the Arch were uplifted about 1,000 m above regional basement elevation (Cant, 1988). The structure map (Fig. 5-1A), representing the top of Precambrian basement, shows that the present PRA is still about 400 m above regional basement elevation at the Phanerozoic base. The isopachs in Figures 5-1B to 5-1D represent the entire Phanerozoic, cratonic platform, and foreland basin, respectively. PRA activity mainly affected the cratonic platform through block faulting parallel to the Arch axes.

Eighteen isopach maps from the Cambrian to Upper Cretaceous were selected and illustrated in Figure 5-2. Corresponding to the isopach maps, sixteen cross sections were constructed along the short axis of the PRA (Fig. 5-3). The preserved thicknesses of the systems/formations illustrate a continuous evolution of the PRA. During Phanerozoic time, the PRA has existed in different forms: an Early-Middle Paleozoic arch, a Late Paleozoic to earliest Mesozoic embayment, and a foreland basin component during most of Mesozoic time. The Peace River Embayment can be recognized at least in Cretaceous Albian time (Upper Mannville, Fig. 2-5) and the PRA appeared again at least in late Turonian (Cardium, Figs. 2-7B, 4-15C) and Coniacian (Muskiki, Fig. 4-15D) time.

To compare formations and trace basin floor motion, time spans for sediment accumulation were considered and depositional rates were calculated for the Phanerozoic formations (Fig. 5-4). The trend of basin floor is shown in Figure 5-4. Although isopachs

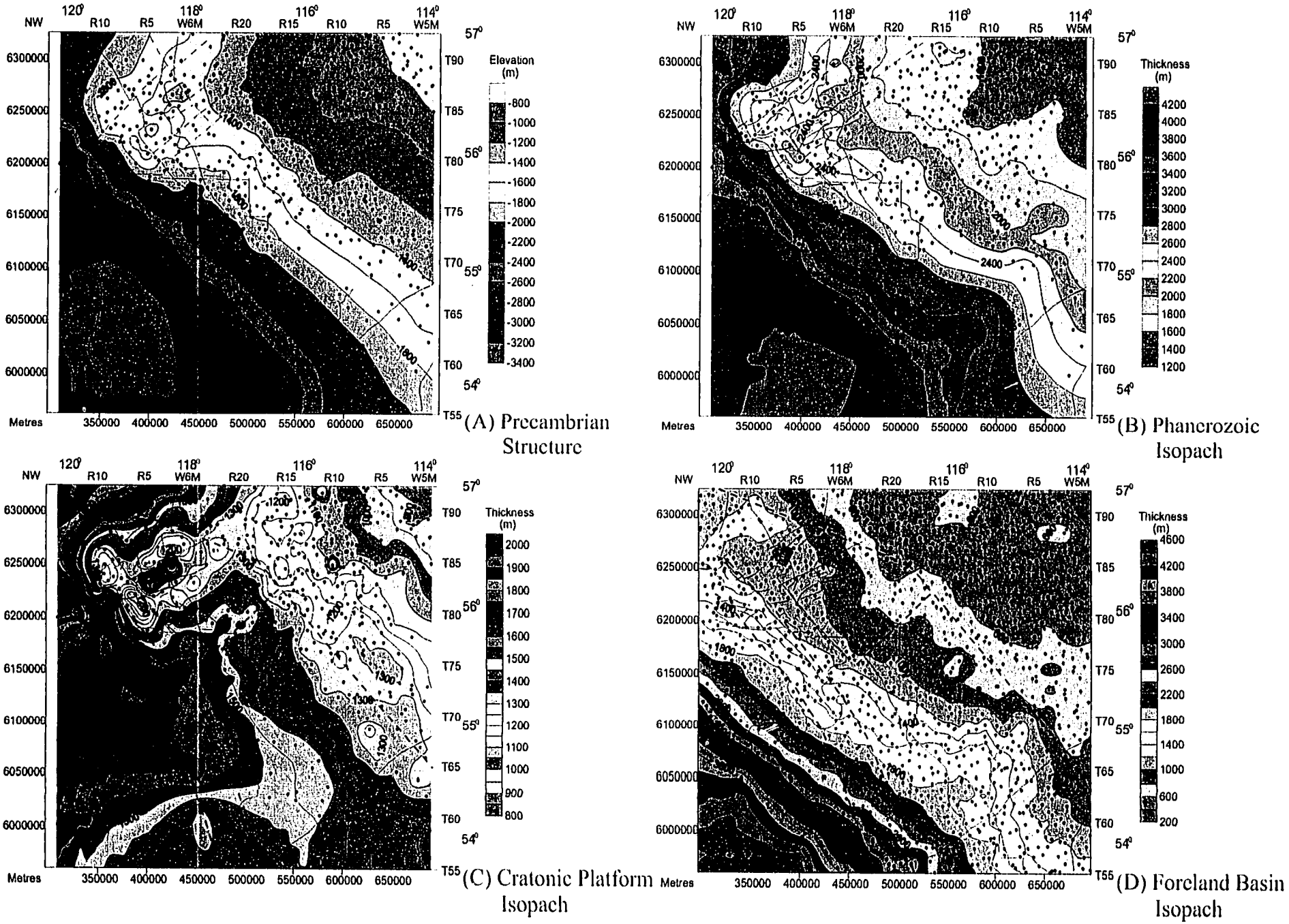

Figure 5-1. Structure and isopach maps. Blue line, Proterozoic domain boundary (refer to Fig. 1-8). Dashed purple line, inferred Precambrian fault/shear zone (refer to Fig. 1-8). Red line, Carboniferous extensional fault (refer to Fig. 1-8). Dashed pink line, faults (refer to Fig. 2-2). Green line, seismic line (refer to Fig. 1-2).

show a major collapse of the Arch in the Carboniferous, the highest subsidence rate was during Late Devonian Wabamun time (Fig. 5-4). Regional subsidence began before Wabamun time and there appears to be a lag before Arch subsidence occurs. The Arch had remained a high until Wabamun time. Arch subsidence seems accelerated after the Wabamun. The thinning of preserved sediments on the PRA before Wabamun time was also influenced by the paleotopography and does not necessarily indicate a net uplift of the Arch.

In Early Paleozoic time, the sedimentary record that is commonly used to record Arch evolution was affected by rapid global sea level rise (Fig. 5-4) and broad regional uplift (Mossop, personal communication, 1999). Subsidence of the Arch began in Middle Devonian Elk Point time (Fig. 5-2C). The PRA became an island in Late Devonian Woodbend and Winterburn time (Fig. 5-2E). Subsequently an embayment developed from Late Devonian Wabamun to Permian time (Figs. 5-2F, 5-2G, 5-2H). The Peace River Embayment was resumed in Cretaceous Albian time (Fig. 5-2L). Tectonic events on the western continental margin since the Mesozoic interrupted Arch subsidence (Figs. 5-2I, 5-2J, 5-2K) and originated its final uplift (Figs. 2-7B, 3-1, 4-15). Figures 5-5 and 5-6 summarize formations and related geological events in the PRA region during Paleozoic and Mesozoic time.

5-1. Cambrian to Late Devonian: Peace River Arch to Peace River Island

The initial uplift of the PRA is suggested to be latest Proterozoic time (McMechan, 1990). The Middle Cambrian Gog Group unconformably overlies uplifted and truncated sediments of the Upper Proterozoic Windermere Supergroup (McMechan, 1990) in the exposed Cordillera about 200 km west of the PRA. The basal Gog Group contains eroded

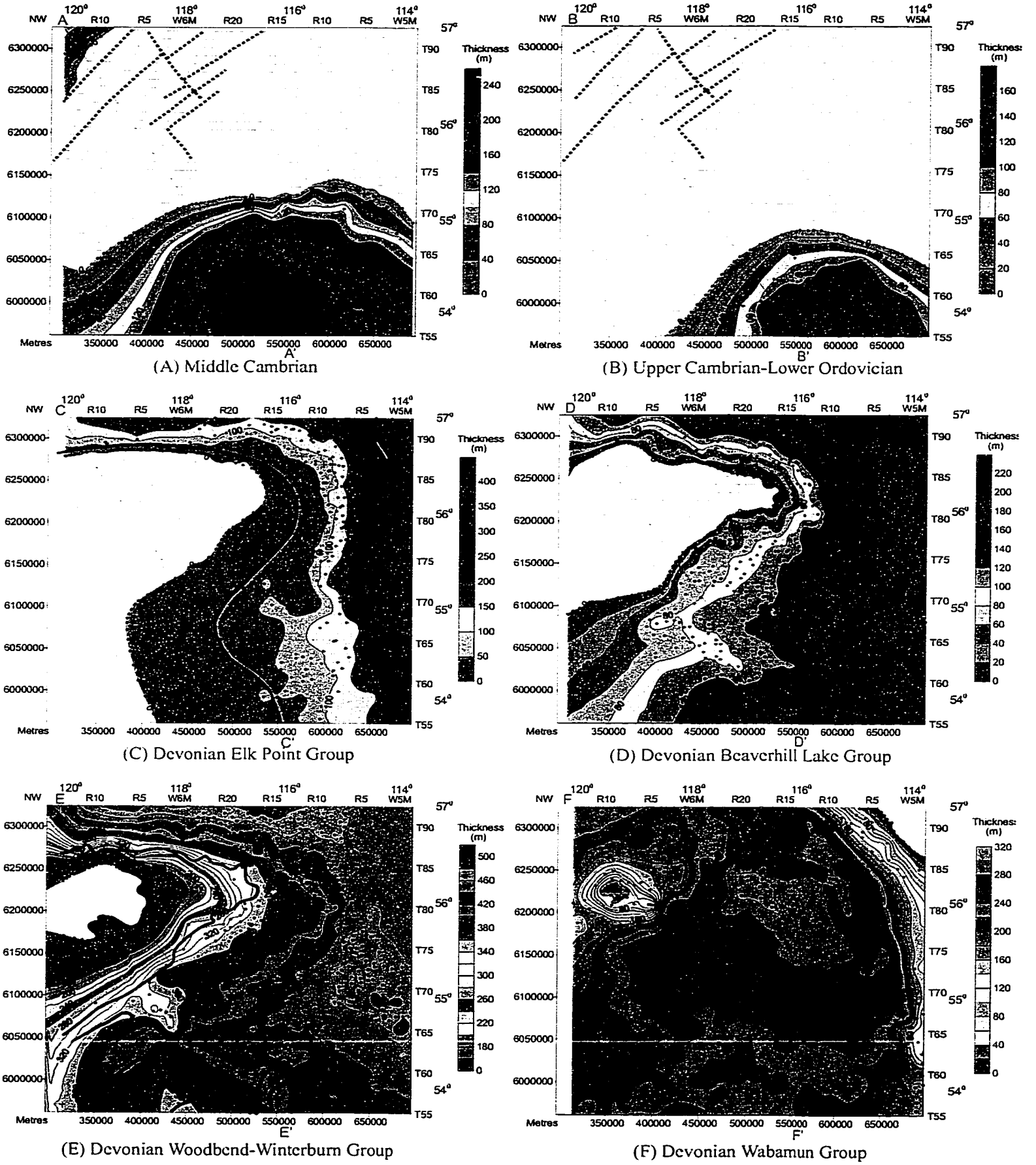

Figure 5-2. Palcozoic Isopach maps for Peace River Arch region. Black dot, mapping control point. Black dashed line, inferred Precambrian fault/shear zone (Burwash *et al.*, 1994). Light blue line, depositional limit of Muskey/Prairie evaporite. Pink line, Leduc reef outline.

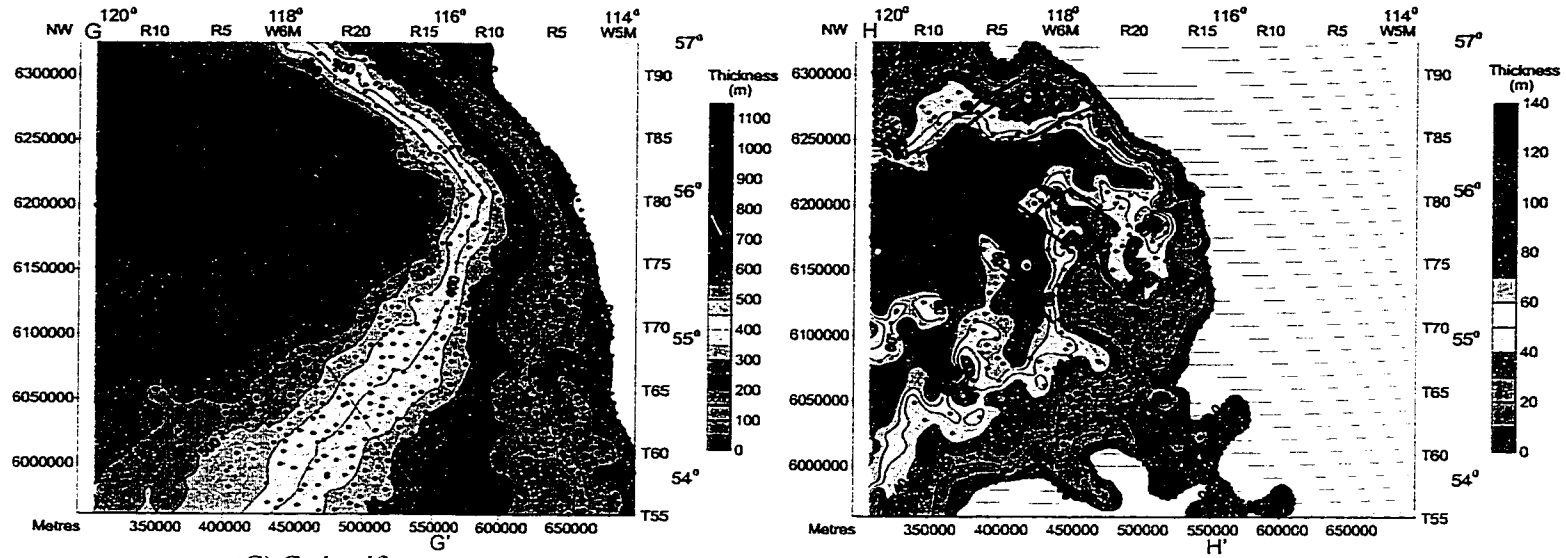

(G) Carboniferous

(H) Permian

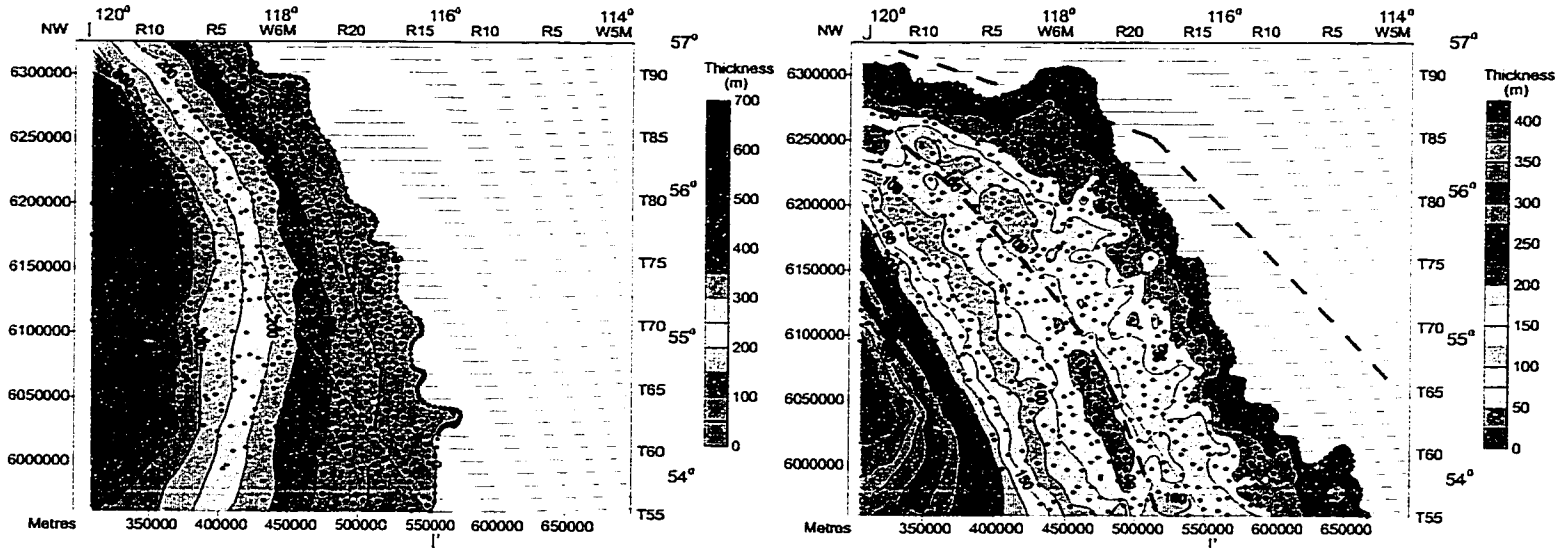

(I) Triassic

(J) Jurassic

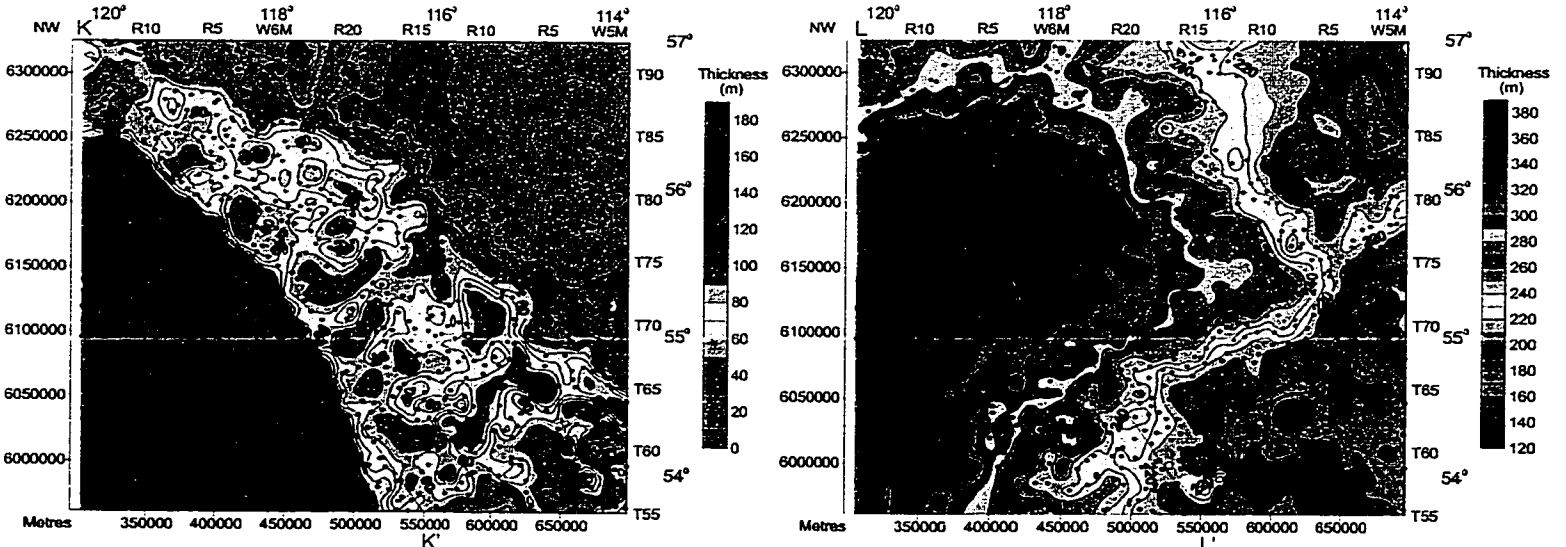

(K) Cretaceous Lower Mannville Group

(L) Cretaceous Upper Mannville Group

Figure 5-2. Isopach maps (C-K_l). Black dot, control point. Red line, Carboniferous fault. Red dashed line, foreland zone boundary. Cross section, refer to Fig. 5-3.

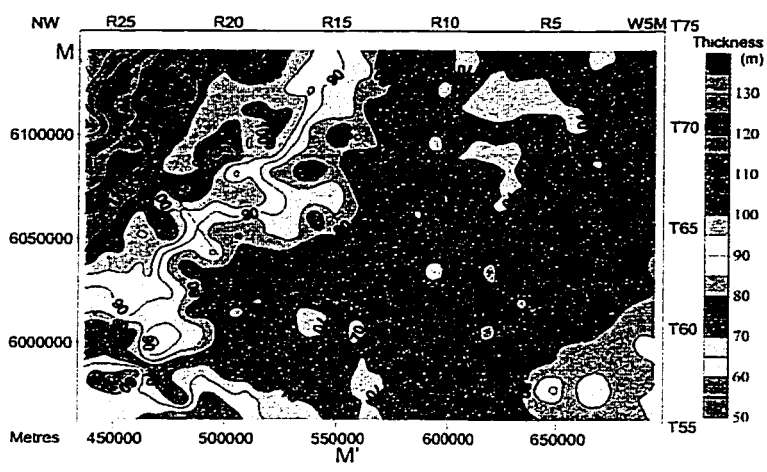

(M) Cretaceous Peace River Group

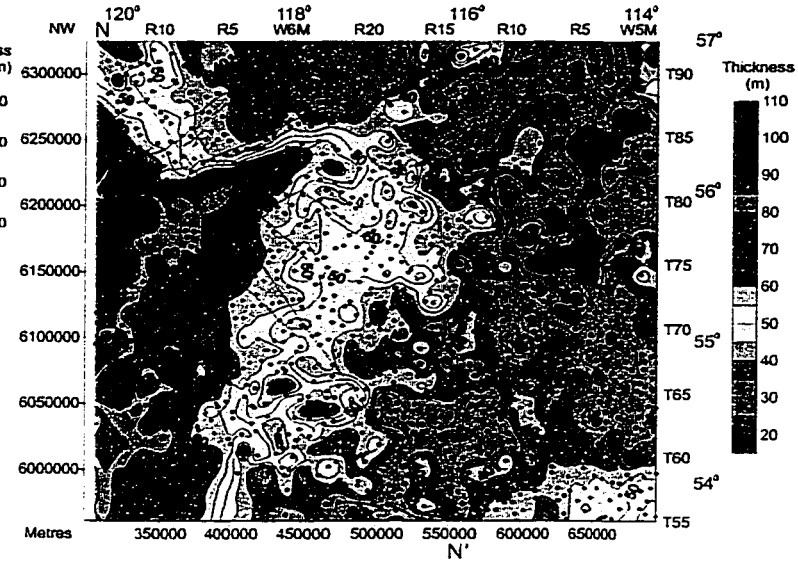

(N) Cretaceous Viking Formation

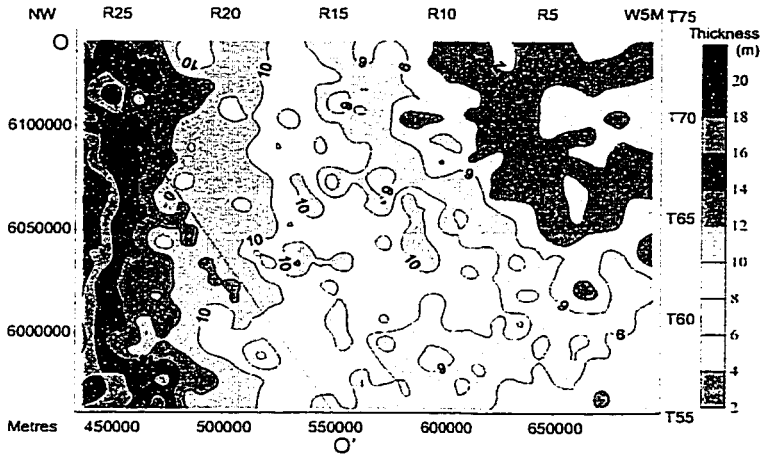

(O) Cretaceous Fish Scale Formation

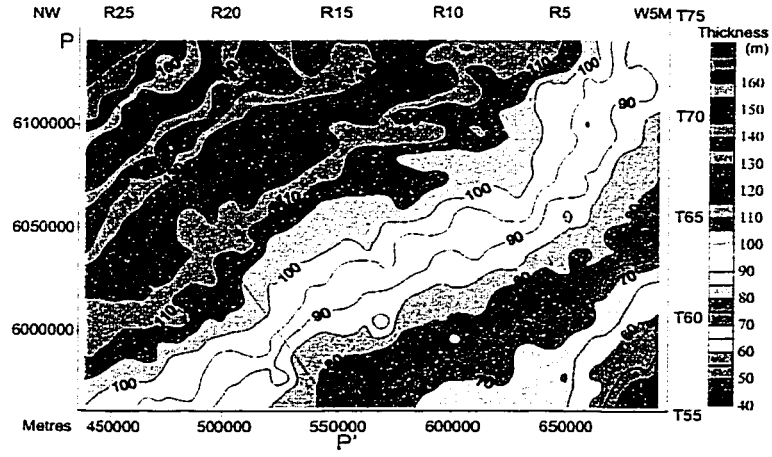

(P) Cretaceous Shaftesbury-Dunvegan Formations

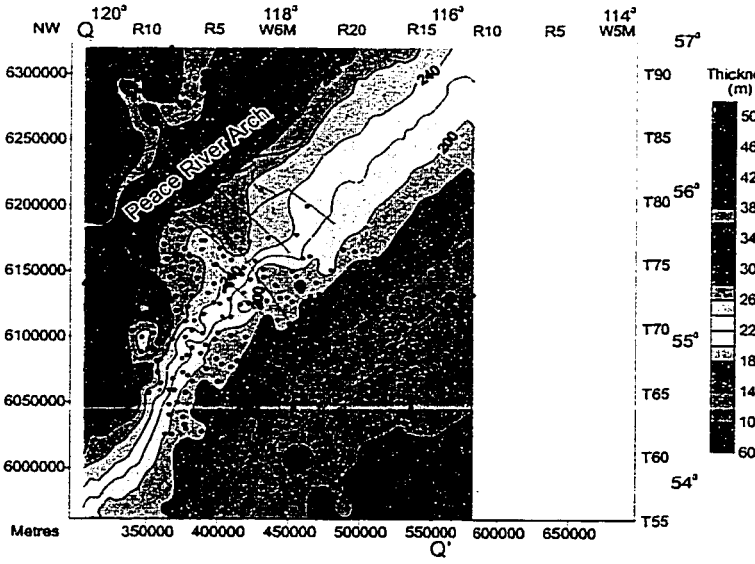

(Q) Cretaceous Dunvegan Formation

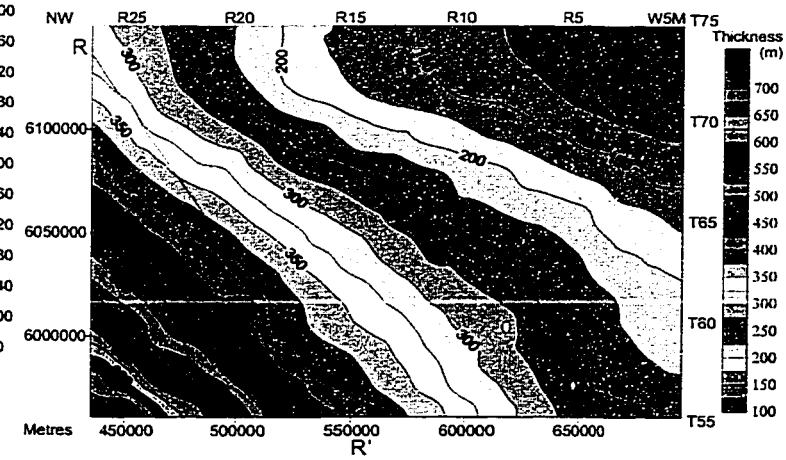

(R) Cretaceous Pouce Coupe-First White Speckled Shale

Figure 5-2. Cretaceous isopach maps for Peace River Arch region. Black dot, mapping control point. Cross section for each isopach, refer to Fig. 5-3.

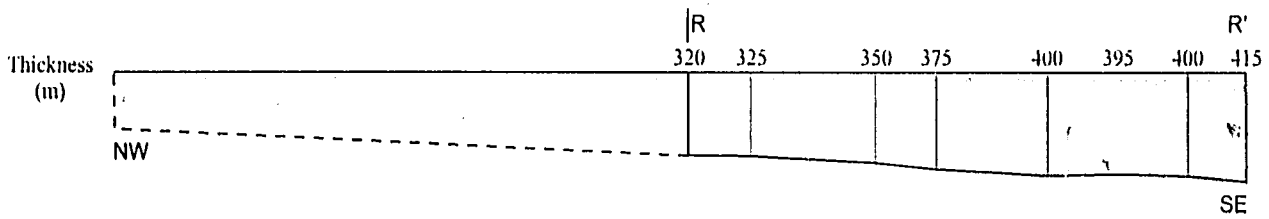

Cretaceous Pouce Coupe-First White Speckled Shale, ca. 7 m.y.

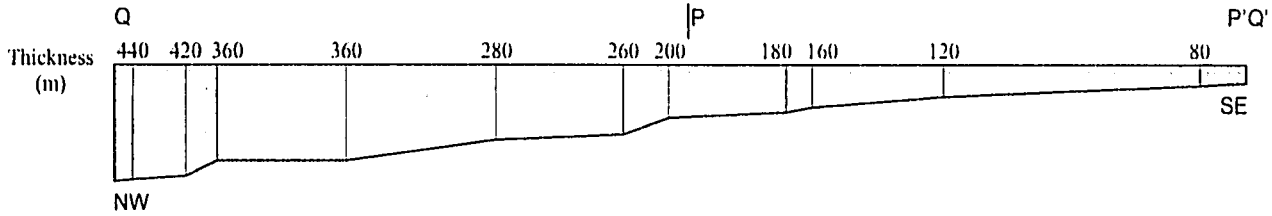

Cretaceous Shaftesbury-Dunvegan, ca. 6.5 m.y.

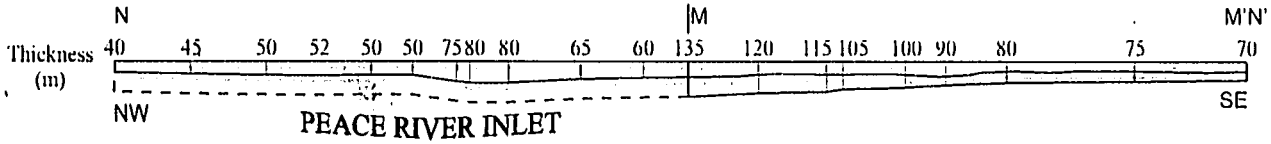

Cretaceous Viking (upper) and Peace River (lower), ca. 6.5 m.y.

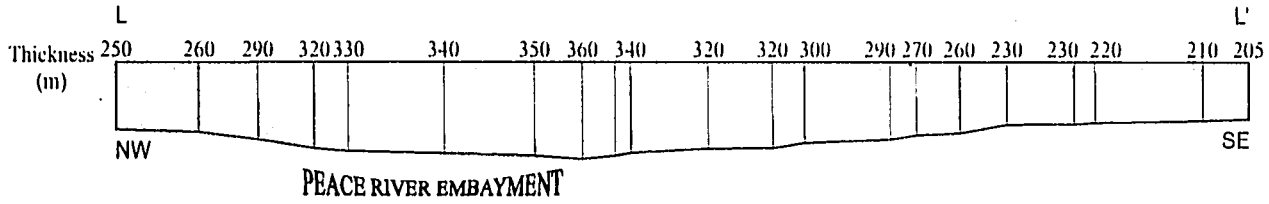

Cretaceous Upper Mannville, ca. 9 m.y.

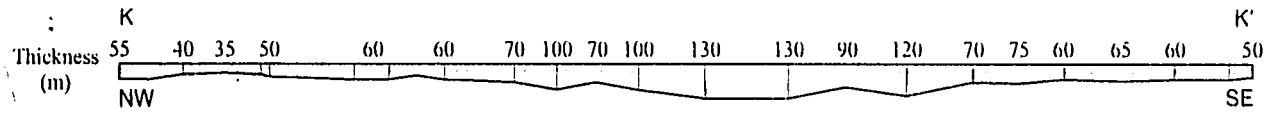

Cretaceous Lower Mannville, ca. 6 m.y.

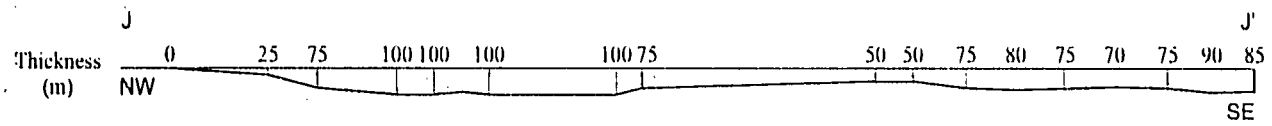

Jurassic, ca. 44 m.y.

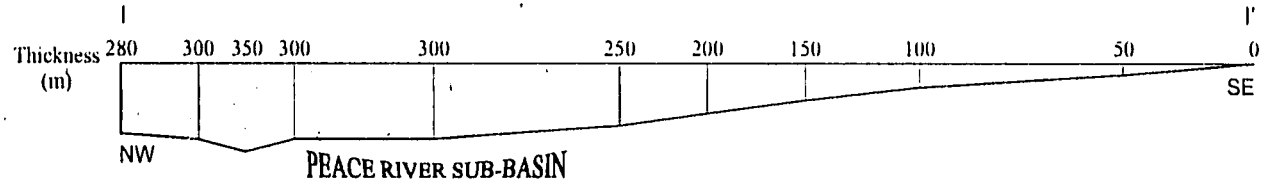

Triassic, ca. 34 m.y.

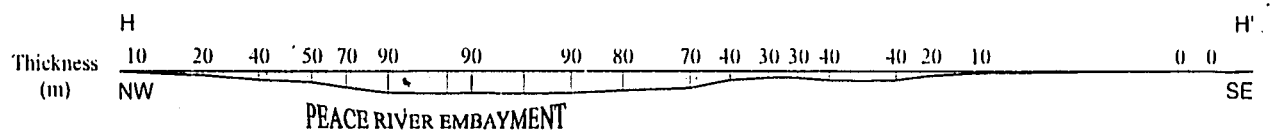

Permian, ca. 14 m.y.

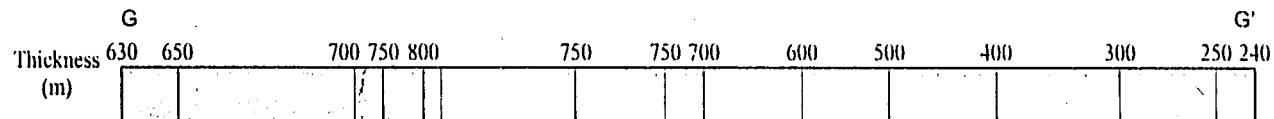

Carboniferous, ca. 62 m.y.

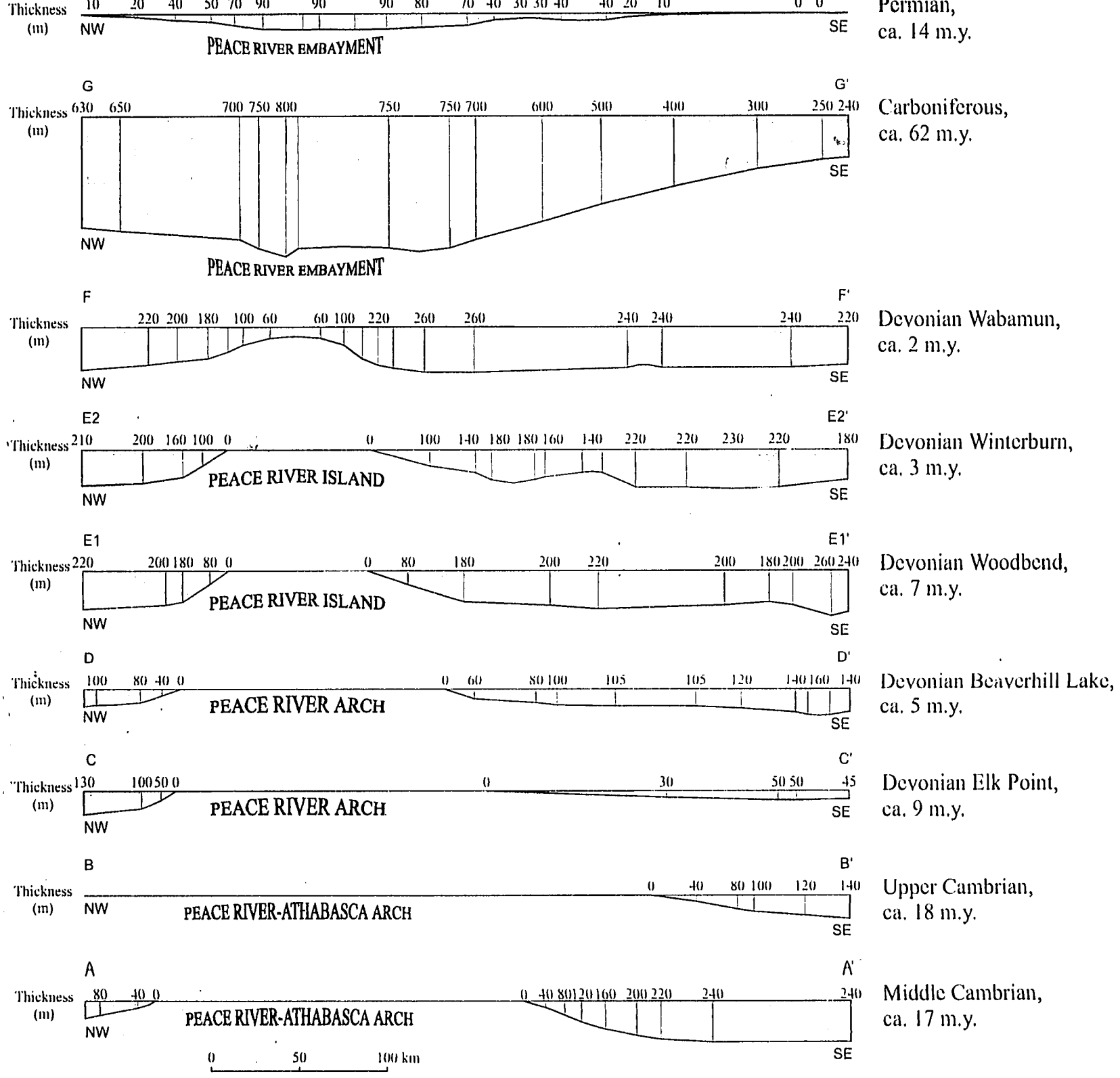

Figure 5-3. Cross sections showing Peace River Arch evolution. A-A' to D-D' and F-F' to R-R' correspond to isopach maps in Fig. 5-2. E1-E1' and E2-E2' correspond to isopach maps in Fig. 2-8. T

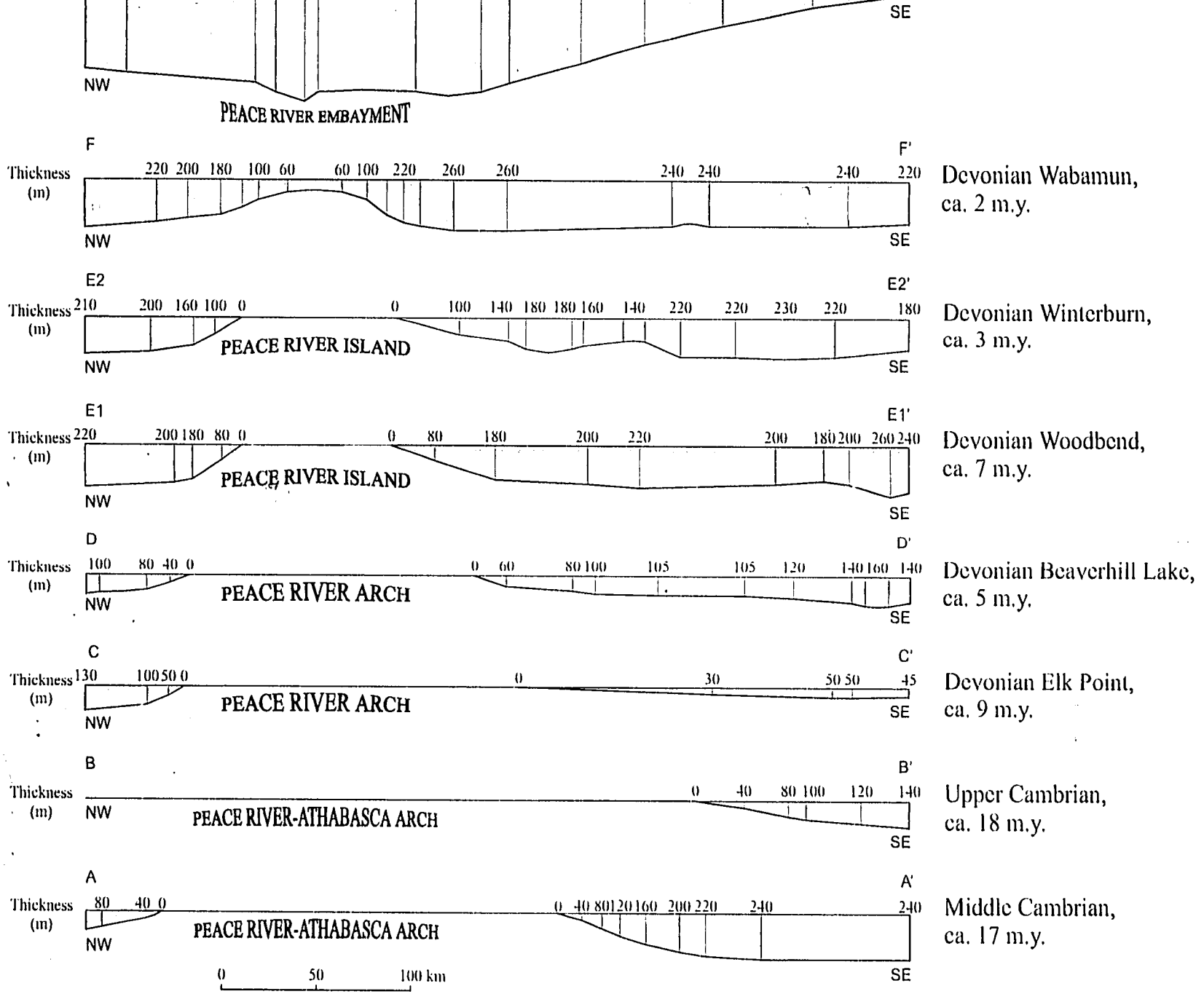

Figure 5-3. Cross sections showing Peace River Arch evolution. A-A' to D-D' and F-F' to R-R' correspond to isopach maps in Fig. 5-2. E1-E1' and E2-E2' correspond to isopach maps in Fig. 2-8. T ime spans exclude none depositional/erosional intervals.

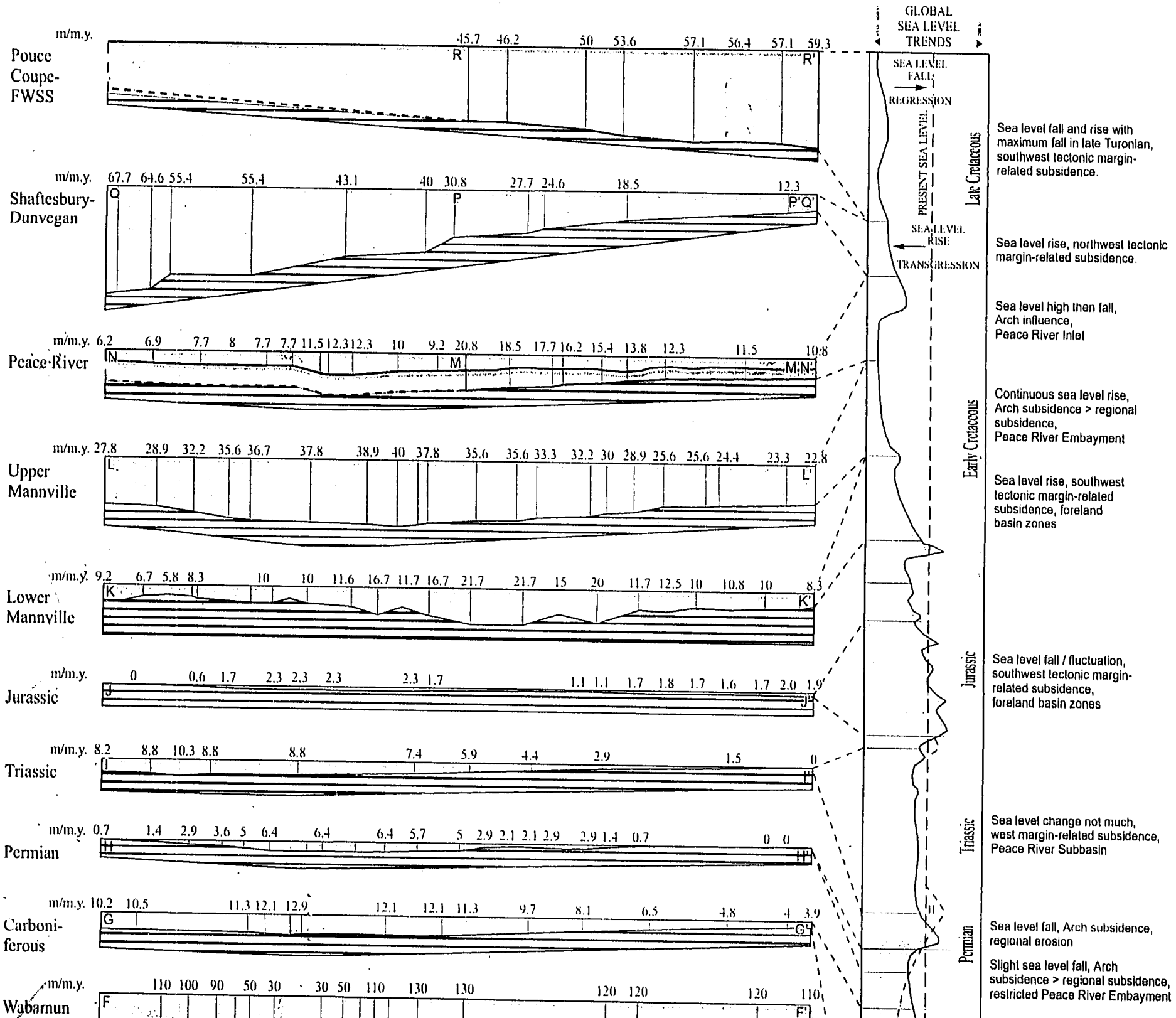
GLOBAL SEA LEVEL TRENDS
SEA LEVEL FALL
REGRESSION
PRESENT SEA LEVEL
SEA-LEVEL RISE
TRANSGRESSION
Late Cretaceous
Early Cretaceous
Jurassic
Triassic
Permian
m/m.y.
Pouce Coupe-FWSS
45.7 46.2 50 53.6 57.1 56.4 57.1 59.3
R R'
m/m.y.
Shaftesbury-Dunvegan
67.7 64.6 55.4 55.4 43.1 40 30.8 27.7 24.6 18.5 12.3
Q P P'Q'
m/m.y.
Peace River
6.2 6.9 7.7 8 7.7 7.7 11.5 12.3 12.3 10 9.2 20.8 18.5 17.7 16.2 15.4 13.8 12.3 11.5 10.8
N M M'N'
m/m.y.
Upper Mannville
27.8 28.9 32.2 35.6 36.7 37.8 38.9 40 37.8 35.6 35.6 33.3 32.2 30 28.9 25.6 25.6 24.4 23.3 22.8
L L'
m/m.y.
Lower Mannville
9.2 6.7 5.8 8.3 10 10 11.6 16.7 11.7 16.7 21.7 21.7 15 20 11.7 12.5 10 10.8 10 8.3
K K'
m/m.y.
Jurassic
0 0.6 1.7 2.3 2.3 2.3 2.3 1.7 1.1 1.1 1.7 1.8 1.7 1.6 1.7 2.0 1.9
J J'
m/m.y.
Triassic
8.2 8.8 10.3 8.8 8.8 7.4 5.9 4.4 2.9 1.5 0
I I'
m/m.y.
Permian
0.7 1.4 2.9 3.6 5 6.4 6.4 6.4 5.7 5 2.9 2.1 2.1 2.9 2.9 1.4 0.7 0 0
H H'
m/m.y.
Carboni-ferous
10.2 10.5 11.3 12.1 12.9 12.1 12.1 11.3 9.7 8.1 6.5 4.8 4 3.9
G G'
m/m.y.
Wabamun
110 100 90 50 30 30 50 110 130 130 120 120 120 110
F F'
Sea level fall and rise with maximum fall in late Turonian, southwest tectonic margin-related subsidence.
Sea level rise, northwest tectonic margin-related subsidence.
Sea level high then fall, Arch influence, Peace River Inlet
Continuous sea level rise, Arch subsidence > regional subsidence, Peace River Embayment
Sea level rise, southwest tectonic margin-related subsidence, foreland basin zones
Sea level fall / fluctuation, southwest tectonic margin-related subsidence, foreland basin zones
Sea level change not much, west margin-related subsidence, Peace River Subbasin
Sea level fall, Arch subsidence, regional erosion
Slight sea level fall, Arch subsidence > regional subsidence, restricted Peace River Embayment

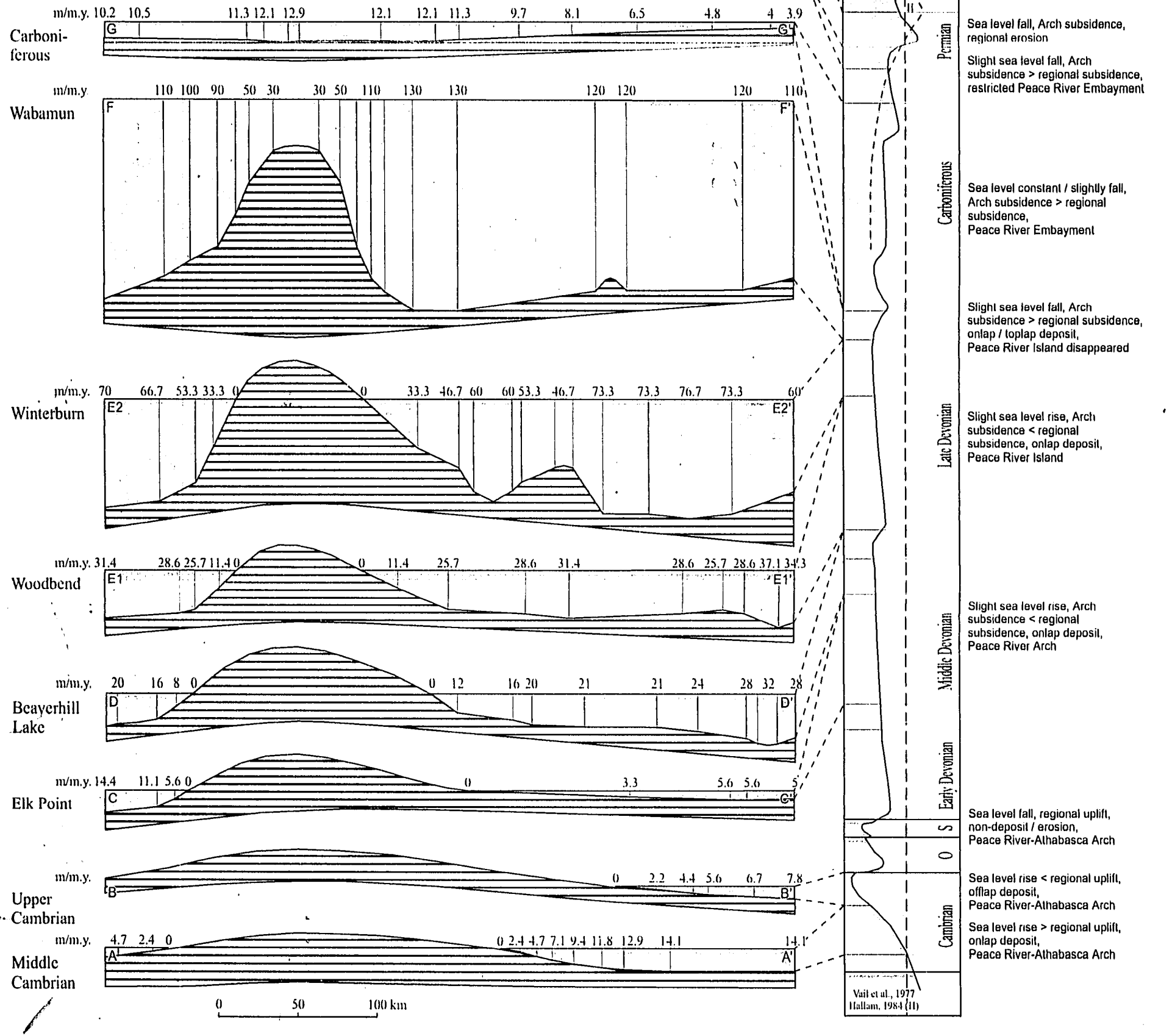
m/m.y. 10.2 10.5 11.3 12.1 12.9 12.1 12.1 11.3 9.7 8.1 6.5 4.8 4 3.9
Carboni-ferous
G
G'
m/m.y.
Wabamun
110 100 90 50 30 30 50 110 130 130 120 120 120 110
F
F'
m/m.y. 70 66.7 53.3 33.3 0 0 33.3 46.7 60 60 53.3 46.7 73.3 73.3 76.7 73.3 60
Winterburn
E2
E2'
m/m.y. 31.4 28.6 25.7 11.4 0 0 11.4 25.7 28.6 31.4 28.6 25.7 28.6 37.1 34.3
Woodbend
E1
E1'
m/m.y. 20 16 8 0 0 12 16 20 21 21 24 28 32 28
Beaverhill Lake
D
D'
m/m.y. 14.4 11.1 5.6 0 0 3.3 5.6 5.6 5
Elk Point
C
C'
m/m.y.
Upper Cambrian
0 2.2 4.4 5.6 6.7 7.8
B
B'
m/m.y. 4.7 2.4 0 0 2.4 4.7 7.1 9.4 11.8 12.9 14.1 14.1
Middle Cambrian
A
A'
0 50 100 km
Permian
Carboniferous
Late Devonian
Middle Devonian
Early Devonian
S
O
Cambrian
Vail et al., 1977
Hallam, 1984 (II)
Sea level fall, Arch subsidence, regional erosion
Slight sea level fall, Arch subsidence > regional subsidence, restricted Peace River Embayment
Sea level constant / slightly fall, Arch subsidence > regional subsidence, Peace River Embayment
Slight sea level fall, Arch subsidence > regional subsidence, onlap / toplap deposit, Peace River Island disappeared
Slight sea level rise, Arch subsidence < regional subsidence, onlap deposit, Peace River Island
Slight sea level rise, Arch subsidence < regional subsidence, onlap deposit, Peace River Arch
Sea level fall, regional uplift, non-deposit / erosion, Peace River-Athabasca Arch
Sea level rise < regional uplift, offlap deposit, Peace River-Athabasca Arch
Sea level rise > regional uplift, onlap deposit, Peace River-Athabasca Arch

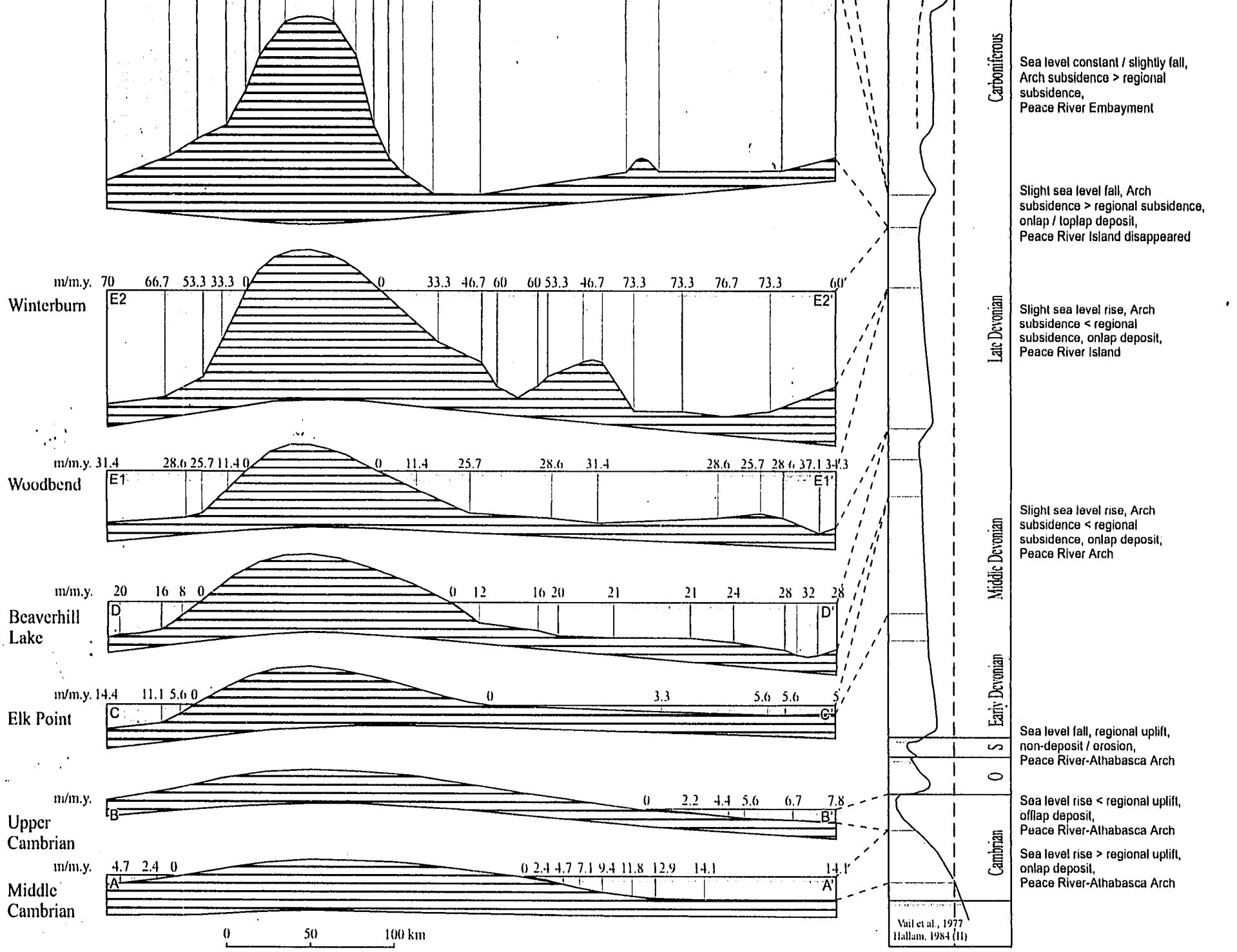

Figure 5-4. Trends of basin floor, global sea level, and depositional rates of formations calculated from Fig. 5-3.

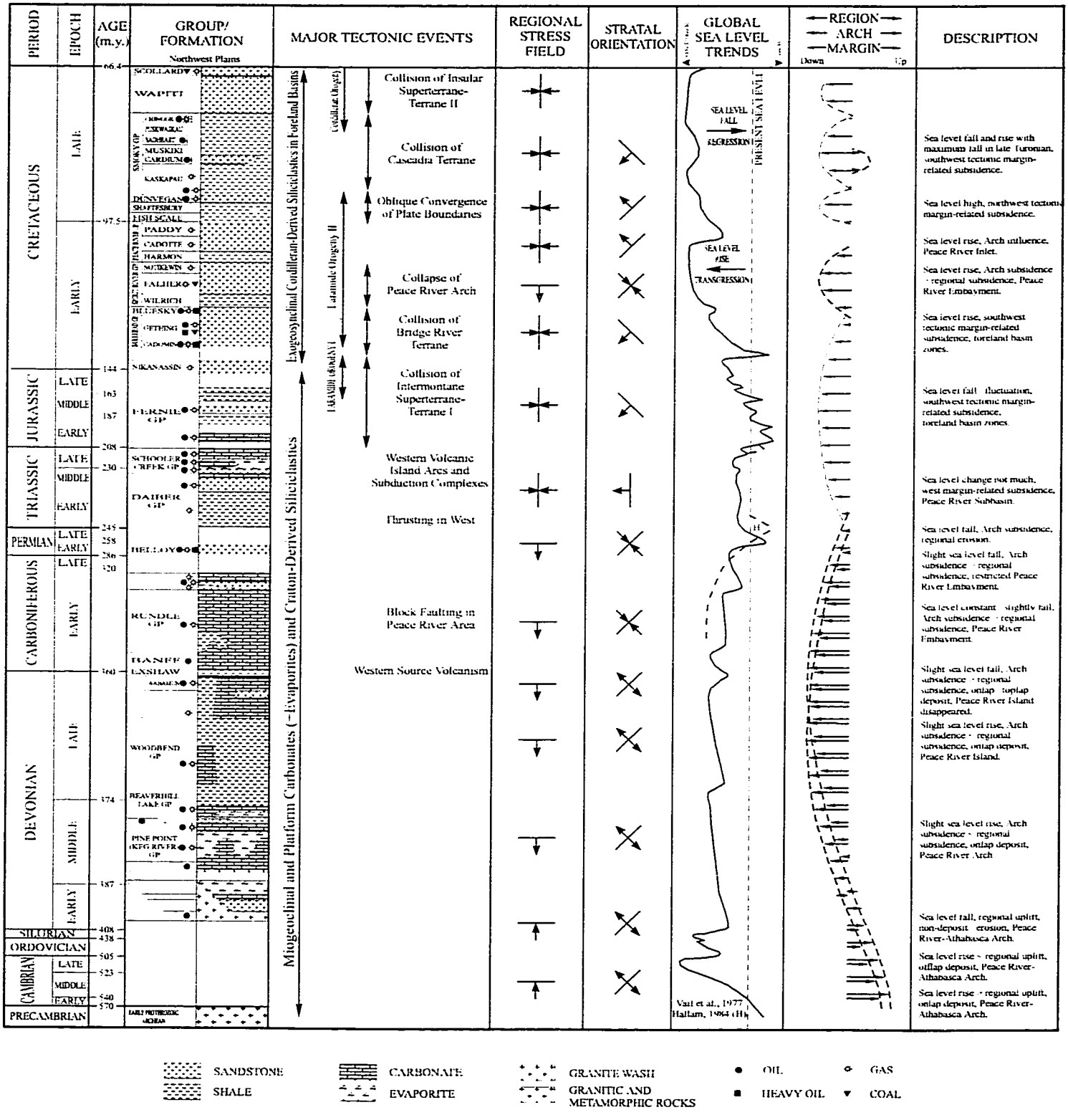

Figure 5-5. Summary of formations and related geological events in the Peace River Arch region during the Paleozoic and Mesozoic eras. Global sea level, modified from Vail *et al.* (1977), Hallam (1984), and AGAT Laboratories (1987). Tectonic events, summarized from Coney *et al.* (1980), Monger (1983), Cant and Stockmal (1989), van der Heyden (1992), Armstrong and Ward (1993). Other component, suggested by this study.

Proterozoic sediments and latest Late Proterozoic to Early Cambrian fossils derived from the uplifted PRA (McMechan, personal communication, 1999).

From Cambrian to Early Devonian time, the Arch region remained as a high, as part of the Peace River-Athabasca Arch (Kent, 1994). The Lower Cambrian is missing from the Arch region. The Middle Cambrian (Fig. 5-2A) was transgressively deposited on the margins of the Arch. Seismic reflectors can be seen at the base of the Middle Cambrian that progressively onlap toward the Arch (Fig. 1-10; Eaton *et al.*, 1997). A comparison to the global sea level trend (Fig. 5-5; Vail *et al.*, 1977; Hallam, 1984) suggests that the Middle Cambrian transgression may have been dominated by a major sea level rise.

Global sea level rose during Late Cambrian time, was shallow during Ordovician and Silurian time, and remained low in Early Devonian time (Fig. 5-5; Ross and Ross, 1988). The retreat of Upper Cambrian and Ordovician deposits and missing of Silurian and Lower Devonian deposits from the Arch region (Fig. 5-2B) many have resulted from regional uplift. A much broader regional uplift prevented Ordovician-Silurian deposition/preservation over all of the WCSB except in the Williston Basin and MacDonald platform (Mossop, personal communication, 1999).

During Middle and Late Devonian time, global sea level was shallow, stable and fell slightly in latest Middle and latest Late Devonian time (Fig. 5-5). Sediment accumulation was accelerated from the Elk Point to Wabamun groups (Fig. 5-4) and the PRA became an embayment toward the Late Paleozoic (Figs. 5-2C, 5-2D, 5-2E, 5-2F, 5-2G, 5-2H). The accommodation space was mainly created by Arch subsidence. The initiation of Arch subsidence began in Middle Devonian time. Normal faulting formed horsts and grabens

oriented parallel and normal to the arch long axis by the Mid-Devonian (Cant, 1988). The emergent Arch landmass (Figs. 5-2C to 5-2F) was progressively onlapped by siliciclastic, evaporitic and shallow marine carbonate sediments during the late Middle and Late Devonian and was buried by the end of Devonian (O'Connell *et al.*, 1990). The subsidence/depositional rate of the Arch and surrounding areas was increased and reached a maximum in Wabamun time (Fig. 5-4). The development of the PRA had a profound influence on Devonian sedimentation by affecting the carbonate platforms and basin fill histories (Dix, 1990). The depositional limit of Muskeg/Prairie evaporite (Fig. 5-2C) and development of the Leduc reefs (Fig. 5-2E) are restricted to the submerged flanks of the PRA. The reefs were initiated and controlled by complex, small-scale, Arch-related tectonics (Keith, 1990).

5-2. Carboniferous to Triassic: Peace River Embayment to Peace River Subbasin

Global sea level remained constant and fell slightly during Carboniferous time but dropped significantly toward Late Permian time (Fig. 5-5). The Arch area continued to subside and became the Peace River Embayment during Carboniferous and Permian time (Figs. 5-2G, 5-2H). Carboniferous formations were thickening toward the Arch and the unique depo-centre was continuously developed on the Arch crest (Fig. 5-3), indicating that subsidence rate was greater on the Arch than surrounding areas during this time. However, the rates of both Arch subsidence and regional subsidence were much slower than in Devonian time (Figs. 5-4).

A graben system developed during the Carboniferous (Richards *et al.*, 1994) and normal faulting was believed to involve rejuvenation of basement blocks. Carbonate deposits were dominant in the Mississippian and Permo-Pennsylvanian formations. The depocentre in the core of the Peace River Embayment (Dawson Creek Graben Complex) formed by numerous internal horst and graben blocks records growth-fault-controlled syntectonic infilling and differential subsidence. Deposition in the Dawson Creek Graben Complex was controlled mainly by tectonic rather than by eustatic process (Barclay *et al.*, 1990).

Global sea level remained low during Triassic time (Fig. 5-5; Haq *et al.*, 1988). Although the PRA area continued to subside in this time (Williams, 1958) and the large depositional centre is still referred to as the Peace River Embayment (Edwards *et al.* 1994), collapse of the Arch ceased and the Peace River Embayment no longer existed in the sense of the Carboniferous and Permian Embayment (Fig. 5-2I). The Triassic depositional centre of the Alberta Basin appears to be related more to the events in the Canadian Cordillera rather than the collapse of the PRA. The Triassic Peace River Embayment was a sub-basin of the Alberta Basin that was connected to the Liard sub-basin in the north and to deposits in the Rocky Mountains and foothills in the south (Edwards *et al.* 1994). The basin had its depositional centre along the foothills of northeastern British Columbia. Triassic deposits in the PRA area comprise marine to marginal-marine siliciclastic and carbonate rocks and lesser amounts of evaporite that form a westward-thickening sedimentary wedge on a westward-deepening stable continental shelf and shoreline (Edwards *et al.*, 1994).

5-3. Jurassic to Cretaceous Aptian: Foreland Zones and Southwest Subsidence

Global sea level fell considerably during Early and Middle Jurassic time and rose slightly in Late Jurassic time (Fig. 5-5; Haq *et al.*, 1988). The Intermontane Superterrane (Terrane I) was interpreted to have accreted to the west margin of North America during this time (Fig. 2-1, Monger *et al.*, 1982). During this compressional regime, no PRA in any sense – arch/embayment existed in the Jurassic (Fig. 5-2J). Jurassic subsidence in the Arch region was exclusively related to the western collisional event (in the southwest corner of the mapping area, the contour pattern was caused by lack of control points at the corner). The Late Jurassic narrow, elongated, foreland trough was formed parallel to the present Rocky Mountain front and rests on Early and Middle Jurassic pre-orogenic Western Platform and Rocky Mountain Trough deposits (Poulton *et al.* 1994). The west-thickening sedimentary wedge is dominated by Lower Jurassic platform and shelf deposits, Middle Jurassic more localized siliciclastic units, and Upper Jurassic non-marine clastics. The effects of differential compaction over different fault blocks along the locus of the ancient PRA are recorded in minor thickness variations in the Jurassic units (Poulton, *et al.* 1990).

Global sea level remained shallow in the earliest Cretaceous and rose in Early Cretaceous Aptian time (Fig. 5-6; Haq *et al.*, 1988). Following the docking of Terrane I (Fig. 2-1, Monger *et al.*, 1982), the Bridge River Terrane was believed to be accreted to the west margin of North America during Aptian time (Cant and Stockmal, 1989). A Rocky Mountain rooted subsidence in the southwest was recorded on the isopach map of the Lower Mannville Group (Fig. 5-2K). The foreland basin was cut into elongate structural zones by the Deep-

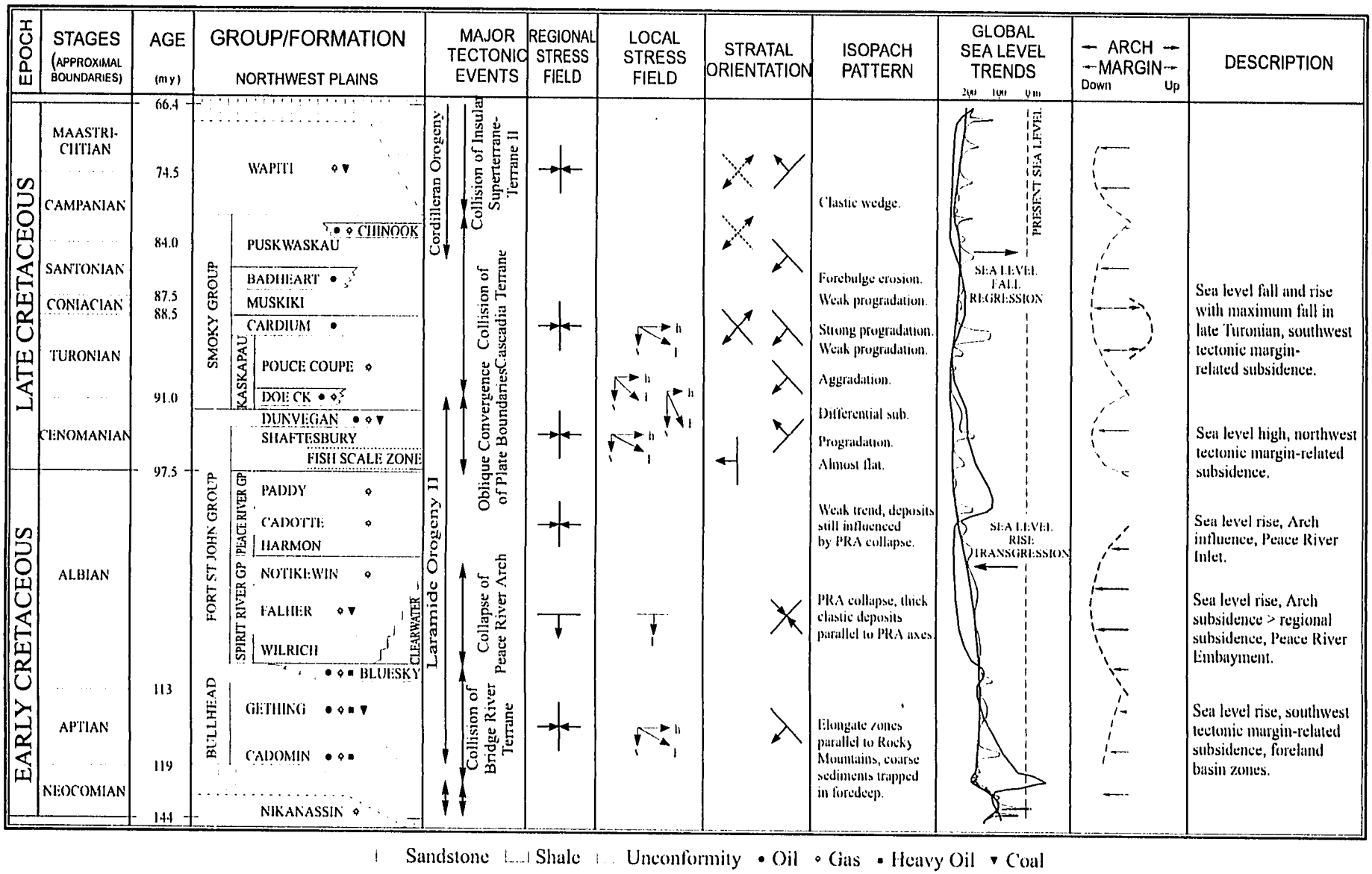

Figure 5-6. Summary of Cretaceous stratal characteristics, global sea-level change, Peace River Arch movement, tectonic events, and stress field. Black curve of sea level, modified from Vail *et al.* (1977) and AGAT Laboratories (1987). Pink (long term) and green (short term) curves of sea level, modified from Haq *et al.* (1988). Tectonic events, summarized from Coney *et al.* (1980), Monger (1983), Cant and Stockmal (1989), van der Heyden (1992), Armstrong and Ward (1993). Other component, suggested by this study.

CROSS SECTION OF UPPER MANNVILLE GROUP

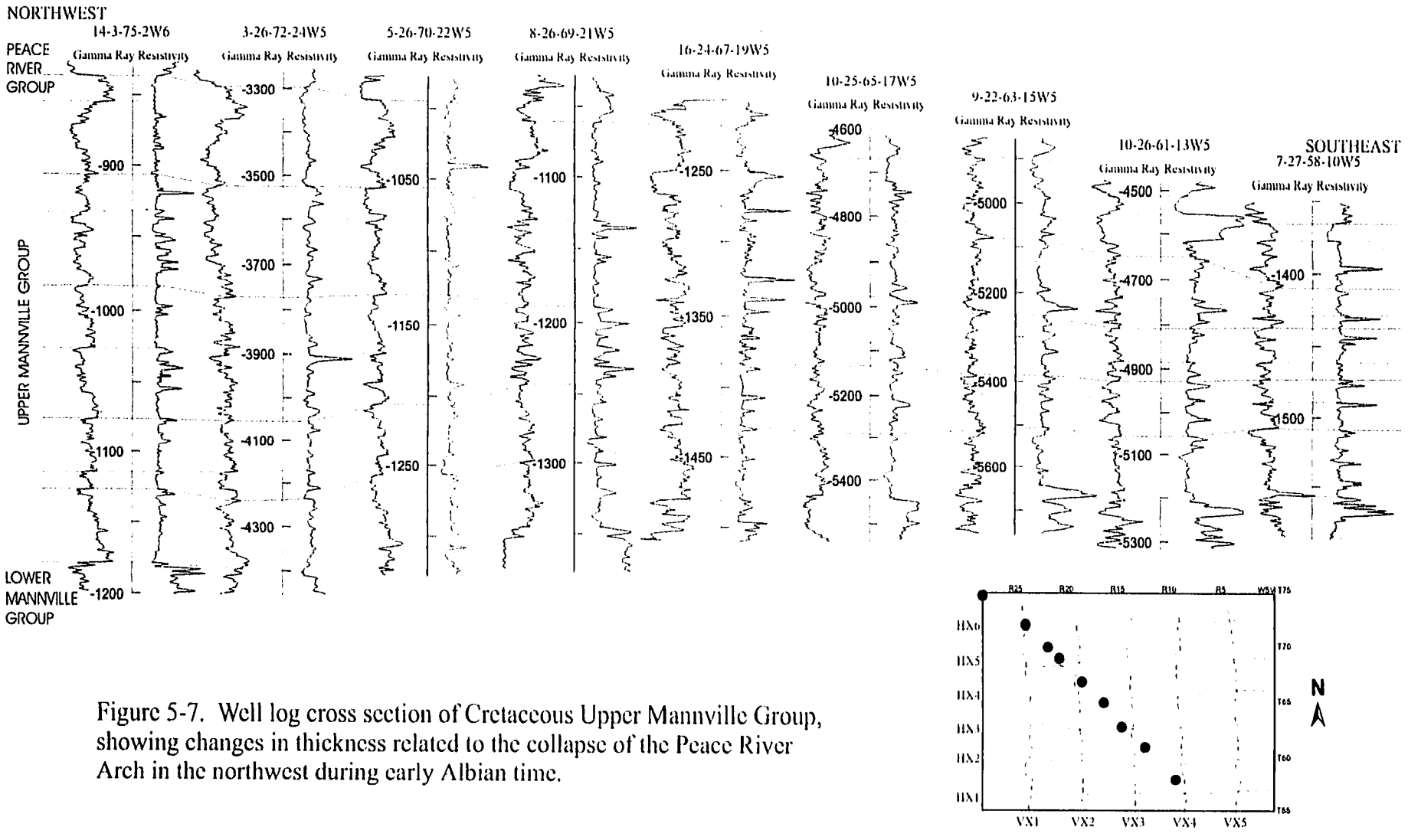

Figure 5-7. Well log cross section of Cretaceous Upper Mannville Group, showing changes in thickness related to the collapse of the Peace River Arch in the northwest during early Albian time.

Bulge and Bulge-Trough hinges. Coarse sediments were trapped mainly in the western foredeep. Deriving from the terrane collision, the supply of clastics for the Lower Mannville Group was abundant from the west. Unconformities formed in the Lower Mannville Group, probably resulting from a decrease in the rate of subduction because of changes in terrane accretion or relative plate motions (Currie, 1997). Several unconformity-bounded units that become muddier upward are distinguished from each other in the group (Cant and Abrahamson, 1996).

5-4. Cretaceous Albian: Resumed Peace River Embayment to Regional Quiescence

Global sea level continued to rise during Early Cretaceous Albian time (Fig. 5-6; Haq *et al.*, 1988). There was no documented collisional event on the west margin of the Canadian craton during this time. Coincidentally with the lack of collisional events on the west margin, the PRA collapsed and the Peace River Embayment was resumed (Fig. 5-2L). The collapse of the PRA during early Albian time has been reported by Cant (1988) and McPhee (1994). There was no forced progradation of successions in the Upper Mannville Formation (Fig. 5-7) as observed in basal deposits of the Cardium (Figs. 4-9, 4-10) and Shaftesbury (Figs. 4-11, 4-16) formations. Stacking of Upper Mannville Group successions (Fig. 5-7) demonstrates a process of syn-depositional down-warping toward the PRA in the northwest. Comparable to the Carboniferous (Fig. 5-2G, 5-2L) and free of regional tectonic events during Albian time, the Albian collapse of the Arch is suggested to represent a regional extension. The mechanism

causing long lasting Arch subsidence from Middle Devonian time may have become the dominant control after the effect from the Terrane I and Bridge River Terrane collisions tapered off during the Cretaceous Albian time.

Clastic supplies from the west were abundant and attributed to the lag effect of source areas from the collisions of Terrane I and the Bridge River Terrane (Underschultz and Erdmer, 1991). Conglomerate and sandstone were deposited in the rapidly subsiding PRA region, forming large deltas (e.g., Falher, Cant, 1988; Rouble and Walker, 1994; Leckie, 1984).

Thick sedimentary sequences deposited in the upper Lower Cretaceous are also observed in the U.S. portion of the Western Interior Basin and the wavelength and magnitude of the accommodation trends are more than can be generated by either flexural foreland basin subsidence or eustatic sea-level rise (Currie, 1997). Currie (1997) proposed that a subducting oceanic plate generates mantle convection beneath the overriding continental lithosphere and long wavelength subsidence into the continental interior. Increased subduction rates during late Early Cretaceous time restored dynamic subsidence beneath the Western Interior Basin and allowed the deposition of thick sedimentary successions in areas beyond the flexural wavelength of the developing Cordilleran foreland-basin system.

Global sea level remained very high during most of the late Albian stage (Haq *et al.*, 1988). Influenced by Arch collapse, the Peace River Group trends NE-SW with the depositional centre in the northwest (Fig. 5-2M). The penecontemporaneously subsiding PRA affected sedimentation and erosional patterns of the Peace River Group in the PRA area (Leckie *et al.*, 1990). The pre-existing faulting system appears to have an influence on deposition of the Peace River Group. Viking contour lines are bent ENE along the trend of the

former Hines Creek Graben (Fig. 5-2N). Clastic supplies were still abundant but fine upward (Fig. 4-3) in the Peace River Group. Stratal trends were less pronounced upward and potato-shaped contours became common (Figs. 5-8A to 5-8D), indicating topographic relief. Thick marine shale deposits in the uppermost Peace River Group were formed in a paleo-environment of deep water (Fig. 5-6) and less coarse clastic supply. Deep water (more accommodation space) could be generated by (1) sea level rise, (2) basement collapse, and (3) tectonic loading on plate margins. Less coarse clastic supply may have resulted from relief of earth topography and long distance transportation of sediments. During Albian time, global sea level rise, basement collapse, and relief of earth topography may have been responsible for the fine clastic deposits in the uppermost Peace River Group in the PRA region.

5-5. Late Cretaceous: Alterations of Basin Floor Tilting and Stratal Orientation

The Base of Fish Scales marker, representing the base of the Upper Cretaceous, consists mainly of sandy silty beds with abundant fish remains that are attributed to an anoxic event caused by a stratified water column (McCrae, 1996). The Base of Fish Scale marker is stable over a large area and the gradients of the basin floor are very gentle, about 5-11 cm/km dipping west (Fig. 5-2O).

Global sea level remained high during most of the Late Cretaceous except late Turonian time (Fig. 5-6; Haq *et al.*, 1988). However, the orientation of strata and the location of maximum subsidence were shifting in the PRA region. The sequence trends NE-SW with

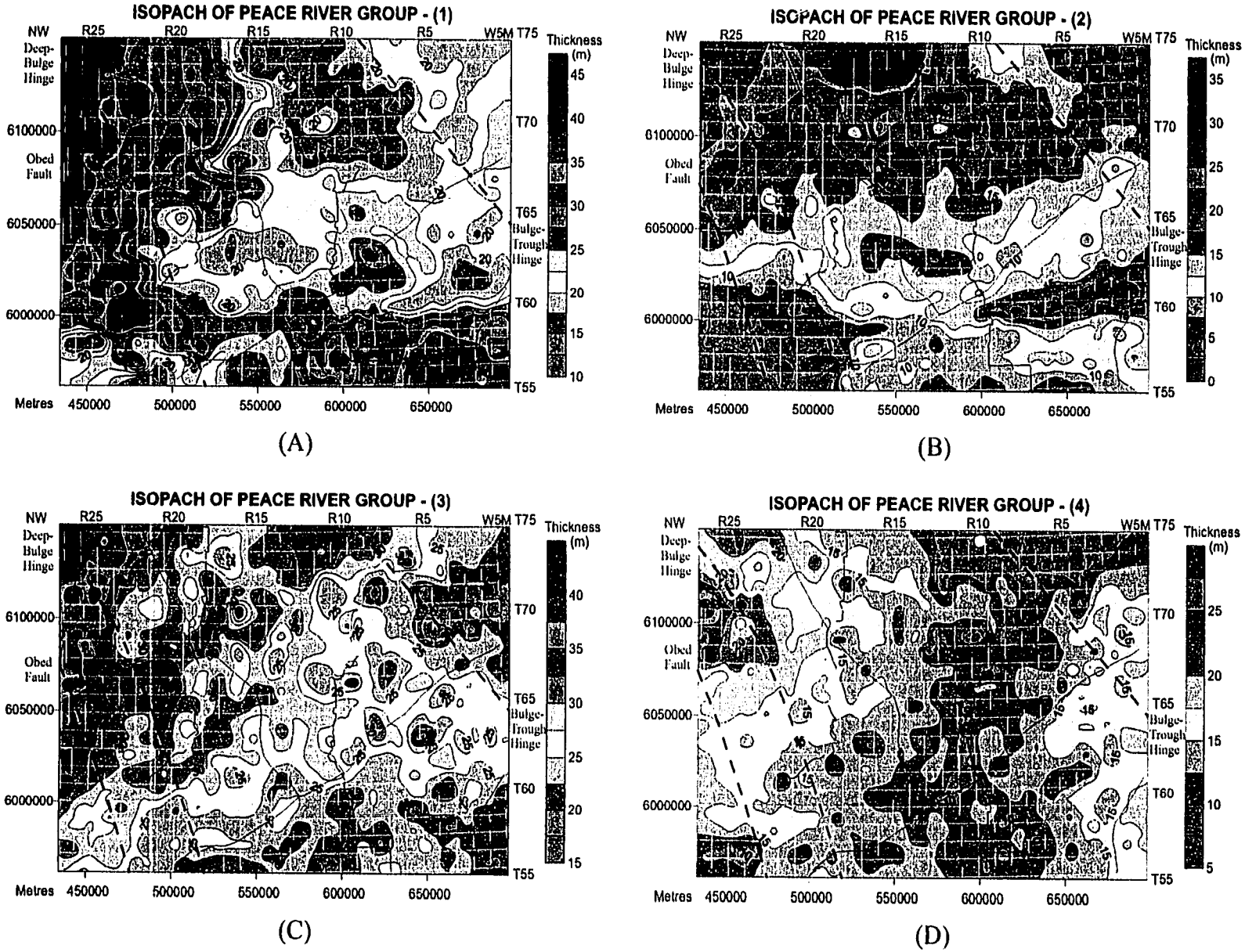

Figure 5-8. Isopach maps of Peace River Group, showing stacking process of the group. Number of formation, refer to Fig. 4-3. Blue line, Proterozoic domain boundary (refer to Fig. 1-8). Purple line, seismic line (refer to Fig. 1-2).

subsidence in the NW from middle Cenomanian to earliest Turonian (Fig. 5-2P), NW-SE with subsidence in the SW from late early Turonian to Santonian (Fig. 5-2R), and NE-SW with subsidence in the NW from Campanian to Maastrichtian (Figs. 3-1, 4-5B). The abrupt changes in regional trends of strata and location of maximum subsidence appears to be related to changes in the regional stress field.

5-5-1. Middle Cenomanian to Earliest Turonian: Northwest Subsidence

During the period from middle Cenomanian to earliest Turonian, compressional orogenic activity in the Cordillera and drifting of the Canada Basin continental margins were active (Dixon, 1993). Northward translation of materials occurred along the continental margin on dextral strike-slip faults caused by oblique convergence that resulted from terrane docking and Pacific plate drift (Coney *et al.*, 1980; Eisbacher, 1981; Monger, 1993). The northward slip of the Canadian cordillera is estimated to be more than 600 km (Monger, 1993).

Local faults were reactivated in early Late Cretaceous time (Leckie *et al.*, 1990). Great thicknesses of Dunvegan sediments accumulated in the PRA area (Williams, 1958). With the exception of marginal areas, all parts of the Cordillera were uplifted by mid-Cretaceous time, and may be responsible for the abundant clastic supplies in the Dunvegan Formation. There is no collapse of the PRA recorded on the isopach map of the Dunvegan Formation (Fig. 5-2Q). The major subsidence of the Dunvegan was beyond the PRA and rooted in the northwest continental boundary. The forced progradation in early deposits of the Shaftesbury/Dunvegan (Fig. 4-16) may have been related to an increase in regional compression. The differential

subsidence in the upper Shaftesbury/Dunvegan and Doe Creek formations (Fig. 4-12) may indicate the wane of the regional compression related to changes in the regional stress fields.

5-5-2. Late Early Turonian to Santonian: Southwest Subsidence with Peace River Arch Uplift in Cardium

Formations from the Pouce Coupe to First White Speckled Shale were oriented NW-SE with maximum subsidence in the SW. With the exception of the Cardium and Bad Heart formations, which consist mainly of coarse siliciclastic sediments, the Pouce Coupe, Blackstone, Muskiki, and lower Puskwaskau formations contain primarily fine siliciclastic sediments (Fig. 1-7). There were two levels of progradation: a long period from the late early Turonian to Santonian time (Fig. 4-15) and a short period in latest Turonian time (Fig. 4-10). The deposition of the six formations (Fig. 4-15) shows a succession from aggradation through progradation to aggradation and is interpreted to correspond to changes in horizontal compression from medium strong through very strong to medium strong. The compressional process was possibly related to convergence of plate boundaries or docking of the Cascadia Terrane in the west (Fig. 2-1; Cant and Stockmal, 1989). The docking of the small Cascadia Terrane should have occurred during late early Turonian and Santonian time and may be responsible for the formation of the Cardium clastic wedge.

The tectonic loading may have reached its peak in late Turonian time (Cardium Formation). Under very strong horizontal compression, elongate structural zones cut by basement faults migrated back and forth perpendicularly to the Cordilleran deformation front. Tectonic events appear to have played a critical role in controlling the motion of basement

blocks, although the slight fall of global sea level at about 90 m.y. (Fig. 5-6; Haq *et al.*, 1988) may have affected deposition of the Cardium Formation and assisted the basinward movement of sediments.

The PRA was uplifted during latest Turonian time (Cardium Formation, Fig. 2-7B; Hart and Plint, 1990). In the northwest of the study area, contour lines on the Cardium isopach map trend NE-SW parallel to the PRA long axis (Fig. 2-7B). Arch activity appears to have slightly affected the Muskiki Formation (Fig. 4-15D) and had ceased in earliest Santonian time (Bad Heart Formation).

5-5-3. Campanian to Maastrichtian: Northwest Subsidence

During Campanian and Maastrichtian time, short-term sea level was fluctuating slightly and long-term sea level was at still stand (Fig. 5-6; Haq *et al.*, 1988). Lea Park fine clastic deposits were thinning toward northwest and overlying Belly River coarse clastic deposits were thickening toward the northwest (Figs. 3-1, 4-5B). The northwest thinning of the Lea Park Formation and northwest thickening of the Belly River Formation may have been dominated by tectonic events during this time.

The depositional environment in the PRA region appears to have been strongly affected by the accretion of the Insular Superterrane (Terrane II) on to the continental margin (Monger *et al.*, 1982; Cant and Stockmal, 1989) and the northward translation of previously accreted and accreting material along the continental margin on dextral strike-slip faults (Coney *et al.*, 1980; Eisbacher, 1981; Monger, 1993). It is not clear if the thickening of the Belly River Formation toward the northwest was related to an Arch subsidence (as in the Upper

Mannville) or a tectonic event in the continental margin (as in the Dunvegan). According to the seismic cross sections (Fig. 3-1), the final uplift of the Arch appears to have started in Maastrichtian time (Edmonton Group).

CHAPTER 6: SUMMARY AND SUGGESTIONS

6-1. Highlights of Key Points

Detailed isopach and structural maps for most of the Cretaceous formations on the southeast flank of the PRA have been constructed for this thesis. These maps have allowed for the 1) documentation of stratigraphic changes and processes. 2) identification of areas of possible basement-sediment interaction in the Arch region. and 3) analysis of possible influences from basement and tectonic events.

6-1-1. Existing Problems

(1) There have not been substantial measurements and calculations for Arch subsidence driven by thermal decay (Cant, 1988).

(2) Basement-prism-floating isostatic adjustment can not accommodate a collapse in an extensional field like the Peace River Embayment in the Carboniferous, Permian, and Early Cretaceous Albian time (Walcott, 1970; Jones, 1980).

(3) A few hundred metres of sediment loading/unloading in the Williston Basin could not generate an uplift/subsidence of the lithosphere in the PRA (Figs. 3-2, 3-3, 3-4; Beaumont, personal communication, 2000).

(4) Post-glacial rebound could not account for the repeated 90^0 changes in the Cretaceous. There is no documented glaciation in the Cretaceous. The time scale of glacial isostatic adjustment process (0.001-0.1 m.y.) is probably not responsible for the basement tilting in the Cretaceous that occurred on a scale of 5-15 m.y. The time frame is consistent

with the time scale recorded for tectonic processes (1-100 m.y.: Pirazzoli *et al.*, 1993; Wu, 1998).

(5) Sedimentologic processes and eustatic sea level fluctuations could not account for the right-angle stratal re-orientations observed in the PRA region during Cretaceous time (Tillman and Martinsen, 1984; Bergman and Walker, 1987; Pattison and Walker, 1992; Posamentier *et al.*, 1992).

(6) Previous studies suggesting basement control have not documented underlying tectonic mechanisms in a continuous process of stratal change and provided evidence from basement. Many basement faults are not associated with linear aeromagnetic anomalies (Smith *et al.*, 1984; Hart and Plint, 1993; Plint *et al.*, 1993; Donaldson *et al.*, 1998).

(7) In addition to missing the Upper Cretaceous Cardium clastic wedge, the collision-clastic wedge model mixed up the Lower Mannville Group with the Upper Mannville Group and mismatched the Dunvegan clastic wedge to the docking of the Cascadia Terrane (Cant and Stockmal, 1989).

(8) The age of the WRS is poorly constrained (Ross and Eaton, 1996, 1997; Figs. 1-10, 2-13, 3-6, 3-7, 3-8). It is unlikely that thin layers (70±10 m) of mafic magma in the WRS were intruded at least 120,000 km^2 in the middle and upper crust without conduits and/or local thickening during a brittle indentation (Delaney, 1980; Ahern, 1980; Kang, 1981; Furling and Myers, 1985; Bruce and Huppert, 1990; Ross and Eaton, 1996, 1997; Brown and Solar, 1999). The reverse polarity in the WRS has been observed by this study (Fig. 2-13; unpublished data; Ross, Eaton, Brent, Dietrich, personal communications, 1999, 2000) and existing seismic modeling tests (Ross and Eaton, 1996, 1997) do not show a reverse polarity.

(9) Many formation boundaries in the Cretaceous are time transgressive surfaces, such as, the boundaries between the Belly River sandstone and the Lea Park shale (Fig. 4-1), between the Bad Heart sandstone and the Puskwaskau shale (Fig. 4-2), and between the Viking sandstone and the Joli Fou shale (Fig. 4-3).

6-1-2. Cretaceous Stratal Re-orientations

(1) Three major stratal re-orientations occurred from NW-SE in the Lower Mannville Group to NE-SW in the Upper Mannville Group (Figs. 2-3, 2-5), from NE-SW in the Dunvegan Formation to NW-SE in the Pouce Coupe Formation (Fig. 4-4), and from NW-SE in the lower Puskwaskau Formation to NE-SW in the Lea Park Formation (Fig. 4-5).

(2) The stratal change between the Aptian and Albian marked a time when the effect from the collisions of Terrane I and the Bridge River Terrane had tapered off and the mechanics causing PRA collapse became the dominant control (Fig. 2-1; Haq *et al.*, 1988; Cant, 1988; Cant and Stockmal, 1989; Leckie and Smith, 1992; Currie, 1997).

(3) Oblique convergence of plate boundaries and the accretion of the Cascadia Terrane on the continental margin may have been responsible for the changes in regional seafloor tilting during latest Cenomanian and earliest Turonian time (Fig. 2-1; Coney et al., 1980; Monger, 1983; van der Heyden, 1992; Armstrong and Ward, 1993).

(4) The northward translation along the continental margin on dextral strike-slip faults and the accretion of Terrane I to western North America may have been responsible for the basin floor tilting and source area alteration during Campanian time (Fig. 2-1; Cant and Stockmal, 1989; Armstrong and Ward, 1993; Monger, 1993).

6-1-3. Cretaceous Stacking Processes

(1) There could be no time delay for sediments to be denuded in the orogen and then trapped in the basin. An orogeny could be responsible for contemporaneous siliciclastic sediments trapped in the basin (Schumm, 1982; Wolman and Miller, 1982; Duk-Rodkin and Hughes, 1994; Fig. 2-7).

(2) Three stacking processes of sediments occurred in the Cretaceous. They are linear progradation of elongate zones (Figs. 4-9, 4-10), differential subsidence (Figs. 4-11, 4-12), and aggradation (Figs. 4-13, 4-14).

(3) Cardium incised shoreface sandbodies stack in particular locations (Hart and Plint, 1993). In the Cardium and lower Shaftesbury/Dunvegan formations, elongate zones slivered by basement faults migrated back and forth perpendicularly to the tectonic front (Figs. 2-1, 2-7B, 4-10).

(4) In the upper Shaftesbury/Dunvegan and Doe Creek formations, quadrilateral blocks subsided differentially crossing basement discontinuities (Fig. 4-12).

(5) In the Pouce Coupe Formation, the whole basement floor functioned as a uniform sheet and subsided in place (Figs. 4-13, 4-14).

(6) Horizontal compression/extension and vertical buoyancy/subsidence appear to have varied through time and have dominated subsidence processes in the Cretaceous. Linear shifting of elongate zones occurred when the lateral compression was strong; differential

subsidence took place when the lateral compression was weak; and aggradation occurred when the lateral compression was moderate.

6-1-4. Basement Objects and Influences

(1) In the PRA region, two sets of basement faults intersect each other at high angles. One trends NW-SE parallel to the Rocky Mountain deformation front and the other trends NE-SW (NEE-SWW) parallel to the long axis of the PRA (Figs. 2-2, 4-8; Cant, 1988; Richards *et al.*, 1994; unpublished data of this study).

(2) The Obed Fault (Figs. 2-2, 2-7A, 2-8), Deep-Bulge Hinge (Figs. 2-2, 2-3, 2-7A, 2-8, 2-9, 2-10), Bulge-Trough Hinge (Figs. 2-2, 2-3, 2-7B, 2-8A, 2-11), and Donnelly Fault (Figs. 2-12, 2-13) are long acting basement faults and have persistently influenced Phanerozoic formations. Basement faults cut the basement into elongate zones and assist the migration of the foreland zones. Reverse motion on faults has been observed in the PRA region. Many faults experienced both episodes of normal and reverse faulting (e.g., Deep-Bulge Hinge, Figs. 2-2, 2-7A; Obed Fault, Fig. 2-8).

(3) The Proterozoic domains (Fig. 1-8) assembled in Paleoproterozoic time (Ross, 1990) appear to have been welded together and functioned as a uniform crustal block during most of the Phanerozoic Era (Figs. 5-1, 5-2). The boundaries of the domains appear to have had a minor impact on sedimentation (Figs. 2-7B, 4-12). The boundaries may have been weak planes in the crust and could be mobilized under certain conditions.

(4) The WRS appears to be elongate and crosscuts Proterozoic domain boundaries (Fig. 3-7A). The WRS is developed along the steeper side of the asymmetric forebulge in the

foreland basin (Figs. 3-7B, 3-8). There is a positive correlation between the topography of the present Phanerozoic cover and the topography of the crustal sheet top (Figs. 1-10, 2-13). The WRS may have been modified by foreland basin processes.

6-1-5. Evolution of Peace River Arch

(1) The initial uplift of the PRA is suggested to be in latest Proterozoic time (McMechan, 1990; O'Connell, *et al.*, 1990). The Arch region remained high, as part of the Peace River-Athabasca Arch from Cambrian to Early Devonian time (Kent, 1994).

(2) There is no Cambrian record on the PRA (Figs. 1-10, Cant, 1988) and the Lower Cambrian is missing from the PRA region (Fig. 5-2). The Middle Cambrian was transgressively deposited on the margins of the Arch (Fig. 1-10; Eaton *et al.*, 1997) as global sea level rose rapidly (Fig. 5-5; Vail *et al.*, 1977; Hallam, 1984).

(3) Deposits retreated from the Arch during the Upper Cambrian to Lower Ordovician (Fig. 5-2B) because of the decrease in the rate of sea level rise (Fig. 5-5) and a much broader regional uplift in the WCSB (Mossop, personal communication, 1999). There is no depositional record (accumulated/prevented) from the Late Ordovician to Early Devonian in the PRA region (Figs. 1-10, 5-2).

(4) Arch rise was terminating toward Middle Devonian time and the Arch region began subsiding in Middle Devonian time (Figs. 5-2C, 5-5). The subsidence/depositional rate of the Arch and surrounding areas increased from Middle to Late Devonian time and reached its peak in Late Devonian Wabamun time (Fig. 5-4).

(5) The PRA became an island in Late Devonian Woodbend and Winterburn time (Fig. 5-2E) and subsequently an embayment from Late Devonian Wabamun to Permian time (Figs. 5-2F, 5-2G, 5-2H, 5-3; O'Connell, *et al.*, 1990; Barclay *et al.*, 1990; Richards *et al.*, 1994).

(6) During Triassic time, collapse of the Arch ceased and the Peace River Embayment became a sub-basin of the Alberta Basin (Fig. 5-2I; Edwards *et al.* 1994).

(7) The long subsidence history of the PRA was interrupted by Mesozoic convergent events on the western margin (Coney *et al.*, 1980; Monger *et al.*, 1982). Jurassic subsidence in the Arch region may have been dominated by the collision of Terrane I (Fig. 5-2J). The Rocky Mountain rooted subsidence of the Lower Mannville Group (Fig. 5-2K) may have been related to the accretion of the Bridge River Terrane to the western margin (Cant and Stockmal, 1989).

(8) The collapse of the PRA (Cant, 1988; McPhee, 1994) was resumed during Early Cretaceous Albian time (Fig. 5-2L). The Arch collapse and pre-existing faulting system had an influence on the Upper Mannville and Peace River groups (Figs. 5-2M, 5-2N). Fine clastic deposits in latest Early Cretaceous were attributed to global sea level rise (Fig. 5-6; Haq *et al.*, 1988), Arch collapse (Figs. 5-2M, 5-2N), and relief of Earth topography (Fig. 5-8).

(9) The orientation of strata and the location of maximum subsidence were shifting during Late Cretaceous time (Figs. 5-2O, 5-2P, 5-2Q, 5-2R). The abrupt changes in depocentre appear to be related to changes in the stress field by oblique convergence of plates and collisions of the Cascadia Terrane and Terrane II (Coney *et al.*, 1980; Eisbacher, 1981; Cant and Stockmal, 1989; Monger, 1993; Dixon, 1993).

(10)The loading of the Cascadia Terrane may have reached its peak and initiated an Arch uplift in late Turonian time (Cardium Formation, Fig. 4-15). The final uplift of the Arch began in Maastrichtian time (Edmonton Group, Fig. 3-1).

6-2. Potential Areas for Petroleum Exploration

The PRA region is one of the most productive oil and gas bearing areas in the WCSB. Since 1949 when the first well was drilled in the Arch (deMille, 1958), more than thirty-three thousand wells (GSC-Calgary SAMS Database) have been drilled in the study area and 39% of the wells have intersected oil and gas pools. Prolific oil and gas fields have been found in the region, including Devonian Normandville Field, Carboniferous Dunvegan Field, Permian Eagle Field (Horner *et al.*, 1994), Triassic Boundary Lake Field, and Cretaceous Elmworth Field (Masters, 1984).

The Cretaceous is one of the most important exploration target intervals in the PRA region. Figure 6-1 illustrates the fields producing oil and gas from the Cretaceous. Among the producing wells, 37% are hosted in the Cretaceous (Devonian 39%, Triassic and Jurassic 18%, Carboniferous and Permian 6%). Oil and gas pools are unevenly distributed in Cretaceous formations. The Lower Cretaceous contains 68% of the pools and 32% were found in the Upper Cretaceous. Among the Lower Cretaceous oil and gas wells, 43% produce oil and gas from the Spirit River (Upper Mannville) Group, 36% from the Lower Mannville Group, and 21% from the Peace River Group.

Formation of oil and gas reservoirs is controlled by many factors, such as hydrocarbon generation and migration, conditions of reservoirs, cap rocks, entrapment, and reservation. In

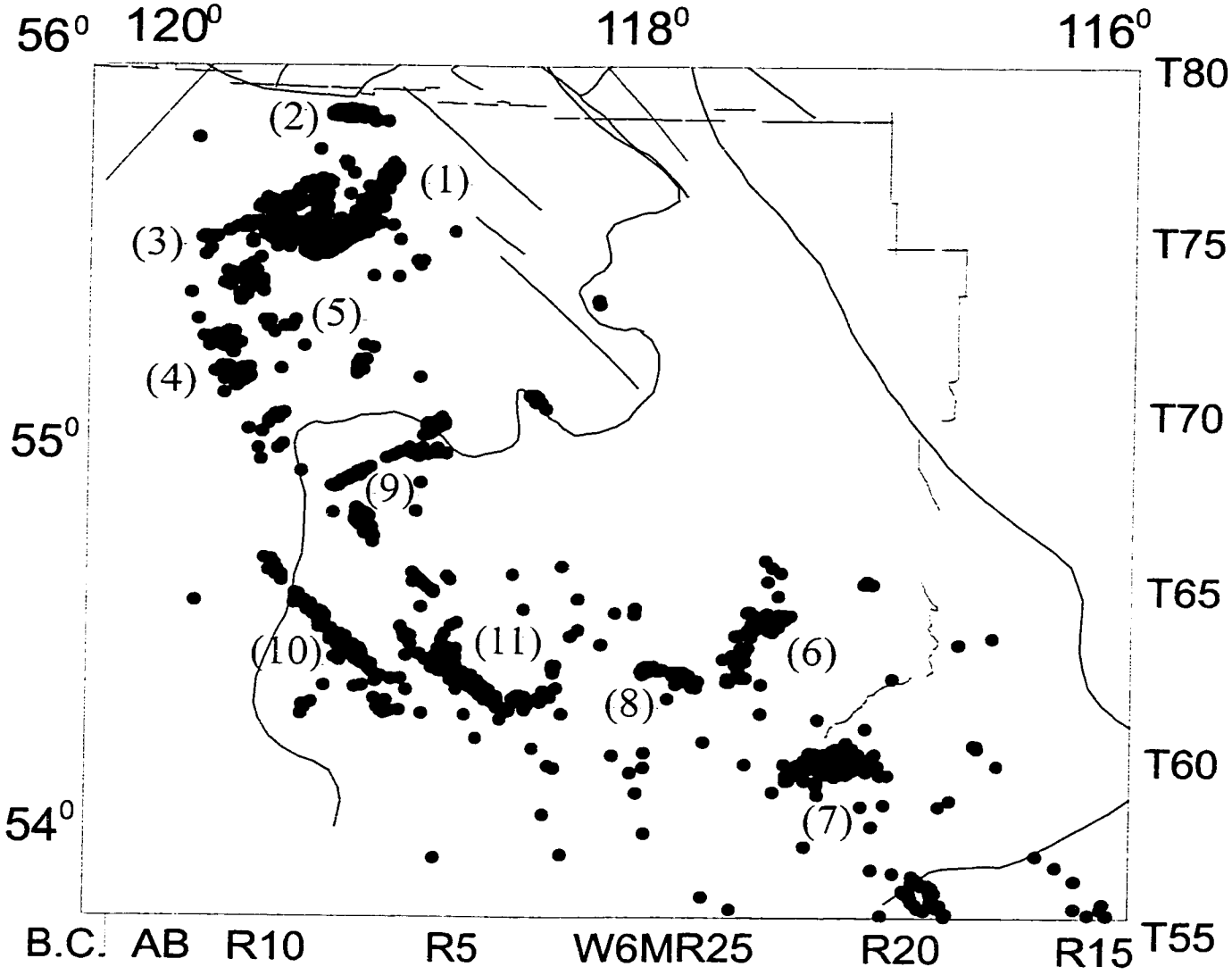

Figure 6-1. Cretaceous oil and gas fields. (1) Valhalla, (2) Progress, (3) Sinclair, (4) Elmworth, (5) Knopcik, (6) Waskahigan, (7) Big Stone, (8) Simonette, (9) Wapiti, (10) Red Rock, (11) Kakwa, (12) Pine Creek. Black dot, oil and gas well. Green line, seismic line (refer to Fig. 1-2). Blue line, Proterozoic domain boundary; purple line, inferred Precambrian fault/shear zone; red line, Carboniferous fault (refer to Fig. 1-8).

a basin where hydrocarbon generation, maturity, migration, and entrapment have been calculated, the distribution of reservoir rocks, reservoir structures, and cap rock conditions become critical to exploration. Generally speaking, in a petroleum province, larger structural reservoirs are likely found in early stages of exploration and smaller stratigraphic reservoirs come later. As exploration matures in an area, it becomes more and more important to integrate geological, geophysical, and engineering data to analyze facies distribution, lithologic change, and petro-physical properties of the target formations.

Figures 6-2 and 6-3 illustrate isopach maps overlain by structural contour lines and wells. Figure 6-2 shows the Dunvegan isopach (color strips), present Dunvegan structure top (blue contours), and wells (red and pink dots, black circles). The red and pink dots are Dunvegan and Doe Creek oil and gas wells and black circles are abandoned/other holes drilled for Upper Cretaceous targets. Figure 6-3 shows the isopach map of the formations between the First and Second White Speckled shales (color strips), present Cardium structure top (blue contours), and wells (red and pink dots, black circles). The red and pink dots are Cardium and Chinook oil and gas wells and black circles are abandoned/other holes drilled for Upper Cretaceous targets.

The structure of the Dunvegan and Cardium tops dip largely SSW. Neither large anticline nor significant faulting offset can be detected on the structures. There is no apparent relation between present structural tops and the successful wells in the Upper Cretaceous. The relation between patches of successful wells and structural contour lines demonstrates that the current tectonic configuration has only local control on petroleum accumulations in the mapping area. In contrast, there is a relationship between the locations of reservoirs and

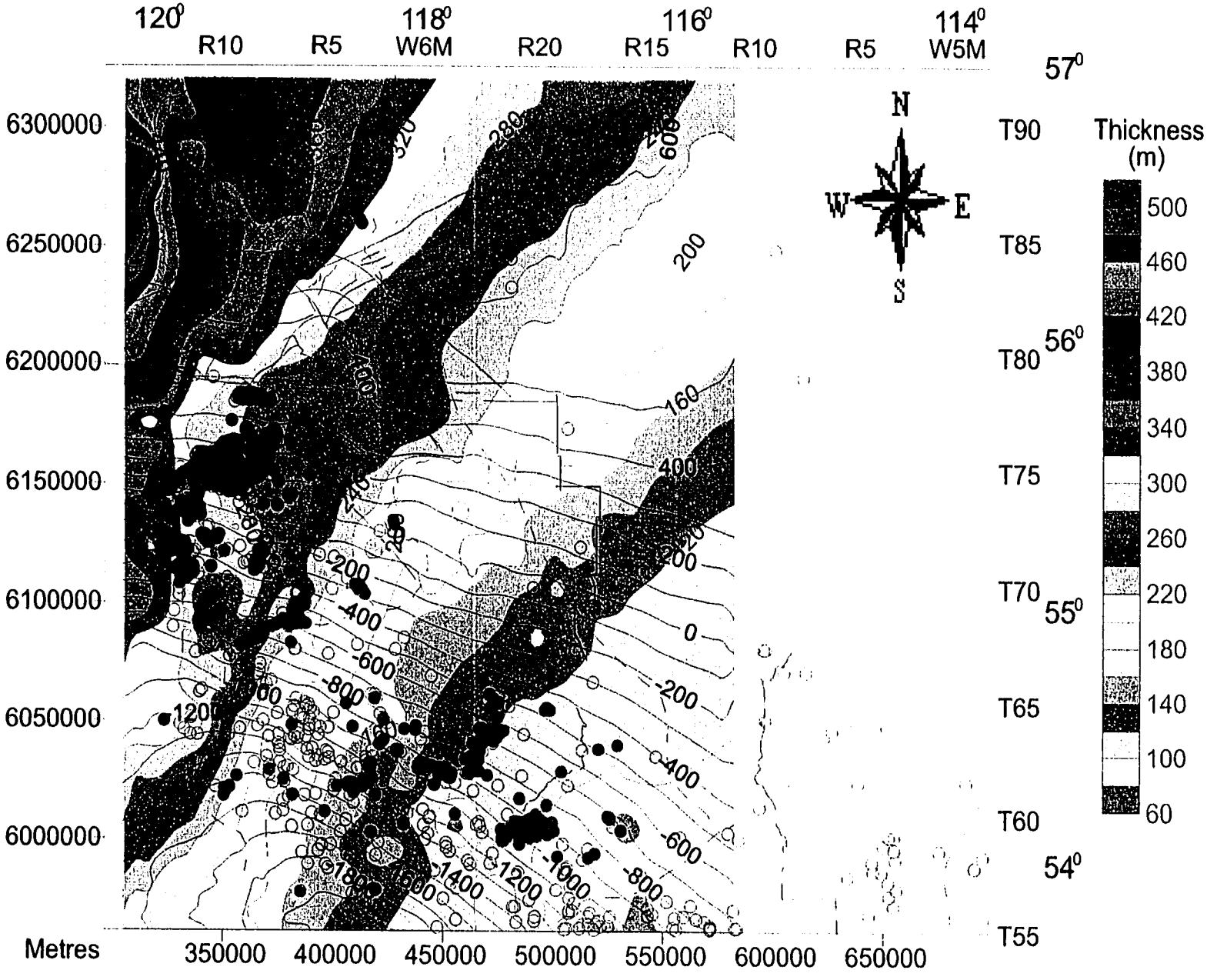

Figure 6-2. Overlain themes of structure, isopach, and wells. Blue line, structural contour of present Dunvegan top, elevation in metres. Orange line, isopach contour of the Dunvegan. Black circle, dry or abandoned well drilled for Upper Cretaceous targets. Red dot, Dunvegan oil and gas well. Pink dot, Doe Creek oil and gas well. Red line, fault. Dashed black line, domain boundary. Purple line, seismic line.

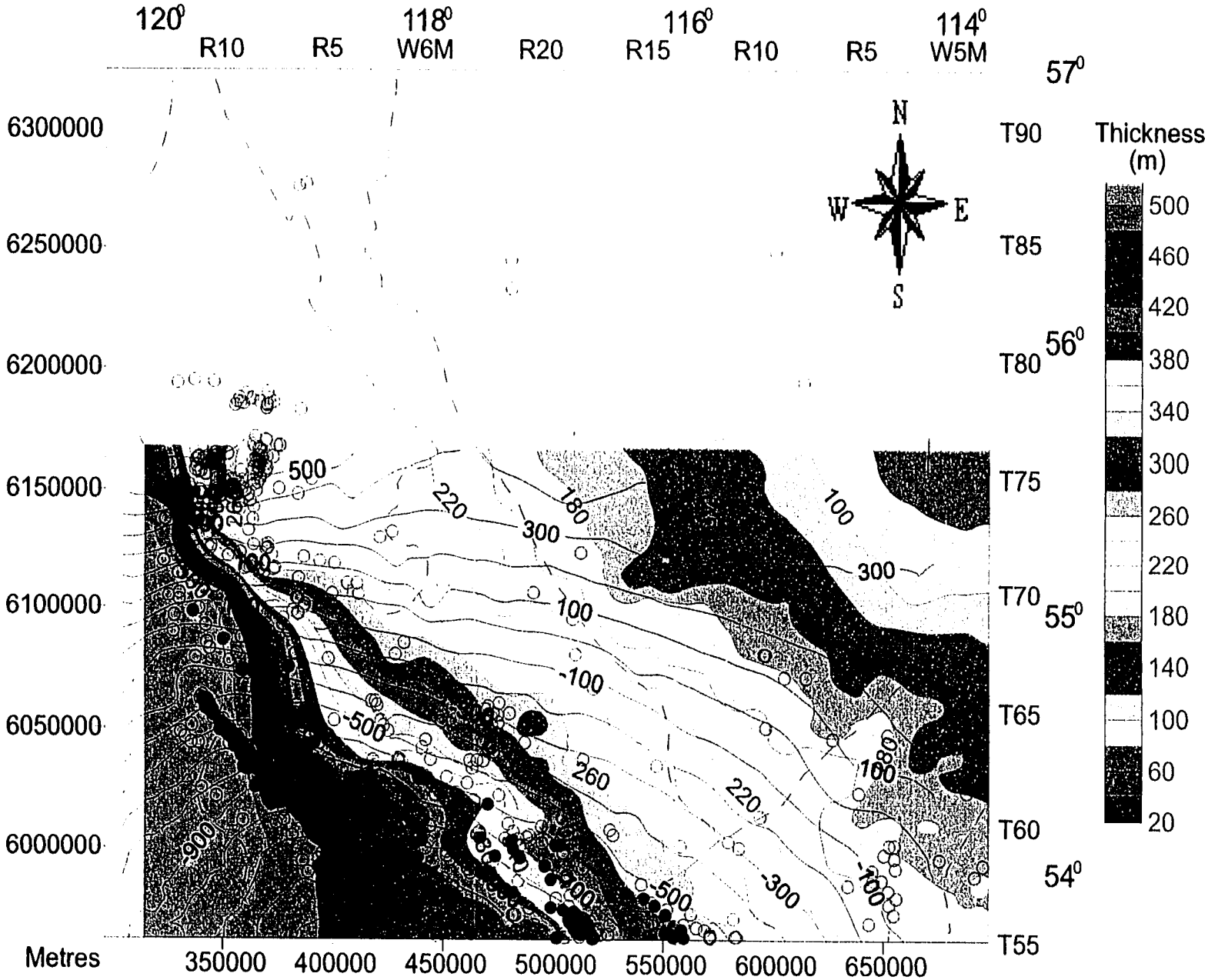

Figure 6-3. Overlain themes of structure, isopach, and wells. Blue line, structural contour line of present Cardium top, elevation in metres. Orange line, isopach contour line of the formations between the First and Second White Speckled Shales. Black circle, dry or abandoned well drilled for Upper Cretaceous targets. Red dot, Cardium oil and gas well. Pink dot, Chinook oil and gas well.

distribution of contemporaneous sandbodies. The Dunvegan and Doe Creek successful wells follow a NE-SW trend (Fig. 6-2) while the Cardium and Chinook successful wells follow a NW-SE trend (Fig. 6-3). The successful wells correspond to the stratal orientation of the host formations.

6-3. Suggestions for Future Work

Many aspects in the study area need further work. Suggestions for the future study are as follows:

(1) Correlate and construct isopach maps for the formations above the upper Lea Park Formation. Without isopach maps, it is not clear whether the thickening of the Belly River Formation and thinning of the Edmonton Group toward the northwest are related to PRA activities or boundary collisional events.

(2) Correlate and construct isopach maps for detailed successions in the Lower Cretaceous Upper Mannville Group to document the process of the Arch collapse during early Albian time.

(3) Design a variety of geological models for the WRS and test seismic responses to determine (a) origin of the reverse polarity, (b) reason for the constancy of the reverse polarity over a large area and insensitivity to depth (frequency) changes, and (c) reason for the high continuation of strong amplitude to be developed to the reflections with reverse polarity and not to be developed in the reflections with normal polarity in the observed WRS sheet.

(4) Investigate the relationship between the distribution of Cretaceous pools and sandbodies.

(5) Examine the relation between isolated shallow marine sandbodies and basement anomalies in other parts of the WCSB.

REFERENCES

AGAT Laboratories. 1987. Table of Formations of Alberta.

Ahern. J.L.: 1980. Magma Migration. Ph.D. thesis. Cornell University. 80-15628.

Armstrong. R.L. and Ward. P.L.: 1993. Late Triassic to earliest Eocene magmatism in the North American Cordillera: implications for the Western Interior Basin. In: Caldwell. W.G.E. and Kauffman. E.G.. eds.. Evolution of the Western Interior Basin. Geological Association of Canada. Special Paper 39. p. 49-72.

Baird. D.J.: Knapp. J.H.: Steer. D.N.: Brown. L.D.: and Nelson. K.D.: 1995. Upper-mantle reflectivity beneath the Williston basin. phase-change Moho. and the origin of intracratonic basins. Gology. v. 23. no. 5. p. 431-434.

Barclay. J.E.: Drause. F.F.: Campbell. R.I.: and Utting. J.: 1990. Dynamic casting and growth faulting: Dawson Creek Graben Complex. Carboniferous-Permian Peace River Embayment. Western Canada. Bulletin of Canadian Petroleum Geology. v. 38A. p. 115-145.

Beaumont. C.: Quinlan. G.M.: and Stockmal. G.S.: 1993. The evolution of the Western Interior Basin: causes. consequences and unsolved problems. In: Caldwell. W.G.E. and Kauffman. E.G.. eds.. Evolution of the Western Interior Basin. Geological Association of Canada. Special Pager 39. p. 97-117.

Bergman. K.M. and Walker. R.G.: 1987. The importance of sea level fluctuations in the formation of linear conglomerate bodies: Carrot Creek Member of Cardium Formation. Cretaceous Western Interior Seaway. Alberta. Canada. Journal of Sedimentary Petrology. v. 57. p. 651-665.

Brown. M. and Solar. G.S.: 1999. The mechanism of ascent and emplacement of granite magma during transpression: a syntectonic granite paradigm. Tectonophysics. v. 312. no. 1. p. 1-33.

Bruce. P.M. and Huppert. H.E.: 1990. Solidification and melting along dykes by the laminar flow of basaltic magma. In: Ryan. M.P.. ed.. Magma Transport and Storage. p. 87-102.

Burk. C.F. Jr.: 1962. Upper Cretaceous structural development of the southern flank of the Peace River Arch. Journal of the Alberta Society of Petroleum Geologists. v. 10. no. 5. p. 223-227.

Burwash. R.A.: 1957. Reconnaissance of subsurface Precambrian of Alberta. AAPG Bulletin. v. 41. no. 1. p. 70-103.

Burwash, R.A.; McGregor, C.R.; and Wilson, J.A.; 1994. Precambrian basement beneath the Western Canada Sedimentary Basin. In: Mossop, G.D. and Shetsen, I., comilers, Geological Atlas of the Western Canada Sedimentary Basin. Canadian Society of Petroleum Geologists and the Alberta Research Council, p. 49-56.

Cant, D.J. and Abrahamson, B.; 1996. Regional distribution and internal stratigraphy of the Lower Mannville. Bulletin of Canadian Petroleum Geology, v. 44, no. 3, p. 508-529.

Cant, D.J. and Stockmal, G.S.; 1989. The Alberta foreland basin: relationship between stratigraphy and Cordilleran terrane-accretion events. Canadian Journal of Earth Sciences, v. 26, no. 10, p. 1964-1975.

Cant, D.J.; 1984. Development of shoreline-shelf sandbodies in a Cretaceous epeiric sea deposit. Journal of Sedimentary Petrology, v. 54, p. 541-556.

Cant, D.J.; 1988. Regional structure and development of the Peace River Arch, Alberta: A Paleozoic failed-rift system? Bulletin of Canadian Petroleum Geology, v. 36, p. 284-295.

Catuneanu, O.; Beaumont, C.; and Waschbusch, P.J.; 1997. Interplay of static loads and subduction dynamics in foreland basins, reciprocal stratigraphies and the "missing" peripheral bulge. Geology (Boulder), v. 25, no. 12, p. 1087-1090.

Chen, D. and Bergman, K.M.; 1997. High-resolution stratigraphic analysis of Cretaceous formations in the Peace River Arch area of the Western Canada Sedimentary Basin: depositional processes and possible controlling mechanisms. LITHOPROBE Report #59, p. 129-162.

Chen, D. and Bergman, K.M; 1999. Stratal reorientation, depositional processes, and sequence evolution of the Cretaceous in the Peace River Arch region of the Western Canada Sedimentary Basin. Bulletin of Canadian Petroleum Geology, v. 47, no. 4, p. 594-620.

Coney, P.J.; Jones, D.L.; and Monger, J.W.H.; 1980. Cordilleran suspect terranes. Nature, v. 288, no. 27, p. 329-333.

Crough, S.T.; 1983. Rifts and swells: geophysical constraints on causality. In: Morgan, P. and Baker, B.H., eds., Processes of continental rifting. New York, Elsevier, p. 23-28.

Currie, B.S.; 1997. Jurassic-Cretaceous accommodation development in the Western Interior Basin, linking basin subsidence with oceanic plate subduction. Geological Society of America, 1997 Annual Meeting. Abstracts with Programs - Geological Society of America, v. 29, no. 6, p. 202.

Currie. B.S.: 1998. Upper Jurassic-Lower Cretaceous Morrison and Cedar Mountain formations. NE Utah-NW Colorado: relationships between nonmarine deposition and early Cordilleran foreland-basin development. Journal of Sedimentary Research. v. 68. no. 4. p. 632-652.

Delaney. P.T.. 1980. Magma flow. heat transport and brecciation of host rocks during dike emplacement near Ship Rock. New Mexico. Ph.D. thesis. Stanford University. 80-24639.

deMille. G.: 1958. Pre-Mississippian history of the Peace River Arch. In: Scott. J.C.. ed.. Symposium on the Peace River Arch. Journal of the Alberta Society of Petroleum Geologists. v. 6. no. 3. p. 61-69.

Dix. G.R.: 1990. Stages of platform development in the Upper Devonian (Frasnian) Leduc Formation. Peace River Arch. Alberta. Bulletin of Canadian Petroleum Geology. v. 38A. p. 66-92.

Dixon. J.: 1993. Cretaceous tectonics and sedimentation in northwest Canada. In: Caldwell. W.G.E. and Kauffman. E.G.. eds.. Evolution of the Western Interior Basin. Geological Association of Canada. Special Pager 39. p. 119-129.

Donaldson. W.S.: Plint. A.G.: and Longstaffe. F.J.: 1998. Basement tectonic control on distribution of the shallow marine Bad Heart Formation: Peace River Arch area. northwest Alberta. Bulletin of Canadian Petroleum Geology. v. 46. no. 4. p. 576-598.

Duk-Rodkin. A. and Hughes. O.L.: 1994. Tertiary-Quaternary drainage of the pre-glacial Mackenzie Basin. Quaternary International. v. 22/23. p. 221-241.

Eaton. D.W.: Lemieux. S.: and Ross. G. M: 1997. Regional seismic perspectives on the evolution of the Peace River Arch. Lithoprobe Report#59. p. 91-111.

Eaton. D.W.: Ross. G.M.: and Hope. J.: 1999. The rise and fall of a cratonic arch: a regional seismic perspective on the Peace River Arch. Alberta. Bulletin of Canadian Petroleum Geology. v. 47. no. 4. p. 346-361.

Edwards. D.E.: Barclay. J.E.: Gibson. D.W.: Kvill. G.E.: and Halton. E: 1994. Triassic Strata of the Western Canada Sedimentary Basin. In: Mossop. G.D. and Shetsen. I.. comilers. Geological Atlas of the Western Canada Sedimentary Basin. Canadian Society of Petroleum Geologists and the Alberta Research Council. p. 259-276.

Eisbacher. G.H.: 1981. Late Mesozoic - Paleogene Bower Basin molasse and Cordilleran tectonics. western Canada. Geological Association of Canada Special Paper 23. p. 125-151.

ERCBA (Energy Resources Conservation Board of Alberta). 1992. Table of Formations. Alberta.

Furlong, K.P. and Myers, J.D.: 1985. Thermal-mechanical modeling of the role of thermal stresses and stoping in magma contamination. Journal of Volcanology and Geothermal Research. v. 24. p. 179-191.

Garland, G.D. and Bower, M.E.: 1959. Interpretation of aeromagnetic anomalies in northeastern Alberta. Fifth World Petroleum Congress. Section 1. Paper 42. P.787-800.

Goodman, A.J: 1951. Tectonics of east side of Cordillera in western Canada. AAPG Bulletin. v. 35. no. 4. p. 783-796.

Hallam, A.. 1984. Pre-Quaternary sea-level changes. Annual Review of Earth and Planetary Sciences. v. 12. p. 205-243.

Haq, B.U.: Hardenbol, J.: and Vail, P.R.: 1987. Chronology of fluctuating sea levels since the Triassic. Science. v. 235. p.1156-1167.

Haq, B.U.: Hardenbol, J.: and Vail, P.R.: 1988. Mesozoic and Cenozoic Chronostratigraphy and cycles of sea-level change. In: Wilgus, C.K. *et al.*. eds.. Sea-Level Changes: An Integrated Approach SEPM Special Publication No. 42. p. 72-108.

Hart, B.S. and Plint, A.G.: 1990. Upper Cretaceous warping and fault movement on the southern flank of the Peace River Arch. Alberta. Bulletin of Canadian Petroleum Geology. v. 38A. p. 190-195.

Hart, B.S. and Plint, A.G.: 1993. Tectonic influence on deposition and erosion in a ramp setting: Upper Cretaceous Cardium Formation. Alberta foreland basin. AAPG Bulletin. v. 77. no. 12. p. 2092-2107.

Hein, F.J. and McMechan, M.E.: 1994. Proterozoic and Lower Cambrian strata of the Western Canada Sedimentary Basin. In: Mossop, G.D. and Shetsen, I.. comilers. Geological Atlas of the Western Canada Sedimentary Basin. Canadian Society of Petroleum Geologists and the Alberta Research Council. p. 57-68.

Hope, J.: Eaton, D.W.; and Ross, G.M.; 1999. Lithoprobe seismic transect of the Alberta Basin: compilation and overview. Bulletin of Canadian Petroleum Geology. v 47. no. 4. p. 331-345.

Horner. R.B.: Barclay. J.E.: and MacRae. J.M.: 1994. Earthquakes and hydrocarbon production in the Fort St. John area of northeastern British Columbia. Canadian Journal of Exploration Geophysics. v. 30. no. 1. p. 39-50.

Hubbard. R.J.: Pape. J.: Roberts. D.G.: 1985. Depositional sequence mapping as a technique to establish tectonic and stratigraphic framework and evaluate hydrocarbon potential on a passive continental margin. In: O.R. Berg and D.G. Woolverton. eds.. Seismic stratigraphy II: an integrated approach to hydrocarbon exploration. AAPG Memoir 39. p. 79-91.

Jones. R.M.P.: 1980. Basinal isostatic adjustment faults and their petroleum significance. Bulletin of Canadian Petroleum Geology. v. 28. no. 2. p. 211-251.

Kang. Joo-Myung. 1981. Finite element analysis of the heat and mass transfer in magma body. Ph.D. thesis. University of Oklahoma. 82-09428.

Kauffman. E.G. and Caldwell. W.G.E.: 1993. The Western Interior Basin in Space and Time. In: Caldwell. W.G.E. and Kauffman. E.G.. eds.. Evolution of the Western Interior Basin. Geological Association of Canada. Special Paper 39. p. 1-30.

Kauffman. E.G.. 1984. Paleobiogeography and evolutionary response dynamic in the Cretaceous Western Interior seaway of North America. In: Westermann. G.E.G.. ed.. Jurassic-Cretaceous Biochronology and Paleogeography of North America. Geological Association of Canada. Special Pager 27. p. 273-306.

Keen. C.E.: 1985. The dynamics of rifting: deformation of the lithosphere by active and passive driving forces. Geophysics. v. 80. p. 95-130.

Keith. J.W.: 1990. The influence of the Peace River Arch on Beaverhill Lake sedimentation. Bulletin of Canadian Petroleum Geology. v. 38A. p. 55-65.

Kent. D.M.: 1994. Paleogeographic evolution of the cratonic platform – Cambrian to Triassic. In: Mossop. G.D. and Shetsen. I.. comilers. Geological Atlas of the Western Canada Sedimentary Basin. Canadian Society of Petroleum Geologists and the Alberta Research Council. p. 69-86.

Kinoshita. W.T.: Koyanagi. R.Y.: Wright. T.L.: and Fiske. R.S: 1969. Kilauea volcano: the 1967-68 summit eruption. Science. v. 166. p. 459-468.

Kirby, S.H., 1985. Rock mechanics observations pertinent to the rheology of the continental lithosphere and the location of strain along shear zones. In: Carter, N.L. and Uyeda, S., eds., Collision Tectonics: Deformation of Continental Lithosphere. Tectonophysics, 119: 1-27.

Lavoie, D.H. 1958. The Peace River Arch during Mississippian and Permo-Pennsylvanian time. In: Scott, J.C., ed., Symposium on the Peace River Arch. Journal of the Alberta Society of Petroleum Geologists, v. 6, no. 3, p. 69-74.

Leckie, D.A.; 1984. Sedimentology of the Moosebar and Gates formations (Lower Cretaceous). 85-14732.

Leckie, D.A.; 1986. Rates, controls, and sand-body geometries of transgressive-regressive cycles: Cretaceous Moosebar and Gates formations, British Columbia. AAPG Bulletin, v. 70, p. 516-535.

Leckie, D.A.; Staniland, M.R.; and Hayes, B.J.; 1990. Regional maps of the Albian Peace River and lower Shaftesbury formations on the Peace River Arch, northwestern Alberta and northeastern British Columbia. Bulletin of Canadian Petroleum Geology, v. 38A, p. 176-189.

Leckie, D.A. and Reinson, G.E.; 1993. Effects of middle to late Albian sea-level fluctuation in the Cretaceous Interior Seaway, Western Canada. In: Caldwell, W.G.E. and Kauffman, E.G., eds., Evolution of the Western Interior Basin. Geological Association of Canada, Special Paper 39, p. 151-175.

Masters, J.A.; 1984. Elmworth - case study of a deep basin field. AAPG Memoir 38.

McCrae, S.L.; 1996. Geometric analysis of high frequency sequences in the lower Shaftesbury Formation, Northwest Alberta and Northeast British Columbia. University of Western Ontario, London, Ontario, Canada.

McMechan, M.E.; 1990. Upper Proterozoic to Middle Cambrian history of the Peace River Arch: evidence from the Rocky Mountains. Bulletin of Canadian Petroleum Geology, v. 38A, p. 36-44.

McPhee, D.A.; 1994. Sequence stratigraphy of the Lower Cretaceous Mannville Group of east-central Alberta. University of Alberta, Edmonton, Alberta, Canada.

Monger, J.W.H.; 1993. Cretaceous Tectonics of the North American Cordillera. In: Caldwell, W.G.E. and Kauffman, E.G., eds., Evolution of the Western Interior Basin. Geological Association of Canada, Special Paper 39, p. 31-47.

Monger, J.W.H.; Price, R.A.; and Tempelman-Kluit, D.J.; 1982. Tectonic accretion and the origin of the two major metamorphic and plutonic welts in the Canadian Cordillera. Geology, v. 10, p. 70-75.

Morgan, W.J.; 1983. Hotspot tracks and the early rifting of the Atlantic. In: Morgan, P. and Baker, B.H., *eds.*, Processes of continental rifting. New York, Elsevier, p. 123-140.

Mossop, G.D. and Shetsen, I.; *comp.*; 1994. Geological Atlas of the Western Canada Sedimentary Basin. Canadian Society of Petroleum Geologists and the Alberta Research Council.

Nelson, K.D.; Baird, D.J.; Walters, J.J.; Hauck, M.; Brown, L.D.; Oliver, J.E.; Ahern, J.L.; Hajnal, Z.; Jones, A.G.; and Sloss, L.L.; 1993. Trans-Hudson orogen and Williston basin in Montana and North Dakota: New COCORP deep-profiling results. Geology, v. 21, p. 447–450.

O'Connell, S.C.; Dix, G.R.; and Barclay, J.E.; 1990. The origin, history, and regional structural development of the Peace River Arch, western Canada. Bulletin of Canadian Petroleum Geology, v. 38A, p. 4-24.

Pattison, S.A.J. and Walker, R.G.; 1992. Deposition and interpretation of long, narrow sandbodies underlain by a basinwide erosion surface: Cardium Formation, Western Interior Seaway, Alberta, Canada. Journal of Sedimentary Petrology, v. 62, no. 2, p. 292-309.

Peltier, W.R.; 1998. Global glacial isostasy and relative sea level: implications for solid earth geophysics and climate system dynamics. In: Wu, P., ed., Dynamics of the Ice Age Earth – A Modern Perspective. GeoResearch Forum, v. 3-4, p. 17-54.

Plint, A.G.; Hart, B.S.; and Donaldson, W.S.; 1993. Lithospheric flexure as a control on stratal geometry and facies distribution in Upper Cretaceous rocks of the Alberta foreland basin. Basin Research, v. 5, no. 2, p. 69-77.

Posamentier, H.W.; Allen, G.P.; James, D.P. and Tesson, M.; 1992. Forced regressions in a sequence stratigraphic framework: concepts, examples and exploration significance. AAPG bulletin, v. 76, p. 1687-1709.

Poulton, T.P.; Christopher, J.E.; Hayes, B.J.R.; Losert, J.; Tittemore, J.; and Gilchrist, R.D.; 1994. Jurassic and Lowermost Cretaceous strata of the Western Canada Sedimentary Basin. In: Mossop, G.D. and Shetsen, I., comilers, Geological Atlas of the Western Canada Sedimentary Basin. Canadian Society of Petroleum Geologists and the Alberta Research Council, p. 297-316.

Poulton, T.P.; Tittemore, J.; Dolby, G.; 1990. Jurassic strata of northwestern (and west-central) Alberta and northeastern British Columbia. Bulletin of Canadian Petroleum Geology, v. 38A, p. 159-175.

Quinlan, G. and Beaumont, C.; 1984. Appalachian thrusting, lithospheric flexure and the Paleozoic stratigraphy of the eastern interior of North America: Canadian Journal of Earth Sciences, v. 21, p. 973-996.

Richards, B.C.; Barclay, J.E.; Bryan, D.; Hartling, A.; henderson, C.M.; Hinds, R.C.; 1994. Carboniferous strata of the Western Canada Sedimentary Basin. In: Mossop, G.D. and Shetsen, I., compilers, Geological Atlas of the Western Canada Sedimentary Basin. Canadian Society of Petroleum Geologists and the Alberta Research Council, p. 221-250.

Ross, C.A. and Ross, J.R.P., 1988. Late Paleozoic transgressive-regressive deposition. In: Wilgus, C.K. *et al.*, eds., Sea-Level Changes: An Integrated Approach SEPM Special Publication No. 42, p. 227-247.

Ross, G.M. and Eaton, D.W.; 1996. The Winagami reflection sequence: Seismic evidence for post-collisional magmatism in the Proterozoic of western Canada. Lithoprobe - Alberta Basement Transects, p. 50-60.

Ross, G.M. and Eaton, D.W.; 1997. Winagami reflection sequence: Seismic evidence for postcollisional magmatism in the Proterozoic of western Canada. Geology, v.25, no. 3, p. 199-202.

Ross, G.M.; 1990. Deep crust and basement structure of the Peace River Arch region: constraints on mechanisms of formation. Bulletin of Canadian Petroleum Geology, v. 38A, p. 25-35.

Ross, G.M.; Villeneuve, M.E.; Parrish, R.R.; and Bowring, S.A.; 1989. Tectonic subdivision and U/Pb geochronology of the Precambrian basement of the Alberta basin, western Canada. Open File Dossier Public 2103, Geological Survey, Ottawa.

Rouble, R.G. and Walker, R.G.; 1994. Sequence stratigraphy and controls of barrier-strandplain systems in Falher Members A and B of the Lower Cretaceous Spirit River Formation, north-western Alberta, Canada. AAPG Annual Meeting Abstract, p. 247.

Schiffries, C.M., 1988. Magmatic and hydrothermal processes in layered intrusions. Ph.D. thesis, Harvard University. 89-01643.

Schiffries. C.M. and Skinner. B.J.: 1987. The Bushveld hydrothermal system: field and petrologic evidence. American Journal of Science. v. 287. p. 566-595.

Schumm. S.A.. 1982. Disparity between present rates of denudation and orogeny. In: Laronne. J.B. and Mosley. M.P.. eds.. Erosion and sediment yield. p. 51-63.

Scott. J.C.. *ed.*: 1958. Symposium on the Peace River Arch. Journal of the Alberta Society of Petroleum Geologists. v. 6. no. 3.

Sheriff. R.E.. 1977. In: Payton. C.E. ed.. Seismic Stratigraphy – application to hydrocarbon exploration.

Sheriff. R.E. and Geldart. L.P.: 1995. Exploration Seismology. Published by the Press Syndicate of the University of Cambridge.

Smith. D.G.: Zorn. C.E.: and Sneider. R.M.: 1984. The paleogeography of the Lower Cretaceous of western Alberta and northeastern British Columbia in and adjacent to the deep basin of the Elmworth area. In: Masters. J.A.. ed.. Elmworth - Case study of a deep basin gas field. AAPG Memoir 38. p. 79-114.

Speed. R. C.: 1994. Phanerozoic Evolution of North American Continent-Ocean Transitions. Geological Society of America. DNAG Continent-Ocean Transect Volume.

Swanson. D.A.: 1972. Magma supply rate at Kilauea volcano. 1952-1971. Science. v. 175. p. 169-170.

Swanson. D.A: Wright. T.L.: and Helz. R.T.: 1975. Linear vent systems and estimated rates of magma production and eruption for the Yakima basalt on the Columbia Plateau. American Journal of Science. v. 275. p. 877-905.

Tillman. R.W. and Martinsen. R.S.: 1984. The Shannon shelf-ridge sandstone complex. Salt Creek anticline area. Powder River Basin. Wyoming. In: Tillman R.W. and Siemers. C.T.. eds.. Siliciclastic shelf sediments. Society of Economic Paleontologists and Mineralogists. Special Publication 34. p. 85-142.

Underschultz. J.R. and Erdmer. P.: 1991. Tectonic loading in the Canadian Cordillera as recorded by mass accumulation in the foreland basin. Tectonics. v. 10. no. 2. p. 367-380.

Underschultz. J.R.: 1991. Tectonic loading. sedimentation. and sea-level changes in the foreland basin of north-west Alberta and north-east British Columbia. Canada. Basin Research. v. 3.

no. 3. p. 165-174.

van der Heyden. P.: 1992. A Middle Jurassic to Early Tertiary Anden-Sierran arc model for the coast belt of British Columbia. Tectonics. v. 11. no. 1. p. 82-97.

Vail. P.R.; Mitchum. R.M. Jr.; Todd. R.G.; Widmier. J.M.; Thompson. S. III; Sangree. J.B.; Bubb. J.N.; and Hatlelid. W.G; 1977. Seismic stratigraphy and global changes of sea level. In: Payton C.E.. ed.. Seismic Stratigraphy – applications to hydrocarbon exploration. AAPG Memoir 26. p. 49-212.

Wadsworth. J.A.; 1989. Morphology and origin of erosion surfaces within the Cardium Formation. Upper Cretaceous. Alberta. McMaster University. Hamilton. Ontario. Canada.

Walcott. R.E.; 1970. Flexural rigidity. thickness. and viscosity of the lithosphere: Journal of Geophysical Research. v. 75. p. 3941-3954.

Walker. R.G. and Eyles. C.H.; 1991. Topography and significance of a basinwide sequence-bounding erosion surface in the Cretaceous Cardium Formation. Alberta. Canada. Journal of Sedimentary Petrology. v. 61. p. 473-496.

Williams. G.K.; 1958. Influence of the Peace River Arch on Mesozoic strata. In: Scott. J.C.. ed.. Symposium on the Peace River Arch. Journal of the Alberta Society of Petroleum Geologists. v. 6. no. 3. p. 74-81.

Wolf. D.; 1993. The changing role of the lithosphere in models of glacial isostasy: a historical review. In: Pirazzoli. P.A.; Plag. H.-P.; Sabadini. R.; and Zerbini. S.; eds.. Vertical movements. earth rheology and sea level measurement. Global and Planetary Change. v. 8. p. 95-106.

Wolman. M.G. and Miller. J.P.; 1982. Magnitude and frequency of forces in geomorphic processes. In: Laronne. J.B. and Mosley. M.P.. eds.. Erosion and sediment yield. p. 13-33.

Wu. P.; 1998. ed.. Dynamics of the Ice Age Earth – A Modern Perspective. GeoResearch Forum. v. 3-4.